

**HYPERACTIVATION OF HUMAN SPERM BY  
4-AMINOPYRIDINE: KEY ROLE FOR MOBILISATION OF  
STORED  $\text{Ca}^{2+}$  IN THE SPERM NECK**

by

**SARAH MARY COSTELLO**

A thesis submitted to  
The University of Birmingham  
For the degree of  
DOCTOR OF PHILOSOPHY

School of Biosciences  
The University of Birmingham  
May 2010



## **University of Birmingham Research Archive**

### **e-thesis repository**

This unpublished thesis/dissertation is copyright of the author and/or third parties. The intellectual property rights of the author or third parties in respect of this work are as defined by The Copyright Designs and Patents Act 1988 or as modified by any successor legislation.

Any use made of information contained in this thesis/dissertation must be in accordance with that legislation and must be properly acknowledged. Further distribution or reproduction in any format is prohibited without the permission of the copyright holder.

## **ABSTRACT**

When first deposited in the female reproductive tract mammalian sperm show progressive (activated) motility, with high flagellar beat frequency but low bend angle, particularly of the proximal flagellum. Hyperactivated motility is triggered by increased flagellar  $\text{Ca}^{2+}$  resulting in deep flagellar bends and exaggerated head movement. Two sources of  $\text{Ca}^{2+}$  may contribute to the regulation of hyperactivation.  $\text{Ca}^{2+}$  influx at the plasma membrane is crucial and CatSper, sperm-specific, pH regulated,  $\text{Ca}^{2+}$ -permeable channels expressed in the principal piece of mammalian sperm are of great importance. In addition, studies on sperm from rodents, bulls and humans have provided strong evidence that  $\text{Ca}^{2+}$  stored in the region of the sperm neck contributes to regulation of flagellar activity. 4-aminopyridine caused robust and persistent hyperactivation of motility in human sperm.  $\text{Ca}^{2+}$  imaging showed that treatment with 4-aminopyridine induced a parallel elevation of  $[\text{Ca}^{2+}]_i$ , which initiated at the sperm neck/midpiece and was associated with asymmetric flagellar bending in this region. The data presented here demonstrates that 4-aminopyridine induced hyperactivation in human sperm is not solely pH/CatSper channel dependent and that mobilisation of stored  $\text{Ca}^{2+}$ , possibly causing activation of store-operated  $\text{Ca}^{2+}$  influx, is essential for hyperactivation in a population of human sperm. Furthermore, 4-aminopyridine induced  $\text{IP}_3\text{R}$  and  $\text{RyR}$  store release in sacroplasmic reticulum and brain microsomal vesicles.

Although the physiological factor(s) that activate hyperactivation *in vivo* remains elusive we can conclude that release of the neck/midpiece intracellular  $\text{Ca}^{2+}$  store was sufficient to initiate hyperactivation in a population of human sperm.

## **ACKNOWLEDGEMENTS**

I would like to say an enormous thanks to my supervisor Dr. Steve Publicover, for his support, advice, patience, and encouragement throughout my PhD.

Thank you to all the members of the Publicover group past and present, especially Meg, Kweku, Gisela, Aduen, Kate and Jen. Despite the endless cups of tea and general silliness, we made it through and I really appreciate your friendship and support. Thanks to the staff at the Assisted Conception Unit and the Reproductive and Genetics group especially Chris and Jackson. I would also like to thank the donors who provided the samples.

I am forever grateful to my mother, father, brothers and sisters for their support and love. I would also like to thank Padraig's parents for all their help and generous support during my studies.

Most importantly, thanks to my husband Padraig, for his love, patience and support, friendship and ability to keep me sane during all the crazy times. And to my wonderful children, Jack and Ellen, thanks for all the hugs and kisses and unconditional love. I love you with all my heart and soul.

I would like to thank the School of Biosciences, University of Birmingham for providing financial support during my PhD studies and for allowing me to carry out my research.

# **TABLE OF CONTENTS**

<b>CHAPTER ONE: SIGNAL TRANSDUCTION IN HUMAN SPERM</b>	<b>1</b>
<b>Foreword to Chapter One</b>	<b>2</b>
<b>1.1 Mammalian Spermatogenesis</b>	<b>3</b>
1.1.1 The Sperm Cell	5
1.1.2 Semen	8
<b>1.2 Oogenesis</b>	<b>9</b>
<b>1.3 Sperm transport in the female reproductive tract and fertilisation</b>	<b>10</b>
<b>1.4 Capacitation</b>	<b>11</b>
<b>1.5 Acrosome reaction</b>	<b>12</b>
1.5.1 Zona pellucida3 induced acrosome reaction	13
1.5.2 Progesterone induced acrosome reaction	18
<b>1.6 The sperm calcium signalling ‘toolkit’</b>	<b>20</b>
1.6.1 Voltage gated calcium channels and CatSper channels	21
1.6.2 Cyclic nucleotide-gated channels	23
1.6.3 Store operated channels	24
1.6.4 Calcium stores in sperm	25
1.6.5 Calcium clearance mechanisms in sperm	27
<b>1.7 Sperm <math>E_m</math> and <math>K^+</math> channels</b>	<b>28</b>
<b>1.8 Intracellular pH and sperm</b>	<b>30</b>
<b>1.9 sAC/cAMP/PKA and motility</b>	<b>31</b>
<b>1.10 Calmodulin-dependent protein kinase and motility</b>	<b>34</b>
<b>1.11 Motility – the mechanics of movement</b>	<b>34</b>
1.11.1 Quantitation of sperm movement	36
<b>1.12 Chemotaxis and sperm</b>	<b>40</b>
<b>1.13 Hyperactivation</b>	<b>41</b>
1.13.1 CatSper channels and hyperactivation	44
1.13.2 Intracellular $Ca^{2+}$ store release/capacitation $Ca^{2+}$ entry and hyperactivation	45
1.13.3 4-aminopyridine and hyperactivation	47
<b>1.14 Summary</b>	<b>50</b>
<b>RESEARCH AIMS</b>	<b>51</b>

## **CHAPTER TWO: 4-AMINOPYRIDINE INDUCED HYPERACTIVATION AND ELEVATION OF $[Ca^{2+}]_i$ IN HUMAN SPERM IS INDEPENDENT OF $K^+$ FLUX AND MEMBRANE DEPOLARISATION**

<b>2.1 Abstract</b>	<b>54</b>
<b>2.2 Introduction</b>	<b>55</b>
<b>2.3 Materials and methods</b>	<b>58</b>
2.3.1 Materials	58
2.3.2 Preparation and capacitation of spermatozoa	58
2.3.3 Single cells imaging	59
2.3.4 Imaging data processing	59
2.3.5 Evaluation of 4-aminopyridine fluorescence quenching	60
2.3.6 Evaluation of sperm hyperactivation	61
2.3.7 High speed imaging of sperm motility	62
2.3.8 Statistical Analysis	62
<b>2.4 Results</b>	<b>63</b>
2.4.1 4-aminopyridine induced hyperactivation in human spermatozoa	63
2.4.2 4-aminopyridine elevated $[Ca^{2+}]_i$ fluorescence in OGB labelled spermatozoa	64
2.4.3 4-aminopyridine did not significantly quench OGB emission signal	65
2.4.4 4-aminopyridine induced hyperactivation and increased $[Ca^{2+}]_i$ fluorescence does not act through $K^+$ channel block and modulation of $E_m$	67
<b>2.5 Discussion</b>	<b>69</b>

## **CHAPTER THREE: EFFECT OF pH ON 4-AMINOPYRIDINE INDUCED HYPERACTIVATION AND ELEVATION OF $[Ca^{2+}]_i$**

<b>3.1 Abstract</b>	<b>74</b>
<b>3.2 Introduction</b>	<b>75</b>
<b>3.3 Materials and methods</b>	<b>77</b>
3.3.1 Materials	77
3.3.2 Spermatozoa preparation and capacitation	77
3.3.3 Fluorimetry	77
3.3.4 Evaluation of sperm hyperactivation	78
3.3.5 Evaluation of extracellular pH on degree of 4-aminopyridine ionisation	79
3.3.6 Single Cell Imaging	79

3.3.7 Imaging data processing	79
3.3.8 Statistical Analysis	79
3.4 Results	80
3.4.1 Ionisation state of 4-aminopyridine is dependent of pH <sub>o</sub>	80
3.4.2 4-aminopyridine induced hyperactivation was significantly increased at extracellular pH8.5	81
3.4.3 Extracellular pH effects 4-aminopyridine induced [Ca <sup>2+</sup> ] <sub>i</sub> fluorescence response in human sperm	84
3.4.4 Effects of NH <sub>4</sub> Cl on intracellular pH and 4-aminopyridine induced hyperactivation and [Ca <sup>2+</sup> ] <sub>i</sub> fluorescence response	88
3.4.5 Effect of propionate pre-treatment on 4-aminopyridine induced [Ca <sup>2+</sup> ] <sub>i</sub> fluorescence response	92
3.5 Discussion	94
<b>CHAPTER FOUR: 4-AMINOPYRIDINE INDUCED HYPERACTIVATION IS NOT SOLELY CATSPER DEPENDENT</b>	99
4.1 Abstract	100
4.2 Introduction	101
4.3 Materials and methods	103
4.3.1 Materials	103
4.3.2 Spermatozoa preparation and capacitation	103
4.3.3 Single cell imaging	103
4.3.4 Evaluation of Ni <sup>2+</sup> fluorescence enhancement	103
4.3.5 Motility Analysis	104
4.3.6 Statistical Analysis	104
4.4 Results	105
4.4.1 The putative CatSper channel blockers (nickel, cadmium and ruthenium red) reduce 4-aminopyridine induced hyperactivation in human spermatozoa	105
4.4.2 Effects of Ni <sup>2+</sup> and 4-aminopyridine on OGB fluorescence emission	108
4.4.3 Effects of nickel on 4-aminopyridine induced [Ca <sup>2+</sup> ] <sub>i</sub> fluorescence response	110
4.5 Discussion	112
<b>CHAPTER FIVE: 4-AMINOPYRIDINE INDUCED INTRACELLULAR Ca<sup>2+</sup> STORE MOBILISATION</b>	115
5.1 Abstract	116

<b>5.2 Introduction</b>	<b>117</b>
<b>5.3 Materials and method</b>	<b>119</b>
5.3.1 Materials	119
5.3.2 Spermatozoa preparation and capacitation	119
5.3.3 Single cell imaging	120
5.3.4 Evaluation of sperm hyperactivation	120
5.3.5 Evaluation of $\text{Ca}^{2+}$ uptake and release in microsomal vesicles	121
5.3.6 Evaluation of acrosomal reaction	122
5.3.7 Statistical analysis	123
<b>5.4 Results</b>	<b>124</b>
5.4.1 The response to 4-aminopyridine initiates at the sperm neck	124
5.4.2 4-aminopyridine mobilises stored $\text{Ca}^{2+}$	126
5.4.3 4-aminopyridine induced $\text{Ca}^{2+}$ mobilisation and hyperactivation	130
5.4.4 Effects of 4-aminopyridine on intracellular $\text{Ca}^{2+}$ uptake and $\text{Ca}^{2+}$ release proteins	132
5.4.4.1 Effect of 4-aminopyridine on fluo3 emission	132
5.4.4.2 Effect of 4-aminopyridine on $\text{Ca}^{2+}$ uptake and $\text{Ca}^{2+}$ -ATPase activity	133
5.4.4.3 Effect of 4-aminopyridine on $\text{IP}_3\text{Ca}^{2+}$ release channels	133
5.4.4.4 Effect of 4-aminopyridine on ryanodine receptor $\text{Ca}^{2+}$ release channels	134
5.4.5 Effect of low dose $\text{P}_4$ on the 4-aminopyridine induced $[\text{Ca}^{2+}]_i$ response	137
5.4.6 Effect of tetracaine on the 4-aminopyridine induced $[\text{Ca}^{2+}]_i$ response	138
5.4.7 4-aminopyridine and mitochondrial $\text{Ca}^{2+}$	140
5.4.8 4-aminopyridine and the acrosome reaction	142
<b>5.5 Discussion</b>	<b>143</b>
<b>CHAPTER SIX: 4-AMINOPYRIDINE AND CAPACITATIVE <math>\text{Ca}^{2+}</math> ENTRY</b>	<b>152</b>
<b>6.1 Abstract</b>	<b>153</b>
<b>6.2 Introduction</b>	<b>154</b>
<b>6.3 Materials and methods</b>	<b>156</b>
6.3.1 Materials	156
6.3.2 Spermatozoa preparation and capacitation	156
6.3.3 Evaluation of sperm hyperactivation	156
6.3.4 Single cell imaging	156
6.3.5 Data analysis	156



<b>6.4 Results</b>	<b>157</b>
<b>6.4.1</b> 4-aminopyridine enhanced $\text{Ca}^{2+}$ influx in $\text{Ca}^{2+}$ store depleted sperm cells	<b>157</b>
<b>6.4.2</b> Pharmacological inhibition of store operated $\text{Ca}^{2+}$ channels modified the 4-aminopyridine induced $[\text{Ca}^{2+}]_i$ response	<b>163</b>
<b>6.5 Discussion</b>	<b>167</b>
<b>CHAPTER SEVEN: GENERAL DISCUSSION</b>	<b>171</b>
<b>7.1 Future research</b>	<b>181</b>
<b>APPENDIX I: Supplement <math>\text{Ca}^{2+}</math> channel information</b>	<b>182</b>
<b>APPENDIX II: Media</b>	<b>188</b>
<b>APPENDIX III: Research Publications</b>	<b>190</b>
<b>REFERENCES</b>	<b>191</b>

## **LIST OF FIGURES**

Figure 1.1: Epithelium of the seminiferous tubule	4
Figure 1.2: Schematic representation of mammalian sperm cell and ultrastructure of the flagellum	7
Figure 1.3: Mechanism of sperm-egg interaction	17
Figure 1.4: Summary of the sperm cell $[Ca^{2+}]_i$ signalling toolkit	21
Figure 1.5: Diagrammatic cross-section of mammalian sperm tail	35
Figure 1.6: Motility patterns for capacitated human sperm	39
Figure 1.7: Motility pattern for activated and hyperactivated sperm	42
Figure 1.8: Structure of 4-aminopyridine	48
Figure 1.9: Experimental matrix/workpath linking research aims with results chapters	52
Figure 2.1a: 4-aminopyridine induced hyperactivation of capacitated sperm in HEPES buffered sEBSS (pH 7.3)	63
Figure 2.1b: Series of phase contrast images for sperm hyperactivated by 4-aminopyridine	63
Figure 2.2: The effects of 4-aminopyridine on $[Ca^{2+}]_i$ in capacitated sperm bathed in standard saline (pH7.3)	64
Figure 2.3a: Emission spectra for de-esterified OGB in the presence of 4-aminopyridine	66
Figure 2.3b: Emission spectra for de-esterified OGB in the absence of 4-aminopyridine	66
Figure 2.3c: Stern Volmer plot for OGB emission fluorescence	66
Figure 2.4a: The effects of valinomycin on 4-aminopyridine induced $[Ca^{2+}]_i$ fluorescence response	68
Figure 2.4b: The effects of valinomycin on 4-aminopyridine induced hyperactivation	68
Figure 3.1: 4-aminopyridine % ionization	80
Figure 3.2a: 4-aminopyridine induced hyperactivation was enhanced at pH <sub>o</sub> 8.5	83
Figure 3.2b: 4-aminopyridine induced hyperactivation in non-capacitated cells	83
Figure 3.2c: 4-aminopyridine induced hyperactivation remained constant over an extended period	83
Figure 3.3a: The effect of 4-aminopyridine on $[Ca^{2+}]_i$ fluorescence at pH <sub>o</sub> 6.5	86

Figure 3.3b: The effect of 4-aminopyridine on $[Ca^{2+}]_i$ fluorescence at $pH_0 8.5$	86
Figure 3.3c: 4-aminopyridine induced $[Ca^{2+}]_i$ fluorescence response did not required prior sensitisation	86
Figure 3.3d: Dose dependent 4-aminopyridine induced $[Ca^{2+}]_i$ fluorescence response	86
Figure 3.3e: Fluorimetric responses of 4-aminopyridine on $[Ca^{2+}]_i$ at $37^\circ C$ and $25^\circ C$	86
Figure 3.4a: An example of a BCECF calibration plot	90
Figure 3.4b: BCECF traces obtained from cells treated with 4-aminopyridine or $NH_4Cl$	90
Figure 3.4c: The effects of $NH_4Cl$ on 4-aminopyridine induced $[Ca^{2+}]_i$ fluorescence response	90
Figure 3.4d: The effects of $NH_4Cl$ or 4-aminopyridine on hyperactivation rates	90
Figure 3.5a: The effects of propionate (intracellular acidification) on 4-aminopyridine $[Ca^{2+}]_i$ fluorescence response	90
Figure 3.5b: Frequency distribution of the proportion of responsive cells and amplitude of the 4-aminopyridine induced $[Ca^{2+}]_i$ fluorescence response in the presence and absence of propionate ( $pH_0 8.5$ )	90
Figure 3.5c: The effects of propionate on 4-aminopyridine induced hyperactivation	90
Figure 4.1: 4-aminopyridine induced hyperactivation on capacitated sperm in the presence of $Ni^{2+}$ , $Cd^{2+}$ and ruthenium red.	106
Figure 4.2a: The effect of $Ni^{2+}$ OGB emission	109
Figure 4.2b: Stern Volmer plot for the effect of $Ni^{2+}$ on OGB emission	109
Figure 4.2c: The effect of $Ni^{2+}$ and 4-aminopyridine on OGB emission	109
Figure 4.3a: The effect of $Ni^{2+}$ on sperm $[Ca^{2+}]_i$ in standard saline	111
Figure 4.3b: The effect of $Ni^{2+}$ pre-treatment on the 4-aminopyridine induced $[Ca^{2+}]_i$ response in standard saline	111
Figure 4.3c: The effect of $Ni^{2+}$ pre-treatment on the 4-aminopyridine induced $[Ca^{2+}]_i$ response in simplified saline	111
Figure 4.3d: The effect 4-aminopyridine induced $[Ca^{2+}]_i$ response in simplified saline	111
Figure 5.1a: 4-aminopyridine induced $[Ca^{2+}]_i$ fluorescence response	125
Figure 5.1b: Pseudocolour images series of $[Ca^{2+}]_i$ fluorescence response in sperm cell exposed to 4-aminopyridine (5.1a)	125

Figure 5.1c: Plot showing delayed mobilization of $\text{Ca}^{2+}$ in the sperm neck in response to 4-aminopyridine	125
Figure 5.1d: Pseudocolour image series for cell (5.1c)	125
Figure 5.2a: Effect of 4-aminopyridine on $[\text{Ca}^{2+}]_i$ in nominal $\text{Ca}^{2+}$ free saline	128
Figure 5.2b: Amplitude of 4-aminopyridine induced $[\text{Ca}^{2+}]_i$ fluorescence response in nominal $\text{Ca}^{2+}$ free saline and standard saline	128
Figure 5.2c: Effect of 4-aminopyridine on $[\text{Ca}^{2+}]_i$ in EGTA buffered saline	128
Figure 5.3a: 4-aminopyridine induced hyperactivation in nominal $\text{Ca}^{2+}$ free and normal saline	131
Figure 5.3b: Effect of suspension in EGTA buffered saline on 4-aminopyridine induced hyperactivation	131
Figure 5.3c: Effect of suspension in EGTA buffered saline on % motility	131
Figure 5.4: Effects of 4-aminopyridine on fluo3 emission	133
Figure 5.5a: Effects of 4-aminopyridine on $\text{Ca}^{2+}$ ATPase in SR microsomes	135
Figure 5.5b: Effects of 4-aminopyridine on $\text{IP}_3\text{R}$ $\text{Ca}^{2+}$ in brain microsomes	135
Figure 5.5c: Effects of 4-aminopyridine on $\text{RyR}$ $\text{Ca}^{2+}$ release SR microsomes	135
Figure 5.5d: Dose-dependent effect of 4-aminopyridine on $\text{RyR}$ $\text{Ca}^{2+}$ release in SR	135
Figure 5.6: The effects of $\text{P}_4$ (100pM) on the 4-aminopyridine induced $[\text{Ca}^{2+}]_i$ fluorescence response	137
Figure 5.7a/b: Effect of tetracaine (1mM) on the 4-aminopyridine induced $[\text{Ca}^{2+}]_i$ fluorescence response	139
Figure 5.8a: Effects of DNP pre-treatment on 4-aminopyridine induced $[\text{Ca}^{2+}]_i$ fluorescence response	141
Figure 5.8b: 4-aminopyridine induced $[\text{Ca}^{2+}]_i$ fluorescence response in the presence or absence of DNP pre-treatment	141
Figure 5.8c: Effects of 4-aminopyridine on Rho123 fluorescence emission	141
Figure 5.9: Effects of 4-aminopyridine on the acrosome reaction	142
Figure 6.1a: Effects of 4-aminopyridine on $[\text{Ca}^{2+}]_i$ fluorescence response in store depleted cells (pre-treated with EGTA for 10 minutes).	158
Figure 6.1b: Effects of restoration of $\text{Ca}^{2+}$ (100 $\mu\text{M}$ ) on $[\text{Ca}^{2+}]_i$ fluorescence response in store	

depleted cells	158
Figure 6.2a: Effects of bis-phenol pre-treatment on 4-aminopyridine induced $[Ca^{2+}]_i$ response in the standard saline.	161
Figure 6.2b: Effects of bis-phenol pre-treatment on 4-aminopyridine induced $[Ca^{2+}]_i$ response in nominal $Ca^{2+}$ free saline.	161
Figure 6.2c: Effects of bis-phenol pre-treatment on 4-aminopyridine induced hyperactivation in standard saline or nominal $Ca^{2+}$ free saline.	161
Figure 6.3a: The effects of 2-APB pre-treatment on 4-aminopyridine induced $[Ca^{2+}]_i$ fluorescence response.	165
Figure 6.3b: The effects of 2-APB pre-treatment on $NH_4Cl$ induced $[Ca^{2+}]_i$ fluorescence response.	165
Figure 6.3c: The effects of SKF-96365 pre-treatment on 4-aminopyridine induced $[Ca^{2+}]_i$ fluorescence response.	165
Figure 7.1a: Schematic diagram of female reproductive tract, indicating gamete direction of travel	179
Figure 7.1b: Schematic diagram of sperm gamete interaction	179
Figure 7.1c: Schematic diagram of sperm cell highlighting neck/midpiece putative store	179
Figure 7.1d: Summary model for the effects of 4-aminopyridine on $[Ca^{2+}]_i$ fluorescence and the components of the $Ca^{2+}$ signalling toolkit that may be involved in these response at the neck/midpiece store region.	179
Figure 8.0: Subunit structure of $Ca_v1$ channel	183

## **LIST OF TABLES**

Table 1.1: Summary of putative ZP3 receptors identified in the mouse	14
Table 1.2: Summary of putative P <sub>4</sub> receptors identified in mammalian sperm	19
Table 3.1: Effect of increased pHi and 4-aminopyridine on sperm motility parameters	91
Table 4.1: Effects of Ni <sup>2+</sup> , Cd <sup>2+</sup> and ruthenium red on 4-aminopyridine induced hyperactivation	107
Table 6.1: Effect of bis-phenol pre-treatment on 4-aminopyridine induced hyperactivation in standard or nominal calcium free saline	161
Table 7.0: Appendix I Supplement Ca <sub>v</sub> channel information	186
Table 8.0: Appendix I Supplement CatSper channel information	187
Table 9.0: Appendix I Supplement TRPC channel information	187

## **LIST OF ABBREVIATIONS**

**AA** – Arachidonic acid

**ACE** – Angiotension-converting enzyme

**ADA** – N-(2-acetamido)iminodiacetic acid

**ADP** – Adenosine 5'-diphosphate

**AKAP** - A-Kinase anchor protein

**ALH** - Amplitude of lateral head displacement

**ALH<sub>max</sub>** - The maximum ALH found along the trajectory

**2-APB** - 2-aminoethoxydipenylborane

**AR** – Acrosome reaction

**ART** - Assisted reproductive techniques

**ATP** – Adenosine 5'-triphosphate

**BCECF**- 2'-7'-bis-(2-carboxyethyl)-5-(and-6-)-carboxyfluorescein acetoxymethyl ester

**8-bromo cGMP** - 8-bromoguanosine-3'-5'-cyclophosphate sodium salt

**BSA** - Bovine serum albumin

**Ca<sup>2+</sup>** - Calcium ion

**[Ca<sup>2+</sup>]<sub>i</sub>** - Intracellular calcium concentration

**CaM** – Calmodulin

**CaMK** – calmodulin kinase

**cAMP** - Cyclic adenosine 3',5'- monophosphate

**CASA** - Computer-assisted semen analysis

**Ca<sub>v</sub>** – Voltage activated calcium channel

**CCE** – Capacitative calcium entry

**CD** – Cluster of differentiation, cell membrane molecule identified by monoclonal antibodies and used to classify leukocytes into subsets.

**CD9** – A type III transmembrane protein crosses the plasma membrane more than once

**Cd<sup>2+</sup>** - Cadmium ion

**CFsEBSS** – Nominal Ca<sup>2+</sup>-free supplemented Earle's balanced salt solution

**CFTR** - Cystic fibrosis transmembrane conductance regulator

**cGMP** - Cyclic guanosine 3',5'-monophosphate

**CICR** - Ca<sup>2+</sup>-induced Ca<sup>2+</sup> release

**Cl<sup>-</sup>** - Chloride ions

**4CmC** - Chloro-m-cresol

**CNG** - Cyclic nucleotide-gated

**CRAC** –  $\text{Ca}^{2+}$  release activated  $\text{Ca}^{2+}$

**DNA** – deoxyribonucleic acid

**DAG** - Diacylglycerol **DMSO** - Dimethyl sulfoxide

**EGTA** - Ethylene glycol-bis ( $\beta$ -amino-ethylether)-N,N,N',N'-tetraacetic acid

**E<sub>m</sub>** – Membrane potential

**ENaC** - Epithelial  $\text{Na}^+$  channels

**ER**- Endoplasmic reticulum

**Fluo3** - 1-[2-Amino-5-(2,7-dichloro-6-hydroxy-3-oxy-9-xanthenyl)phenoxy]-2-(2-amino-5-methylphenoxy)ethane-N,N,N',N'-tetraacetic acid ammonium potassium salt

**FS** - Fibrous sheath

**FSH** - Follicle stimulating hormone

**Fura2/AM** – 5-Oxazolecarboxylic acid, 2-6-(bis(2-((acetloxy)methoxy)-2-oxoethyl)amino)-5-methylphenoxy)ethoxy)-2-benzofuranyl)-, (acetyloxy)methyl ester

**GABA<sub>A</sub>** - Gamma-aminobutyric acid type A

**GalTase** –  $\beta$  1,4-galactosyltransferase

**GAPDH** – glyceraldehyde phosphate dehydrogenase

**GC** – Guanylyl cyclase

**GLR** - Glycine receptor/ $\text{Cl}^-$  channel

**H<sup>+</sup>** - Hydrogen ions

**HCO<sub>3</sub><sup>-</sup>** - Bicarbonate ion

**Hepes** - 4-(2-hydroxyethyl)-1-piperazineethanesulfonic acid

**HOS** – Hypo-osmotic swelling solution

**HNG** - hyperpolarisation-activated nucleotide-gated

**HPG** – Hypothalamic-pituitary-gonadal

**Hv1**- Voltage gated proton pump 1

**IBMX**- 3-isobutyl-1-methylxanthine (phosphodiesterase inhibitor)

**ICS** – Intra-calcium store

**IP<sub>3</sub>** - Inositol-1,4,5-triphosphate

**IP<sub>3</sub>R** - Inositol-1,4,5-triphosphate receptor



**IVF** - *In vitro* fertilization

**K<sup>+</sup>** - Potassium ion

**Kir** – Inwardly rectifying K<sup>+</sup> channel

**KO** – Knock out

**La<sup>3+</sup>** - Lanthanum ion

**LH** - Luteinizing hormone

**LIN** - % linearity (straight line velocity/ curvilinear velocity x 100)

**mAC** - Membrane-associated adenylyl cyclase

**MCU** – Mitochondrial Ca<sup>2+</sup> uniporter

**mPR** - Membrane progesterone receptor

**MS** - Mitochondrial sheath

**Na<sup>+</sup>** - Sodium ions

**NaK-ATPase** – Sodium potassium ATPase

**NCX** – Sodium calcium exchanger

**Ni<sup>2+</sup>** - Nickel ion

**NKCC** – Na<sup>+</sup>/K<sup>+</sup>/Cl<sup>-</sup> co-transporter

**1NM-PP1** – pyrazolo[3,4-*d*]pyrimidine (novel inhibitor)

**NO** – Nitric oxide

**ODFs** - Outer dense fibers

**OGB-1AM** - Oregon green 488 BAPTA 1-acetoxymethyl

**OR** - Olfactory receptor

**Orai** - A protein that forms a calcium channel in the plasma membrane

**PBS** - Phosphate buffered saline

**PDL** - Poly-D-lysine

**PGRMC1** - Progesterone membrane receptor component 1

**PGRMC2** - Progesterone membrane receptor component 2

**pH<sub>i</sub>** - intracellular pH

**PIP<sub>2</sub>** - Phosphatidylinositol 4,5-biphosphate

**PKA** - Protein kinase A

**PKC** - Protein kinase C

**PKG** - Protein kinase G

**PLA** – Phospholipase A

**PLC** - Phospholipase C

**PMCA** - Plasma membrane  $\text{Ca}^{2+}$ -ATPase

**PP** – protein phosphatase

**PTP** – Phosphotyrosine phosphatase

**PTP** - Permeability transition pore

**RNE** - Redundant nuclear envelope

**Rh123** - Rhodamine 123 (2-(6-Amino-3-imino-3H-xanthen-9-yl)benzoic acid methyl ester)

**RNE** – Redundant nuclear envelope

**ROC** – Receptor operated channels

**RR** – Ruthenium red dye

**RyRs** - Ryanodine receptors

**sAC** - Soluble adenylyl cyclase

**sEBSS** - Supplemented Earle's balanced salt solution

**SED1**- secondary zona-binding factor1

**SERCA** - Sarcoplasmic-Endoplasmic  $\text{Ca}^{2+}$ -ATPase

**sGC** - Soluble guanylyl cyclase

**SKF96365** - 1-[ $\beta$ -[3-(4-Methoxyphenyl)propoxy]-4-methoxyphenethyl]-1H-imidazole, HCL

**SNARE** - Soluble N-ethylmaleimide-sensitive factor-attachment protein receptor

**sNHE** – Sperm specific sodium hydrogen exchanger

**SOAF** - Sperm oocyte activating factors

**SOC** - Store-operated  $\text{Ca}^{2+}$  channel

**SP56**- Sperm protein 56

**SPAM1** – Sperm adhesion molecule 1

**SPCA** - Secretory pathway  $\text{Ca}^{2+}$ -ATPase

**SR** – Sarcoplasmic reticulum

**STIM1** – Stromal interacting protein 1

**tmACs** - Transmembrane adenylyl cyclases

**TAPS** - [(2-hydroxy-1,1-bis(hydromethyl)ethyl)amino]-1-propanesulfonic acid

**2TM** – 2 transmembrane

**6TM** – 6 transmembrane

**tmAC** – Transmembrane adenylyl cyclase

**TRP** - Transient receptor potential

**TRPC** - Transient receptor potential canonical

**Tsp-2** – Tyrosylprotein sulfotransferase-2

**VAP** - Average path velocity

**VCL** - Curvilinear velocity

**VSL** – Straight line velocity

**VGCC** - Voltage-gated  $\text{Ca}^{2+}$  channels

**VOC** – Voltage-operated channels

**VOCCs** - Voltage-operated  $\text{Ca}^{2+}$  channels

**VSL** - Straight-line velocity

**WHO** - World Health Organization

**ZP** – Zona pellucida

**ZPBP1** – Zona pellucida binding protein 1

**ZPBP2** – Zona pellucida binding protein 2

# **CHAPTER ONE**

## **SIGNAL TRANSDUCTION IN HUMAN SPERMATOZOA**

<b>Foreword to Chapter One</b>	<b>2</b>
<b>1.1 Mammalian spermatogenesis</b>	<b>3</b>
1.1.1 The Sperm Cell	5
1.1.2 Semen	8
<b>1.2 Oogenesis</b>	<b>9</b>
<b>1.3 Sperm transport in the female reproductive tract and fertilisation</b>	<b>10</b>
<b>1.4 Capacitation</b>	<b>11</b>
<b>1.5 Acrosome reaction</b>	<b>12</b>
1.5.1 Zona pellucida <sup>3</sup> induced acrosome reaction	13
1.5.2 Progesterone induced acrosome reaction	18
<b>1.6 The sperm calcium signalling ‘toolkit’</b>	<b>20</b>
1.6.1 Voltage gated calcium channels and CatSper channels	21
1.6.2 Cyclic nucleotide-gated channels	23
1.6.3 Store operated channels	24
1.6.4 Calcium stores in sperm	25
1.6.5 Calcium clearance mechanisms in sperm	27
<b>1.7 Sperm E<sub>m</sub> and K<sup>+</sup> channels</b>	<b>28</b>
<b>1.8 Intracellular pH and sperm</b>	<b>30</b>
<b>1.9 sAC/cAMP/PKA and motility</b>	<b>31</b>
<b>1.10 Calmodulin-dependent protein kinase and motility</b>	<b>34</b>
<b>1.11 Motility- the mechanics of movement</b>	<b>34</b>
1.11.1 Quantitation of sperm movement	36
<b>1.12 Chemotaxis and sperm</b>	<b>40</b>
<b>1.13 Hyperactivation</b>	<b>41</b>
1.13.1 CatSper channels and hyperactivation	44
1.13.2 Intracellular Ca <sup>2+</sup> store release/capacitation Ca <sup>2+</sup> entry and hyperactivation	45
1.13.3 4-aminopyridine and hyperactivation	47
<b>1.14 Summary</b>	<b>50</b>
<b>RESEARCH AIMS</b>	<b>51</b>

## **Foreword to Chapter One**

This chapter summarises the recent progress that has been made in understanding the complex series of activities that spermatozoa must perform to fertilise the oocyte. This chapter describes the physical structure of the human gametes, in particular the spermatozoa. Emphasis is placed on regulation of motility and hyperactivation and the  $\text{Ca}^{2+}$  signalling events that occur within the sperm cell.

## 1.1 Mammalian spermatogenesis

Spermatogenesis is a complex process of proliferation and differentiation, occurring in the seminiferous tubules of the testis, resulting in the continuous production of highly differentiated spermatozoa (figure 1.1) (Sutovsky and Manandhar, 2006). During embryogenesis, the primordial germ cells migrate to the testis and are incorporated within the tubules to form spermatogonia. The reproductive system and germ line remain relatively quiescent until the peri-pubertal period (Sutovsky and Manandhar, 2006). At puberty, the diploid spermatogonia are re-activated and undergo mitosis in the basal compartment of the seminiferous tubules to form a reservoir of self renewing stem cells or differentiate to A1 type spermatogonia (figure 1.1). A1 spermatogonia undergo a number of mitotic divisions to form a clone of cells, some of which differentiate to primary spermatocytes before migrating through the blood-testis barrier. The blood-testis barrier is formed by intricate cell-cell junctions (Setchell, 2008) between adjacent cytoplasmic projections of Sertoli cells (nurse cells). Primary spermatocytes penetrate through this barrier to enter the immunoprivileged adluminal compartment and undergo meiotic divisions to form round haploid spermatids (Sutovsky and Manandhar, 2006).

Spermiogenesis involves the differentiation of the spermatid into elongated spermatid and finally spermatozoa. This process involves extensive cellular remodeling and the reduction of many spermatid organelles synchronised with the formation of specialised sperm structures such as the acrosome, flagellum and nucleus. Spermatogenesis is terminated at spermiation, when fully differentiated sperm detach from each other and from the apical surface of the seminiferous epithelium. Spermatozoa within the testis are quiescent and passage through the male reproductive tract is facilitated by the the flow of testicular secretions and ciliated epithelial cells. Following release from the seminiferous tubules, spermatozoa are transported through the epididymis and vas deferens where further biochemical and functional modifications (maturation) occurs (Marengo, 2008). Sperm are subsequently stored in the

cauda epididymis prior to ejaculation (Wassarman and Florman, 1997). Spermatogenesis is controlled by the hypothalamic-pituitary-gonadal (HPG) axis. The hypothalamus releases gonadotrophin-releasing hormone which stimulates the anterior pituitary to release the hormones, luteinizing hormone (LH) and follicle stimulating hormone (FSH). The human spermatogenic cycle takes approximately 70 days to complete (Sutovsky and Manandhar, 2006).

**Figure 1.1**

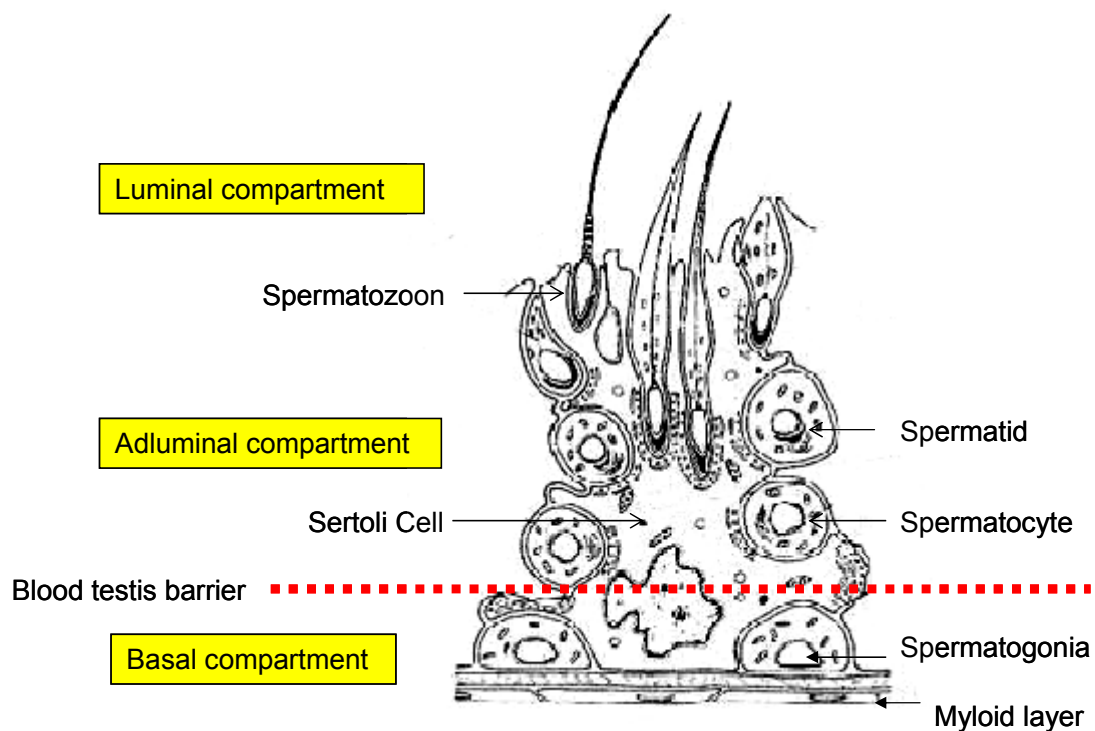


Figure 1.1: Epithelium of the seminiferous tubule, showing the relationship between Sertoli cells and developing sperm cells. As sperm cells mature, they progress towards the lumen of the seminiferous tubule (adapted from Glover *et al.*, 1990).

### 1.1.1 The Sperm cell

Mature spermatozoa are highly polarised, compartmentalised, terminally differentiated cells (Barratt, 1995; Flesch and Gadella, 2000; Naz and Rajesh, 2004). The ungulate, carnivore and primate sperm head is pleomorphic, oval in shape and slightly bilaterally flattened, whereas a rodent sperm head is hook shaped. Taking into consideration any shrinkage that fixation and staining induce, the World Health Organisation (WHO, 1999) morphology guidelines state that the human spermatozoon head should be 4.0-5.0 $\mu$ m in length and 2.5-3.5 $\mu$ m in width. All eutherian mammalian sperm share the general features of the head and tail as described below.

The head contains the nucleus, acrosome and cytoplasmic droplet(s) (figure 1.2). The highly condensed nucleus contains tightly packed chromatin consisting of haploid supercoiled DNA (transcriptionally and translationally inactive) complexed with highly basic protamines. The nuclear envelope pore complexes are reduced during spermiogenesis with some nuclear pores remaining in the redundant nuclear envelope (RNE) located at the base of the nucleus (Ho, 2010). The perinuclear theca forms a unique cytoskeletal shell that encapsulates and protects the mammalian sperm nucleus. This extranuclear structure can be subdivided into three structurally continuous regions: the subacrosomal layer, equatorial segment and the postacrosomal sheath. The subacrosomal layer underlies the acrosomal segment of the sperm head, and functions to anchor the Golgi derived acrosome cap. The inner and outer acrosomal membranes encase the dense acrosomal matrix. The equatorial segment is a folded-over complex of perinuclear theca, inner and outer acrosomal membranes which remains intact following the acrosome reaction. The equatorial segment carries receptors (including the Izumo proteins- Inoue *et al.*, 2005; Isotani and Okabe, 2005; Ellerman *et al.*, 2009; Ikawa *et al.*, 2008, 2010) involved in secondary sperm-oolemma binding. The postacrosomal sheath of the sperm perinuclear theca is believed to contain a complex of sperm borne, oocyte activating factors (including phospholipase C  $\zeta$  (PLC $\zeta$ )) (Ciapa and Chiri, 2000; Swann and Lai, 2002;



Swann *et al.*, 2004, 2006; Swann and Yu, 2008; Dale *et al.*, 2010).

During spermatogenesis approximately 50% of the mitochondria are lost and the remainder migrate to the base of the nucleus and are arranged in a helix around the proximal piece of the flagella surrounded by the mitochondrial sheath (Cataldo *et al.*, 1996). The cytoplasmic droplet(s) contains redundant cytoplasm and organelles such as mitochondria and ribosomes. The head is separated from the midpiece by the posterior ring.

Spermatozoa are immotile in the testis and are activated upon release into physiological fluid (containing  $\text{HCO}_3^-$  and  $\text{Ca}^{2+}$ ). The function of the flagellum (figure 1.2) is to produce energy and propel the spermatozoon from the site of semen deposition in the vagina, through the female reproductive tract and finally aid penetration of the outer vestments of the oocyte. The innermost structure of the flagellum consists of the axoneme paralleled by the outer dense fibres (ODF). Sperm motility is provided by the 9+2 arrangement of microtubules that form the axoneme. The nine outer microtubule doubles (figure 1.2a) are paralleled by nine outer dense fibers that provide flexibility and support. The external structure of the sperm flagellum can be divided into four subdivisions – the connecting piece, the mid-piece, the principal piece and the end-piece (Fawcett, 1975). The connecting piece is a short linking segment and is most proximal portion of the flagellum that attaches to the sperm head (0.5 $\mu\text{m}$ ). The connecting piece contains the sperm proximal centriole (the distal centriole disintegrates during spermiogenesis). The proximal centriole marks the origin of the pair of central microtubule of the axoneme. The midpiece is covered by the mitochondrial sheath containing the helical arrangement of mitochondria (3.5 $\mu\text{m}$ ). The principal piece (~55 $\mu\text{m}$ ) is covered by the fibrous sheath, composed of two longitudinal columns running parallel to the outer dense fibres three and eight, and stabilised by circumferential or transverse ribs (figure 1.2b). Finally, the end-piece is a terminal portion of the flagellum containing the axoneme only surrounded by plasma membrane (~3 $\mu\text{m}$ ) (Turner, 2006).

**Figure 1.2**

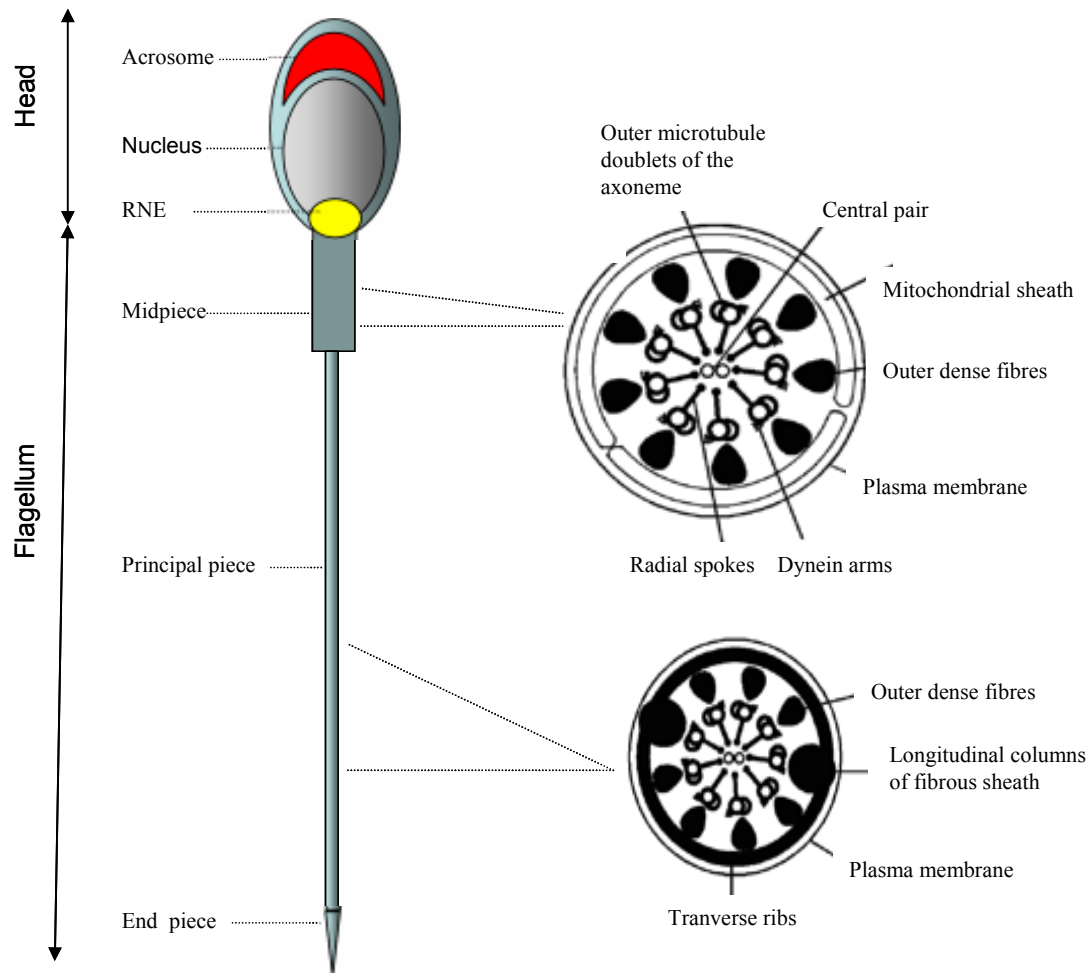


**Figure 1.2:** Schematic representation of a mammalian sperm cell and the ultrastructure of the flagellum. (a) Schematic cross-section through the midpiece showing the plasma membrane, mitochondrial sheath surrounding the 9 outer dense fibres. Within the outer dense fibres (ODF) are the components of the axoneme: the 9 outer microtubule doublets with associated dynein arms, radial spokes and the central pair of microtubule doublets. (b) Schematic cross-section through the principal piece showing the plasma membrane surrounding 7 ODFs (3 and 8 have been replaced with longitudinal columns of fibrous sheath. The two columns are connected by transverse ribs) (adapted from Turner, 2006 and Lefèvre *et al.*, 2009)

### 1.1.2 Semen

Seminal fluid is a heterogeneous mixture consisting of ejaculated spermatozoa (1-5%) and accessory gland secretions mainly from the prostate gland (30%) and seminal vesicles (60%) (Polakoski *et al.*, 1976; Mann and Lutwak-Mann, 1981; Coffey, 1995). The ejaculate of normozoospermic males contains  $\geq 20$  million spermatozoa per ml,  $\geq 50\%$  of these sperm are progressively motile and  $\geq 30\%$  of the sperm are morphologically normal (WHO, 1990). The function of seminal fluid is to provide nutrients, a transport medium and to facilitate sperm movement. Prostate gland secretions include citrate (a nutrient source), inositol, calcium, zinc, magnesium, fibrinolysin and acid phosphatase (involved in activating sperm). Seminal vesicle secretions include fructose, ascorbic acid, vesiculase (a coagulating enzyme) and prostaglandins. Sperm stored in the cauda epididymis are immotile but are immediately activated when sperm are released from the epididymis into semen (high bicarbonate ( $\text{HCO}_3^-$ ) and calcium ( $\text{Ca}^{2+}$ ) conc.) (Visconti and Kopf, 1998; Visconti *et al.*, 1998; 2002; Visconti, 2009). Sperm maintained in seminal plasma are unable to capacitate due to the presence of de-capacitating factors (de Lamirande *et al.*, 1997; Luconi *et al.*, 2000; Fraser, 2010). The first fraction of the ejaculate contains the majority of the spermatozoa which quickly swim out and penetrate the cervical mucus (Katz *et al.*, 1978a). Human semen coagulates immediately following ejaculation, although the exact physiological role remains unclear (Burkman, 1995; Mortimer, 1995).

## 1.2 Oogenesis

During embryogenesis, oogonia develop from the primordial germ cells and undergo a limited number of mitotic divisions. Many of these primary oocytes undergo degeneration or follicular atresia. The primary oocytes (2N) that continue to develop are enclosed in a primary follicle and arrest at meiotic prophase1.

At birth the eutherian primary oocyte is surrounded by the zona pellucida (ZP) glycoproteins and enveloped by a follicle consisting of a single layer of epithelial cells and a less organised layer of mesenchymal thecal cells. With the onset of puberty and stimulated by hormones a number of oocytes periodically mature and complete meiosis 1. The cytoplasm of the primary oocyte divides asymmetrically so that the one of the daughter cells or secondary oocyte (2N) retains most of the cytoplasm and the other cell is a nonviable small polar body (2N). Secondary oocyte maturation proceeds to metaphase 11 and arrests until fertilisation. The follicle undergoes folliculogenesis until it forms a mature pre-ovulatory Graafian follicle. The Graafian follicle consists of several layers of concentric cumulus cells, a fluid filled antrum and the secondary oocyte surrounded by the corona radiata granulosa cells. At ovulation the arrested secondary oocyte is released from the ovary surrounded by ZP and the cumulus oophorus. Upon fertilisation the oocyte is stimulated to complete meiosis 11 whereby the secondary oocyte divides asymmetrically to produce an ovum (1N) and another polar body (1N).

The zona pellucida (ZP) is a thick, translucent extra-cellular sulphated glycoprotein matrix (Wassarman, 1999; Wassarman *et al.*, 2001; 2004). This oocyte specific structure is secreted during folliculogenesis and comprises 3 or 4 ZP glycoproteins which interact via non-covalent bonds (Greve and Wassarman, 1985; Wassarman *et al.*, 2004). Due to a paucity of human zona pellucida most ZP research involves murine models. Mouse zona pellucida is composed of three glycoproteins (ZP1, ZP2 and ZP3). The ZP1 glycoprotein acts as a linker molecule between ZP filaments and provides the structural integrity of the ZP matrix (Green, 1997). The

human oocyte expresses four ZP genes (ZP1, ZP2, ZP3 and ZP4 or ZPB, ZP4 is a pseudogene in mice) (Lefièvre *et al.*, 2004; Conner *et al.*, 2005; Gupta *et al.*, 2009). The role of mammalian ZP is to ensure species-specific sperm-oocyte binding, prevent polyspermy and protection of the embryo until blastocyst implantation in the uterus (Flesch and Gadella, 2000; Wassarman *et al.*, 2001; 2004).

The cumulus oophorus surrounds the ovum and consists of an inner layer (corona radiata) and outer layers of follicular granulosa cells dispersed in a hyaluronic acid matrix. Mammalian spermatozoa must initially penetrate the cumulus matrix in order to bind to ZP proteins. Before ovulation the cumulus oophorus supports oocyte maturation and during ovulation it guides the oocyte into the oviduct (Tanghe *et al.*, 2002). Cumulus cells facilitate sperm capacitation and the acrosome reaction in human, bovine, porcine and hamster spermatozoa (Laufer *et al.*, 1984; Tanghe *et al.*, 2002). The cells of the cumulus secrete steroids including progesterone and synthesise nitric oxide (Tesarik *et al.*, 1988, 1990; Osman *et al.*, 1989; Patrat *et al.*, 2000; Kirkman-Brown *et al.*, 2000, 2002; Sun *et al.*, 2005; Machado-Oliveira *et al.*, 2008).

### **1.3 Sperm transport in the female reproductive tract and fertilisation**

If coitus occurs mid-cycle, a limited number of sperm quickly leave the seminal plasma, and begin the physiological maturation process of capacitation as they penetrate the cervical mucus and travel through the female reproductive tract (Katz *et al.*, 1978a; Burkman, 1995). Passage of spermatozoa through the female tract is regulated to maximise the chance of fertilisation and ensure that sperm with normal morphology and vigorous motility will be the ones that arrive in the Fallopian tube. The cervical mucus serves as a filter to trap damaged (by physical stress during ejaculation) or abnormal spermatozoa (with poor motility and morphology) (Suarez and Pacey, 2006). Since, spermatozoa are allogenic and targeted by the female immune system they have a limited time within the female reproductive tract (Austin, 1957; Menge and

Edwards, 1993). In humans, contractions of the uterine muscle may draw spermatozoa from the cervix into the uterus (Kunz *et al.*, 1996). Spermatozoa may be inseminated days (humans, cattle, pigs and horses) or months (some bat species) prior to oocyte arrival and sperm may be stored or trapped at the uterotubal junction (Suarez, 2002a). Although there is little evidence for a human sperm storage reservoir in the Fallopian tubes, oviduct cells prolong sperm survival *in vitro* (De Mott *et al.*, 1995; Pacey *et al.*, 1995a, 1995b; De Jonge, 2005; Suarez and Pacey, 2006).

## 1.4 Capacitation

Mammalian spermatozoa are unable to fertilize the oocyte immediately after ejaculation but must undergo a maturation process termed capacitation (Austin 1951; Chang, 1951). Physiologically, capacitation occurs as spermatozoa leave the seminal plasma and swim through the female genital tract (Yanagimachi, 1970). Capacitation is a complex series of molecular events that occurs in spermatozoa after epididymal maturation and confers on spermatozoa the ability to fertilise an oocyte (Austin 1951; Chang, 1951; Burkman, 1995; Ho and Suarez, 2001a; Visconti *et al.*, 2002). Capacitation can therefore be described as a time dependent activation process where sperm must reside in the female genital tract or a defined culture medium for a period of time (Visconti *et al.*, 1998; Visconti and Kopf, 1998; Flesch and Gadella, 2000; Baldi *et al.*, 2000, 2002; Gadella and Visconti, 2006). Capacitated spermatozoa have the ability to exhibit hyperactivated motility (section 1.13) and undergo the ZP-induced acrosome reaction (section 1.5.1) (Yanagimachi and Usui, 1974; Suarez and Osman, 1987; Cross *et al.*, 1988; Suarez, 2002b; 2008a; Schuffner *et al.*, 2002).

The molecular mechanisms involved in capacitation are still under investigation. Capacitation includes reorganisation of the plasma membrane, increase in protein tyrosine phosphorylation (section 1.9), hyperpolarisation of the plasma membrane potential ( $E_m$ ) (section 1.7) and

increase in intracellular pH ( $\text{pH}_i$ ) (section 1.8) and  $\text{Ca}^{2+}$  ( $[\text{Ca}^{2+}]_i$ ) (section 1.6) (Parrish *et al.*, 1989; Burks *et al.*, 1995; Zeng *et al.*, 1995, 1996; Darszon *et al.*, 2001; Visconti *et al.*, 2002; Hernandez-Gonzalez *et al.*, 2006, 2007). Capacitation may be induced *in vitro* by removal of sperm from the seminal plasma followed by incubation in defined culture media containing calcium, serum albumin (to serve as a cholesterol acceptor) and bicarbonate (activation of bicarbonate sensitive soluble adenylyl cyclase (sAC)(section 1.9)) (Wuttke *et al.*, 2001; Chen *et al.*, 2000; Gadella and Visconti, 2006).

Sperm hyperactivation is critical for *in vivo* fertilisation, enabling sperm to detach from the oviduct epithelium and facilitating penetration of the outer vestments of the oocyte (section 1.3) (Morales *et al.*, 1988; Suarez, 2008b; Ho *et al.*, 2009). The acrosome reaction induced by a physiological stimulus (ZP or progesterone) is used as a marker for the completion of capacitation as only capacitated sperm can acrosome react (Cummins and Yanagimachi, 1986; Morales and Llanos, 1996; Jaiswal *et al.*, 1998) .

## 1.5 The acrosome reaction

The acrosome, is a Golgi derived membrane bound cap like secretory vesicle (Curry and Watson, 1995; Moreno *et al.*, 2000), which comprises 40-70% of the anterior head volume (WHO, 1999) containing various hydrolytic enzymes including hyaluronidase, protease, phosphatase, neuraminidase and inactive zymogens. The function of the acrosome is to facilitate passage of the sperm through the outer vestments of the oocyte. The acrosome reaction (AR) is a  $\text{Ca}^{2+}$  dependent secretory event characterised by multiple fusions of the plasma membrane. The plasma membrane of the anterior sperm head fuses with the outer acrosomal membrane (Baibakov *et al.*, 2007) to produce numerous hybrid membrane vesicles and expose new membrane domains, both of which are essential for fertilisation to proceed. Dispersion of the acrosomal contents dissolves the ZP matrix and the inner acrosomal membrane forms a continuous membrane hairpin like structure with the plasma membrane

(figure 1.3) (Flesch and Gadella, 2000). The acrosome reacted spermatozoa enter the perivitelline space to initiate secondary binding, including Izumo sperm protein binding with CD9 on the oolemma (figure 1.3) (Miyado *et al.*, 2000; 2008). Following membrane fusion the sperm borne oocyte activating factors (including PLC $\zeta$ ) are released to trigger calcium oscillations and the resumption of meiosis in the oocyte (Swann and Lai, 2002; Swann *et al.*, 2006; Swann and Yu, 2008). Izumo null mice sperm maintain the ability to penetrate the ZP but accumulate within the perivitelline space and fail to bind with the oocyte (Ikawa *et al.*, 2008, 2010; Ellerman *et al.*, 2009). Oocyte re-activation releases the cortical granules (specialised secretory vesicles just under the oolemma) to alter the structure of the ZP and prevent polyspermy (Bleil *et al.*, 1981). In mouse the physiological inducer of the acrosome reaction *in vivo* is the ZP3 glycoprotein (Bleil and Wassarman, 1980a, 1980b, 1983; Bailey and Storey, 1994; Arnoult *et al.*, 1996a, 1996b). Both ZP3 and ZP4 are required to induce the acrosome reaction in capacitated human spermatozoa (Chakravarty *et al.*, 2008; Gupta *et al.*, 2009). Progesterone synthesised by the cumulus cells surrounding the oocyte may have a priming effect on sperm AR (Morales and Llanos, 1996; Schuffner *et al.*, 2002).

### **1.5.1 Zona Pellucida3 induced acrosome reaction**

A plethora of molecules have been investigated in sperm-oocyte interactions but the identity of the sperm ZP3 receptor(s) remains unclear (table 1.1). Given the number of candidates it is possible that a number of structurally/functionally distinct receptors exist (Shur *et al.*, 2006; Correia *et al.*, 2007; Shur, 2008; José *et al.*, 2010). It has been demonstrated that the acrosome reaction occurs in stages whereby components of the acrosomal matrix peripherally re-locate to the surface and interact with the ZP (Buffone *et al.*, 2009). There is evidence of a degree of redundancy in mouse as mutations to many of the putative sperm ZP3 receptor (targeted deletion of secondary zona-binding factor (SED-1),  $\beta$ -1,4-galactosyltransferase (GalTase), zona pellucida binding protein (ZPB1 or ZPB2) or proacrosin do not necessarily interfere with



sperm-ZP binding and AR (Shur, 2008). However, the ability of knockout (KO) animals to remain fertile may reflect spontaneous AR during IVF. The AR is a pre-requisite for fertilisation in mammalian sperm (Nagae *et al.*, 1986; Yanagimachi, 1994a, 1994b) as only reacted sperm can fuse with the egg plasma membrane (Yanagimachi 1994a; Florman *et al.*, 1999).

Table 1.1- Putative mouse sperm ZP3 receptor	
Beta 1,4-galactosyltransferase (GalTase)	KO mice are fertile, ZP3-induced AR defective (Lu and Shur, 1997; Shur <i>et al.</i> , 2006).
Secondary zona-binding factor (SED1)	KO mice fertile (Ensslin and Shur, 2003). SED1 undergoes sulfation (mediated in Golgi by Tyrosylprotein sulfotransferase-2 (TSP-2). <i>Tpst-2</i> KO mice infertile, severe defects in motility (Hoffhines <i>et al.</i> , 2009).
Zonadhesion	KO mice are fertile, normal ZP3 binding. Confers species specificity to ZP adhesion (component of acrosomal matrix) (Shur <i>et al.</i> , 2006).
Angiotensin-Converting Enzyme (ACE)	<i>ACE</i> KO mice are fertile, mild defect in ZP binding, impaired migration into the oviduct (Hagaman <i>et al.</i> , 1998; Inoune <i>et al.</i> , 2010).
Fertilin $\beta$ (ADAM2)	<i>Fertilin <math>\beta</math></i> KO fertile, decreased sperm-oocyte fusion, defective ZP binding, impaired migration into oviduct (Primakoff and Myles, 2000; 2002; Kim <i>et al.</i> , 2006). Calmegin (testis-specific chaperone protein) KO mice reduced fertility due to loss of Fertilin $\alpha\beta$ and ZP binding (Ikawa <i>et al.</i> , 1997)
Cyritestin (ADAM3)	KO mice were infertile, defective ZP binding, impaired migration into the oviduct (Yamaguchi <i>et al.</i> , 2009). ADAM3 is a pseudogene in humans (Frayne <i>et al.</i> , 1999).
sp56	Potential ZP3 receptor, however sp56 is located within acrosomal matrix. Sp56 relocated to capacitated plasma membrane where may interact with ZP3 (Wassarman, 2009).
Proacrosin/acrosin	KO mice fertile but penetration of ZP delayed compared to wild type, located acrosomal matrix (Buffone <i>et al.</i> , 2009).
PH-20 or SPAM1 (sperm adhesion molecule 1)	KO mice fertile, slow to disperse cumulus cells (Baba <i>et al.</i> , 2002).
Zona Pellucida Binding Protein 1(sp38) Zona Pellucida Binding Protein2	Components of acrosomal matrix. ZPBP1 KO mice are sterile, ZPBP2 KO mice are subfertile (small defects in sperm) (Lin <i>et al.</i> , 2007)
Glycine receptor/ Cl <sup>-</sup> channel (GLR)	Mice with mutations in GLR $\alpha$ or GLR $\beta$ defective ZP3 or glycine induced AR (Sato <i>et al.</i> , 2000).

**Table 1.1** Summary of putative sperm ZP3 receptors identified in mouse (including the effects of mutations on male fertility and sperm motility).

Sperm binding with ZP3 triggers various responses required to produce a sustained calcium influx which drive the acrosome reaction. ZP3 induced signal transduction includes activation of a pertussis toxin-sensitive  $G_i$ -coupled receptor resulting in cytoplasmic alkalinisation (Florman *et al.*, 1989; Ward *et al.*, 1994; Arnoult *et al.*, 1996b, 1998). Sperm-ZP3 binding activates phospholipase C (PLC). The resulting inositol triphosphate ( $IP_3$ ) dependent mobilisation of stored acrosomal calcium is essential (De Blas *et al.*, 2002; Herrick *et al.*, 2005) and likely to induce store operated  $Ca^{2+}$  influx possibly via canonical Transient Receptor Potential (TRP) channels (Clapham *et al.*, 2005). Jungnickel *et al.*, (2001) reported that TRPC2 co-localised with ZP3 binding sites and application of a TRPC2 antibody prevented the sustained calcium response to ZP3. However, TRPC2 is a pseudogene in humans (Wes *et al.*, 1995; Vannier *et al.*, 1999) and bovine sperm (Wissenbach *et al.*, 1998) and TRPC2 mutant mice remain fertile (Leypold *et al.*, 2002). These results suggest that other channels in the anterior head (including other TRPC channels) are involved in the sustained calcium influx and substitute for TRPC2. In addition ZP3 binding triggers a transient  $Ca^{2+}$  influx, the activation time course and effects of pharmacological antagonists suggest this transient calcium entry is carried by a low voltage calcium channel (possibly Cav3) (Arnoult *et al.*, 1996a; Jimenez-Gonzalez *et al.*, 2006; Florman *et al.*, 2008). However, a recent study provided evidence for an alternative model in which the initial transient  $[Ca^{2+}]_i$  influx in mouse sperm was via CatSper channels (section 1.13.1) located in the flagellum, the signal propagating rapidly ( $\sim 3$  sec at  $37^\circ C$ ) from the principal piece to the head (Xia and Ren, 2009b).

Combined calcium channel opening and depletion of  $Ca^{2+}$  from acrosomal stores results in elevation of  $[Ca^{2+}]_i$  to drive exocytosis of the acrosomal contents (Florman *et al.*, 1989; Florman, 1994).

The fusion proteins SNARE (soluble N-ethylmaleimide-sensitive attachment protein receptors), which are localised to the outer acrosomal membrane of mammalian and sea urchin sperm (Schulz *et al.*, 1997; Michaut *et al.*, 2000; Hutt *et al.*, 2002; Tomes *et al.*, 2002) couple calcium

influx with exocytosis (Evans and Florman, 2002). Relatively high  $[Ca^{2+}]_i$  activates actin severing proteins such as gelsolin, inducing actin filament depolymerisation between the outer acrosomal membrane and the overlaying plasma membrane (Cabello-Agueros *et al.*, 2003). The apical plasma membrane of the sperm head fuses with the underlying outer acrosomal membrane at multiple sites, forming mixed vesicles that disperse and the acrosomal contents are released (figure 1.3) (Breitbart, 2003).

Other molecular components of the acrosome reaction include calcium dependent Phospholipase A<sub>2</sub> (PLA<sub>2</sub>). Hydrolysis of phospholipids in the acrosome reaction generates free fatty acids (arachidonic acid (AA)) and formation of lysophosphatidylcholine, metabolites involved in membrane fusion and activation of Protein Kinase C (PKC) (Yuan *et al.*, 2003; Abou-haila and Tulsiani, 2009). PKC activators and inhibitors modulate the AR in sperm cells (De Jonge *et al.*, 1991; Roldan and Harrison, 1993).

**Figure 1.3**

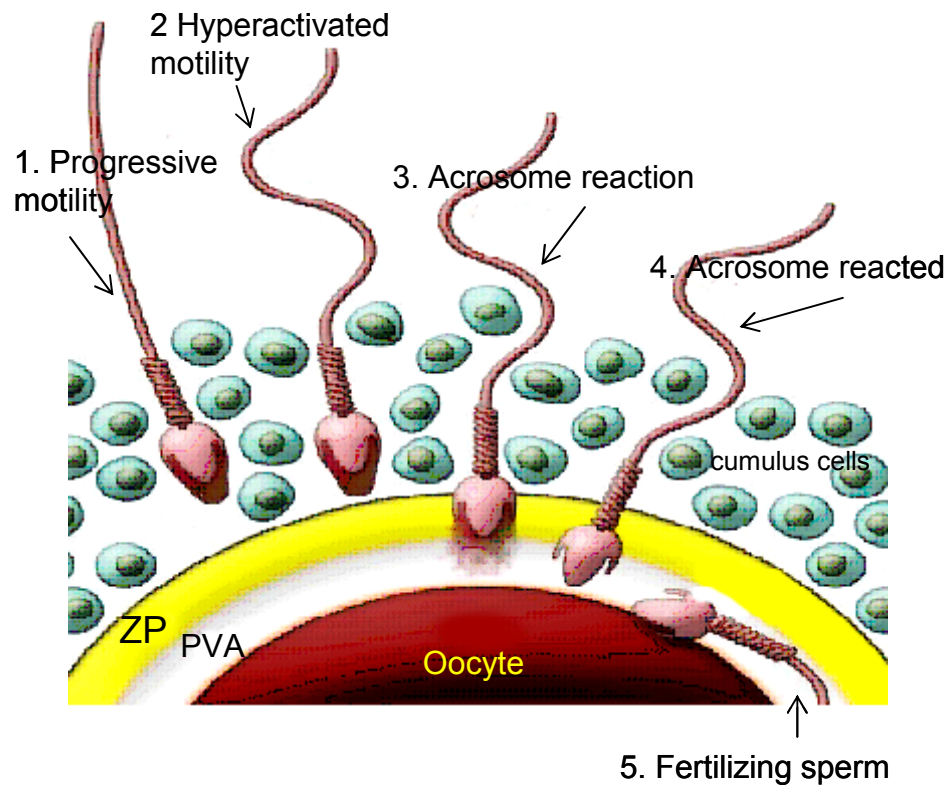


**Figure 1.3** Mechanism of sperm-egg interaction. As spermatozoa move through the female reproductive tract they undergo a maturation process termed capacitation. As capacitation progresses, spermatozoa alter motility from progressive motility (1) to the relatively non-progressive hyperactivated motility (2) enabling cells to push through the cumulus cells surrounding the oocyte. (3) Sperm undergo the zona pellucida induced acrosome reaction and (4) release of the acrosomal contents enables the sperm cell to enter the perivitelline space. (5) The equatorial segment carries receptors involved in secondary sperm-oolemma binding and fusion with the oolemma (adapted from Ikawa *et al.*, 2010)

### 1.5.2 Progesterone induced acrosome reaction

Progesterone is synthesised by the cumulus cells and present in micromolar concentrations surrounding the oocyte (Osman *et al.*, 1989; Thomas and Meizel, 1989). Due to the paucity of human ZP, the dose-dependent progesterone induced acrosome reaction has been extensively studied in human sperm (Blackmore *et al.*, 1990; Baldi *et al.*, 1991; Foresta *et al.*, 1993; Plant *et al.*, 1995; Aitken *et al.*, 1996; Yanagimachi, 1994b; Kirkman-Brown *et al.*, 2000; Harper *et al.*, 2003, 2006, 2008). Progesterone binds to a cell surface receptor (Meizel and Turner, 1991), although the identity of the receptor remains unclear (table 1.2) and may consist of more than one candidate receptor forming a complex progesterone binding molecule (Correia *et al.*, 2007). It has been shown that progesterone and follicular fluid act in synergy with ZP3 to induce the acrosome reaction in mouse sperm (Roldan *et al.*, 1994; Schuffner *et al.*, 2002).

In human spermatozoa, progesterone effects are not associated with G<sub>i</sub>-protein activation (Tesarik *et al.*, 1993; Abou-haila and Tulsiani, 2009). Capacitated human spermatozoa respond to progesterone *in vitro* with a rapid influx of calcium due to receptor operated mechanism and activation of a non-specific calcium ion channel (Meizel *et al.*, 1997; Blackmore and Eisoldt, 1999). A role for voltage operated calcium channels (VOCC, section 1.6.1) in this effect is unclear (Blackmore and Eisoldt, 1999; Garcia and Meizel, 1999). As with mouse ZP3 induced AR, the initial transient influx is followed by a slower, more sustained increase in intracellular calcium possibly triggered by store mobilisation and capacitative calcium entry (CCE, section 1.6.4) (Thomas and Meizel, 1989; Bedu-Addo *et al.*, 2007). Progesterone also stimulates PLA<sub>2</sub> in murine acrosomal reaction (Pietrobon *et al.*, 2005). Fukami *et al.*, (2003) demonstrated that the initial  $[Ca^{2+}]_i$  response initiated in the acrosome in mice treated with ZP3 whereas the progesterone induced calcium signal initiated in the neck/midpiece region.

Furthermore, human spermatozoa undergo the acrosome reaction in response to low dose progesterone *in vitro* (Harper *et al.*, 2004). Should this happen *in vivo* as the sperm cell

approaches the cumulus-oocyte complex these prematurely reacted cells would lose their ability to fertilise (Harper and Publicover, 2005). Premature acrosome reaction may serve as a quality control function potentially removing poorer quality cells (Harper and Publicover, 2005).

Table 1.2- Putative sperm progesterone receptor	
Truncated classical progesterone receptor	hmPR1/PGRMC1 and hmPR2/PGRMC2 immunolocalised PGRMC1 to the inner plasma membrane of permeabilised porcine spermatozoa (Losel <i>et al.</i> , 2004, 2005). Progesterone may diffuse through the membrane to bind on the inner plasma membrane.
G-coupled membrane progesterone receptors	Novel G-coupled PR identified, cloned and characterised in humans and other vertebrates (Zhu <i>et al.</i> , 2003). However, Krietsch <i>et al.</i> (2006) found that no progesterone binding activity or calcium mobilisation when receptors expressed in mammalian cell systems.
$\gamma$ -aminobutyric acid (GABA <sub>A</sub> )-receptor Cl <sup>-</sup> channel	Inhibition of Cl <sup>-</sup> efflux by channels blockers or incubation in Cl <sup>-</sup> free media reduces the progesterone induced AR rates in murine, porcine and human spermatozoa (Roldan <i>et al.</i> , 1994; Shi and Roldan, 1995; Wistrom and Meizel, 1993; Calogero <i>et al.</i> , 1999). However, others report that inhibition with GABA <sub>A</sub> receptor blocker (bicuculline) did not affect the progesterone induced calcium influx or AR (Baldi <i>et al.</i> , 1991).

**Table 1.2** Summary of putative sperm progesterone receptors identified in mammalian sperm.

## 1.6 The sperm calcium signalling ‘toolkit’

Spermatozoa rely on post translational modifications of existing proteins regulated by second messengers including cyclic adenosine 3',5'-monophosphate (cAMP), nitric oxide (NO) and  $\text{Ca}^{2+}$  (San Agustin and Witman, 1994; Jimenez-Gonzalez *et al.*, 2006). Calcium functions as a ubiquitous second messenger and fluctuations in intracellular  $\text{Ca}^{2+}$  concentration ( $[\text{Ca}^{2+}]_i$ ) mediate rapid transmission of information from extracellular signals to internal response systems (Berridge, 1997; Breitbart, 2003; Bedu-Addo *et al.*, 2008). Mature spermatozoa are ‘stripped down’ cells lacking an endoplasmic reticulum, have minimal cytoplasm with a highly condensed nucleus and consequently appears to have a much simplified calcium signalling toolkit (figure 1.4) in comparison to somatic cells (Publicover *et al.*, 2007; Bedu-Addo *et al.*, 2008; Barratt *et al.*, 2009). Numerous studies have established that changes in  $\text{Ca}^{2+}$ -signalling regulate or contribute to the regulation of many different aspects of mammalian sperm function (Kirkman-Brown *et al.*, 2002; Ho and Suarez, 2003; Jimenez-Gonzalez *et al.*, 2006; Suarez *et al.*, 2007; Publicover *et al.*, 2007). Spermatozoa generate discrete, spatiotemporal  $\text{Ca}^{2+}$  signals to selectively regulate specific activities in response to extracellular cues (e.g. ZP induced acrosome reaction, chemotaxis in response to low dose progesterone) (Publicover *et al.*, 2007; Machado-Oliveira *et al.*, 2008; Teves *et al.*, 2006, 2009).  $[\text{Ca}^{2+}]_i$  has been shown to increase during capacitation, hyperactivation and the acrosome reaction in several mammalian species including human (Baldi *et al.*, 1991; Yanagimachi, 1994a; Garcia and Meizel, 1999). Impairment of calcium signalling in sperm is associated with male sub-fertility (Baldi *et al.*, 1999, Espino *et al.*, 2009). The application of standard cell electrophysiological techniques is technically demanding in spermatozoa therefore identification and characterisation of the sperm calcium ‘toolkit’ is complex (figure 1.4).

**Figure 1.4**

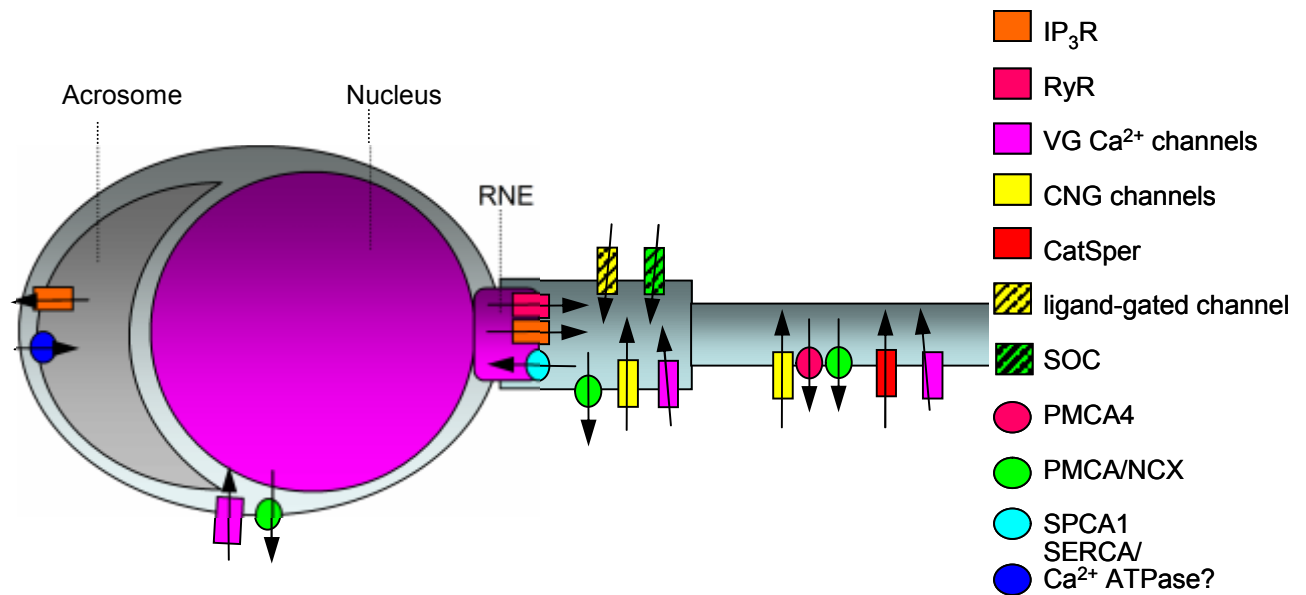


**Figure 1.4** Summary of sperm cell [ $\text{Ca}^{2+}$ ]<sub>i</sub> signalling toolkit (refer to text for details) (adapted from Publicover *et al.*, 2008; Bedu-Addo *et al.*, 2008)

### 1.6.1 Voltage Gated Calcium Channels and CatSper Channels

Voltage gated calcium channels ( $\text{Ca}_v$ , refer to appendix I and table 7.0 for further details) are multi-subunit transmembrane channels which open in response to membrane depolarisation (figure 8.0) (translate membrane potential ( $E_m$ )) (Darszon *et al.*, 2006). Molecular and immunohistochemistry studies show that several types of  $\text{Ca}_v$  are present in sperm (Wennemuth *et al.*, 2000; Jagannathan *et al.*, 2002; Felix, 2005). Park *et al.* (2003) detected transcripts for  $\text{Ca}_v1$  and  $\text{Ca}_v2$  (high voltage activated channels) and  $\text{Ca}_v3$  (low voltage activated channels) in human spermatozoa.  $\text{Ca}_v3.1$  and  $\text{Ca}_v3.2$  have been immunolocalised to the sperm



head and  $\text{Ca}_v3.3$  is limited to the mid-piece region of human sperm (Trevino *et al.*, 2004; Jimenez-Gonzales *et al.*, 2006). High voltage activated ( $\text{Ca}_v1$  and  $\text{Ca}_v2$ ) channels has shown similar localisation in mouse and human. However, electrophysiological studies on mouse and human spermatogenic cells generate only  $\text{Ca}_v3$  (transient) currents (Trevino *et al.*, 2004). Faire-Zamora and Gonzalez-Martinez (2004) demonstrated that intracellular alkalinisation stimulated a depolarisation-evoked calcium influx in human sperm and this effect was enhanced in capacitated cells (Neri-Vidaurre Pdel *et al.*, 2006). However, disruption of the genes that encode  $\text{Ca}_v3.1$  and  $\text{Ca}_v3.2$  channels did not affect fertility in mice (Escoffier *et al.*, 2007; Florman *et al.*, 2008). Similar results were obtained with  $\text{Ca}_v2.2$  and  $\text{Ca}_v2.3$  deficient mice (Sakata *et al.*, 2002). Recently, Xia and Ren (2009b) detected  $\text{Ca}_v3$  currents in mouse spermatocytes and spermatids but the current gradually decreased as sperm became more mature. No current was detectable in mouse epididymal sperm.

CatSper (refer to Appendix I, table 8.0) are a novel family of  $\text{Ca}^{2+}$  permeable cation channels, resembling voltage-gated  $\text{Ca}^{2+}$  channels, which are expressed exclusively in sperm. Recent studies have shown that CatSper channels are important in hyperactivation and the acrosome reaction in mouse models (Xia and Ren, 2009b). The CatSper channels (formed from putative 6TM subunits), are voltage gated,  $\text{Ca}^{2+}$  permeant channels that mediate  $I_{\text{CatSper}}$  (Quill *et al.*, 2001; Clapham and Garbers, 2005). CatSper channel subunits are structurally most closely related to individual domains of  $\text{Ca}_v$  channels (Ren *et al.*, 2001). The CatSper proteins are located on the plasma membrane of the principal piece the largest segment of the flagellum (Ren *et al.*, 2001; Quill *et al.*, 2001, 2003; Xia *et al.*, 2007). Four different proteins have been identified, CatSper1-4 (Ren *et al.*, 2001; Quill *et al.*, 2001, 2003; Lobje *et al.*, 2003; Jin *et al.*, 2007).  $I_{\text{CatSper}}$  is constitutively active, weakly facilitated by membrane depolarisation but strongly augmented by cytoplasmic alkalinisation (Navarro *et al.*, 2007). Alkalinisation shifts the voltage dependence of activation towards negative potentials ( $V_{1/2}$  @ pH6.0 = +87mV;  $V_{1/2}$  @ pH7.5 = +11mV). CatSper channels may regulate basal  $\text{Ca}^{2+}$  levels and motility since

elimination of any of the CatSper proteins gradually decreases sperm motility (Quill *et al.*, 2003; Qi *et al.*, 2007). Calcium entry through CatSper channels is induced by alkalinisation leading to increased flagellar bending. Targeted disruption of *CatSper1*, 2, 3 or 4 genes results in an identical phenotype in which spermatozoa fail to exhibit hyperactivation. Such disruptions are associated with a deficit in alkalinisation and depolarisation-evoked  $\text{Ca}^{2+}$  entry into sperm (Carlson *et al.*, 2003, 2005; Navarro *et al.*, 2007; Qi *et al.*, 2007). The driving force for  $\text{Ca}^{2+}$  entry is principally determined by the weak outwardly rectifying  $\text{K}^+$  channel ( $I_{\text{KSper}}$ ) that, like CatSper, is activated by intracellular alkalinisation (Navarro *et al.*, 2007). The  $\text{HCO}_3^-$  anion accelerates flagellar beat in CatSper1 and 2 null sperm indicating that downstream cAMP mediated responses are not affected by the CatSper proteins loss of function phenotype. In several experiments it has been shown that the application of extracellular cell permeant cyclic nucleotide analogues induces a rapid increase in  $[\text{Ca}^{2+}]_i$  (Kobori *et al.*, 2000; Ren *et al.*, 2001; Xia *et al.*, 2007). The direct mechanism by which cyclic nucleotides activates  $\text{Ca}^{2+}$  influx is not known but this response is absent in CatSper1 null mice (Carlson *et al.*, 2003). Patch clamp experiments suggests that cyclic nucleotides do not directly open CatSper channels (Ren *et al.*, 2001; Kirichok *et al.*, 2006) it is probable that  $\text{HCO}_3^-/\text{sAC}/\text{cAMP}/\text{PKA}$  (section 1.9) pathway facilitates phosphorylation of CatSper channel on one or more subunits (Carlson *et al.*, 2003, 2005, 2007; Xie *et al.*, 2006; Babcock, 2007; Qi *et al.*, 2007). Recently Ho *et al.*, (2009) demonstrated that CatSper null spermatozoa are unable to detach from oviductal epithelium. Mutations in CatSper protein result in human infertility (Avenarius *et al.*, 2009)

### 1.6.2 Cyclic nucleotide-gated channels

Cyclic nucleotide signalling (cyclic adenosine 3',5'-monophosphate (cAMP) or cyclic guanosine 3',5'-monophosphate (cGMP)) is essential in mammalian sperm function (Leclerc *et al.*, 1996; Lefièvre *et al.*, 2000) and a cyclic-nucleotide gated (CNG),  $\text{Ca}^{2+}$  permeable channel

similar to those found in olfactory neurons has been described in human sperm (refer to Appendix I) (Parmentier *et al.*, 1992; Kaupp, 1995; Wiesner *et al.*, 1998). It has been suggested that the human olfactory receptor (hOR17-4) expressed in sperm are involved in chemotaxis by regulation of cyclic-nucleotide mediated  $\text{Ca}^{2+}$  influx and motility (Spehr *et al.*, 2003, 2004).

### 1.6.3 Store Operated Channels

In both excitable and non-excitable cells, mobilisation of stored intracellular calcium (leading to a fall in the  $[\text{Ca}^{2+}]_i$  in the storage organelle), triggers a  $\text{Ca}^{2+}$  influx across the plasma membrane via store-operated channels (SOC) or calcium release activated  $\text{Ca}^{2+}$  channels (CRAC) by a process termed capacitative  $\text{Ca}^{2+}$  entry (CCE) (Putney, 1990; Parekh and Putney, 2005). Pharmacological mobilisation of stored calcium activates calcium influx in non-capacitated human spermatozoa (Blackmore, 1993). This influx of calcium results in the sustained increase of  $[\text{Ca}^{2+}]_i$  necessary to drive the acrosome reaction (O'Toole *et al.*, 2000; Gonzalez-Martinez *et al.*, 2001; Hirohashi and Vacquier, 2003; Jimenez-Gonzalez *et al.*, 2006; Conner *et al.*, 2007). The molecular components of the highly selective  $I_{\text{CRAC}}$  current have recently been identified including proteins of the STIM (stromal interaction molecule 1) (Roos *et al.*, 2005; Zhang *et al.*, 2005; Lewis, 2007; Luik *et al.*, 2008) and Orai (Feske *et al.*, 2006; Prakriya *et al.*, 2006; Yuan *et al.*, 2007; Várnai *et al.*, 2009) families. STIM1 is the putative sensor for detection of store filling status and Orai1 forms the membrane  $\text{Ca}^{2+}$ -permeable channel (Strange *et al.*, 2007). Upon depletion of the endoplasmic reticulum (ER)  $\text{Ca}^{2+}$  store, STIM1 and Orai protein aggregate into a macromolecular complex. Both STIM1 and Orai1 are expressed in human spermatozoa and immunolocalise mainly to the redundant nuclear envelope (RNE, section 1.6.4) in the neck/midpiece region (Lefièvre, in prep; Costello *et al.*, 2009). These proteins may also combine/interact with members of the canonical transient receptor potential (TRPCs) (refer to Appendix I and table 9.0) to form a SOC macromolecular

complex to facilitate  $\text{Ca}^{2+}$  influx (Abramowitz and Birnbaumer, 2009; Vaca, 2010). Various TRP(s) (refer to appendix 1, table 9.0) have been identified on the head and flagellum of human sperm (Trevino *et al.*, 2001; Castellano *et al.*, 2003). TRPC1, 3, 4 and 6 have been localised to the flagellum in human sperm and SKF96365, a blocker of TRPC channels significantly reduced motility (Castellano *et al.*, 2003). Recently TRPM8, a thermo sensitive channel has been identified and immunolocalised to the tail and head in human sperm (De Blas *et al.*, 2009). TRPM8 agonist (methanol and temperature) induce an increase in  $[\text{Ca}^{2+}]_i$  and AR in a dose dependent manner but did not modify motility.

#### **1.6.4 Calcium stores in sperm**

In many cell types at rest the endoplasmic reticulum (ER)  $\text{Ca}^{2+}$  store is in a dynamic steady-state with cytoplasmic  $\text{Ca}^{2+}$  (Wennemuth *et al.*, 2003b). Although mature spermatozoa lack an ER, there is evidence for the presence of at least three discrete intracellular  $\text{Ca}^{2+}$  stores in mammalian sperm. The acrosome contains  $\text{IP}_3$ -gated calcium channels, a  $\text{Ca}^{2+}$ -ATPase (sacroplasmic-endoplasmic  $\text{Ca}^{2+}$ -ATPases (SERCAs) and calreticulin (a low affinity, high capacity calcium buffering protein) and is thought to serve as an intracellular  $\text{Ca}^{2+}$  store (Walensky and Snyder, 1995; Kuroda *et al.*, 1999; Minelli *et al.*, 2000; Rossato *et al.*, 2001; De Blas *et al.*, 2002; Publicover *et al.*, 2007; Lawson *et al.*, 2007).

A second  $\text{Ca}^{2+}$  store (or stores) is present in the sperm neck/midpiece region. The identity of the membranous compartment in which  $\text{Ca}^{2+}$  is stored is not yet clear, but it appears to involve the redundant nuclear envelope (RNE) and/or calreticulin-containing vesicles in the cytoplasmic droplet (Ho and Suarez, 2001a, 2001b, 2003; Naaby-Hansen *et al.*, 2001; Harper *et al.*, 2004, 2005). Both  $\text{IP}_3\text{R}$  and ryanodine receptors (RyRs) have been localised to this region and are sensitive to local  $\text{Ca}^{2+}$  concentration, increased cytosolic  $\text{Ca}^{2+}$  induces further release from the store, a process known as  $\text{Ca}^{2+}$ -induced  $\text{Ca}^{2+}$  release (CICR). The calcium sensitivity of these channels decreases as cytosolic  $\text{Ca}^{2+}$  increases (i.e. the channels begin to close again).

RyR receptors are large proteins organised into a complicated tetrameric arrangement with only ~20% of the protein associated with channel activity. The remainder form a prominent structure that extends into the cytoplasm and possesses binding sites for a number of physiological modulators including calcium. IP<sub>3</sub>R are also tetramers, each of the component subunits possess 6 transmembrane segments. Both the N- and C-termini lie within the cytosol and possess a number of modulatory sites. IP<sub>3</sub> binds to the IP<sub>3</sub>R (located on the N-terminal) and increases sensitivity of the channel to the local Ca<sup>2+</sup> concentration. IP<sub>3</sub> is generated as a result of PLC induced hydrolysis of inositol 4', 5' bisphosphate (Fukami *et al.*, 2001; 2003). The IP<sub>3</sub>-sensitive calcium channel has been well studied in numerous cell types, including sperm (Jimenez-Gonzalez *et al.*, 2006). Isoform-specific IP<sub>3</sub>R antibody labelling has been used on various mammalian spermatozoa including human where IP<sub>3</sub>R1 antibody predominantly labelled the acrosomal area and IP<sub>3</sub>R3 antibody labelled the posterior head region, mid-piece and part of the flagellum (Kuroda *et al.*, 1999; Minelli *et al.*, 2000; Naaby-Hansen *et al.*, 2001; Ho and Suarez, 2003). It is possible that the Ca<sup>2+</sup> sensitivity of the IP<sub>3</sub>R could be responsible for Ca<sup>2+</sup> induced Ca<sup>2+</sup> release (Taylor *et al.*, 2009) with CatSper dependent Ca<sup>2+</sup> influx increasing IP<sub>3</sub> production. Treatment with the Ca<sup>2+</sup> ionophore (A23187) activates PLC generating diacylglycerol (DAG) and IP<sub>3</sub> in a variety of mammalian sperm (Roldan and Fraser, 1998; Felix, 2005). Furthermore, cAMP can stimulate PLC to generate IP<sub>3</sub> (Schmidt *et al.*, 2001), with various subtypes identified in the head and midpiece of sperm-PLC $\zeta$ , PLC $\delta$ 4 and PLC $\beta$  (Walensky and Snyder, 1995; Choi *et al.*, 2001; Swann *et al.*, 2004; Irino *et al.*, 2005).

In addition to IP<sub>3</sub>-sensitive Ca<sup>2+</sup> channels, there is evidence for the presence of a functional ryanodine (RyRs; so-called because of their sensitivity to the plant alkaloid ryanodine) receptor in sperm cells (Giannini *et al.*, 1995; Minelli *et al.*, 2000; Harper *et al.*, 2004). RyR1 and RyR3 are expressed in mouse spermatocytes and spermatids (Giannini *et al.*, 1995; Trevino *et al.*, 1998; Chiarella *et al.*, 2004), RyR3 immunolocalised to the acrosomal area in mature

spermatozoa (Trevino *et al.*, 1998). Immunolocalisation of RyR in human spermatozoa was focussed at the rear of the head with a lower signal from the acrosomal region (Harper *et al.*, 2004). Pharmacological modulators of RyR have been shown to significantly modify progesterone induced  $[Ca^{2+}]_i$  oscillations (Harper *et al.*, 2004; Machado-Oliveira *et al.*, 2008). In human spermatozoa, the mitochondria are restricted to the midpiece. Mitochondria can act as  $Ca^{2+}$  buffers, accumulating  $Ca^{2+}$  from the cytosol (Gunter *et al.*, 2000; Nicholls and Chalmers, 2004). The mitochondrial  $Ca^{2+}$  uniporter (MCU) brings  $Ca^{2+}$  into the energised mitochondria only when  $Ca^{2+}$  is elevated to  $0.5\mu M$  (Gunter *et al.*, 2000). Treatment with uncouplers has little effect on  $[Ca^{2+}]_i$  signals in human spermatozoa (Wennemuth *et al.*, 2003b; Ho and Suarez, 2003; Harper *et al.*, 2004; Machado-Oliveira *et al.*, 2008).

### 1.6.5 Calcium clearance mechanisms in sperm

$Ca^{2+}$  is a highly effective signalling agent, however, excessive intracellular  $Ca^{2+}$  is cytotoxic and  $Ca^{2+}$  clearance mechanisms are essential to return the cell to resting levels after  $Ca^{2+}$  signalling events have occurred. Sperm  $Ca^{2+}$  clearance mechanisms include the plasma membrane  $Ca^{2+}$ -ATPases (PMCA) and the  $Na^{+}$ - $Ca^{2+}$  exchangers (NCXs), which extrude calcium from the cell (Breitbart *et al.*, 1983; Michelangeli *et al.*, 2005). Plasma membrane  $Ca^{2+}$  ATPase4 is expressed at high levels in the flagellum and is essential to sperm motility and hyperactivation (Okunade *et al.*, 2004; Schuh *et al.*, 2004). A plasma membrane  $Ca^{2+}$  ATPase is also expressed in sea urchin sperm localised to the sperm head. Pharmacological inhibition of this pump disrupts control of  $[Ca^{2+}]_i$  in the sperm and resulting in loss of flagellar activity (Gunaratne and Vacquier, 2006).  $Na^{+}$ - $Ca^{2+}$  exchangers are also present in sperm and contribute to  $[Ca^{2+}]_i$  regulation (Wennemuth *et al.*, 2003b).

There is evidence that the intracellular  $Ca^{2+}$  store pumps (sarcoplasmic-endoplasmic  $Ca^{2+}$ -ATPases (SERCA) and the secretory pathway  $Ca^{2+}$ -ATPase (SPCA)) are involved in calcium

clearance as they sequester calcium to the intracellular calcium stores (Harper *et al.*, 2005; Jimenez-Gonzalez *et al.*, 2006). Analysis of calcium clearance in mouse spermatozoa suggests that both calcium exchangers and calcium pumps are important contributors to intracellular calcium buffering but the relative importance of each is still to be identified (reviewed in Jimenez-Gonzalez *et al.*, 2006; Conner *et al.*, 2007). In sperm, high doses of thapsigargin (inhibits SERCA) does not induce a rapid elevation of  $[Ca^{2+}]_i$  but a gradual release, the effect is irreversible resulting in a loss of motility (Williams and Ford, 2003).

## 1.7 Sperm $E_m$ and $K^+$ channels

Capacitation in mammalian sperm is accompanied by hyperpolarisation of membrane potential ( $E_m$ ) (Espinosa and Darszon, 1995; Zeng *et al.*, 1995, 1996; Arnoult *et al.*, 1999). Hyperpolarisation is observed as an increase in the intracellular negative charge (-30-45mV to -65mV) when compared to the extracellular environment (Arnoult *et al.*, 1996a; 1998, 1999; Espinosa and Darszon, 1995; Muñoz-Garay *et al.*, 2001; Acevedo *et al.*, 2006). Ion channels contribute significantly to  $E_m$ , but electrophysiological characterisation of ion channels is technically demanding in mature sperm cells therefore many studies utilise spermatogenic cells. Capacitation associated elevation of  $pH_i$  may activate  $K^+$  channels permitting  $K^+$  efflux, driving  $E_m$  (-45mV) towards the  $K^+$  equilibrium potential (-90-110mV) and hyperpolarising sperm (-80mV) (Arnoult *et al.*, 1996a; 1999; Espinosa and Darszon, 1995; Muñoz -Garay *et al.*, 2001; Acevedo *et al.*, 2006). In whole cell patch clamp, a constitutively active, weakly outwardly rectifying  $K^+$  current was measured ( $I_{KSper}$ ), localised to the principal piece of mouse sperm flagellum (Navarro *et al.*, 2007). Intracellular alkalinisation strongly potentiates  $I_{KSper}$  and the sperm specific pH sensitive Slo3  $K^+$  channel (identified in mice spermatocytes) (Schreiber *et al.*, 1998) has been proposed as a likely candidate to carry this current (Navarro *et al.*, 2008).  $I_{KSper}$  is not affected by cell permeant cyclic nucleotides (Navarro *et al.*, 2007). Other studies report that Slo3 does not mediate KSper current in mouse since the voltage

dependency of Slo3 current is significantly stronger than KSper (Yang *et al.*, 2009).  $K^+$  currents recorded from *Xenopus* oocytes (expressing Slo3) and mouse sperm were stimulated by increased  $pH_i$  and cAMP (Marinez-Lopez *et al.*, 2009). Slo3 knockout mice are infertile; Slo3 mutant sperm depolarise during capacitation (wild type hyperpolarise during capacitation), lack a pH-sensitive  $K^+$  current and have impaired motility and AR (Santi *et al.*, 2010). In addition, studies indicate the presence of an inwardly rectifying  $pH_i$  sensitive  $K^+$  channel ( $K_{ir}$ ) in mice sperm (Muñoz-Garay *et al.*, 2001).  $K_{ir}$  channels selectively carry larger inward currents at membrane potential ( $E_m$ ) negative to  $E_K$  than outward currents at voltages positive to  $E_K$  even with equal  $[K^+]$  on both sides of the membrane (Nichols and Lopatin, 1997). Uncapacitated sperm cells have a relatively acidic  $pH_i$  which may act as a negative regulator of  $K_{ir}$ , maintaining a depolarised  $E_m$ . Capacitation induced cytoplasmic alkalinisation would enhance the open probability of a small but significant proportion of  $K_{ir}$  channels at potentials more positive than  $E_K$ , leading to  $K^+$  efflux and hyperpolarisation (Muñoz-Garay *et al.*, 2001). The presence of a pH-sensitive  $K_{ATP}$  channels has been shown, blockers of adenosine 5'-triphosphate (ATP) synthesis and channel activators, enhanced whole cell currents in mouse spermatogenic cells. During capacitation ATP content of the cell decreases (Baker and Aitken, 2004) increasing  $K_{ATP}$  channel open time resulting in  $E_m$  hyperpolarisation. Hernandez-Gonzalez *et al.*, 2006 have shown that mouse sperm resting  $E_m$  is  $Na^+$ - dependent and epithelial  $Na^+$  channels participate in the regulation of capacitation in mouse spermatogenic cells. Capacitation associated hyperpolarisation may result from decreased  $Na^+$  permeability. Hernandez-Gonzalez *et al.*, 2006 demonstrated the presence of epithelial  $Na^+$  channels (ENaCs) type currents in mouse sperm. Experiments designed to inhibit ENaC activity (treatment with amiloride) and reduce  $Na^+$  permeability (replacing  $Na^+$  with non-permeant cations) result in  $E_m$  hyperpolarisation.

Furthermore, this group report the involvement of the cystic fibrosis transmembrane conductance regulator (CFTR, a  $Cl^-$  channel) in controlling hyperpolarisation and regulating



the activity of ENaC in human sperm (Hernandez-Gonzalez *et al.*, 2007). Inhibition of CFTR blocks capacitation-associated hyperpolarisation. The CFTR  $\text{Cl}^-$  channel is cAMP/PKA regulated, treatment of noncapacitated sperm with cAMP or IBMX increased  $[\text{Cl}^-]_i$  and significantly diminished ENaC activity (decreased  $\text{Na}^+$  permeability) resulting in  $E_m$  hyperpolarisation in mice sperm. Wertheimer *et al.*, (2008) confirm that in addition to CFTR a  $\text{Na}^+/\text{K}^+/\text{Cl}^-$  co-transporter (NKCC) mediates  $\text{Cl}^-$  transport into the cell. Inward translocation of  $\text{Cl}^-$  is coupled to the activity of the  $\text{Cl}^-/\text{HCO}_3^-$  antiporter (efflux of  $\text{Cl}^-$  and influx of  $\text{HCO}_3^-$ , enhanced cAMP/PKA activity and tyrosine phosphorylation). Demarco *et al.*, (2003) have shown that increased extracellular  $\text{HCO}_3^-$  (that occurs during ejaculation) activates a  $\text{Na}^+/\text{HCO}_3^-$  cotransporter involved in mouse sperm  $E_m$  hyperpolarisation.

In summary, membrane hyperpolarisation associated with capacitation is likely to involve numerous channels and ion fluxes.

## 1.8 Intracellular pH and sperm

Intracellular pH is a critical regulator of sperm motility (Parrish *et al.*, 1989; Zeng *et al.*, 1996; Galantino-Homer *et al.*, 2004). The male reproductive tract renders sperm cytoplasm  $\text{pH}_i$  acidic ( $\text{pH} \sim 6.5$ ), apparently maintaining spermatozoa quiescent prior to ejaculation (Acott and Carr, 1984; Carr and Acott, 1989; Jones and Bavister, 2000; Lishko *et al.*, 2010). Capacitation associated cytoplasmic alkalinisation is essential for normal and hyperactivated motility (Hamamah and Gatti, 1998; Marquez and Suarez, 2007) and the acrosome reaction (Florman *et al.*, 1989; Parrish *et al.*, 1989; Darszon *et al.*, 2006). Proton extrusion from the cytoplasm would increase  $\text{pH}_i$ . Proton transfer may involve a  $\text{Na}^+/\text{H}^+$  exchanger (Garcia and Meizel, 1999; Woo *et al.*, 2002) or a voltage gated proton channel (Hv1) (Lishko *et al.*, 2010)

Lishko *et al.*, (2010) identified a voltage-gated proton channel (Hv1) localised to the principal piece of human sperm flagellum. Hv1 currents were activated by membrane depolarisation, removal of extracellular zinc (a potent Hv1 inhibitor) and an extracellular alkaline environment.

Hv1 allows only the outward transport of protons, resulting in extracellular alkalinisation. Since physiological membrane potential in capacitated sperm cells hyperpolarises to values which should prevent Hv1 channel activity, activity may be regulated by another mechanism (Florman *et al.*, 2010). Lishko *et al.*, (2010) suggest a degree of species specificity in sperm pH regulation; a robust proton current in human sperm but a barely detectable current in mice sperm. The authors conclude that mouse sperm do not have a functional Hv1 channel and that proton extrusion from these cells is mediated by a different mechanism.

Mammalian sperm, including humans have a sperm-specific  $\text{Na}^+/\text{H}^+$  exchanger (sNHE) which plays a role in capacitation (Wang *et al.*, 2003, 2007). The driving force for sNHE activation (proton efflux leading to  $\text{pH}_i$  alkalinisation), would occur as sperm enter the slightly alkaline female tract environment (Wang *et al.*, 2003; Florman *et al.*, 2010). The sNHE plays an important role in maintaining  $\text{pH}_i$ , motility and infertility. The sNHE is present in the principal piece of sperm flagellum. Mutations of the sNHE gene causes complete infertility, sperm immotility was partly rescued by addition of  $\text{NH}_4\text{Cl}$  and completely restored by cell permeant cAMP analogues (Wang *et al.*, 2003; Quill *et al.*, 2006). The soluble adenylyl cyclase (sAC) is mainly responsible for cAMP synthesis in mammalian sperm (Sinclair *et al.*, 2000; Esposito *et al.*, 2004; Fraser *et al.*, 2005; Hess *et al.*, 2005; Xie *et al.*, 2006). sNHE protein contains a voltage sensitive domain and a cyclic nucleotide binding domain and may therefore be sensitive to cAMP and/or membrane potential. cAMP may activate (directly or indirectly) sNHE, which could account for intracellular alkalinisation.

## **1.9 sAC/cAMP/ PKA and motility**

An increase in intracellular pH triggers the activation of sperm flagellum through cAMP-dependent protein kinase A (PKA) (Brokaw, 1987; Lindemann and Goltz, 1988; Scott *et al.*, 2000; Lefièvre *et al.*, 2002; Harayama *et al.*, 2003; Hayashi and Shingyoji, 2009; Goto and Harayama, 2009). Bicarbonate and  $\text{Ca}^{2+}$  ions activate the soluble adenylyl cyclase

(sAC) increasing cAMP synthesis and activation of PKA (Tash and Means, 1982; Visconti *et al.*, 1995; Visconti and Kopf, 1998; Boatman and Robbins, 1991; Buck *et al.*, 1999; Wennemuth *et al.*, 2003a; Marquez and Suarez, 2008) Sperm AC differs molecularly and biochemically from the transmembrane adenylyl cyclase (tmAC), partly because sAC is uniquely sensitive to bicarbonate (Wuttke *et al.*, 2001; Jaiswal and Conti, 2003; Litvin *et al.*, 2003). Motility is defective in sAC null mice sperm and males are sterile but can be rescued with the addition of cell permeant cAMP (Esposito *et al.*, 2004). Targeted mutation of ATP binding pocket of mouse sperm PKAC $\alpha$ 2 catalytic subunit, results in infertility. Mutated sperm lack cAMP, depolarisation induced calcium influx and protein tyrosine phosphorylation (Skalhegg *et al.*, 2002; Nolan *et al.*, 2004). Morgan *et al.*, (2008) engineered a “knockin” mouse that can be switched from expressing wild-type PKAC $\alpha$  to mutated PKAC $\alpha$ . Furthermore, this mutation confers sensitivity to inhibition by 1NM-PP1 (pyrazolo[3,4-*d*]pyrimide, a novel PKA catalytic subunit inhibitor) (Morgan *et al.*, 2008). This group was able to examine the HCO $_3^-$ /sAC/cAMP/ PKA pathway regulated fast and slow capacitation events in mouse sperm (Morgan *et al.*, 2008; Visconti, 2009). When murine sperm are exposed to Ca $^{2+}$  and HCO $_3^-$ , cAMP rises to a maximum within 60 seconds and the increase in PKA-dependent phosphorylation begins after 90 seconds resulting in vigorous flagellar movement (Harrison, 2004; Morgan *et al.*, 2008; Kaneto *et al.*, 2008). Slower sAC/cAMP/ PKA dependent events occur as sperm are capacitated *in vivo* or *in vitro*, resulting in increased tyrosine phosphorylation (Visconti, 2009). Application of HCO $_3^-$  resulted in vigorous flagellar activity in mutated sperm however flagellar beat frequency was quickly lowered in the presence of the inhibitor. Furthermore, continuous incubation with the inhibitor prevented protein tyrosine phosphorylation of late-stage capacitation (Morgan *et al.*, 2008) and loss of motility in the majority of cells. However, acute treatment with inhibitor did not affect the established waveform asymmetry of hyperactivated mutant cells. This agrees with studies that bending of flagellum is Ca $^{2+}$  dependent (Lindemann and Goltz, 1988; Lindemann *et al.*,

1991; Ishijima *et al.*, 2006).

Once activated, PKA phosphorylates various target proteins which initiate several signalling pathways. PKA cannot directly phosphorylate proteins on tyrosine residues which may occur due to the involvement of an intermediate unidentified tyrosine kinase, or inhibition of a phosphotyrosine phosphatase (PTP) or PKA phosphorylation of proteins on serine or threonine residues that prime these proteins for subsequent phosphorylation on tyrosine residues (Breitbart and Spungin, 1997). The majority of tyrosine phosphorylation occurs in the flagellum (Visconti *et al.*, 1995; Carrera *et al.*, 1996; Vijayaraghavan *et al.*, 1997; Si and Okuno, 1999; Naz and Rajesh, 2004; Tomes *et al.*, 2004). Capacitation is associated with increased tyrosine phosphorylation of sperm flagellar proteins and is related to the acquisition of hyperactivated motility. The regulatory subunits of PKA also are important for intracellular localisation of the kinase. Multiple A kinase anchoring proteins (AKAPs) have been localised throughout the sperm and AKAP4 is a major protein of the sperm fibrous sheath. AKAP4 recruits PKA to the fibrous sheath to facilitate phosphorylation of neighbouring proteins and regulate flagellar function (Carrera *et al.*, 1996; Miki *et al.*, 2002; Brown *et al.*, 2003). Targeted disruption of the *Akap4* gene causes defects in sperm flagellum and motility (Miki *et al.*, 2002; Huang *et al.*, 2005). Protein phosphatases (PP) have also been identified in mouse sperm and co-immunoprecipitate with the regulatory subunit of PKA and may be involved in maintaining progressive motility by suppression of PKA activity (Goto and Harayama, 2009) by dephosphorylation of axonemal proteins. Protein phosphatase 1 $\gamma$ 2 is a unique isoform of PP1 which has been detected in the head and flagellar principal piece in mice sperm (Huang *et al.*, 2005; Goto and Harayama, 2009).

## 1.10 Calmodulin -dependent protein kinase and motility

In addition to PKA-dependent phosphorylation, several studies have suggested that  $\text{Ca}^{2+}$ /Calmodulin (CaM)-dependent protein kinase (CaMK) is involved in flagellar motility initiation and regulation (Jones *et al.*, 1980; Tash *et al.*, 1988; Tash, 1989; Tash and Bracho, 1998; Si and Olds-Clarke, 2000; Nomura *et al.*, 2004; Ignatz and Suarez, 2005; Marín-Briggiler *et al.*, 2005; Schlingmann *et al.*, 2007; Suarez, 2008a). CaM has been identified as a component of ciliary and flagellar axonemes and is thought to act as a calcium sensor to mediate motility (Lindemann *et al.*, 1991). CaM kinase (CaMK) has been immunolocalised to the flagellum in human sperm and incubation with CaMK inhibitors reduced motility and sperm ATP content but does not alter patterns of protein tyrosine phosphorylation or induce the acrosome reaction (Marín-Briggiler *et al.*, 2005). A recent study in *Chlamydomonas* demonstrated that calcium controls dynein-driven microtubule sliding through the activation of axonemal CaM and CaMK phosphorylation of the radial spoke proteins (Dymek and Smith, 2007). These changes increase flagellar bending and enhance ATP production.

## 1.11 Motility – the mechanics of movement

The axoneme or axial filament stretches the full length of the flagellum and is the motor apparatus of the sperm tail consisting of a classical 9+2 pattern (2 central microtubules (figure 1.5 (yellow boxed region) surrounded by 9 evenly spaced microtubule doublets (figure 1.5 (red boxed region)) (Curry and Watson, 1995; Porter and Johnson, 1989). Nine radial spokes, each derived from one of the outer microtubular doublet pairs, extend inwards towards the central pair in a helical fashion. Permanently attached to the A tubule of each doublet microtubule are the inner and outer dynein arm. Activation of the ( $\text{Ca}^{2+}$   $\text{Mg}^{2+}$  dependent) dynein ATPase (ATP hydrolysis and phosphorylation of dynein arms (Gibbons and Rowe, 1965) causes the dynein arms to interact with their B tubule of the neighbouring microtubular doublet and produce a

power stroke, causing the microtubules to slide past each other (Satir 1968; Brokaw, 1972, 1987, 1989; Shingyoji *et al.*, 1977, Summers and Gibbons, 1971; Tash and Means, 1983, 1987; Tash, 1989; Ishijima and Hamaguchi, 1993; Ishijima *et al.*, 2002a, 2002b; Turner, 2006). The axoneme is connected to the base of the sperm so that sliding force generates bending of the flagellum and involves mechanically induced switching of dynein activity between the two sides of the central pair (Nakano *et al.*, 2003; Hayashi and Shingyoji, 2008, 2009). The peripheral microtubules are connected to the adjacent microtubule by nexin, acting as an elastic element, regulating the extent of sheer force while retaining the symmetry of the axoneme. The key regulatory proteins required for modulating motility are located in the flagellum and involves key calcium sensors calmodulin and calmodulin dependent kinases (Yang *et al.*, 2001; Smith, 2002; Nomura *et al.*, 2004; Morita *et al.*, 2009). Regulation of dynein activity by  $\text{Ca}^{2+}$  involves the central pair or apparatus and the radial spoke complex (Ishijima *et al.*, 1996; Smith, 2002; Nakano *et al.*, 2003). Axonemes are highly conserved in ciliated and flagellated eukaryotic cells although the outer dense fibres, mitochondrial sheath and fibrous sheath are exclusive to mammalian spermatozoa flagellum (Turner, 2006).

**Figure 1.5**

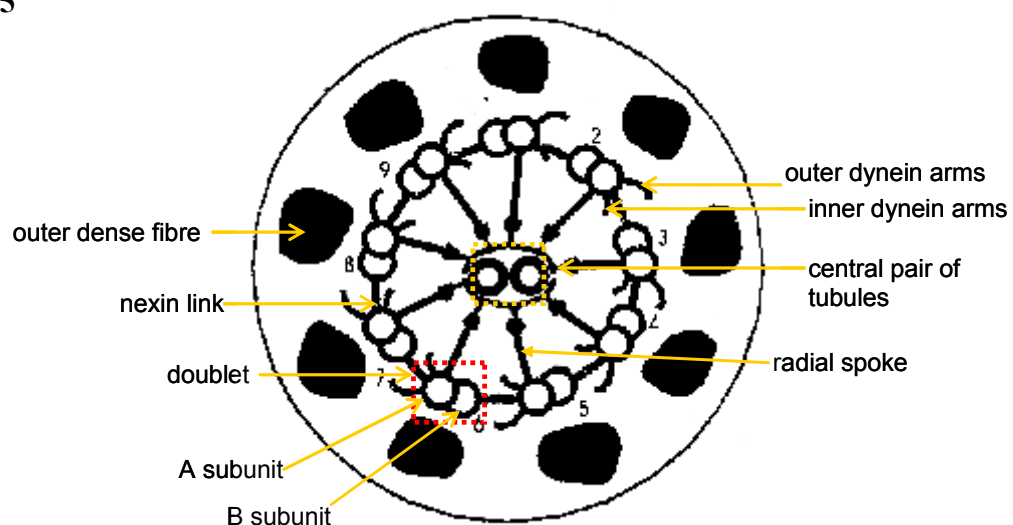


Figure 1.5: Diagrammatic cross-section of a mammalian sperm tail in the proximal region of the principal piece (refer to text for details, adapted from Mortimer, 2000).

In spermatozoa, mitochondria are restricted to the mid-piece and generate ATP through aerobic respiration. Sperm specific mitochondrial proteins include isoforms of lactate dehydrogenase and hexokinase but due to their location production of sufficiently high levels ATP and effective diffusion to supply dynein ATPases is unlikely (Williams and Ford, 2003; Turner *et al.*, 2003; Miki *et al.*, 2004; Ford, 2006). Mice spermatozoa defective in mitochondrial oxidative phosphorylation remain fertile but motility is reduced with lower levels of ATP generated (Narisawa *et al.*, 2002). This data suggests oxidative phosphorylation is not the sole source of ATP and motility. Dynein ATPases generate ATP locally by glycolysis along the length of the principal piece for flagellar movement (Eddy *et al.*, 2007). The glycolytic enzymes hexokinase, lactate dehydrogenase and glyceraldehyde-3-phosphate dehydrogenase (GAPDH) have been identified in the fibrous sheath/principal piece of mammalian species (Westhoff and Kamp, 1997; Bunch *et al.*, 1998; Miki *et al.*, 2004). All the glycolytic enzymes downstream of GAPDH are tightly bound to the cytoskeleton, even after membrane removal suggesting they are components of either the fibrous sheath or ODFs. Furthermore mammalian sperm produce lactate from glucose under aerobic conditions (Storey and Kayne, 1975). Ejaculated sperm can produce 90% of their ATP by anaerobic metabolism and blocking aerobic ATP production does not significantly reduce ATP levels or motility (Mukai and Okuno, 2004). Null mutant mice for the sperm's fibrous sheath-specific GAPDH are immotile (Miki *et al.*, 2004). Both ATP and adenosine 5'-diphosphate (ADP) binding to dynein regulates motile activity of the flagellum (Inoue and Shingyoji, 2007; Yoshimura *et al.*, 2007).

### **1.11.1 Quantitation of Sperm Movement**

Axonemal bending and the flagellar wave occur as a result of attachment-detachment cycles between the dynein arms and the adjacent doublet although the exact mechanism has not been fully elucidated (figure 1.5) (Ishijima, 1995; Mortimer, 1997; Ishijima *et al.*, 2002a). The flagellar wave is seen as a flattened helical beat of the tail, the wave travels the length of the

tail to propel the sperm cell forward, while the sperm head is forced to rotate along the axis of the direction of travel. The initial phase of the flagellar wave occurs near the head and if small in amplitude the sperm head has little lateral movement (figure 1.6a) and a pronounced forward movement. When the flagellar waves are of higher amplitude the head movement has a more pronounced, wider lateral movement (figure 1.6b). Movement patterns of sperm are influenced by their external environment. Recently, Smith *et al.*, (2009) utilised high frame rate digital imaging to examine in detail bend propagation in the flagella of free swimming human sperm in low viscosity and high viscosity medium (to mimic tract mucus). They report that sperm swimming in high viscosity medium had a lower wavespeed (frequency X wavelength) than sperm swimming in low viscosity medium (200 $\mu$ m/s and 890 $\mu$ m/s respectively) but that progressive velocity remained similar (62 $\mu$ m/s and 65 $\mu$ m/s respectively). In summary, cells in high viscosity media flagella beat less frequently (11Hz versus 23Hz) and have shorter wavelength (18 $\mu$ m versus 39 $\mu$ m) but progression per beat was >50% higher (5.8 $\mu$ m versus 2.7 $\mu$ m). Sperm swimming in low viscosity medium have a high head rolling rate because of the non-planarity of the flagellar bend. The flagellar envelope is described as an elliptical cone with a head rolling rate between 9-11 Hz. Ishijima *et al.*, (1992) reported the rotational movement of sperm attached vertically to a coverslip but swimming freely in media. Human spermatozoa rolled counter clockwise (viewed from the anterior end) and occasionally changed rotational direction (head rolling rate~9Hz). Smith *et al.*, (2009) report that sperm migrating through high viscosity media have a reduced head rolling rate and an almost planar flagellar beat to maintain effective cell progression despite increased resistance. Analysis of motility in low viscosity media is essential to understanding how cells swim in IVF media or follicular fluid around the time of ovulation (Smith *et al.*, 2009).

Since flagellar beat pattern determines the pattern of head movement computer assisted semen analysis (CASA) instruments exploits this relationship to track the sperm head movement, which does not move as fast as the flagellum. CASA analysis is routinely used in clinics to



assess motility parameters in human spermatozoa and has two main advantages over manual method – high precision and provision of quantitative data on sperm kinematics.

Motility kinematic values determined include the velocity of movement, the width of the sperm head trajectory and the frequency of change of direction of the sperm head (Mortimer, 2000). Velocity values ( $\mu\text{m}/\text{sec}$ ) include curvilinear velocity (VCL), straight line velocity (VSL) and average path velocity (VAP). VCL refers to the total distance the sperm head travels and is the highest value (figure 1.6, red line linking black dots (dots represent individual head position points)). VSL is determined from the straight line distance between the first head position point and the last point (figure 1.6a and b; blue lines). VAP is the distance the sperm has travelled in the average direction of movement during the observation period. VAP is calculated by taking the (x,y) coordinates for each head position point as well as those of two track point on either side, to give a smoothed (x,y) coordinate for that track point. When all the track points are smoothed the average path is calculated from the total distance travelled in the observation period. In cases, where the sperm position points are regular and linear, VAP (broken line, figure 1.6a) is similar to VSL (blue line, figure 1.6a). Linearity (%) can be used to describe the trajectory of the cells ( $\text{VSL}/\text{VCL} \times 100$ ). The amplitude of lateral head displacement (ALH,  $\mu\text{m}$ ) is used to approximate the flagellar beat envelope. To determine ALH manually, parallel lines are drawn between adjacent peaks and troughs and the perpendicular distance is measured, for regular trajectories the true head position point is perpendicular to the smoothed point on the average path (figure 1.6a). CASA calculates ALHmax (the maximum ALH found along the trajectory) using the Risers method, the distance from the true track coordinate (figure 1.6c, black dots linked with red lines) to the corresponding smoothed track coordinate (green dots) is calculated (Mortimer, 2000).

It is unusual for all spermatozoa (especially human) in a preparation to have the same motility pattern therefore population averages are unlikely to give an indication of the proportion of hyperactivated cells. However, since the motility pattern of hyperactivated sperm is very

different to non-hyperactivated sperm (compare sperm tracks in figure 1.7a with 1.7c and d), a defined range of kinematic criteria (Boolean argument) has been published (Mortimer, 2000). For a human sperm to be considered hyperactivated it must meet all the following criteria: curvilinear velocity  $\geq 150\mu\text{m/s}$  AND linearity  $< 50\%$  AND lateral head displacement  $\geq 7\mu\text{m}$  (Mortimer, 2000).

**Figure 1.6**

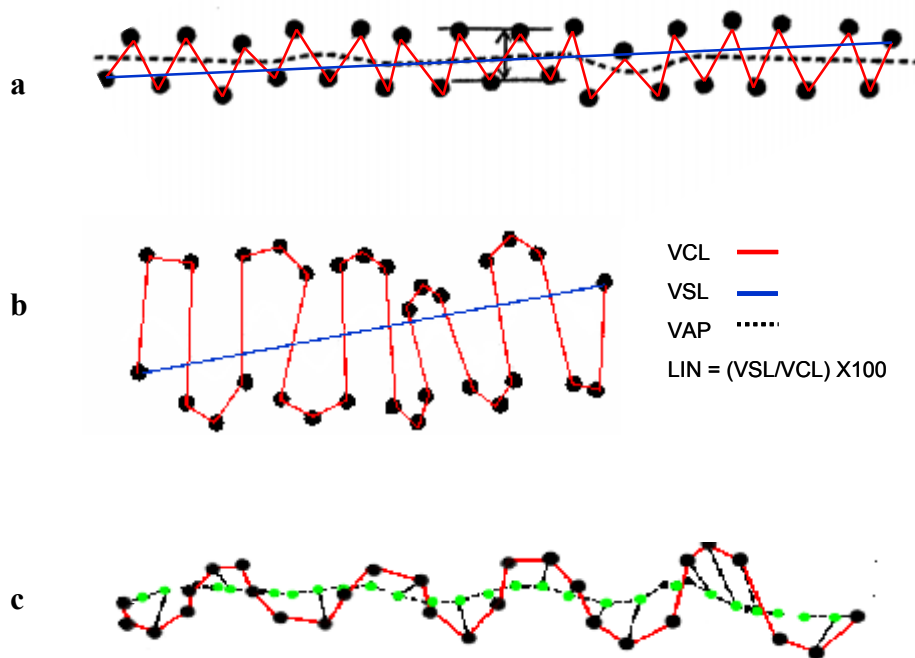


**Figure 1.6:** Motility patterns for capacitated human sperm. Individual head position points (black dots with red links) are shown. Refer to text for VSL (blue line) and VCL (red line) details (a) head position points of sperm (black dots) with regular motility pattern and (b) irregular motility pattern. (c) Risers method for determining ALH using smoothed head position points (green dots) and true head position points (black dots linked with red lines). Refer to text for ALH calculation details (adapted from Mortimer, 2000).

## 1.12 Chemotaxis and Sperm

Sperm are attracted and swim towards chemical factors released by the oocyte- a process called chemotaxis (Kaupp *et al.*, 2003, 2008). Much of the chemotatic research has centered on marine sperm where chemotatic factors from the egg jelly causes the sperm to re-orientate and swim towards the oocyte following a concentration gradient (Cohen-Dayag *et al.*, 1994; Eisenbach, 1999; Eisenbach and Giojalas, 2006; Neill and Vacquier, 2004). Binding of the egg derived factor to the receptor guanylyl cyclase (GC) activates cGMP synthesis. cGMP opens a  $K^+$  selective cyclic nucleotide-gated (KCNG) channel, causing  $E_m$  hyperpolarisation (Strünker *et al.*, 2006; Bönigk *et al.*, 2009). Hyperpolarisation activates a cyclic-nucleotide gated channel (HCN) and low voltage activated  $Ca^{2+}$  channels (LVA  $Ca^{2+}$ ) allowing the influx of  $Na^+$  and  $Ca^{2+}$  respectively (Strünker *et al.*, 2006). The opening of high voltage activated  $Ca^{2+}$  channels may be involved in the sustained elevation of  $[Ca^{2+}]_i$ . As previously described,  $Ca^{2+}$  interacts with the motor proteins of the axoneme to cause a change in flagellar beat and finally a change in the swimming trajectory (Kaupp *et al.*, 2008).

Spehr *et al.*, (2003; 2004) identified the presence of an odorant receptor (h-OR17-4) which responds to bourgeonal (floral scent) stimulating chemotatic behaviour in human sperm. Similarly lylal (floral scent) binds to a mouse odorant receptor (mOR23) and stimulates chemotaxis (Fukuda *et al.*, 2004). Binding of the odorant to the OR activates a G protein ( $G_{olf}$ ) and activation of the transmembrane adenylyl cyclase (tmAC) to induce a cAMP  $[Ca^{2+}]_i$  response. The specific components of this cAMP signalling pathway have not been unequivocally identified (Kaupp *et al.*, 2008).

Progesterone is secreted by the cumulus cells surrounding the oocyte and may form a chemotatic gradient (Jaiswal *et al.*, 1999). Recently Teves *et al* (2006) demonstrated a chemotatic response in (5-10%) of sperm (rabbit or human) to picomolar concentrations of

progesterone. The progesterone-signalling pathway mediating chemotaxis is unknown but  $[Ca^{2+}]_i$  signals generated could lead to chemotactic turns and orientation of cells up the chemotactic gradient (Kaupp *et al.*, 2008). Human sperm stimulated with a progesterone gradient (nanomolar to micromolar) to represent more closely the physiological stimulus that a sperm will encounter upon approaching the oocyte, generate a slow tonic rise in  $[Ca^{2+}]_i$  superimposed with  $Ca^{2+}$  oscillations in the neck region of sperm (Harper *et al.*, 2004). In loosely tethered human sperm, increased flagellar excursion and flagellar asymmetry occur during the initial progesterone-induced  $[Ca^{2+}]_i$  response and  $Ca^{2+}$  oscillations synchronise with flagellar asymmetry even in calcium free saline (Harper *et al.*, 2004; Bedu-Addo *et al.*, 2007). Evidence also indicates that cumulus oophorus express nitric oxide synthase and as spermatozoa approach or enter the cumulus they experience increased concentrations of NO (similar to progesterone gradient). Treatment of spermatozoa with nitric oxide (NO) donors affects sperm motility (Herrero *et al.*, 1994; Zhang and Zheng, 1996; Yeoman *et al.*, 1998; Herrero and Gagnon, 2001) and causes a sustained rise in  $[Ca^{2+}]_i$  due to mobilisation of a calcium store (Machado-Oliveira *et al.*, 2008). NO was shown to affect nitrosylation of RyR and act as a functional switch (Lefièvre *et al.*, 2007; Machado-Oliveira *et al.*, 2008). Machado-Oliveira *et al.*, (2008) demonstrated that progesterone and NO act synergistically. Human spermatozoa pre-treated with low dose progesterone and NO donor induce an immediate large transit  $[Ca^{2+}]_i$  signal which was often followed by  $Ca^{2+}$  oscillations synchronised with bending of the proximal flagellum, leading to flagellar asymmetry.

### 1.13 Hyperactivation

Mammalian spermatozoa exhibit two forms of physiological motility – activated and hyperactivated. Within semen or low viscosity media activated spermatozoa move in a relatively straight path with minimal head rolling and the flagellum generates symmetrical,

lower amplitude waveform that propel the cell forward (figure 1.7a) (Ho and Suarez, 2001a; Turner, 2006; Marquez *et al.*, 2007).

As spermatozoa reach the oviduct the pattern of flagellar motility alters to an asymmetric, high amplitude beat termed hyperactivated motility. Hyperactivated spermatozoa (*in vitro*) display extreme bending of the flagellum (high amplitude, high curvature) resulting in large side to side movements of the sperm head (greater lateral displacement of the head) (figure 1.7c and d). *In vitro* hyperactivated sperm have limited forward progression and when viewed on a microscope slide are often swimming in circles (starspin) or figures of eight (Ho and Suarez, 2001a). This pattern of motility is biphasic as spermatozoa can switch from one swimming pattern to another (Katz and Yanagimachi, 1980; Pacey *et al.*, 1995a; Mortimer and Swan, 1995).

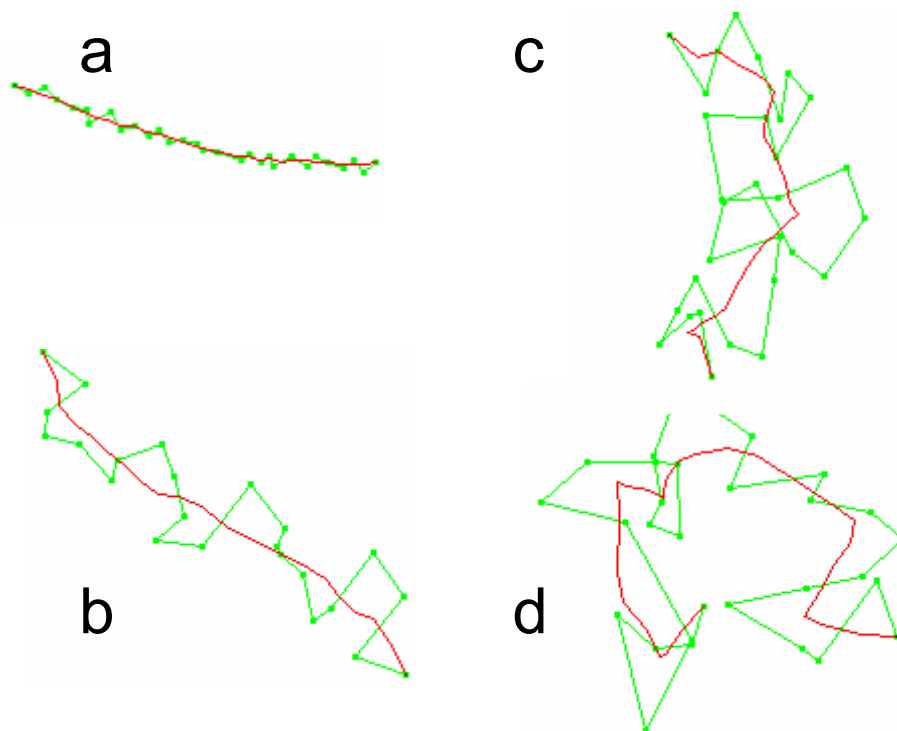


**Figure 1.7:** Motility pattern for activated and hyperactivated sperm. Sperm tracks show typical motility of cells suspended in (a) control media and (b) stimulated with 3 $\mu$ M progesterone or (c and d) with 2mM 4-AP (adapted from Gu *et al.*, 2004).

Yanagimachi (1970) first observed *in situ* hyperactivated spermatozoa through the walls of the oviductal ampulla of golden hamster indicating a physiological role in fertilisation. Hyperactivation has since been observed *in vitro* for all eutherian spermatozoa studied (Yanagimachi and Mahi, 1976; Battalia and Yanagamachi, 1979; Katz and Yanagamachi, 1980; Overstreet *et al.*, 1980; Mortimer *et al.*, 1984; Burkman *et al.*, 1984). There are a number of similarities in the hyperactivated movement patterns of mammalian spermatozoa, although interspecies differences have been observed. The hyperactivated sperm recovered from the ampulla were observed to swim in circular trajectories, due to the development of asymmetric flagellar beats whereas ejaculated sperm had linear trajectories due to symmetrical flagellar beat patterns. As mentioned previously, motility is influenced by the external environment and in high viscosity media hyperactivated mouse cells are more progressive than activated cells (Suarez and Dai, 1992).

The changes in motility patterns of hyperactivated spermatozoa have been shown to be due to change in flagellar bending rather than to a change in the viscous drag associated with acrosomal loss, as hyperactivated motility has been observed in headless spermatozoa from guinea pig and hamster (Katz *et al.*, 1978b). *In vivo* hyperactivation enables spermatozoa to detach from the oviductal epithelium (Ho *et al.*, 2009) and move progressively through the oviduct and effectively penetrate the outer vestements of the oocyte (Ho and Suarez, 2001a, 2003; Quill *et al.*, 2003; Suarez *et al.*, 1991; Stauss *et al.*, 1995; Marquez *et al.*, 2007).

The *in vivo* signals which regulate hyperactivation may include oviductal luminal fluid (containing hormones, ions and secretions), cumulus oophorus and/or follicular fluid but the specific triggers that induce hyperactivation are unknown (Mendoza and Tesarik, 1990; Uhler *et al.*, 1992; Ho and Suarez, 2001b). Hyperactivation is regularly associated with capacitation but can occur independently (Marquez and Suarez, 2004).

The signalling mechanisms that govern *in vivo* HA are not known however, evidence for

increased intracellular  $\text{Ca}^{2+}$ , a role for plasma membrane channels and intra-calcium store (ICS) mobilisation have been demonstrated (Marquez *et al.*, 2007). Various calcium channels including the sperm specific CatSper channels have been localised to the flagellum (Marquez *et al.*, 2007). Mobilisation of stored calcium has been shown to initiate hyperactivation in mice, bovine and human sperm (Ho and Suarez, 2001b; 2003).

Calcium regulates the axonemal waveform in both activated and hyperactivated motility (Suarez *et al.*, 1987, 2007; Ho *et al.*, 2002). The axonemal response to changes in calcium concentration has been well reported. Axonemes isolated for sea urchin sperm are reactivated *in vitro* under low calcium concentrations and beat with a symmetrical waveform. Increasing calcium enhanced an asymmetrical axonemal beat (Brokaw *et al.*, 1974; Browkaw, 1979) and in high extracellular conditions the axoneme are motionless (Gibbons and Gibbons, 1980; Sale, 1986).

### **1.13.1 CatSper channels and hyperactivation**

Calcium entry through CatSper channels is important to sustain sperm hyperactivated motility in mouse sperm (Carlson *et al.*, 2003, 2009) enhanced calcium influx is induced by alkalinisation leading to increased flagellar bending. Kirichok *et al.*, (2006) reported that the calcium current ( $I_{\text{CatSper}}$ ) is absent in CatSper null mice. The current was weakly voltage sensitive, but this sensitivity showed a pronounced negative shift (to physiological values of membrane potential) when  $\text{pH}_i$  was raised from its basal value of  $<7$  to  $\sim 7.5$  or 8. Recently the same lab detected a weakly outwardly rectifying  $\text{K}^+$  current ( $I_{\text{KSper}}$ ) in the principal piece of murine sperm. Alkalinisation activates the  $\text{pH}_i$  sensitive  $I_{\text{KSper}}$ , setting  $E_m$  to negative potentials where  $\text{Ca}^{2+}$  entry via  $I_{\text{CatSper}}$  is maximized (Navarro *et al.*, 2007). CatSper null sperm are unable to penetrate the outer vestments of the intact oocyte but can fertilise denuded oocytes *in vitro* (Ren *et al.*, 2001; Quill *et al.*, 2003; Carlson *et al.*, 2005). CatSper null sperm have normal patterns of tyrosine phosphorylation and are able to undergo ZP3-induced acrosome reaction

(Xia *et al.*, 2007).

Recently a flagellar voltage-gated proton channel (Hv1) has been identified in human sperm and proton extrusion from the cytoplasm would lead to cytoplasmic alkalinisation and CatSper channel activation (Lishko *et al.*, 2010).

Xia *et al.*, (2007) recorded relative  $[Ca^{2+}]_i$  along the length of the mouse tail using a  $Ca^{2+}$  sensitive fluorescent dye after the application of cell permeable cyclic analogues (8-Br-cAMP or 8-Br-cGMP). Increased intracellular  $Ca^{2+}$  started in the principal piece and propagated rapidly to the midpiece and head (3.2 sec) (Xia *et al.*, 2007). However, with ionomycin, a  $Ca^{2+}$  ionophore that facilitates  $Ca^{2+}$  transport across the plasma membrane, was applied extracellularly the fluorescence signal was seen immediately in all regions of the cell. Furthermore no significant response to 8-Br-cAMP was seen in CatSper null mutants. Xia *et al.*, (2007) concluded that 8-Br-cAMP indirectly opens CatSper channels,  $Ca^{2+}$  influx through the principal piece which propagates rapidly to the midpiece and head. CatSper channels have been implicated in regulating basal motility (Quill *et al.*, 2003; Qi *et al.*, 2007). Marquez *et al.*, (2007) observed that in CatSper null mice the flagellar bend amplitude is lowered but could be raised to normal pre-hyperactivation levels with the addition of thimerosal (ethyl (2-mercaptobenzoato-(2-)-O,S)mercurate(1-)-sodium (thimerosal) is a thiol reactive agent that stimulates  $Ca^{2+}$  flux in  $IP_3R$  by an as yet unidentified mechanism (Bultynck *et al.*, 2004). CatSper channels are also thought to be involved in ZP3 induced  $[Ca^{2+}]_i$  increase and therefore CatSper could play a role in the acrosome reaction (Xia and Ren, 2009b).

### **1.13.2 Intracellular $Ca^{2+}$ store release/capacitative $Ca^{2+}$ entry and hyperactivation**

Marquez *et al.*, (2007) provided evidence that release of calcium from intracellular stores contributes to increased  $[Ca^{2+}]_i$  in sperm that can induce hyperactivation in sperm lacking CatSper proteins. Ho and Suarez (2001b, 2003) reported that the redundant nuclear envelope



(RNE) may act as a calcium store having immunolocalised both IP<sub>3</sub>R and calreticulin to this region. In Ca<sup>2+</sup> free conditions, the release of stored calcium by thimerosal was sufficient to initiate hyperactivation in mice sperm although extra-cellular calcium influx was required to maximise and sustain hyperactivation for longer periods (Marquez *et al.*, 2007). CatSper1 and CatSper2 null sperm stimulated by thimerosal responded in this way, confirming mobilisation of stored calcium in the neck region was capable of supporting hyperactivation independently of influx through CatSper channels (Marquez *et al.*, 2007). Recently Xia *et al.* (2007) demonstrated that the CatSper dependent transient calcium influx signal initiated in the principal piece propagates rapidly to the midpiece and sperm head. Both the initial calcium elevation and the forward progression were lost in CatSper null mice. Suarez *et al.*, (1993) demonstrated that relative intracellular Ca<sup>2+</sup> was observed to be highest in the head region of intact hyperactivated hamster sperm. But can diffusion account for the sustained increase in head [Ca<sup>2+</sup>]<sub>i</sub> to maintain hyperactivation or is the CatSper dependent Ca<sup>2+</sup> influx stimulating CICR and mobilising stored Ca<sup>2+</sup>? A recent paper from Olson *et al.*, (2010) used mathematical modelling of sperm Ca<sup>2+</sup> dynamics to investigate a pump (PMCA)/ leak system and diffusion. They demonstrated that Ca<sup>2+</sup> influx through CatSper channels located in the principal piece could increase Ca<sup>2+</sup> in the principal piece and head but the response in the head could not be sustained (as Ca<sup>2+</sup> would be pumped out). By extending the model to include IP<sub>3</sub>, IP<sub>3</sub>R and RNE Ca<sup>2+</sup> store mobilisation, increased [Ca<sup>2+</sup>]<sub>i</sub> in the head region was sustained for as long as IP<sub>3</sub> was synthesised and Ca<sup>2+</sup> released from RNE store. In summary, CatSper derived Ca<sup>2+</sup> propagated along tail midpiece and head triggered IP<sub>3</sub> dependent Ca<sup>2+</sup> release resulting in a sustained increase in head calcium (characteristic of hyperactivated cells). The presence of IP<sub>3</sub>R in mammalian sperm has been confirmed in many studies (Costello *et al.*, 2009). Furthermore RyR may play a role in amplifying the signal initiated by Ca<sup>2+</sup> influx via the CatSper channel. The acrosome is not thought to be involved since experiments using Ca<sup>2+</sup> release agents to induce hyperactivation did not enhance acrosome reaction rates (Ho and

Suarez, 2001b).

### 1.13.3 4-aminopyridine and hyperactivation

4-aminopyridine (figure 1.8) is a widely used voltage-sensitive  $K^+$  channel blocker (Aronson *et al.*, 1992). 4-aminopyridine has also been used therapeutically for a number of neurological and neuromuscular junction disorders, such as Alzheimer's disease, multiple sclerosis and myasthenia gravis. Clinical application of 4-aminopyridine is thought to improve symptoms through blockage of voltage-activated  $K^+$  channels and in turn cause neuronal depolarisation and potentiation of neurotransmission (Smith *et al.*, 2000).

In addition to  $K^+$  channels inhibition, 4-aminopyridine disrupts intra-cellular calcium homeostasis in a number of cell types (Guse *et al.*, 1994; Ishida and Honda, 1993; Gobet *et al.*, 1995; Grimaldi *et al.*, 2001) and also functions as a cell-permeant weak base. Grimaldi and colleagues (2001) demonstrated that the 4-aminopyridine induced mobilisation of intracellular  $Ca^{2+}$  stores, potentiation of neurotransmitter-induced calcium transients and CCE in type 1 astrocytes, neurons and skeletal muscle cells. The  $[Ca^{2+}]_i$  elevation induced by 4-aminopyridine was concentration-dependent and consisted of two phases: the first was dependent on store mobilisation and the second was dependent on extra-cellular calcium influx. 4-aminopyridine also enhanced the second messenger  $IP_3$  in both neurons and astrocytes. In astrocytes, 4-aminopyridine potentiate the sustained phase of the  $[Ca^{2+}]_i$  elevation induced by ATP and bradykinin. The 4-aminopyridine induced effects were fully reversible. Other voltage-sensitive  $K^+$  channel blockers did not affect agonist-induced calcium transients or CCE indicating that 4-aminopyridine effects on  $[Ca^{2+}]_i$  was not caused by blockade of voltage gated  $K^+$  channels.

4-aminopyridine has been shown to have a particularly potent effect on human sperm motility. Data from our laboratory and others show that application of 4-aminopyridine induces a

dramatic increase in hyperactivation in both non-capacitated and capacitated human spermatozoa, with the proportion of hyperactivated sperm increased from 3-5% to 40-50% (Gu *et al.*, 2004; Barfield *et al.*, 2005). As previously discussed the initiation and maintenance of hyperactivation requires enhanced  $[Ca^{2+}]_i$  in mammalian sperm.

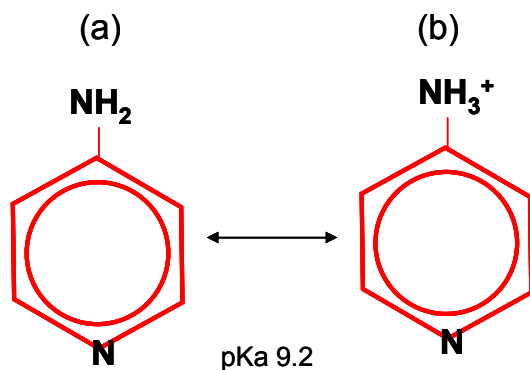


**Figure 1.8:** Structure of 4-aminopyridine. 4-aminopyridine can exist in an uncharged (a) or protonated form (b). The % of protonated 4-aminopyridine (pKa 9.2 at 25°C, Albert *et al.*, 1948; Babiak and Testa, 1976) is dependent on  $pH_o$  (Howe and Ritchie, 1991; Stephens *et al.*, 1994).

In mice sperm, 4-aminopyridine (weak organic base, pKa 9.2) induced cytoplasmic alkalinisation and enhanced  $I_{K_{Sper}}$  induced hyperpolarisation to increase the driving force for  $Ca^{2+}$  entry through CatSper channels (Navarro *et al.*, 2007). Similarly, cytoplasmic alkalinisation with 25mM  $NH_4Cl$  resulted in hyperactivation in bovine sperm (Marquez and Suarez, 2007). In addition, the weak base procaine had a similar effect and induced hyperactivation in mammalian sperm which further implicates pH as a component in the signalling pathway that control  $Ca^{2+}$  entry and hyperactivation (Mújica *et al.*, 1994; Marquez and Suarez, 2004; McPartlin *et al.*, 2009). Despite the importance of  $pH_i$  and CatSper activation, studies in rodent and bovine sperm have provided strong evidence that the elevation of  $[Ca^{2+}]_i$  that occurs upon mobilisation of  $Ca^{2+}$ , from a store in the sperm neck/midpiece region also contribute to regulation of flagellar activity, including (or at least facilitating) aspects of hyperactivation (Ho *et al.*, 2001b; 2003). Hyperactivation can also be induced by thimerosal induced store mobilisation in CatSper null mice. Experiments in human sperm cells have demonstrated that manipulations of the store located at the neck/midpiece result in

oscillations which are synchronised to asymmetrical binding of the proximal piece of the flagellum (Machado-Oliveira *et al.*, 2008). As mentioned previously mathematical modelling demonstrated that CatSper channel  $\text{Ca}^{2+}$  tail to head propagation is insufficient to maintain a sufficiently high  $[\text{Ca}^{2+}]_i$  and that store mobilisation and SOC induced  $\text{Ca}^{2+}$  influx was required (Olson *et al.*, 2010).

Since capacitative  $\text{Ca}^{2+}$  entry (influx of  $\text{Ca}^{2+}$  through store operated  $\text{Ca}^{2+}$  channels) has been observed in sperm (Blackmore, 1993; Williams & Ford, 2003; Harper *et al.*, 2005; Costello *et al.*, 2009), store mobilisation might even recruit this mechanism to supplement  $\text{Ca}^{2+}$  influx through CatSper channels. Alternatively this second pathway for induction of hyperactivation may play a separate role from that mediated by CatSper. Observations of sperm, primarily in humans but also other mammals, suggest that the cells can ‘switch’ rapidly and probably repeatedly between activated and hyperactivated motility (Pacey *et al.*, 1995a, 1995b; Mortimer and Swan, 1995), a behaviour that may mediate interactions with cells of the female tract (Pacey *et al.*, 1995b). Mobilisation of stored  $\text{Ca}^{2+}$ , which is rapidly reversible and localised, may be better suited to such transient regulation of motility whereas pH regulated activation of CatSper could support the prolonged hyperactivation that permits ‘permanent’ detachment from the cells of the female tract (Ho *et al.*, 2009) and penetration of the zona. It is however not clear how store mobilisation contributes and interacts with the CatSper channels (Olson *et al.*, 2010). The effects of 4-aminopyridine on human sperm hyperactivation and  $[\text{Ca}^{2+}]_i$  response has been examined in the following chapters. In particular, the relative contribution of cytoplasmic alkalinisation (CatSper activation) and store mobilisation (SOC entry) in 4-aminopyridine induced hyperactivation in human spermatozoa was investigated.

## 1.14 Summary

The mature sperm cell is a highly specialized cell despite lacking much of the intracellular structure and organisation present in somatic cells. Mammalian sperm are capable of long distance travel through the female reproductive tract to the oviduct, in which fertilisation takes place (Ikawa *et al.*, 2010). Transit through the female reproductive is accomplished by the flagellum driving the sperm cell towards its target. Due to ethical constraints very little is known about the human sperm's journey and interaction with the oocyte *in vivo*. This review focused on the  $\text{Ca}^{2+}$  signalling toolkit essential for sperm motility and hyperactivation (Publicover *et al.*, 2007).

## RESEARCH AIMS

Assess the effects of 4-aminopyridine on  $[Ca^{2+}]_i$  and hyperactivation in human spermatozoa and the importance of  $K^+$  flux and  $E_m$  depolarisation in this process (Q1 and Q2 figure 1.9, results chapter 2).

Investigate the effects of extracellular pH on 4-aminopyridine entry into sperm. Examine the effects of  $pH_i$  modulators on 4-aminopyridine induced hyperactivation and  $[Ca^{2+}]_i$  response (Q3, Q4 and Q5 figure 1.9, results chapter 3).

Assess the contribution of CatSper induced  $Ca^{2+}$  influx in 4-aminopyridine induced hyperactivation and  $[Ca^{2+}]_i$  response (Q6 figure 1.9, results chapter 4)

Examine the effects of 4-aminopyridine on intracellular  $Ca^{2+}$  store release and the consequent effects on human sperm functions (Q7 figure 1.9, results chapter 5)

Investigate the effects of store operated channels modulation in the 4-aminopyridine induced  $[Ca^{2+}]_i$  response (Q8 figure 1.9, results chapter 6).

An experimental matrix/workpath linking the project research aims (and experimental questions Q1-Q8) with results chapters (2-6) is illustrated in figure 1.9 (also included are methods utilised to investigate and results obtained).

Figure 1.9

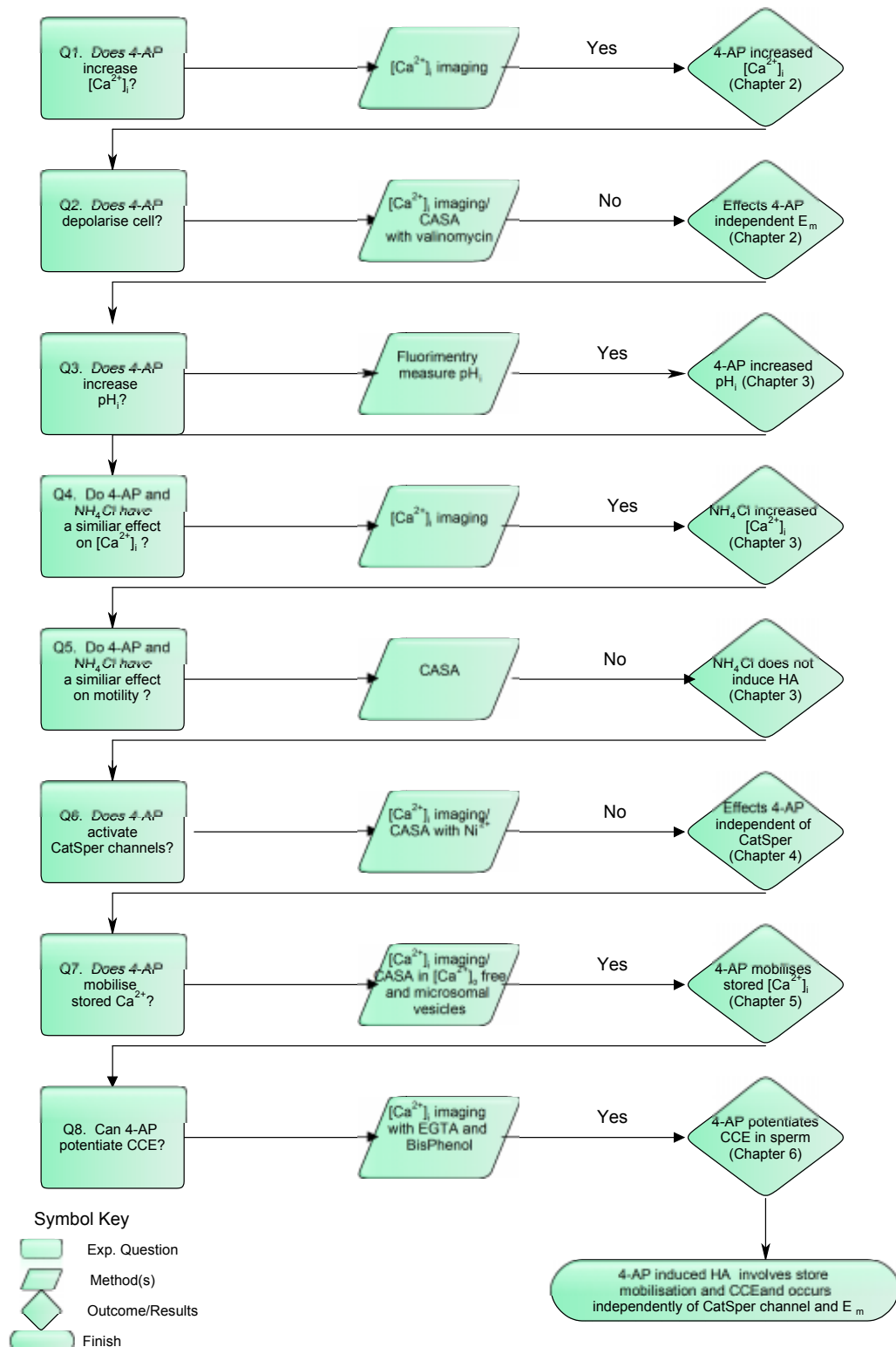


Figure 1.9: Experimental matrix/workpath linking research aims and experimental questions with results chapters

## **CHAPTER TWO**

# **4-AMINOPYRIDINE INDUCED HYPERACTIVATION AND ELEVATION OF $[Ca^{2+}]_i$ IN HUMAN SPERM IS INDEPENDENT OF $K^+$ FLUX AND MEMBRANE DEPOLARISATION**

<b>2.1 Abstract</b>	54
<b>2.2 Introduction</b>	55
<b>2.3 Materials and methods</b>	58
2.3.1 Materials	58
2.3.2 Preparation and capacitation of spermatozoa	58
2.3.3 Single cell imaging	59
2.3.4 Imaging data processing	59
2.3.5 Evaluation of 4-aminopyridine fluorescence quenching	60
2.3.6 Evaluation of sperm hyperactivation	61
2.3.7 High speed imaging of sperm motility	62
2.3.8 Statistical Analysis	62
<b>2.4 Results</b>	63
2.4.1 4-aminopyridine induced hyperactivation in human spermatozoa	63
2.4.2 4-aminopyridine elevates $[Ca^{2+}]_i$ fluorescence in OGB labelled spermatozoa	64
2.4.3 4-aminopyridine did not significantly quench OGB emission signal	65
2.4.4 4-aminopyridine induced hyperactivation and increased $[Ca^{2+}]_i$ fluorescence does not act through $K^+$ channel block and modulation of $E_m$	67
<b>2.5 Discussion</b>	69



## 2.1 Abstract

4-aminopyridine (4-AP), a blocker of voltage-activated  $K^+$  channels, is one of the most potent inducers of human sperm hyperactivation yet described (Gu *et al.*, 2004). Since data from both our studies and those of others laboratories have shown that  $[Ca^{2+}]_i$  plays a central role in regulating the activity of the flagellum, we have investigated the effects of 4-aminopyridine on  $[Ca^{2+}]_i$  fluorescence in human spermatozoa. We report that 4-aminopyridine (2mM) enhanced  $[Ca^{2+}]_i$  fluorescence in OGB labelled sperm and induced hyperactivated motility. These 4-aminopyridine induced effects are independent of  $K^+$  flux and membrane potential.

## 2.2 Introduction

During fertilisation the highly specialised sperm cell fuses with the oocyte to deliver paternal genetic material and trigger egg activation (Swann *et al.*, 2004). Mammalian sperm are unable to fertilise the oocyte immediately after ejaculation but must undergo a maturation process termed capacitation as they journey through the female reproductive tract (Austin 1951; Chang 1951; Yanagimachi and Usui, 1974). Spermatozoa acquire the ability to undergo the agonist induced acrosome reaction and modify motility pattern from activated to hyperactivated (Gadella and Visconti., 2006). Activated or progressive motility is characterised by high flagellar beat frequency with low bend angle, particularly of the proximal flagellum. Transition to hyperactivated swimming involves deep flagellar bends, due to increased flexure of the midpiece/proximal flagellum and a concomitant decreased beat frequency resulting in greater lateral displacement of the head (Ho and Suarez, 2001a; Ishijima, 2007a, 2007b).

*In situ* hyperactivation was first reported by Yanagimachi (1970) and observed through the oviductal walls of golden hamster. Hyperactivated motility has been described *in vitro* for all eutherian spermatozoa (Suarez and Osman, 1987; Mortimer, 2000) and has been shown to be essential for *in vivo* fertilisation, enabling the sperm to effectively penetrate mucus, detach from the oviductal epithelium and penetrate the outer vestments of the oocyte (Stauss *et al.*, 1995; Ren *et al.*, 2001; Quill *et al.*, 2003; Carlson *et al.*, 2003; Ho *et al.*, 2009).

The signalling mechanisms that govern *in vivo* hyperactivation in sperm are not fully understood but various studies have shown that pH (Parrish *et al.*, 1989) and cAMP are important regulatory components (Marquez and Suarez, 2007). However the increase in intracellular  $\text{Ca}^{2+}$ , particularly in the mid-piece, is key to the initiation and maintenance of hyperactivation, probably by strongly enhancing flagellar bending (Lindemann and Goltz 1988; Suarez and Dai 1992; Yanagimachi *et al.*, 1994b; Visconti *et al.*, 1995; Ho *et al.*, 2002; Ishijima *et al.*, 2006, Ohmuro and Ishijima, 2006; Marquez *et al.*, 2007).

Two sources of  $\text{Ca}^{2+}$  may contribute to the regulation of hyperactivation in sperm.  $\text{Ca}^{2+}$  influx at the plasma membrane is crucial and/or release of stored intracellular calcium and activation of capacitative calcium entry (CCE). The sperm-specific, pH regulated,  $\text{Ca}^{2+}$ -permeable CatSper channels expressed in the principal piece of mammalian sperm are of great importance in this process (Kirichok *et al.*, 2006; Qi *et al.*, 2007). In addition, studies on sperm from rodents, bulls and humans have provided strong evidence that  $\text{Ca}^{2+}$  stored in the region of the sperm neck contributes to regulation of flagellar activity (Chandler and Battersby, 1976; De Blas *et al.*, 2002; Herrick *et al.*, 2005).

Due to the ethical constraints, *in vivo* hyperactivation cannot be observed in the human Fallopian tube however failure of human sperm to hyperactivate may be an important contributory factor to infertility (Nikpoor *et al.*, 2004).

A major problem in human sperm samples is the highly asynchronous motility response within a population of cells. However, since the motility pattern of hyperactivated sperm is very different to non-hyperactivated sperm (compare sperm tracks in figure 1.7a with 1.7c and d), it has been possible to define specific kinematic criteria (Mortimer, 2000). As mentioned previously (section 1.11.1), for a human sperm to be considered hyperactivated it must meet all the following criteria: curvilinear velocity  $\geq 150\mu\text{m/s}$  AND linearity  $< 50\%$  AND lateral head displacement  $\geq 7\mu\text{m}$  (Mortimer, 2000). More detailed characterization of flagellar movement involves digital frame by frame analysis which is both tedious and time-consuming and normally depends on some form of cell attachment.

Gu *et al.*, (2004) previously described 4-aminopyridine (2mM) as a potent inducer of hyperactivation in human spermatozoa and potentially a useful tool to assess patient sperm hyperactivation ability. 4-aminopyridine is a widely used and effective blocker of  $\text{K}^+$  channels and has been shown to disrupt intra-cellular calcium homeostasis in a number of cell types.

We have examined the effects of 4-aminopyridine on  $[Ca^{2+}]_i$  fluorescence and motility (assessed by CASA) of human sperm.

## **2.3 Materials and Methods**

### **2.3.1 Materials**

Supplemented Earle's balanced salt solution (sEBSS) was prepared in the laboratory and contained 1.0167mM  $\text{NaH}_2\text{PO}_4$ , 5.4mM KCl, 0.811mM  $\text{MgSO}_4 \cdot 7\text{H}_2\text{O}$ , 5.5mM  $\text{C}_6\text{H}_{12}\text{O}_6$ , 2.5mM  $\text{C}_3\text{H}_3\text{NaO}_3$ , 19.0mM  $\text{CH}_3\text{CH}(\text{OH})\text{COONa}$ , 1.8mM  $\text{CaCl}_2 \cdot 2\text{H}_2\text{O}$ , 25.0mM  $\text{NaHCO}_3$ , 118.4mM NaCl and 15mM HEPES (pH 7.35, 285-295 mOsm), supplemented with 0.3% (w/v) fatty acid free BSA. Chemicals used in preparation of media were from Sigma Aldrich (Poole, Dorset, UK). Fatty acid-free BSA was from SAFC Biosciences (Lenexa, KS, USA). Osmotic strength (285-295mOsmol) was maintained by adjusting NaCl. OGB and fura-2/AM were from Invitrogen Molecular Probes (Paisley, UK). PDL was from BD Biosciences (Oxford, UK). All other chemicals referred in the text were from Calbiochem (San Diego, CA, USA), except 4-aminopyridine and Pluronic F-127 were from Sigma-Aldrich (Poole, Dorset, UK). All chemicals were cell-culture-tested grade where available.

### **2.3.2 Preparation and capacitation of spermatozoa**

All donors were recruited in accordance with the Human and Embryology Authority Code of Practice (Version 7) and gave informed consent (LREC 2003/239 and University of Birmingham Life and Health Sciences ERC 07-009). Cells from more than 20 donors were used over the duration of the study and all showed similar responses to stimulation with 4-aminopyridine. Semen was collected by masturbation after 2-3 days of sexual abstinence and allowed to liquefy for approximately 30 minutes, at 37°C and 5.5%  $\text{CO}_2$ . Highly motile spermatozoa were harvested by direct swim-up (Mortimer, 1994) into supplemented Earle's balanced salt solution (sEBSS) medium (15mM Hepes, pH 7.3-7.4) with 0.3% Bovine Serum Albumin (BSA). Briefly, 1 ml of medium was underlayered with 0.3 ml of semen in Falcon round-bottom tubes. After 1 hour incubation at 37°C and 5%  $\text{CO}_2$ , the top 0.7ml was removed, pooled and spermatozoa concentration was determined using a Neubauer haemocytometer and

adjusted to  $6 \times 10^6$  cells/ml. Aliquots of 200 $\mu$ l (for single-cell imaging and motility analysis) were left to capacitate for 5-6 hours. .

### **2.3.3 Single Cell Imaging**

200 $\mu$ l aliquots of capacitated spermatozoa at  $3-6 \times 10^6$  cells/ml were loaded with Oregon Green bis-(o-aminophenoxy)ethane-*N,N,N',N'*-tetra-acetic (BAPTA 1)-AM (12 $\mu$ M final concentration dispersed with Pluronic F-127). Fluorescence of Oregon Green BAPTA shows negligible pH sensitivity over the range pH 6-9 (Haugland and You, 2008) making it suitable for the experiments in which pH<sub>i</sub> is varied. After incubation for 30 min at 37°C and 5.5% CO<sub>2</sub>, cells were transferred to an imaging chamber (volume 180  $\mu$ l) in which the lower surface was a 1% (w/v) poly-D-lysine coated coverslip. A further 30 min incubation was then allowed for the cells to adhere. The chamber was connected to the perfusion apparatus (peristaltic pump and header tank; perfusion rate 0.4ml min<sup>-1</sup>) and cells were superfused with approximately 10 ml of fresh medium to remove unattached cells and excess dye. All experiments were performed at 25 $\pm$ 0.5°C in a continuous flow of medium.

Spermatozoa were imaged on a Nikon TE200 inverted fluorescence microscope. Images were obtained at 10 s intervals using a 40x objective and a Hamamatsu Orca 1 or Q Imaging Rolera-XR cooled CCD camera controlled by a PC running iQ software (Andor Technology, Belfast, UK). For high speed fluorescence imaging (9 Hz) the protocol was as above but cells were viewed using a 60x oil immersion objective and images were captured with an Andor iXon EM<sup>+</sup> camera controlled by a PC running iQ software.

### **2.3.4 Imaging Data Processing**

Data were processed offline using iQ software. A region of interest was drawn around the rear of the head of each sperm in the field of view. The image series was then replayed several

times, enabling close visual inspection of each cell. Cells were excluded from analysis if they moved outside the region of interest or if the fluorescence faded to zero within the duration of the experiment (assumed to reflect loss of dye due to cell death). Raw intensity values were imported into Microsoft Excel and normalized utilizing the equation

$$R = [(F - F_{\text{rest}}) / F_{\text{rest}}] \times 100\%,$$

where R is normalised fluorescence intensity, F is Fluorescence intensity at a time t and  $F_{\text{rest}}$  is the mean of 20-30 determinations of F obtained during the control period. At each time point the average normalised head fluorescence ( $R_{\text{tot}}$ ) was calculated. The total series of  $R_{\text{tot}}$  was then plotted to give the mean normalized fluorescence intensity for that experiment. For each cell, Microsoft Excel was used to calculate the mean and 95% confidence interval of fluorescence intensity for at least 15 images during the control period ( $Con \pm con$ ) and 8-10 images at a selected time point after stimulation ( $X \pm X$ ). The response was considered significant if

$$X - x > Con + con$$

where 'X' and 'x' are the mean and 95% confidence interval for that sampling point, and 'Con' and 'con' are the mean and 95% confidence interval for the control period. Cells were sorted into those showing either an increase, decrease or no change in fluorescence after treatment. Visual examination of fluorescence-time plots for the sorted cells confirmed that this technique resulted in successful sorting of the different response categories. Where more complex  $[Ca^{2+}]_i$  responses were observed, quantification of responses was carried out by direct observation of time-fluorescence intensity plots.

### **2.3.5 Evaluation of 4-aminopyridine fluorescence quenching**

Following swim-up approximately 7mls of highly motile spermatozoa ( $6 \times 10^6$  cells/ml) were pooled and loaded with Oregon Green BAPTA 1-AM (6 $\mu$ M final concentration dispersed with Pluronic F-127). To allow maximal de-esterification of the dye, cells were incubated for

approximately 5 hours at 37°C and 5% CO<sub>2</sub> then centrifuged (300g for 5 min). The supernatant was retained (6mls) and diluted with 20mM Hepes buffer deionised H<sub>2</sub>O (pH 7.3) so that final Ca<sup>2+</sup> concentration was 3.6 X 10<sup>-4</sup>M. Experiments were carried out using a Perkin-Elmer LS50B fluorescence spectrofluorimeter running FLWinlab version 3.0. Fluorimetry was performed with 2ml aliquot of de-esterified dye in a magnetically stirred methylacrylate cuvette maintained at 25°C by a water jacket. An emission spectrum was recorded with 4-aminopyridine (0-5mM final concentration) using the fixed excitation wavelength of 494nm with slit width set at 3nm. Emission was scanned between 495 to 600nm with slit width set at 3nm and scan speed 1000 (nm/min). Fluorescence quenching was measured quantitatively using the Stern-Volmer equation.

$$K_{sv} = ((F_0/F_{[Q]})-1)/[Q]$$

$K_{sv}$  – Stern Volmer Constant

[Q]- concentration of quencher (4-aminopyridine)

$F_0$  - measured fluorescence intensity in the absence of quencher

$F_{[Q]}$ - measured fluorescence intensity in the presence of [Q].

### 2.3.6 Evaluation of sperm hyperactivation

For motility assessment 200µl aliquots of spermatozoa ( $\geq 6 \times 10^6$  cells.ml<sup>-1</sup>) were prepared by direct swim-up into standard media (sEBSS) and incubated for 5-6 hours. 200µl aliquots were treated with either saline (control) or 4-aminopyridine and immediately introduced into a chamber (depth 20µm) (Microcell, Conception Technologies Ltd.) at a concentration of 6-15 million/ml on a Hamilton Thorne HTM IVOS semen analyzer (37°C). Hyperactivation was defined as curvilinear velocity  $\geq 150\mu\text{m/s}$ ; linearity  $< 50\%$ ; lateral head displacement  $\geq 7\mu\text{m}$ . Only cells where tracks of  $\geq 13$  points were obtained were included in calculation of %



hyperactivated cells. At least 20 fields were scored across each slide. Playback feature also help to ensure the accuracy of the system

### **2.3.7 High speed imaging of sperm motility**

Image series of swimming sperm for assessment of flagellar movement were collected using 200µl aliquots of spermatozoa which were prepared for fluorescence imaging but diluted to approximately 0.5 million cells.ml<sup>-1</sup> before use. Aliquots were treated with either saline (control) or 4-aminopyridine immediately before recording. For low-speed image series, phase contrast images of free-swimming cells were collected at 10 Hz using the same chamber, camera and software as that employed for fluorescence imaging (see above). For high speed imaging cells were introduced into a Model P-2, series 20 imaging chamber (Warner Instruments Inc) and observed using a positive phase contrast lens (203/0.40 1/0.17 Ph1, depth of field 5.8 µm) on an Olympus BX50 microscope. Data capture was via a Hamamatsu Photonics C9300 CCD camera at approximately 150 frames per second, streaming data directly to a Dell Dimension 64 bit Workstation, running Wasabi software (Hamamatsu). The stage was maintained at 37°C using a LINKAM C0102 stage heater.

### **2.3.8 Statistical analysis**

Values in the text giving frequency of each response type are stated as mean ± s.e.m.

Microsoft Excel was used to perform paired or unpaired *t* tests as appropriate. Statistical significance was set at  $P < 0.05$ . Percentage data were arcsine transformed before testing

## 2.4 Results

### 2.4.1 4-aminopyridine induced hyperactivation in human spermatozoa

As described previously (Gu *et al.*, 2004), 2mM 4-aminopyridine induced an immediate transition to hyperactivated motility in a proportion of human sperm. Since 4-aminopyridine acts as a weak base, CASA experiments were carried out in HEPES buffered (15-25mM sEBSS, pH7.3) saline. In capacitated cells (5-6 h) the proportion of hyperactivated sperm (as assessed by CASA) increased from  $3.5 \pm 1.1\%$  to  $16.2 \pm 2.8\%$  (15-25mM HEPES buffered saline,  $n = 6$ , paired  $t$ -test,  $P < 0.001$ ),  $< 2$  minutes (minimum delay prior to assessment) (figure 2.1a). Series of phase contrast images of sperm (10 frames/second) showing 'typical' activated sperm under control conditions (left column) and sperm hyperactivated by 2mM 4-aminopyridine (right column) (figure 2.1b).

Figure 2.1

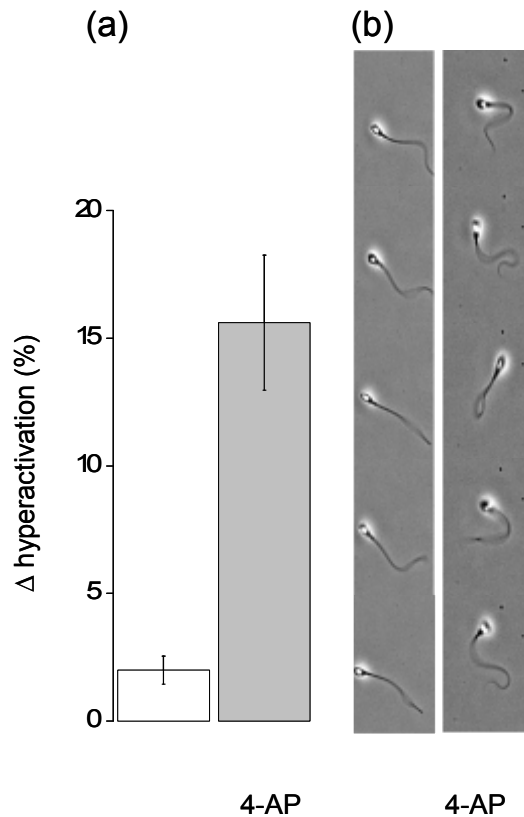


**Figure 2.1.** 4-aminopyridine (4-AP, 2mM) induced hyperactivation of capacitated human spermatozoa (assessed by CASA) in HEPES buffered sEBSS at pH7.3. **(a)** 4-AP causes an increase in the % of hyperactivated sperm from control conditions (open bar) and after exposure to 4-AP for  $\approx 2$ min (grey bar). Each bar shows mean  $\pm$  s.e.m. of 6 experiments ( $P < 0.001$ ; paired  $t$ ). **(b)** Series of phase contrast images of sperm (left column) and sperm hyperactivated by 2mM 4-AP (right column) (inter-frame interval 100ms).

#### 2.4.2 4-aminopyridine elevates $[Ca^{2+}]_i$ fluorescence in OGB labelled spermatozoa

Application of 2mM 4-aminopyridine to cells loaded with Oregon Green BAPTA 1 (OGB) showed that  $\approx 75\%$  of imaged cells responded with a significant increase in fluorescence (see methods, paired  $t$ -test,  $P < 0.05$ ). Fluorescence increased within 10-30 s and stabilized at an elevated level 1-5 min after application. The mean amplitude of this response ( $\Delta$  fluorescence), 5 minutes after application of 4-aminopyridine was  $15.0 \pm 1.4\%$  (8 experiments; 515 cells; figure 2.2). Upon washout of 4-aminopyridine  $[Ca^{2+}]_i$  fell rapidly to levels at or near those observed before treatment, sometimes with an ‘undershoot’ of 2-3 minute duration (figure 2.2).

Figure 2.2

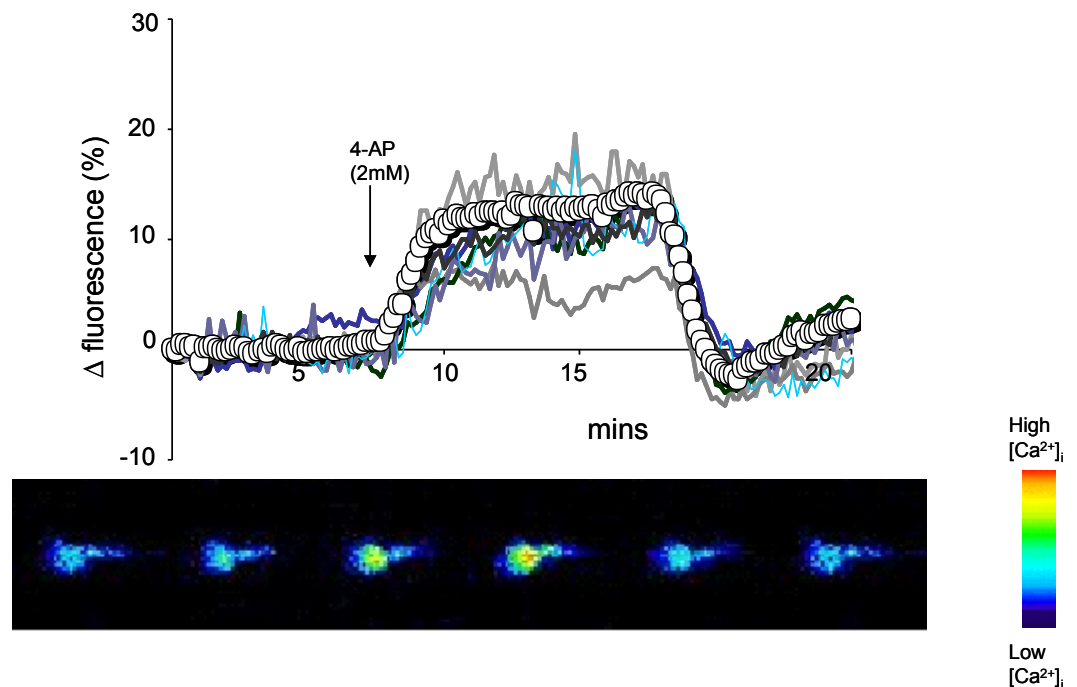


**Figure 2.2.** The effects of 2mM 4-AP on  $[Ca^{2+}]_i$  (Oregon Green BAPTA-1 fluorescence) in capacitated human sperm bathed in standard saline (pH7.3). Traces show 7 responses of representative cells and also mean response (o-o) of all 55 cells in this experiment. Lower panel shows pseudo-colour images (warm colours show high  $[Ca^{2+}]_i$ ) of OGB fluorescence response in a ‘typical’ sperm cell at various points in the experiment. First two images are prior to treatment, images 3 and 4 are during 4-aminopyridine superfusion and images 5 and 6 are during washout.

### 2.4.3 4-aminopyridine did not significantly quench OGB emission signal

Aminopyridines are N-heterocyclic tertiary amines and have inherent fluorescent properties. There are three isomeric amines of pyridine depending on the position (2, 3 or 4) of the ring nitrogen. 4-aminopyridine absorbs light at  $\lambda$  245nm but is essentially non fluorescent in polar and non-polar solvents, with a low quantum yield (0.001) and a molar extinction coefficient of  $\sim 11,600 \text{ cm}^{-1}\text{M}^{-1}$  (Steck and Ewing, 1948; Dega-Szafran *et al.*, 1994). Direct effects of 4-aminopyridine on the recorded fluorescent signal are therefore unlikely.

Aromatic amines have been shown to quench or decrease the intensity of fluorophore emission. We have therefore examined the effects of 4-aminopyridine on OGB emission intensity. To investigate, de-esterified OGB (as described in the methods) was prepared, OGB fluorescence emission recorded in the presence ( $F$ , figure 2.3a) and absence ( $F_0$ , figure 2.3b) of 4-aminopyridine (0.5-5mM). Fluorescence emission intensity quenching can be quantified by the Stern-Volmer equation (see methods). By plotting 4-aminopyridine concentrations (0.5-5mM) against the ratio of  $F_0$  to  $F$ , the value for  $K_{sv}$  (Stern-Volmer constant) can be obtained from the slope using linear regression ( $K_{sv} = 0.023$  at  $25^\circ\text{C}$ ). Addition of 4-aminopyridine did not change the shape of the fluorescence spectra and slightly quenched OGB emission (figure 2.3a). The Stern-Volmer constant serves as a direct measure of the efficiency of the fluorescence quenching process. It is useful to note that  $1/K_{sv}$  is the 4-aminopyridine concentration at which  $F_0/F_{[Q]}=2$  (or 50% of the fluorescence intensity is quenched), therefore  $>50\text{mM}$  4-aminopyridine would be required to quench fluorescence intensity by 50%.

Figure 2.3

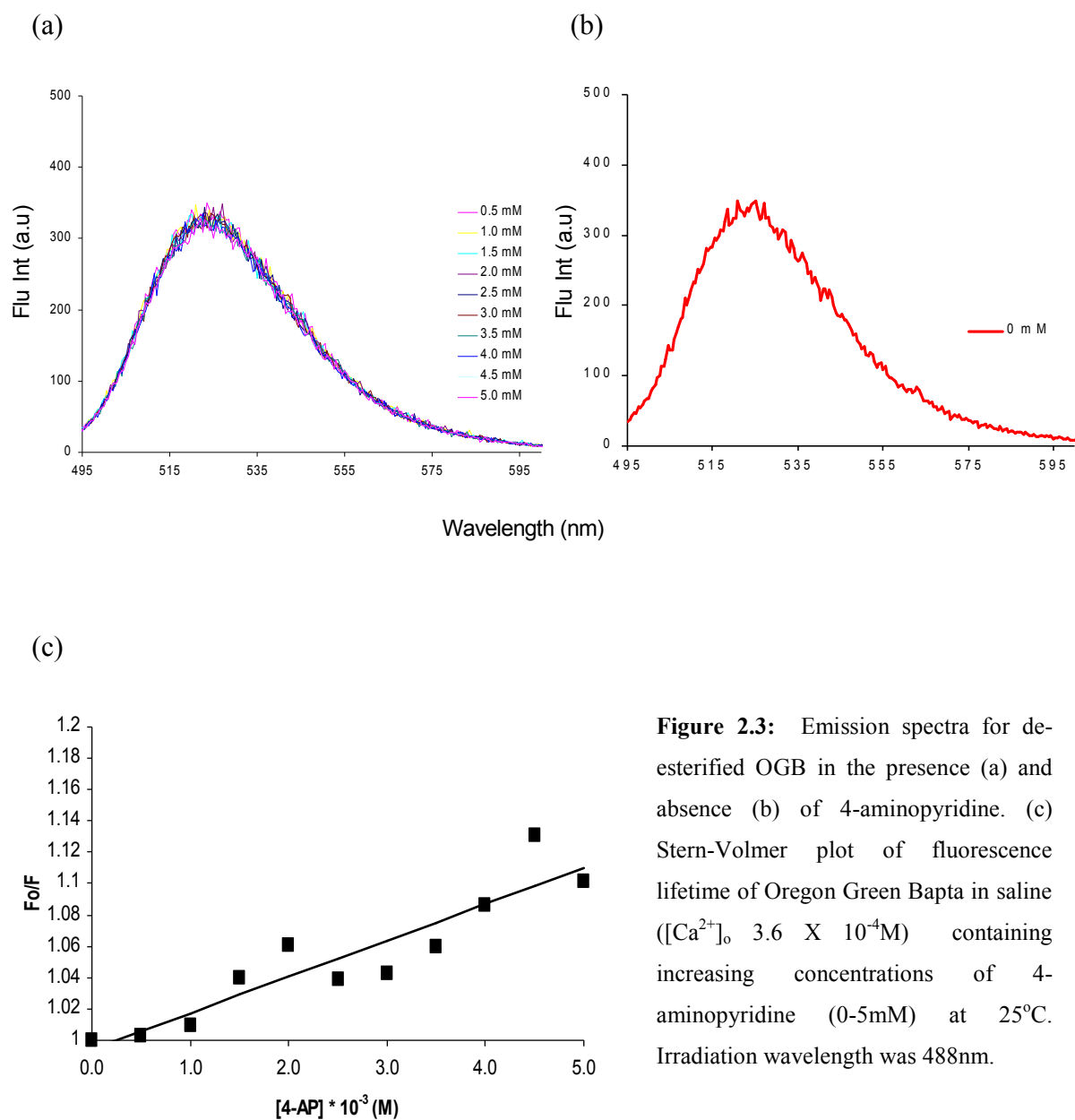


**Figure 2.3:** Emission spectra for de-esterified OGB in the presence (a) and absence (b) of 4-aminopyridine. (c) Stern-Volmer plot of fluorescence lifetime of Oregon Green Bapta in saline ( $[Ca^{2+}]_0$   $3.6 \times 10^{-4} M$ ) containing increasing concentrations of 4-aminopyridine (0-5mM) at 25°C. Irradiation wavelength was 488nm.

#### **2.4.4 4-Aminopyridine induced hyperactivation and increased $[Ca^{2+}]_i$ fluorescence does not act through $K^+$ channel block and modulation of $E_m$**

4-aminopyridine is a widely used and effective blocker of  $K^+$  channels, where it acts at an intracellular site after entering the cell in its uncharged form (Howe and Ritchie, 1991, Stephens *et al.*, 1994). Such an action, for instance leading to depolarisation of the sperm membrane potential ( $E_m$ ), might underlie the effect of 4-aminopyridine on  $[Ca^{2+}]_i$  and hyperactivation. To investigate this possibility, we ‘clamped’ sperm membrane potential at the potassium equilibrium potential ( $E_K$ ) by pre-incubating cells with the  $K^+$ -ionophore valinomycin (1  $\mu$ M) (Nernst calculation for  $E_K = -83$  mV (125 mM intracellular  $K^+$  and 5.4 mM extracellular  $K^+$ ) for 5 min prior to 4-aminopyridine addition. In 7 sets of paired observations, brief pre-treatment with valinomycin (~2 mins time taken to load sample and record motility) reduced only slightly the proportion of cells that showed hyperactivated motility in response to 2 mM 4-aminopyridine (2 mM 4-aminopyridine =  $26.6 \pm 5.3\%$ ; valinomycin followed by 2 mM 4-aminopyridine =  $21.1 \pm 4.9\%$ ; paired *t*-test,  $P > 0.05$ ) (figure 2.4b). In single cell imaging experiments, pre-treatment with 1  $\mu$ M valinomycin had a significant effect on resting  $[Ca^{2+}]_i$ , increasing fluorescence by  $12.4\% \pm 0.8\%$ ;  $n = 4$  experiments; 226 cells, paired *t*-test,  $P < 0.05$ ) (figure 2.4a), an effect that may reflect action of valinomycin at the mitochondria (Salvioli *et al.*, 2000; Foreman *et al.*, 2006). However, the response to 4-aminopyridine was essentially unchanged, the mean increase in fluorescence 5 min after exposure to 4-aminopyridine being  $24.8 \pm 2.0\%$  after valinomycin pre-treatment (normalized to fluorescence intensity in the presence of valinomycin; 4 experiments; 220 cells) and  $20.8 \pm 2.0\%$  in parallel controls (4 paired experiments, 195 cells; paired *t*-test,  $P > 0.05$ ).

Figure 2.4

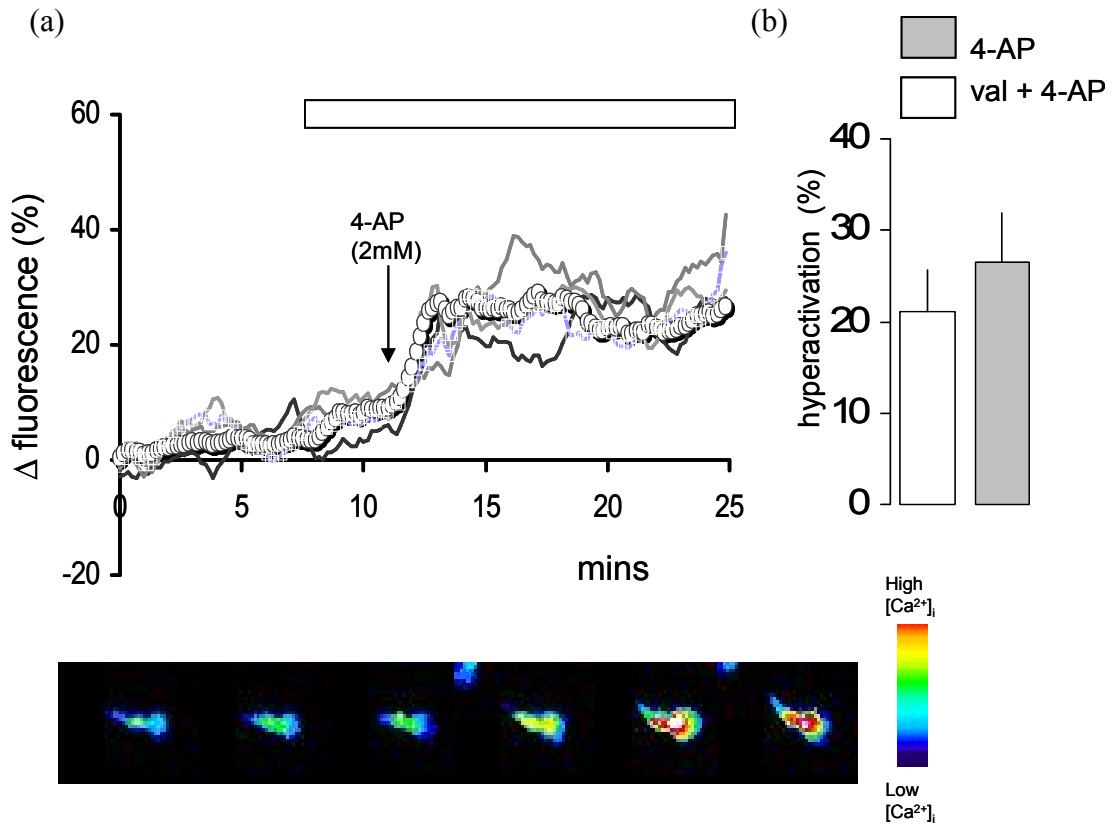


**Figure 2.4.** Investigation whether modulation of  $E_m$  (due to  $K^+$  channel blockade) might underlie the action of 4-aminopyridine. **(a)**  $E_m$  was clamped at  $E_k$  (-83mV) by pre-incubating cells with the  $K^+$  -ionophore valinomycin (1 $\mu$ M, white bar) and incubation with 2mM 4-aminopyridine (black arrow) on  $[Ca^{2+}]_i$  (Oregon Green BAPTA-1 fluorescence) in capacitated human sperm bathed in standard saline. Traces show 6 responses of representative cells and also mean response (o-o) of all 76 cells in this experiment. Lower panel shows pseudo-colour images (warm colours show high  $[Ca^{2+}]_i$ ) of Oregon Green-1 BAPTA fluorescence in sperm cell at various points in the experiment. First two images are prior to treatment, images 3 and 4 are during valinomycin superfusion and images 5 and 6 are during valinomycin and 4-aminopyridine superfusion. **(b)** Exposure to valinomycin and 4-aminopyridine (open bar) reduced slightly the % of hyperactivation (paired  $t$ -test,  $P > 0.05$ ,  $n = 7$  experiments).

## 2.5 Discussion

Hyperactivation is essential for sperm detachment from oviductal epithelium and penetration of the outer vestments of the oocyte (Stauss *et al.*, 1995; Carlson *et al.*, 2003; Ho and Suarez, 2001a; Ho *et al.*, 2009). Hyperactivated motility occurs when the flagellum develops high amplitude waves in the proximal rather than the distal region (Mortimer *et al.*, 1997). When the wave is propagated its movement away from the proximal region of the tail results in the sperm head being moved back toward the average path at a high velocity much like a whiplash. To identify hyperactivated sperm CASA thresholds for human sperm analyzed at 60Hz are  $VCL \geq 150\mu\text{m/s}$  and  $Lin \leq 50\%$  and  $ALH_{\text{max}} \geq 7.0\mu\text{m}$  (section 1.11.1) (Mortimer *et al.*, 1997). This is an indirect measure of flagellar bend amplitude, because the head is displaced from side-to-side by the developing principal and reverse bends and it gets wagged further by deeper flagellar bends. Because ALH is not a direct measure of flagellar bends it is imperfect however CASA compensates by precision and acquisition of data from hundreds of sperm.

### *4-aminopyridine induced hyperactivation in capacitated human spermatozoa*

Previously our group demonstrated the potent effect of 4-aminopyridine on human sperm motility. Gu *et al.* (2004) found that application of 4-aminopyridine (2mM) induced a dramatic increase in hyperactivated motility in capacitated human spermatozoa (Gu *et al.*, 2004; Barfield *et al.*, 2005). The proportion of hyperactivated sperm increased from 3-5% in control experiments to 40-50% following stimulation with 4-aminopyridine (Gu *et al.*, 2004). The potency of 4-aminopyridine is strongly dependent upon  $\text{pH}_o$  which explains the discrepancy between the results presented here and those reported by Gu *et al.*, (2004). At elevated  $\text{pH}_o$  ( $>8.0$ ) the proportion of the compound which in a non-ionised form and therefore membrane permeable is greatly enhanced (Howe and Richie, 1991; Stephens *et al.*, 1994). 4-aminopyridine is a weak organic base ( $\text{pK}_a$  9.2, Albert *et al.*, 1948; Babiak and Testa, 1976) and at physiological pH exists in equilibrium between the neutral (figure 1.8a) and protonated



forms (figure 1.8b) that strongly favors the charged form. By maintaining extracellular pH at 7.3, membrane permeability of the compound is lowered, resulting in a lower proportion of spermatozoa displaying hyperactivated motility ( $3.0 \pm 2.5$  in control experiments to  $15.6 \pm 4.0\%$  following stimulation with 4-aminopyridine ( $n=9$ ;  $P<0.001$ ; figure 2.1a). Furthermore throughout these experiments we have utilized 20 $\mu$ m depth CASA chambers rather than 50 $\mu$ m depth chamber often used in hyperactivation experiments. Use of these chambers may result in some constraint of flagellar movements and further explain the lower proportion of 4-aminopyridine induced hyperactivation rates. Despite this, application of 4-aminopyridine increased the proportion of hyperactivated cells three fold in comparison to parallel controls.

#### *4-aminopyridine increased $[Ca^{2+}]_i$ fluorescence in human spermatozoa*

Control of motility and hyperactivation is dependent on  $[Ca^{2+}]_i$  signalling in the principal piece and midpiece of the flagellum. Application of 2mM 4-aminopyridine to cells loaded with OGB induced a sustained increase in  $[Ca^{2+}]_i$  in  $\approx 75\%$  human spermatozoa. Fluorescence increased within 10-30 seconds and stabilised at an elevated level 1-5mins after application (figure 2.2). Upon washout of 4-aminopyridine  $[Ca^{2+}]_i$  immediately falls to levels at or near those observed before treatment. It is unclear from these initial experiments as to the source of 4-aminopyridine induced sustained increase in  $[Ca^{2+}]_i$  since human spermatozoa contain both plasma membrane calcium channels and an intracellular calcium store localised at the proximal head/midpiece. These results are consistent with other studies which demonstrate 4-aminopyridine induced  $Ca^{2+}$  mobilisation in a wide variety of cell types including astrocytes, neurons, and skeletal muscle cells (Grimaldi *et al.*, 2001).

Examination of OGB emission spectra in the presence and absence of 4-aminopyridine indicated a degree of fluorescent quenching and decreased fluorescent signal. However, the effect of 4-aminopyridine will lead to an underestimate not an exaggeration of effect on  $[Ca^{2+}]_i$ . Increased intracellular calcium is pivotal for the induction of hyperactivation and therefore

must be examined. Furthermore, the varying nature of human sperm  $[Ca^{2+}]_i$  response justified the examination of individual imaging traces, not visible in population responses.

#### *4-aminopyridine and $K^+$ channel blockade*

4-aminopyridine is a broad spectrum  $K^+$  channel blocker. Human spermatozoa express  $K^+$  channels and blocking these channels could cause  $E_m$  depolarisation induced calcium influx. Therefore, 4-aminopyridine may be modulating  $E_m$  resulting in  $Ca^{2+}$  influx and hyperactivated motility. Spermatozoa were pre-treated with the  $K^+$  ionophore, valinomycin prior to examination of the effects of 4-aminopyridine on  $[Ca^{2+}]_i$  and hyperactivation. 4-aminopyridine induced hyperactivation was not significantly affected by valinomycin. Imaging experiments show that valinomycin caused a significant sustained increase in  $[Ca^{2+}]_i$  in single cell responses however this may be due to modulation of sperm mitochondria. In somatic cells mitochondria play an important role in regulation of intracellular  $Ca^{2+}$  signalling. Mitochondria sequester increased  $[Ca^{2+}]_i$  through the mitochondrial  $Ca^{2+}$  uniporter (MCU), which is driven by the large negative potential across the inner mitochondrial membrane (Parekh, 2003; Breitbart *et al.*, 1983; 1996). Valinomycin has previously been shown to uncouple oxidative phosphorylation and dissipate mitochondrial membrane potential (Salviolo *et al.*, 2000; Amaral and Ramalho-Santos, 2009) and inhibit mitochondrial  $Ca^{2+}$  uptake in rat primary bone marrow stromal cells (Foreman *et al.*, 2006). However, the response to 4-aminopyridine was essentially unchanged, the mean increase in fluorescence 5 min after exposure to 4-aminopyridine was slightly higher than parallel controls. These results, are in agreement with Xia and Ren (2009b) who used a similar approach to show that the recorded  $[Ca^{2+}]_i$  influx was not dependent on  $E_m$  and activation of voltage gated  $Ca^{2+}$  channels. In summary, the 4-aminopyridine induced  $[Ca^{2+}]_i$  increase is not dependent on membrane voltage change which persists when the voltage is “clamped” with valinomycin.

In whole cell patch clamp, a constitutively active, weakly outwardly rectifying  $K^+$  current was measured ( $I_{K_{Sper}}$ ), localised to the principal piece of the flagellum (Navarro *et al.*, 2007). This current activates in response to intracellular alkalinisation, leading to hyperpolarisation and an increased driving force for calcium entry through CatSper channels. Navarro *et al.*, (2008) have suggested that Slo3 channels are the best candidate for the  $K^+$  current ( $I_{K_{Sper}}$ ) principally because of Slo3 pH sensitivity although other disagree due to key differences between  $K_{Sper}$  and Slo3 (Martínez-López *et al.*, 2009). Martínez-López *et al.*, (2009) report that Slo3  $K^+$  currents were inhibited by  $Ba^{2+}$  and stimulated by 8 Br-cAMP whereas  $I_{K_{Sper}}$  was weakly inhibited by  $Ba^{2+}$  and insensitive to cAMP (Navarro *et al.*, 2007). Although  $K^+$  channel activity was not measured directly in this study, recent data on the pharmacological properties of Slo3 channels (expressed in *Xenopus* oocytes) demonstrated that extracellular 4-aminopyridine has little effect on the  $K^+$  current (Tang *et al.*, 2010). The authors conclude that any accumulation of 4-aminopyridine in the cytosol would elevate pH to promote Slo3 activity (act in opposition to any channel blocking effects).

In summary, exposure of capacitated human spermatozoa to 2mM 4-aminopyridine induced hyperactivation in a proportion of sperm and a sustained increase in  $[Ca^{2+}]_i$  in the majority of cells. The 4-aminopyridine induced increase in  $[Ca^{2+}]_i$  was independent of  $K^+$  fluxes however the source of calcium is not clear from these experiments.

## **CHAPTER THREE**

### **EFFECT OF pH ON 4-AMINOPYRIDINE INDUCED**

### **HYPERACTIVATION AND ELEVATION OF $[Ca^{2+}]_i$**

<b>3.1 Abstract</b>	74
<b>3.2 Introduction</b>	75
<b>3.3 Materials and methods</b>	77
3.3.1 Materials	77
3.3.2 Spermatozoa preparation and capacitation	77
3.3.3 Fluorimetry	77
3.3.4 Evaluation of sperm hyperactivation	78
3.3.5 Evaluation of extracellular pH and degree of 4-aminopyridine ionisation	79
3.3.6 Single Cell Imaging	79
3.3.7 Imaging data processing	79
3.3.8 Statistical Analysis	79
<b>3.4 Results</b>	
3.4.1 Ionisation state of 4-aminopyridine was dependent on $pH_o$	80
3.4.2 4-aminopyridine induced hyperactivation was significantly increased at extracellular pH 8.5	81
3.4.3 Extracellular pH effects 4-aminopyridine induced $[Ca^{2+}]_i$ fluorescence Response in human sperm	84
3.4.4 Effects of $NH_4Cl$ on intracellular pH and 4-aminopyridine induced hyperactivation and $[Ca^{2+}]_i$ fluorescence response	88
3.4.5 Effect of propionate pre-treatment on 4-aminopyridine induced $[Ca^{2+}]_i$ fluorescence response	92
<b>3.5 Discussion</b>	94

### 3.1 Abstract

Various studies have shown that a pH-stimulated  $\text{Ca}^{2+}$  increase in sperm, triggers hyperactivation (Mújica *et al.*, 1994; Marquez and Suarez, 2004, 2007). Navarro *et al.*, (2007) demonstrated that 4-aminopyridine (pKa9.2) induced cytoplasmic alkalinisation enhanced the pH-sensitive K<sub>sper</sub> and CatSper currents in mouse sperm. Assessment using BCECF confirmed that 2mM 4-aminopyridine caused an immediate increase in  $\text{pH}_i$  of  $\approx 0.2$  units in human sperm. To investigate whether cytoplasmic alkalinisation of human sperm might underlie the effect of 4-aminopyridine on  $[\text{Ca}^{2+}]_i$  and hyperactivation  $\text{NH}_4\text{Cl}$  was used directly to increase  $\text{pH}_i$ . Exposure of sperm to  $\text{NH}_4\text{Cl}$  had an almost identical effect on  $\text{pH}_i$  and also caused a sustained increase in  $[\text{Ca}^{2+}]_i$  only slightly less than that seen with 2mM 4-aminopyridine. However, there was negligible induction of hyperactivation compared to cells treated with 4-aminopyridine. Treatment of sperm with propionate (to decrease  $\text{pH}_i$  and inhibit CatSper channel) did not significantly effect 4-aminopyridine induced hyperactivation but enhanced the effect of 4-aminopyridine on  $[\text{Ca}^{2+}]_i$ . In summary the 4-aminopyridine induced hyperactivation response in human sperm is not solely pH or CatSper channel dependent.

### 3.2 Introduction

Human spermatozoa are quiescent in the male reproductive system and become activated upon ejaculation (Acott and Carr, 1984; Carr and Acott, 1989; Giroux-Widemann *et al.*, 1991). Intracellular pH is a critical regulator of sperm function and cytoplasmic alkalinisation is essential for the initiation and maintenance of motility, capacitation, chemotaxis, hyperactivation and the acrosome reaction (Acott and Carr, 1984; Parrish *et al.*, 1989; Cook and Babcock, 1993; Jones and Barvister, 2000; Ho *et al.*, 2002; Böhmer *et al.*, 2005; Darszon *et al.*, 2006; Marquez and Suarez, 2007; Shiba *et al.*, 2008). Despite the importance of intracellular alkalinisation to sperm motility the mechanisms enabling or enhancing transition from activated to hyperactivated motility are unclear.

Transition from activated to hyperactivated motility also requires an increase in  $[Ca^{2+}]_i$ . Influx through calcium channels (localised in the flagellum) or release from intracellular stores have been shown to play a role in supporting and sustaining hyperactivation. Calcium channels include transient receptor potential channels, cyclic nucleotide gated calcium channels and voltage-gated  $Ca^{2+}$  channels and the pH sensitive sperm specific CatSper calcium. Male mice lacking functional CatSper1 or CatSper2 genes are sterile (Ren *et al.*, 2001; Quill *et al.*, 2001; Carlson *et al.*, 2003, 2005). . It has been shown that intracellular alkalinisation potentiates an inward  $Ca^{2+}$  current through CatSper-associated channels (Kirichok *et al.*, 2006; Navarro *et al.*, 2007; Xia and Ren, 2009b). The weak base 4-aminopyridine (pKa9.2) induced cytoplasmic alkalinisation enhanced  $I_{K_{Sper}}$  induced hyperpolarisation resulting in an increased driving force for  $Ca^{2+}$  entry through CatSper channels (Navarro *et al.*, 2007). In addition, the weak base procaine has been shown to induce hyperactivation in bovine sperm which further implicates pH as a component in the signalling pathway that control  $Ca^{2+}$  entry and hyperactivation (Mújica *et al.*, 1994; Marquez and Suarez, 2004).

However, studies in rodent and bovine sperm has provided strong evidence that the elevation of  $[Ca^{2+}]_i$  that occurs upon mobilisation of  $Ca^{2+}$ , from a store in the sperm neck/midpiece

region also contribute to regulation of flagellar activity, including (or at least facilitating) aspects of hyperactivation (Ho *et al.*, 2001b; 2003). It is unclear if store mobilisation contributes or interacts with the CatSper channels (Olson *et al.*, 2010).

Since the efficacy of 4-aminopyridine (Howe and Ritchie, 1991; Stephens *et al.*, 1994) is strongly dependent upon pH, this report examines the effects of intracellular and extracellular pH modulation on 4-aminopyridine induced responses in human sperm.

### **3.3 Experimental Procedures**

#### **3.3.1 Materials**

Supplemented Earle's balanced salt solution (sEBSS) was prepared as in chapter two. For maintenance of pH at 8.5, HEPES was replaced with 10mM [(2-hydroxy-1,1-bis(hydromethyl)ethyl)amino]-1-propanesulfonic acid (TAPS). For maintenance of pH at 6.5, HEPES was replaced with 10mM N-(2-acetamido)iminodiacetic acid (ADA). Ammonium supplemented sEBSS (25mM) and proprionate supplemented sEBSS (15mM, pH 8.5) was prepared in the laboratory. Non-capacitating saline was prepared as for standard saline with the omission of  $\text{NaHCO}_3$  and BSA. Osmotic strength was maintained (285-295mOmol) by adjusting NaCl in all saline prepared.

#### **3.3.2 Spermatozoa preparation and capacitation**

As described in chapter two with the following modifications.

Spermatozoa were harvested by direct swim-up into non-capacitating saline without  $\text{NaHCO}_3$  and BSA.

#### **3.3.3 Fluorimetry**

For fluorimetric studies on  $\text{pH}_i$ , 2ml aliquots ( $6 \times 10^6$  cells. $\text{ml}^{-1}$ ) were labelled with  $1\mu\text{M}$  2'-7'-bis-(2-carboxyethyl)-5-(and-6-)-carboxyfluorescein acetoxymethyl ester (BCECF-AM) for 30 min at  $37^\circ\text{C}$  and 5.5%  $\text{CO}_2$  then centrifuged (300g for 5 min). The pellet was re-suspended in sEBSS with pH adjusted and buffered as required. Excitation wavelengths alternated between 440 and 495nm. Emission was recorded at 535nm with slit width was set at 15nm and a sampling rate of 12.5Hz. The  $\text{pH}_i$  values for control and 4-aminopyridine or  $\text{NH}_4\text{Cl}$  were determined using a calibration procedure similar to that described by Fraire-Zamora and Gonzalez-Martinez (2004). Briefly, cells suspended in sEBSS at pH 7.35 were permeabilised with Triton X-100 (final concentration 0.12%) then a series of additions of HCl were made. At



each step (including the one obtained after detergent addition) the pH was determined with a conventional pH electrode to obtain a calibration curve. BCECF ratio values were plotted as a function of pH. As the ratio was linear in the pH range between 6.5 and 7.35 (figure 3.4a) a simple transformation using a straight line equation was performed to estimate  $\text{pH}_i$  values from experimental data.

For fluorimetric studies on sperm  $[\text{Ca}^{2+}]_i$  2ml aliquots ( $6 \times 10^6$  cells. $\text{ml}^{-1}$ ) were labelled with  $1\mu\text{M}$  fura-2 acetoxymethyl ester (fura-2/AM) for 12 min at  $37^\circ\text{C}$  and 5%  $\text{CO}_2$ , centrifuged (300 g for 5 min) and re-suspended in sEBSS for a further 17 min ( $37^\circ\text{C}$ ) to allow for further de-esterification of the dye. Experiments were carried out using a Perkin-Elmer LS50B fluorescence spectrofluorimeter running FLWinlab version 2.01. Fluorimetry was performed in a magnetically stirred methylacrylate cuvette maintained at constant temperature by a water jacket ( $25^\circ\text{C}$  or  $37^\circ\text{C}$ ). Excitation wavelengths alternated between 340 and 380nm. Emission was recorded at 510 nm with slit width was set at 15nm with a sampling rate of 12.5Hz. Calibration of  $[\text{Ca}^{2+}]_i$  was carried out using digitonin ( $50\mu\text{M}$ ) to generate a maximal response and subsequent addition of EGTA (20mM) to provide a minimum. A  $K_d$  value of 224nM was assumed and calibration was performed according to the equation of Grynkiewicz *et al.* (1985).

### **3.3.4 Evaluation of sperm hyperactivation**

For experiments involving TAPS-buffered medium, cells were centrifuged (300 g for 5 min) and the pellet re-suspended in 1ml TAPS buffered saline immediately prior to the experiment. 200 $\mu\text{l}$  aliquots were treated with either saline (control) or 4-aminopyridine and immediately introduced into a 20 $\mu\text{M}$  depth chamber (Microcell, Conception Technologies Ltd.) at a concentration of  $\sim 6$  million/ml on a Hamilton Thorne HTM IVOS semen analyzer ( $37^\circ\text{C}$ ). Hyperactivation was defined as in chapter two.

### 3.3.5 Evaluation of extracellular pH on degree of 4-aminopyridine ionisation

The Henderson-Hasselbalch equation for a weak base is as follows

$$pH = \frac{[B]}{[BH^+]} + pKa \quad (1)$$

Using this equation the % ionisation of the weak base can be calculated from the ratio of the ionised to neutral compound, multiplied by 100.

$$\% \text{ionisation} = \frac{I \bullet 100}{I + N} \quad \begin{array}{l} I = \text{ionised 4-aminopyridine} \\ N = \text{neutral 4-aminopyridine} \end{array} \quad (2)$$

$$\text{Rearranged as } \frac{N}{I} = \text{antilog}(pH - pKa) \quad (3)$$

$$\text{Solved for } N = I \bullet \text{antilog}(pH - pKa) \quad (4)$$

Upon substitution of (4) into (2) the equation for % ionisation for a weak base is as follows:

$$\% \text{ionisation (base)} = \frac{100}{1 + \text{antilog}(pH - pKa)}$$

### 3.3.6 Single Cell Imaging

As in chapter two.

### 3.3.7 Imaging Data Processing

As in chapter two.

### 3.3.8 Statistical analysis

As in chapter two.

### 3.4 Results

#### 3.4.1 Ionisation state of 4-aminopyridine was dependent on pH<sub>o</sub>

The potency and membrane permeability of 4-aminopyridine is dependent upon the ionisation state of the compound. A modified Henderson-Hasselbach equation was used to calculate % ionisation of 4-aminopyridine (pKa9.2 at 25°C, Albert *et al.*, 1948; Babiak and Testa, 1976) over a range of pH values (see methods 3.3.5). At physiological pH, the basic nature of 4-aminopyridine leads to an equilibrium between the ionised (I) and neutral (N) form that strongly favors the protonated form (~99%) (figure 3.1). At pH<sub>o</sub>7.3 the majority of the compound is charged and membrane impermeable (Howe and Richie, 1991; Zhang *et al.*, 1998), whereas at pH<sub>o</sub>8.5 approximately 20% of the compound is in a neutral, membrane permeable form.

Figure 3.1

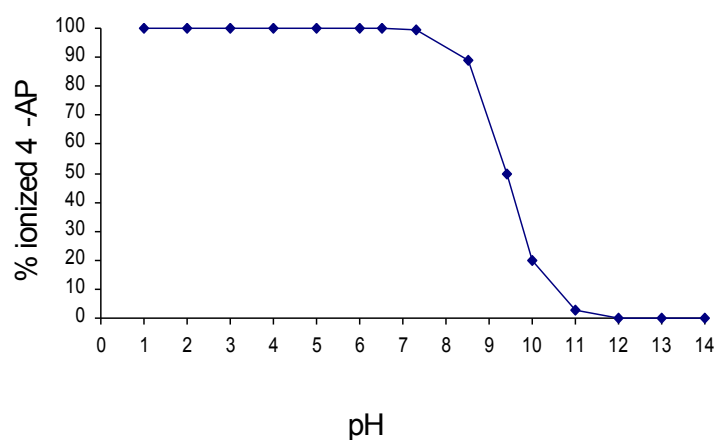


Figure 3.1: 4-aminopyridine % ionisation was calculated (see text) for a range of pH values from the 4-aminopyridine pKa value of 9.2 at 25°C (Albert *et al.*, 1948; Babiak and Testa, 1976)

### ***3.4.2 4-aminopyridine induced hyperactivation was significantly increased at extracellular pH8.5***

Initially we investigated the efficacy of 4-aminopyridine at a  $pH_o$  of 8.5 (sEBSS with HEPES replaced by 10mM TAPS) (figure 3.2a). Elevation of  $pH_o$  had no significant effect on the level of hyperactivation, increasing the proportion of hyperactivated cells assessed by CASA from  $5.1 \pm 1.2$  to  $8.1 \pm 2.2\%$  ( $n=14$ ,  $p=0.09$ , paired  $t$ -test,  $P>0.05$ ). However, upon application of 2mM 4-aminopyridine at  $pH_o 8.5$  the proportion of hyperactivated cells increased to  $33.1 \pm 3.1\%$  ( $n=14$ ;  $P<10^{-6}$  compared to control, paired  $t$ -test) more than double that which was seen at  $pH_o 7.35$  (unpaired  $t$ -test,  $P<0.0005$ ). This action of 4-aminopyridine was clearly dose dependent (figure 3.2a), application of 0.5mM 4-aminopyridine induced hyperactivation in only  $\approx 7.5$  of cells and no effect was detectable at a dose of 0.1mM ( $pH_o 8.5$ , TAPS buffered media). At 10mM 4-aminopyridine induced hyperactivation in  $26.3 \pm 5.3\%$  of cells ( $pH 8.5$ , TAPS buffered media). To facilitate observation of the effect of 4-aminopyridine, all subsequent experiments (unless stated otherwise) were carried out at  $pH_o 8.5$ .

The ability of 4-aminopyridine to induce hyperactivation was independent of capacitation. Highly motile sperm cells were harvested by direct swim-up into non-capacitating sEBSS (NCsEBSS, lacking BSA and  $HCO_3^-$ ) or standard saline as previously described. Motility was immediately assessed by CASA in the presence and absence of 4-aminopyridine (2mM). The proportion of hyperactivated cells did not differ significantly between treatments (NCsEBSS cells=  $27.2 \pm 8.0\%$ , standard sEBSS  $31.5 \pm 2.6\%$ ,  $n=6$  experiments, paired  $t$ -test,  $P>0.05$ ) (figure 3.1b). Similarly, cells capacitated for  $\sim 1$  hour (time taken to swim-up and assess) did not differ significantly from cells capacitated for 5-6 hours in the response to 4-aminopyridine ( $t=1$  hour capacitation  $31.5 \pm 2.6\%$ ,  $t=5-6$  hours capacitation  $30.8 \pm 5.6\%$ ,  $n=6$  paired  $t$ -test,  $P>0.05$ ) (figure 3.2b).

Since inhibition of  $K^+$  channels has been shown to have a deleterious effect on intracellular volume regulation and motility in human sperm (Yeung and Cooper, 2001), the effects of prolonged exposure to 2mM 4-aminopyridine was investigated (figure 3.2c). Sperm were capacitated in standard saline for 4/5 hours and 4-aminopyridine induced hyperactivation assessed by CASA ( $37.3 \pm 8.2\%$  hyperactivation after 2 minutes -minimum time taken to load and assess sample). The effects of 2mM 4-aminopyridine showed only a minor decay when the same aliquot of cells was tested 45 minutes later ( $30.0 \pm 7.5\%$ ) ( $n=3$ exps, paired  $t$ -test,  $P>0.05$ ). Similarly, % motility was not significantly altered despite prolonged exposure to 4-aminopyridine ( $82.8 \pm 3.6\%$   $t=2$ mins,  $82.2 \pm 3.7\%$   $t=45$ mins,  $n=3$ experiments, paired  $t$ -test,  $P>0.05$ ).

Figure 3.2

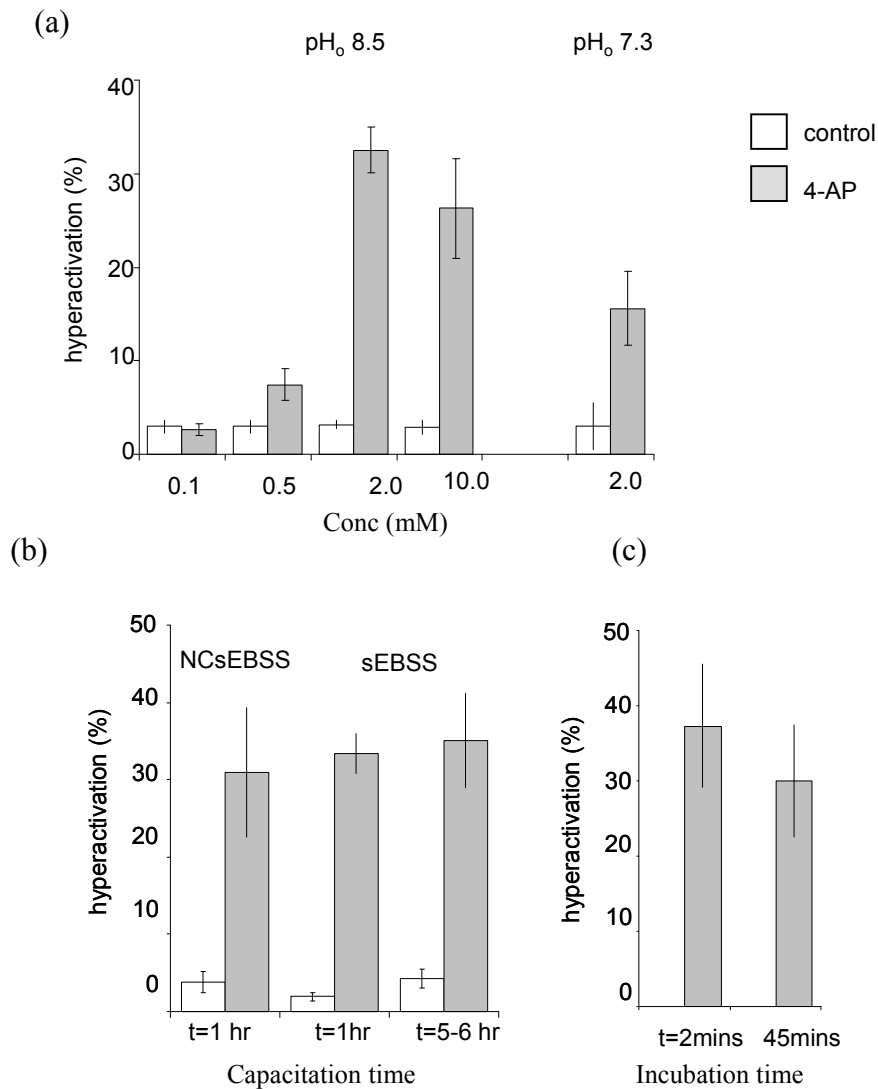


**Figure 3.2.** 4-aminopyridine (2mM) induced hyperactivation in non-capacitated and capacitated human spermatozoa (assessed by CASA) is enhanced at pH<sub>o</sub> 8.5. **(a)** The efficacy of (2mM) 4-aminopyridine to induce hyperactivation was greatly enhanced at pH<sub>o</sub> 8.5 in comparison to pH<sub>o</sub> 7.3. This action of 4-aminopyridine was clearly dose dependent with maximal effect at 2mM, each bar shows mean  $\pm$  s.e.m. of 9 experiments ( $P < 0.001$ ; paired  $t$ -test). **(b)** The ability of 4-aminopyridine to induce hyperactivation did not significantly differ between non-capacitated cells (NCsEBSS,  $n=6$  exps) and capacitated cells (1hr or 5-6hrs) ( $n=6$  exps, paired  $t$ -test,  $P > 0.05$ ). **(c)** The proportion of 4-aminopyridine induced hyperactivated cells remained constant over a prolonged exposure period ( $n=3$ , 45 mins) in capacitated cells.

### 3.4.3 Extracellular pH effects 4-aminopyridine induced $[Ca^{2+}]_i$ fluorescence response in human spermatozoa

Initially the effect of lowering  $pH_o$  (from 7.35 to 6.5), prior to application of 2mM 4-aminopyridine was investigated. Superfusion of cells with saline ( $pH_o$ 6.5) decreased  $[Ca^{2+}]_i$  fluorescence in ~30% of cells (decrease of ~10%) but in many cells there was no discernible effect (figure 3.3 a). Application of 2mM 4-aminopyridine resulted in an increase in  $[Ca^{2+}]_i$  fluorescence in 37% of cells (a transient response of  $21.2 \pm 1.0\%$  in 10% of cells and a sustained increase of  $8.5 \pm 0.3\%$  in 27% of cells ( $n=4$  experiments, 264 cells)).

Increasing  $pH_o$  (from 7.35 to 8.5) caused a detectable increase in  $[Ca^{2+}]_i$  fluorescence in ~95% of cells, fluorescence of OGB stabilising within 2-3 min at 10-15% above control levels (figure 3.3b ) ( $pH_i$  increased from  $7.08 \pm 0.10$  ( $n=23$ ) to  $7.2 \pm 0.10$  ( $n=17$ ; paired  $t$ -test,  $P>0.05$ ). Application of 2mM 4-aminopyridine caused a further significant increase in  $[Ca^{2+}]_i$  fluorescence in 75% of cells, a similar proportion to that observed at pH 7.35. The amplitude of this response ( $24.5 \pm 0.66\%$  of fluorescence intensity at pH8.5; 8 experiments, 580 cells) was greater than at pH7.35 ( $15.0 \pm 1.4\%$ , paired  $t$ -test,  $P=0.01$ ; figure 2.2). It was not necessary to sensitise the cells to high  $pH_o$  with TAPs buffered saline ( $pH_o$ 8.5), addition of 2mM 4-aminopyridine (to non-Hepes buffered saline) resulted in a significant increase in  $[Ca^{2+}]_i$  fluorescence (amplitude of the response was  $25.3 \pm 4.4\%$  in ~85% of cells 5 mins after exposure ( $n=3$  experiments, 311 cells, unpaired  $t$ -test,  $P<0.05$ ) (figure 3.3c), a response similar to that of cell pre-treated with TAPS buffered saline (figure 3.3b), Upon 4-aminopyridine washout  $[Ca^{2+}]_i$  fluorescence dropped rapidly to pre-application levels and the response could be repeated by re-application of the drug (amplitude of second response  $30.3 \pm 2.8\%$  5 mins after exposure, figure 3.3 c). Similar to the effect of 4-aminopyridine on hyperactivation, elevation of  $[Ca^{2+}]_i$  by 4-aminopyridine applied at  $pH_o$ 8.5 showed a marked dose sensitivity over the range 0.1-2.0mM (figure 3.3d).

In some cells an initial peak was clearly discernible upon application of the drug, followed by a plateau phase. In single cell imaging experiments this was detectable in mean responses ( $R_{\text{tot}}$ ) as a 'notch' occurring 2-3 minutes after application of 4-aminopyridine (figure 3.3c). Fluorimetric (population) records of  $[\text{Ca}^{2+}]_i$  response to 2mM 4-aminopyridine in cells incubated at 25°C and 37°C ( $\text{pH}_o 8.5$ , figure 3.3de) was investigated. Application of 4-aminopyridine to cells at 25°C resulted in a similar response to that of single cell imaging experiments. At both temperatures the response appears to comprise an initial transient response followed by a plateau (consistent with store mobilisation followed by  $\text{Ca}^{2+}$  influx) but separation of the phases is more clearly visible at 37°C.

At 37°C an initial transient response peaked at  $\approx 30$  s after application, followed by a plateau (figure 3.3e). At 25°C the response rose more slowly, taking up to 100 s to reach maximum and then decayed slowly to a plateau (figure 3.3e). The estimated amplitude of the response ( $\Delta [\text{Ca}^{2+}]_i$  at peak) was  $112.1 \pm 16.3 \text{ nM}$  ( $n=6$  exps) at 37°C and  $187.2 \pm 19.2 \text{ nM}$  ( $n=7$  exps) at 25°C.



Figure 3.3

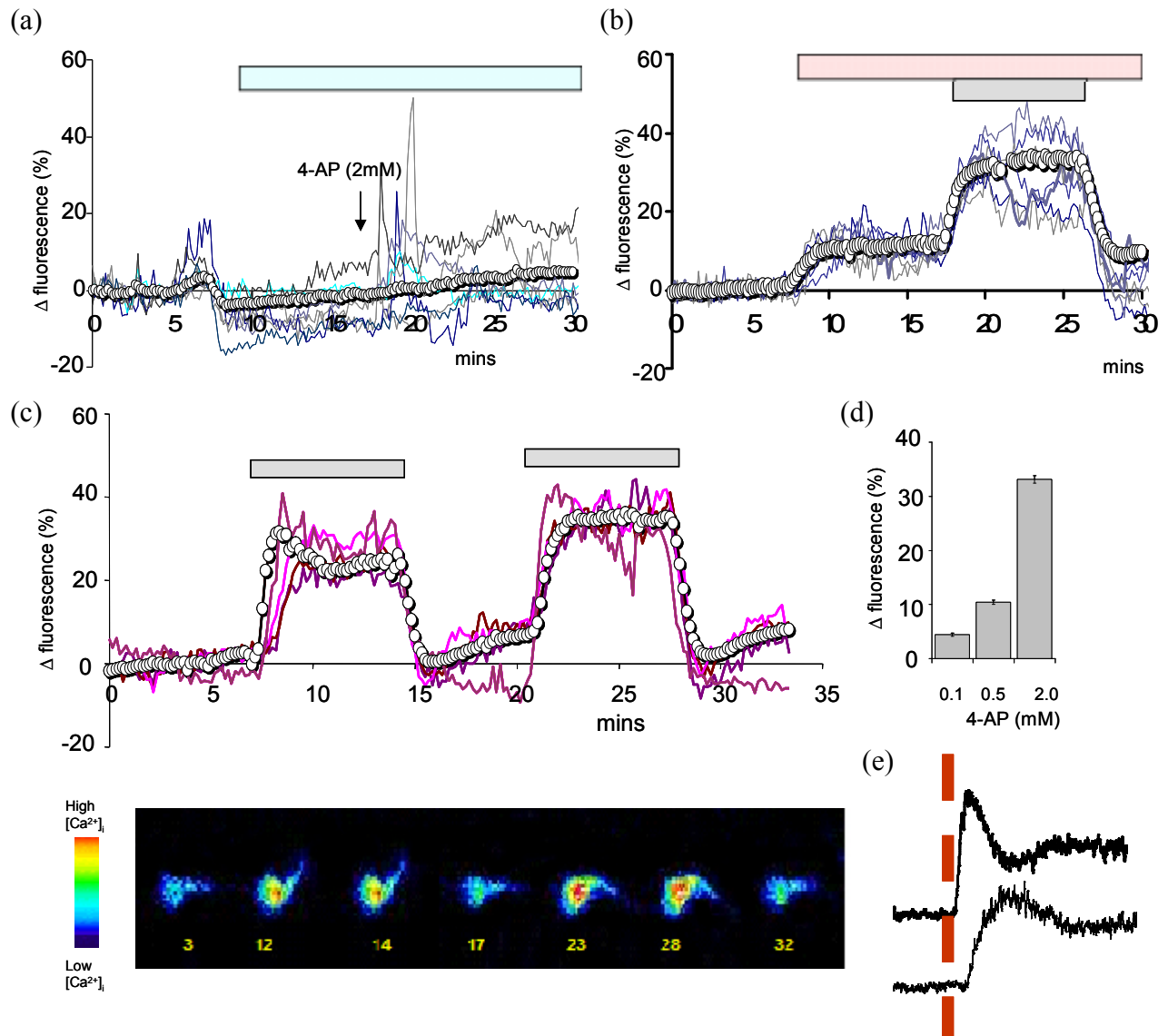


**Figure 3.3.** The effect of extracellular pH on 4-aminopyridine induced  $[Ca^{2+}]_i$  fluorescence response in human sperm. **(a)** Effect of 4-aminopyridine on  $[Ca^{2+}]_i$  fluorescence at pH<sub>o</sub>6.5. Cells were initially superfused with standard sEBSS (~6mins, pH<sub>o</sub>7.35). Superfusion with ADA-buffered saline (pH<sub>o</sub>6.5, blue bar) caused a slight decrease in population  $[Ca^{2+}]_i$  fluorescence. Upon application of 4-aminopyridine (also pH<sub>o</sub>6.5, arrow) there was a transient increase in  $[Ca^{2+}]_i$  fluorescence in a proportion of cells. Responses of 8 representative cells are shown and also mean response (o-o) of all the 66 cells in the experiment. **(b)** Effect of 4-aminopyridine on  $[Ca^{2+}]_i$  (OGB fluorescence) at pH<sub>o</sub>8.5. Cells were initially superfused with standard sEBSS (pH<sub>o</sub>7.35, ~6 mins). Superfusion with TAPS-buffered saline (pH<sub>o</sub>8.5, pink bar) caused a sustained rise in  $[Ca^{2+}]_i$  fluorescence. Upon application of 4-aminopyridine (also pH<sub>o</sub>8.5, grey bar) there was a further and much larger rise in  $[Ca^{2+}]_i$  which reversed immediately upon washout. Responses of 5 representative cells are shown and also mean response (o-o) of all the 70 cells in the experiment. **(c)** 4-aminopyridine enhanced  $[Ca^{2+}]_i$  fluorescence did not require prior sensitisation with TAPS buffered saline. Since 4-aminopyridine can act as a weak base (pK<sub>a</sub>9.2) application in non-buffered

saline (grey bar) caused an increase in  $\text{pH}_o$  and increased  $[\text{Ca}^{2+}]_i$  fluorescence. This effect reversed immediately upon washout and re-application of 4-aminopyridine (grey bar) caused a second significant sustained rise in  $[\text{Ca}^{2+}]_i$  fluorescence which again reversed upon washout. Responses of 10 representative cells are shown and also mean response (o-o) of all the 77 cells in the experiment). Lower panel shows pseudocolour images (warm colours show high  $[\text{Ca}^{2+}]_i$ ) of OGB fluorescence in a sperm cell at various times points (figure in each image shows the time in minutes from start of experiment). **(d)** Elevation of  $[\text{Ca}^{2+}]_i$  by 4-aminopyridine applied at  $\text{pH}_o 8.5$  showed a marked dose sensitivity over the range 0.1-2.0mM **(e)** Fluorimetric (population) records of fura-2/AM labelled  $[\text{Ca}^{2+}]_i$  cell response to 2mM 4-aminopyridine incubated at 37°C (top trace) and 25°C (lower trace). Application of 4-aminopyridine to cells at 25°C resulted a similar response to that of Oregon Green Bapta1 single cell imaging experiments. The response to 4-aminopyridine at 37°C compromised an initial transient response followed by a plateau. Traces have been aligned by the time of 4-aminopyridine application (shown by red dotted line).

### **3.3.4 Effects of NH<sub>4</sub>Cl on intracellular pH and 4-aminopyridine induced hyperactivation and [Ca<sup>2+</sup>]<sub>i</sub> fluorescence response**

As a weak organic base (pK<sub>a</sub>9.2), 4-aminopyridine on entering the cell may directly elevate pH<sub>i</sub>, potentially leading to increased Ca<sup>2+</sup> influx and hyperactivation through activation of pH-regulated CatSper channels. To investigate, we used BCECF directly to monitor intracellular pH in suspensions of human sperm. Fluorimetric experiments on suspended cells (loaded with fura-2) showed that the [Ca<sup>2+</sup>]<sub>i</sub> response to 4-aminopyridine was similar to that of immobilised cells (compare figure 3.3c with 3.3e). In capacitated cells (5-6 hours), the resting pH<sub>o</sub> (calibrated as described in methods, figure 3.4b) was  $7.08 \pm 0.10$  (n=23). Suspension in TAPS-buffered medium (pH<sub>o</sub>8.5) resulted in a slightly increased pH<sub>i</sub> to  $7.2 \pm 0.10$  (n=17; NS). Application of 2mM 4-aminopyridine to cells bathed in TAPS-buffered medium caused an immediate rise in pH<sub>i</sub>, which stabilized within 10-20 s at a value  $0.20 \pm 0.06$  units (n=9) above control level ( $P < 0.01$ ; paired *t*-test; figure 3.4b; grey trace).

To determine whether this effect on pH<sub>i</sub> might be sufficient to explain the observed effects of 4-aminopyridine, we used cell permeant NH<sub>4</sub>Cl to increase pH<sub>i</sub>. In cells suspended in sEBSS held at pH 7.35 (15mM HEPES), 25mM NH<sub>4</sub>Cl rapidly increased pH<sub>i</sub> by  $0.26 \pm 0.06$  units (n=6, figure 3.4b- black trace), consistent with previous studies on human and bovine sperm (Fraire-Zamora and Gonzalez-Martinez, 2004; Marquez and Suarez, 2007). Addition of 4-aminopyridine to cells pre-treated with NH<sub>4</sub>Cl resulted in a further increase of  $\sim 0.10$  (n=4).

In cells suspended in TAPS-buffered (pH<sub>o</sub>8.5) medium, NH<sub>4</sub>Cl increased pH<sub>i</sub> by  $0.18 \pm 0.05$  units (n=9;  $P < 0.01$ ; paired *t*-test), an effect very similar to that caused by 4-aminopyridine ( $P = 0.17$ ; paired *t*-test) figure 3.4b, grey trace).

A similar response occurred in Ca<sup>2+</sup> imaging experiments., upon exposure to 25mM NH<sub>4</sub>Cl we observed a sustained increase in fluorescence in  $\sim 70\%$  of cells (mean response after 5mins exposure  $19.5 \pm 2.6\%$ , 3 mins after exposure; 3 experiments, 168 cells; figure 3.4c) apparently

reflecting CatSper channel activation. However, pretreatment with  $\text{NH}_4\text{Cl}$  did not occlude a subsequent response to 2mM 4-aminopyridine in ~50% of cells (41% of cells responded with 20% increase in  $[\text{Ca}^{2+}]_i$  fluorescence and 9% responded with a transient type response amplitude 32%) (figure 3.4c).

Previous studies have shown that  $\text{NH}_4\text{Cl}$  induced cytoplasmic alkalinisation enhanced  $\text{Ca}^{2+}$  influx and hyperactivation in bovine sperm (Marquez and Suarez, 2007). Surprisingly, the effect of 25mM  $\text{NH}_4\text{Cl}$  (at  $\text{pH}_o 7.3$  or 8.5, figure 3.4d, table 3.1) treatment on hyperactivation was negligible, the proportion of hyperactivated cells increasing from  $3.9 \pm 0.7$  to just  $6.4 \pm 1.3\%$  (at  $\text{pH}_o 7.3$ ) and from  $2.4 \pm 0.8$  to  $7.8 \pm 1.9\%$  ( $\text{pH}_o 8.5$ ) ( $P > 0.05$ ,  $n=7$ ; paired  $t$ -test, figure 3.4d table 3.1). In parallel incubations, 4-aminopyridine increased the proportion of hyperactivated cells from  $3.9 \pm 0.7\%$  to  $15.6 \pm 3.9\%$  ( $\text{pH}_o 7.3$ ) and  $2.4 \pm 0.8\%$  to  $35.6 \pm 1.6\%$  ( $\text{pH}_o 8.5$ ) (paired  $t$ -test,  $P < 0.005$  compared to  $\text{NH}_4\text{Cl}$ ; figure 3.4d, table 3.1). This discrepancy may reflect different criteria for defining hyperactivation. Throughout this report, hyperactivation was defined by the following criteria (Mortimer and Swan, 1995; Mortimer, 2000) - curvilinear velocity  $\geq 150 \mu\text{m/s}$  and linearity  $< 50\%$  and lateral head displacement  $\geq 7 \mu\text{m}$  (analyzed at 60Hz). Examination of overall mean VCL, ALH and LIN (table 3.1) motion parameters demonstrate that addition of  $\text{NH}_4\text{Cl}$  increased ALH and VCL and had a slight effect of %LIN but not to the same extent as parallel 4-aminopyridine treated cells. The application of 4-aminopyridine to  $\text{NH}_4\text{Cl}$  pre-treated cells (at  $\text{pH}_o 8.5$ ) significantly increased the proportion of hyperactivated cells ( $\text{NH}_4\text{Cl}$  only  $7.8 \pm 1.9\%$ , turquoise bar to  $24.7 \pm 7.2\%$   $\text{NH}_4\text{Cl}$  and 4-aminopyridine, stripped bar, figure 3.4d) (paired  $t$ -test,  $P < 0.05$ ). Pre-treatment with  $\text{NH}_4\text{Cl}$  reduced the hyperactivation rates compared to cells treated with 4-aminopyridine only at  $\text{pH}_o 8.5$  (figure 3.4d, table 3.1-  $\text{NH}_4\text{Cl}$  and 4-aminopyridine  $24.7 \pm 7.2\%$  (stripped bar), 4-aminopyridine only  $35.6 \pm 1.6\%$  (grey bar), paired  $t$ -test,  $P > 0.05$ ), apparently due to lowered overall motility rates (table 3.1, TAPS buffered saline % motile =  $90.6 \pm 2.7\%$ ,  $\text{NH}_4\text{Cl}$  and 4-

aminopyridine in TAPS buffered saline % motile=  $78.2 \pm 4.3\%$ , paired *t*-test,  $P < 0.05$ , 7 paired experiments), with some cells observed to arrest with angulated flagellum and became motionless (Gibbons and Gibbons, 1980; Sale, 1986).

**Figure 3.4**

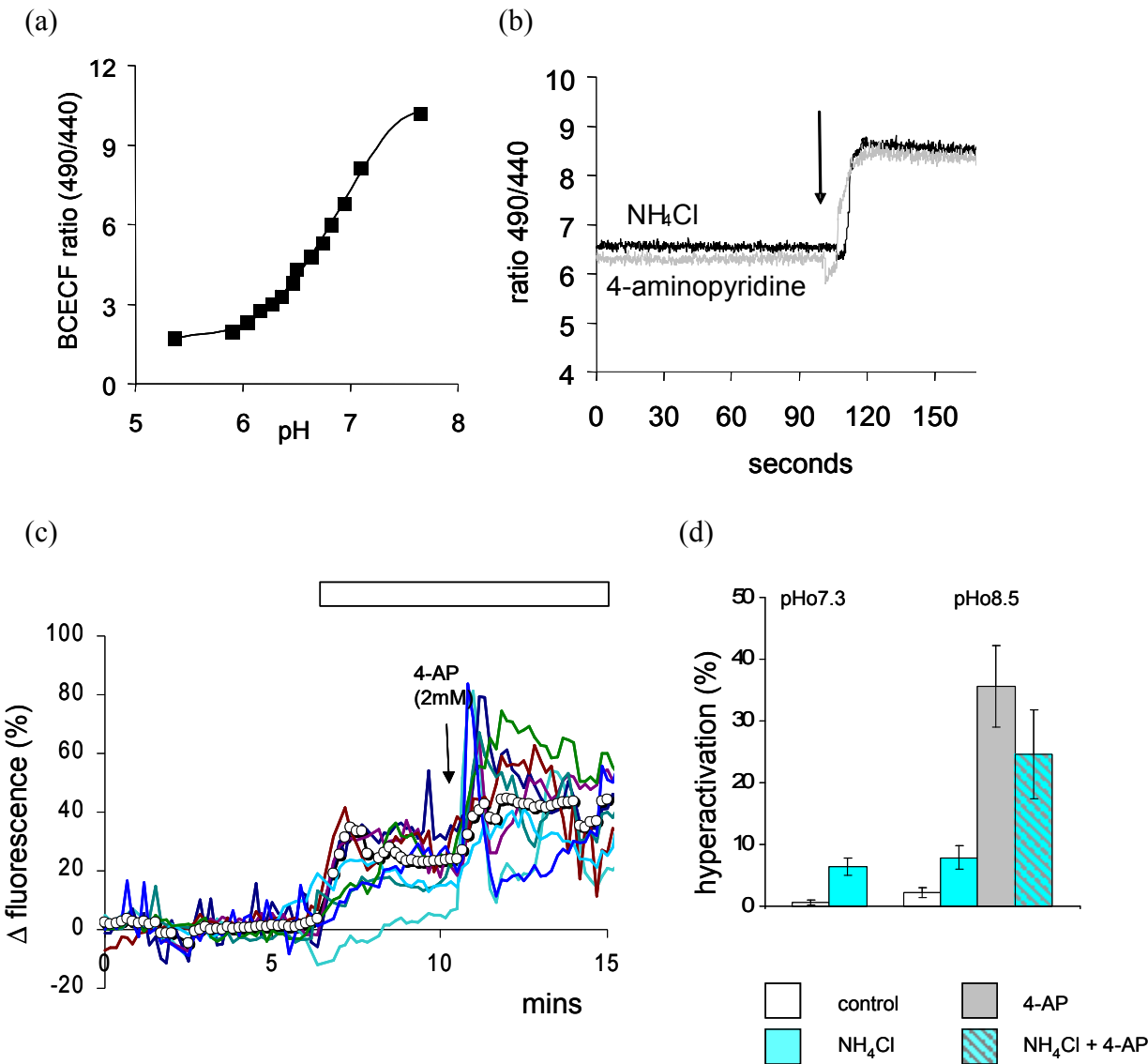


**Table 3.1.** Effect of NH<sub>4</sub>Cl and/or 4-aminopyridine on human sperm motility parameters at pH<sub>i</sub> 7.3 or 8.5 (mean ± s.e.m., n=7 experiments).

	Motile(%)	VCL (μm/sec)	ALH (μm)	LIN (%)	% hyperactivation
Control (pH 7.3)	81.1±3.5	106.6±5.0	4.3±0.2	58.0±1.0	3.9±0.7
+ NH <sub>4</sub> Cl (25mM, pH 7.3)	75.5±4.2	119.5±5.1	5.1±0.2	57.5±0.9	6.4±1.3
+ 4AP (2mM, pH 7.3)	83.6±4.0	121.1±9.4	5.3±0.3	49.6±1.3	15.6±3.9
Control (pH 8.5)	90.6±2.7	117.4±7.3	4.1±0.3	65.1±2.3	2.4±0.8
+ NH <sub>4</sub> Cl (25mM, pH 8.5)	86.3±3.6	137.0±8.1	5.2±0.3	69.0±2.2	7.8±1.9
+ 4-AP (2mM, pH 8.5)	81.4±3.7	190.8±10.2	7.5±0.5	64.7±1.2	35.6±1.6
+ NH <sub>4</sub> Cl (25mM) + 4-AP(2mM) (pH 8.5)	78.2±4.3	168.5±10.1	6.7±0.3	67.0±1.7	24.7±7.4

**Figure 3.4.** The effects of increased intracellular pH on hyperactivation and [Ca<sup>2+</sup>]<sub>i</sub> response in cells exposed to 4-aminopyridine and NH<sub>4</sub>Cl **(a)** an example of calibration plot for BCECF-loaded human sperm. BCECF-loaded sperm suspended in standard sEBSS (pH<sub>o</sub>7.35) were permeabilized with Triton X-100 and the medium was then acidified by serial additions of HCL. After each addition the fluorescence ratio (490/440) was recorded and pH measured with a standard electrode to produce the calibration curve. **(b)** BCECF ratio traces obtained from suspensions of human sperm (from the same sample) exposed to 2mM 4-aminopyridine (grey trace) and 25mM NH<sub>4</sub>Cl (black trace). Additions are marked by the arrow. **(c)** Elevation of [Ca<sup>2+</sup>]<sub>i</sub> fluorescence in response to application of 25mM NH<sub>4</sub>Cl (white bar). Responses of 7 representative cells are shown and also mean response (o-o) of all the 65 cells in the experiment. Application of 2mM 4-aminopyridine (arrow) after exposure to NH<sub>4</sub>Cl induced a further elevation of [Ca<sup>2+</sup>]<sub>i</sub> in 50% of cells (see text). **(d)** The proportion of cells showing hyperactivated motility in TAPS-buffered medium (pH8.5) under control conditions and 2-3 min after addition of 2mM 4-aminopyridine (grey bar) or 25mM NH<sub>4</sub>Cl (turquoise bar) or both compounds (stripped bar). Each bar shows mean ± s.e.m. of 7 experiments. **Table 3.1** CASA motility parameters (% motility, VCL, ALH, LIN and % hyperactivation) for cell treated with NH<sub>4</sub>Cl and/or 4-aminopyridine at pH<sub>o</sub> 7.3 and 8.5 (n=7 exps).

### 3.4.5 Effect of propionate pre-treatment on 4-aminopyridine induced $[Ca^{2+}]_i$ fluorescence response

Previous studies have demonstrated that the ionised form of 4-aminopyridine is most effective intra-cellularly as a  $K^+$  channel blocker (Howe and Richie, 1991; Stephens *et al.*, 1994). Sperm cells were treated with propionate (15mM for 5 mins) to induce intracellular acidification (Cross and Razy-Faulkner, 1997; Sandoval *et al.*, 2007) and enhance ionisation of intracellular 4-aminopyridine. Following the initial control period in standard saline ( $pH_o 7.3 \sim 6$ mins),  $pH_o$  was maintained at 8.5 for the remainder of the experiment (figure 3.5a grey bar). As mentioned previously raising  $pH_o$ , caused a detectable increase in  $[Ca^{2+}]_i$  in  $\sim 80\%$  of cells, fluorescence of OGB stabilising  $\sim 15-20\%$  above control levels. Subsequent addition of propionate (to reduce  $pH_i$ ) caused a slight increase in  $[Ca^{2+}]_i$  calcium (figure 3.5a, blue bar), although in many cells a response was barely discernible. Addition of 2mM 4-aminopyridine (figure 3.5a, black arrow) enhanced  $[Ca^{2+}]_i$  in  $\sim 44\%$  of cells (of these cells 31% responded with a sustained increase of  $43.5 \pm 3.6\%$  and 13% responded with a transient response of  $82.7 \pm 11.0\%$  ( $n=4$  experiments 220 cells figure 3.5b). In paired, non-propionate treated experiments, 82% of cells responded to 4-aminopyridine with an increase of  $23.3 \pm 0.7\%$  ( $n=4$  experiments, 315 cells, figure 3.5b). The frequency distribution of % increase in  $[Ca^{2+}]_i$  amplitude illustrated that although the proportion of propionate pre-treated cells (44%) that responded to 4-aminopyridine was lower in comparison to non-propionate treated control cells (82%), the amplitude of the response was significantly higher (paired  $t$ -test,  $P < 0.05$ , figure 3.5b).

Finally, pre-treatment with propionate enhanced 4-aminopyridine induced hyperactivation rates (at  $pH_o 8.5$ ) although the effect was not significant (figure 3.5c) ( $41.4 \pm 4.9\%$  (stripped bar, figure 3.5c) in comparison to 4-aminopyridine only treated cells  $33.1 \pm 3.6\%$  (grey bar, figure 3.5c) ( $n=7$  experiments, paired  $t$ -test,  $P > 0.05$ ). Motility did not differ significantly between treatments (4-aminopyridine % motility ( $pH_o 8.5$ ) =  $82.4 \pm 3.2\%$  compared with propionate and 4-aminopyridine % motility ( $pH_o$ ) =  $83.0 \pm 3.6\%$ , paired  $t$ -test,  $P > 0.05$ ).

Figure 3.5

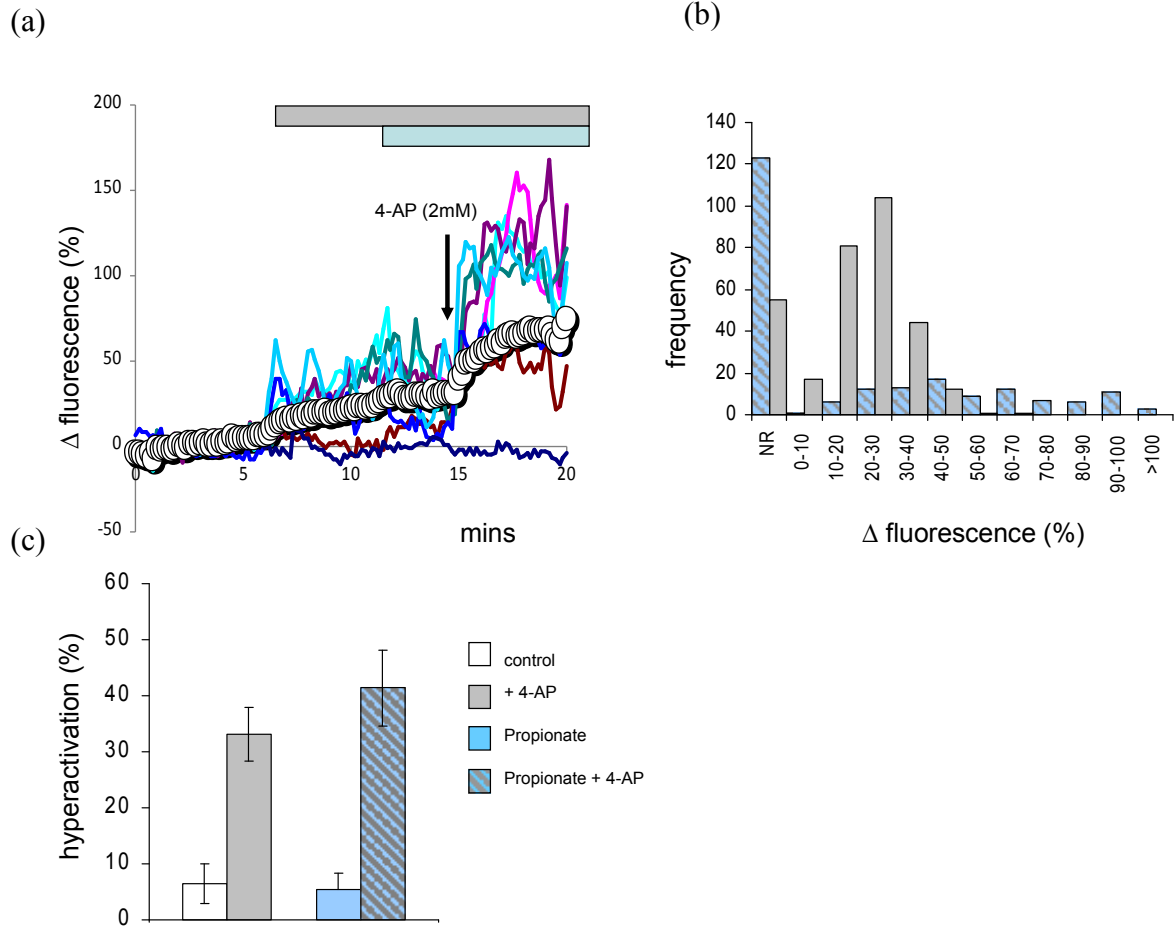


**Figure 3.5** The effect of extracellular alkalinisation and intracellular acidification on the 4-aminopyridine induced hyperactivation and  $[Ca^{2+}]_i$  fluorescence response in human sperm **(a)** Elevation of  $[Ca^{2+}]_i$  (OGB) in response to superfusion with TAPS buffered saline (pH<sub>o</sub>8.5, grey bar) followed by addition of 15mM propionate (~ 5mins, blue bar). Application of 4-aminopyridine (black arrow) resulted in a further significant increase in  $[Ca^{2+}]_i$  fluorescence in  $\approx$  40% of cells. Responses of 8 representative cells are shown and also mean response (o-o) of all the 99 cells in the experiment. **(b)** Although a lower proportion of propionate pre-treated cells responded to 4-aminopyridine (44% versus 82%) the amplitude of the response was significantly increased and is reflected by the frequency distribution shift to higher amplitude of response values. **(c)** Pretreatment of cells with propionate enhanced the proportion of hyperactivated cells in response to 4-aminopyridine at pH<sub>o</sub>8.5 (n=7 paired *t*-test,  $P>0.05$ )



### 3.5 Discussion

Intracellular pH is an important regulator of sperm function reaction (Acott and Carr, 1984; Parrish *et al.*, 1989; Ho *et al.*, 2002, Marquez and Suarez, 2007). During capacitation intracellular pH gradually increases and is associated with flagellar activation, acquisition of progressive motility and transition to hyperactivated motility.

#### *Modulation of $pH_o$ effected 4-aminopyridine induced hyperactivation and $[Ca^{2+}]_i$ response in human sperm*

Membrane permeability of the weak organic base 4-aminopyridine (pKa 9.2, Albert *et al.*, 1948; Babiak and Testa, 1976) was strongly dependent upon  $pH_o$ , consistent with previous reports that the action of the drug depends upon the proportion of the compound that is in the non-ionised (membrane permanent) form (Howe and Richie, 1991; Stephens *et al.*, 1994). Therefore, application of 4-aminopyridine in alkaline saline resulted in an increased proportion of the neutral form of the compound and induced a dose-dependent increase in the proportion of hyperactivated cells (figure 3.2a). 4-aminopyridine induced hyperactivation was independent of capacitation; the response was similar in non-capacitated and capacitated cells. These results agree with Marquez and Suarez (2004) who demonstrated that hyperactivation in bovine cells can occur independently of capacitation.

Sperm, like all mammalian cells, must regulate their volume and treatment with  $K^+$  channel blockers can cause sperm cells to swell significantly effecting motility (Kulkarni *et al.*, 1997; Yeung and Cooper, 2001; Yeung *et al.*, 2004, 2006; Cooper *et al.*, 2005). Human spermatozoa exposed continuously to 4-aminopyridine (2mM) did not show significantly altered % motility over 45 minutes (mean motility  $t=0$  min, 83.3%, and  $t=45$  min 81%,  $n=4$  experiments, paired  $t$ -test,  $P> 0.05$ ). These results are in agreement with Barfield *et al.*, (2005) who found that human spermatozoa exposed to 4-aminopyridine (1mM) for 30 minutes did not significantly

effect cell volume regulation whereas exposure to higher concentrations of 4-aminopyridine (4mM) decreased motility and increased cell volume.

Increased  $\text{pH}_o$  (8.5) enhanced  $[\text{Ca}^{2+}]_i$  in the majority of cells apparently reflecting activation of the pH sensitive CatSper channels. Additionally alkaline  $\text{pH}_o$  affects  $\text{Ca}^{2+}$  clearance, the plasma membrane  $\text{Ca}^{2+}$  ATPase (PMCA) plays a significant role in maintaining basal  $[\text{Ca}^{2+}]_i$  in human sperm and activity is significantly reduced in alkaline  $\text{pH}_o$  but unaffected by cytoplasmic alkalinisation (Xu *et al.*, 2000; Wennemuth *et al.*, 2003b). The sperm sodium calcium exchanger (NCX) also plays a role in  $\text{Ca}^{2+}$  clearance but activity is not significantly affected by high  $\text{pH}_o$  (Linck *et al.*, 1998). Application of 4-aminopyridine in TAPs buffered saline increased the membrane permeable neutral form of the compound, resulting in enhanced  $[\text{Ca}^{2+}]_i$  fluorescence in the majority of cells. The time-course, dose-sensitivity and dependence upon  $\text{pH}_o$  of this effect resembled those for induction of hyperactivation (figure 3.3d). Furthermore since 4-aminopyridine is a weak base ( $\text{pK}_a 9.2$ ) addition to non-Hepes buffered saline induced an immediate reversible  $[\text{Ca}^{2+}]_i$  fluorescence response, cells therefore did not require pre-treatment with alkaline saline to enhance sensitivity to the compound.

Cross (2007) report that BCECF loaded human sperm cells are pH compliant; low  $\text{pH}_o$  reflected by lowered  $\text{pH}_i$ . The sperm specific CatSper channels contribute to resting  $[\text{Ca}^{2+}]_i$  levels (Xia and Ren, 2009a) and are effectively inhibited at low  $\text{pH}_i$  (Carlson *et al.*, 2009). The reduction of  $[\text{Ca}^{2+}]_i$  fluorescence in cells superfused with saline maintained at 6.5 may reflect CatSper channel inactivation. Furthermore application of 4-aminopyridine to saline maintained at  $\text{pH} 6.5$  would result in the majority of the compound been charged and therefore membrane impermeable. However, a proportion of cells responded to 4-aminopyridine with a transient increase in  $[\text{Ca}^{2+}]_i$  fluorescence apparently reflecting store mobilisation.

*Modulation of pHi effected 4-aminopyridine induced hyperactivation and  $[Ca^{2+}]_i$  response in human sperm*

Studies on capacitated human sperm have shown that  $NH_4Cl$  induced cytoplasmic alkalinisation caused a dose-dependent increase in  $[Ca^{2+}]_i$  and enhanced depolarisation-induced  $Ca^{2+}$  influx (Fraire-Zamora and Gonzalez-Martinez, 2004; Neri-Vidaurre Pdel *et al.*, 2006; Publicover *et al.*, 2008). 4-aminopyridine can act as a weak organic base (pKa9.2) and it has been demonstrated recently that cytoplasmic alkalinisation (with 4-aminopyridine or  $NH_4Cl$ ) greatly enhances activity of the pH-sensitive sperm  $K^+$  current ( $I_{KSper}$ ) in the principal piece of mouse sperm by cytoplasmic alkalinisation (Navarro *et al.*, 2007). Since the sperm-specific, pH-sensitive  $Ca^{2+}$ -permeable CatSper channels are similarly localised (Ren *et al.*, 2001; Kirichok *et al.*, 2006), it is possible that 4-aminopyridine induces  $Ca^{2+}$ -influx in the sperm tail (and sustained hyperactivation) may reflect (at least in part) activation of  $I_{CatSper}$ .

Assessment using BCECF confirmed that 2mM 4-aminopyridine caused an immediate increase in  $pH_i$  of  $\approx 0.2$  units in human sperm. Exposure of sperm to 25mM  $NH_4Cl$  had an almost identical effect on  $pH_i$  and also caused a sustained increase in  $[Ca^{2+}]_i$  only slightly less than that seen with 2mM 4-aminopyridine. Surprisingly, there was negligible induction of hyperactivation compared to cells treated with 4-aminopyridine (figure 3.4d). In contrast, Marquez and Suarez (2007) showed that  $Ca^{2+}$ -influx induced by elevation of  $pH_i$  (with 25mM  $NH_4Cl$ ) was sufficient to induce hyperactivation in bovine sperm. Marquez and Suarez reported population mean values for the various hyperactivation motility parameters (enhanced VCL and ALH (by  $\sim 40\%$ ) and decreased % LIN ( $\sim 50\%$ )). In comparison  $NH_4Cl$  induced effects on human sperm motility are muted with enhanced VCL and ALH (by 12% and 19% respectively) and a very slight effect on % LIN. Furthermore, hyperactivation was rescued in  $NH_4Cl$  pre-treated cells with the addition of 4-aminopyridine (stripped bar, figure 3.4d, table 3.1). Similarly, cytoplasmic alkalinisation (with  $NH_4Cl$ ) induced  $[Ca^{2+}]_i$  fluorescence increase

did not occlude the 4-aminopyridine induced  $[Ca^{2+}]_i$  fluorescence response in many cells (figure 3.4c). The negligible effect of  $NH_4Cl$  on human sperm motility may reflect species variation in the mechanisms that control hyperactivation (and sensitivity to hyperactivating stimuli) due to differences in the behavioural requirements for sperm activity to achieve fertilisation in different species (discussed in Chapter 7). These results demonstrate that 4-aminopyridine induced response in human sperm is not solely dependent on cytoplasmic alkalinisation and CatSper activation.

Finally cytoplasmic acidification significantly enhanced the  $[Ca^{2+}]_i$  response in a proportion of cells (44%) exposed to 4-aminopyridine and of these (~25%, the response was altered from a sustained to a transient response indicating  $Ca^{2+}$  store mobilisation. In agreement with other studies these results confirm that the charged form of 4-aminopyridine has a more potent intracellular effect. Furthermore intracellular acidification would reverse the effects of the sodium hydrogen exchanger (NHE) and proton pump (Hv1) (Sandoval *et al.*, 2007) to effectively inhibit  $I_{CatSper}$  (Kirichok *et al.*, 2006; Carlson *et al.*, 2009) providing further evidence that 4-aminopyridine induced  $[Ca^{2+}]_i$  response is pH/CatSper independent. Although intracellular acidification did not significantly enhance the proportion of 4-aminopyridine induced hyperactivation (nor effect % motility) these results suggest the presence of a population of cells that respond to 4-aminopyridine induced hyperactivation independent of CatSper channel activation.

### *Summary*

These results indicate that the 4-aminopyridine induced  $Ca^{2+}$ -influx may not be solely pH/CatSper dependent. CatSper channel activation ( $NH_4Cl$  induced cytoplasmic alkalinisation) and inhibition (propionate induced cytoplasmic acidification) did not occlude the 4-aminopyridine induced hyperactivation or  $[Ca^{2+}]_i$  fluorescence response in human sperm.

We conclude that hyperactivation of human sperm that occurs upon exposure to 4-aminopyridine may, in a number of ways, parallel the induction of hyperactivation in bovine sperm induced by manoeuvres designed to mobilise stored  $\text{Ca}^{2+}$  (Ho and Suarez, 2001b; 2003).

## **CHAPTER FOUR**

### **4-AMINOPYRIDINE INDUCED HYPERACTIVATION IS NOT SOLELY CATSPER DEPENDENT**

<b>4.1 Abstract</b>	100
<b>4.2 Introduction</b>	101
<b>4.3 Materials and methods</b>	103
4.3.1 Materials	103
4.3.2 Spermatozoa preparation and capacitation	103
4.3.3 Single cell imaging	103
4.3.4 Evaluation of $\text{Ni}^{2+}$ fluorescence enhancement	103
4.3.5 Motility Analysis	104
4.3.6 Statistical Analysis	104
<b>4.4 Results</b>	105
4.4.1 The putative CatSper channels blockers (nickel, cadmium and ruthenium red) reduced 4-aminopyridine induced hyperactivation in human spermatozoa	105
4.4.2 Effects of $\text{Ni}^{2+}$ and 4-aminopyridine on OGB fluorescence emission	108
4.4.3 Effects of nickel on 4-aminopyridine induced $[\text{Ca}^{2+}]_i$ fluorescence response	110
<b>4.5 Discussion</b>	112

## 4.1 Abstract

Transition from activated to hyperactivated motility requires an increase in cytoplasmic  $\text{Ca}^{2+}$ , to amplify flagellar bend amplitude and asymmetry of flagellar beat. Increased calcium entry via the sperm specific pH-sensitive flagellar CatSper channels has been shown to be an important contributor to hyperactivation in mouse spermatozoa (Ren *et al.*, 2001; Quill *et al.*, 2001). The effects of calcium channel inhibition on 4-aminopyridine induced hyperactivation was investigated. The divalent metal ions ( $300\mu\text{M Ni}^{2+}$  and  $200\mu\text{M Cd}^{2+}$ ) and ruthenium red ( $10\mu\text{M}$ ) have been shown to reversibly inhibit CatSper channel activity in mice sperm (Kirichok *et al.*, 2006). Inhibition of CatSper channels did not occlude the 4-aminopyridine induced hyperactivation in a population of human spermatozoa. The application of 4-aminopyridine to cells briefly pre-treated with  $\text{Ni}^{2+}$  triggered a transient increase in  $[\text{Ca}^{2+}]_i$  fluorescence indicative of stored  $\text{Ca}^{2+}$  mobilisation in a small proportion of cells. These results provide further evidence that 4-aminopyridine induced hyperactivation is not solely dependent on CatSper dependent calcium influx. The presence of a population of 4-aminopyridine responsive cells suggest that store mobilisation and channels resistant to  $\text{Ni}^{2+}$  and  $\text{Cd}^{2+}$  play a significant role in human sperm hyperactivation.

## 4.2 Introduction

Sperm motility is essential for natural conception, with successful cells altering motility pattern quickly and appropriately, according to extracellular cues as they move through the female reproductive system (chemotaxis, thermotaxis, activated and hyperactivated motility). Intracellular  $\text{Ca}^{2+}$  regulates activated and hyperactivated motility (Ho and Suarez, 2001a; Carlson *et al.*, 2005; Suarez, 2008a), capacitation (Visconti, 2009) and the acrosome reaction (Kirkman-Brown *et al.*, 2003). Spermatozoa generate  $\text{Ca}^{2+}$  signals to selectively regulate specific activities in response to extracellular cues. Increased intracellular  $\text{Ca}^{2+}$  concentration is the central regulator of hyperactivation, required both for initiation and maintenance of hyperactivation, probably by strongly enhancing flagellar bending. (Lindemann and Goltz 1988; Ho *et al.*, 2002, Ishijima *et al.*, 2006; Marquez *et al.*, 2007).  $\text{Ca}^{2+}$  signals are produced by the opening of plasma membrane  $\text{Ca}^{2+}$  channels, mobilisation of intracellular stored  $\text{Ca}^{2+}$  or both, acting together (Berridge, 2005; Felix, 2005; Jimenez-Gonzalez *et al.*, 2006). Increased calcium entry via plasma membrane channels is known to play a role in hyperactivation, the sperm specific pH-sensitive CatSper channels have been shown to be important for mouse fertility (Ren *et al.*, 2001; Quill *et al.*, 2003, Carlson *et al.*, 2005; Kirichok *et al.*, 2006; Qi *et al.*, 2007; Xia *et al.*, 2007). Human spermatozoa can be described as “a stripped down but refined machine” (Barratt *et al.*, 2009), but unlike somatic cells lack an identifiable intracellular calcium storage organelle. Evidence suggests the redundant nuclear envelope (RNE) located at the posterior head functions as a calcium store. Crucially, Marquez *et al.*, (2007) demonstrated that store mobilisation was sufficient to initiate hyperactivation in CatSper null mice, we have examined the importance of CatSper channels in human sperm hyperactivation.

The divalent metal ions (cadmium (200 $\mu\text{M}$ ) and nickel (300 $\mu\text{M}$ )) and the dye ruthenium red (10 $\mu\text{M}$ ) were found to reversibly block  $I_{\text{CatSper}}$  (Kirichok *et al.*, 2006). The effects of the putative CatSper channel blockers (nickel, cadmium and ruthenium red) on the 4-



aminopyridine induced hyperactivation were investigated. Since 4-aminopyridine has been shown to potentiate  $I_{\text{CatSper}}$  current in mouse sperm (Kirichok *et al.*, 2006) the effects of nickel (300 $\mu\text{M}$ ) pre-treatment on the 4-aminopyridine induced increase in  $[\text{Ca}^{2+}]_i$  fluorescence was examined.

## **4.3 Materials and Methods**

### **4.3.1 Materials**

As described in chapter two, with the following modifications.

To limit precipitation, 300uM nickel chloride ( $\text{NiCl}_2$ ) was prepared in a simplified media (4.5mM KCl, 9.0 mM  $\text{C}_6\text{H}_{12}\text{O}_6$ , 2.0mM  $\text{CaCl}_2 \cdot 2\text{H}_2\text{O}$ , 1mM  $\text{MgCl}_2 \cdot 6\text{H}_2\text{O}$ , 132.0mM NaCl and 15mM HEPES (pH 7.3, 285-295 mOsm)), supplemented with 0.3% (w/v) fatty acid free BSA. Osmotic strength (285-295mOsmol) was maintained by adjusting NaCl. Standard saline (sEBSS) was maintained at pH7.3 (15mM Hepes buffer).

All chemicals referred to in the text were from Sigma-Aldrich (Poole, Dorset, UK). All chemicals were cell-culture-tested grade where available.

### **4.3.2 Spermatozoa preparation and capacitation**

As in chapter two.

### **4.3.3 Single cell Imaging**

Single cell fluorescence plots in response to  $\text{Ni}^{2+}$  (300 $\mu\text{M}$ ) were sorted as described in chapter two. Visual examination of fluorescence-time plots for individual sorted cells confirmed that a proportion of cells responded to 4-aminopyridine. Quantification of 4-aminopyridine induced responses was carried out by direct observation of individual time-fluorescence intensity plots.

### **4.3.4 Evaluation of $\text{Ni}^{2+}$ fluorescence enhancement**

As described in chapter two (section 2.3.5). Emission spectrum was recorded in the presence and absence of nickel (0.1-0.5mM final concentration) and the fluorescence enhancement

factor calculated as described in Rai and Kasturi, (1994). The fluorescence enhancement factor Q was defined as

$$Q = F/F_0 - 1$$

where F and  $F_0$  are the fluorescence intensities in the presence (F) and absence ( $F_0$ ) of  $\text{Ni}^{2+}$ . The enhancement factor (1/Q) can be obtained from the intercept of the double reciprocal plot  $F_0/(F-F_0)$  vs  $1/[\text{Ni}^{2+}]$ .

OGB emission spectra were recorded for 4-aminopyridine (0.0 to 5.0mM) in the presence of 300 $\mu\text{M}$  nickel. Fluorescence quenching was measured quantitatively using the Stern-Volmer equation as described in chapter two.

#### **4.3.5 Motility Analysis.**

As in chapter two.

#### **4.3.6 Statistical Analysis**

As in chapter two.

## 4.4 Results

### 4.4.1 The putative CatSper channel blockers (nickel, cadmium and ruthenium red) reduced 4-aminopyridine induced hyperactivation in human spermatozoa

As described previously 4-aminopyridine (2mM) induced an immediate transition to hyperactivated motility in a proportion of human sperm. In capacitated cells (3-4 h) the proportion of hyperactivated sperm (as assessed by CASA) increased from  $3.5 \pm 1.4\%$  to  $36.0 \pm 4.3\%$  (figure 4.1a,  $n = 6$  experiments, paired  $t$ -test,  $P < 0.001$ ).

Brief treatment ( $\sim 2$  mins, minimum loading time) of cells with nickel (300 $\mu$ M), cadmium (200 $\mu$ M) and ruthenium red (10 $\mu$ M) did not significantly effect the proportion of hyperactivated cells (figure 4.1) or affect % motility or hyperactivation motility parameters (VCL, ALH and LIN - table 4.1).

The proportion of 4-aminopyridine induced hyperactivated cells was diminished in the presence of the heavy metal cations (figure 4.1). Pre-treatment with  $\text{Ni}^{2+}$  and  $\text{Cd}^{2+}$  ( $\sim 2$  mins) reduced 4-aminopyridine induced hyperactivation rate by 54.9% and 64.4% respectively. However, a proportion of cells remained responsive to 4-aminopyridine induced hyperactivation in the presence of  $\text{Ni}^{2+}$  (45.1%) and  $\text{Cd}^{2+}$  (35.6%). Pre-treatment of  $\text{Ni}^{2+}$  significantly effected the 4-aminopyridine induced VCL response (decreased by 23%, from  $171.2 \pm 13.0 \mu\text{m/sec}$  to  $131.2 \pm 16.8 \mu\text{m/sec}$ , paired  $t$ -test,  $P < 0.05$ ) but had no significant effect on ALH (decreased by 21% from  $6.8 \pm 0.5 \mu\text{m}$  to  $5.4 \pm 0.6 \mu\text{m}$ , paired  $t$ -test,  $P > 0.05$ ) and % LIN (increased by 7% from  $41.3 \pm 1.7\%$  to  $44.0 \pm 6.5\%$ , paired  $t$ -test,  $P > 0.05$ ) (table 4.1,  $n = 6$  experiments). Pre-treatment with  $\text{Cd}^{2+}$  did not significantly effect 4-aminopyridine induced VCL response (reduced by 15% from  $171.2 \pm 13.0 \mu\text{m/sec}$  to  $143.0 \pm 15.1 \mu\text{m/sec}$ ), ALH (reduced by 10% from  $6.8 \pm 0.5 \mu\text{m}$  to  $6.1 \pm 0.5 \mu\text{m}$ ), and % LIN (increased by 5% from  $41.3 \pm 1.7\%$  to  $44.9 \pm 3.6\%$ ) ( $n = 6$  experiments; paired  $t$ -test,  $P > 0.05$ ). Finally, pre-treatment of cells with ruthenium red decreased the proportion of hyperactivated cells in respond to 4-

aminopyridine by ~30% from 32.5±4.0% to 22.2±6.8% and did not significantly effect other motility parameters (n=6 experiments; paired *t*-test, *P*>0.05).

Figure 4.1

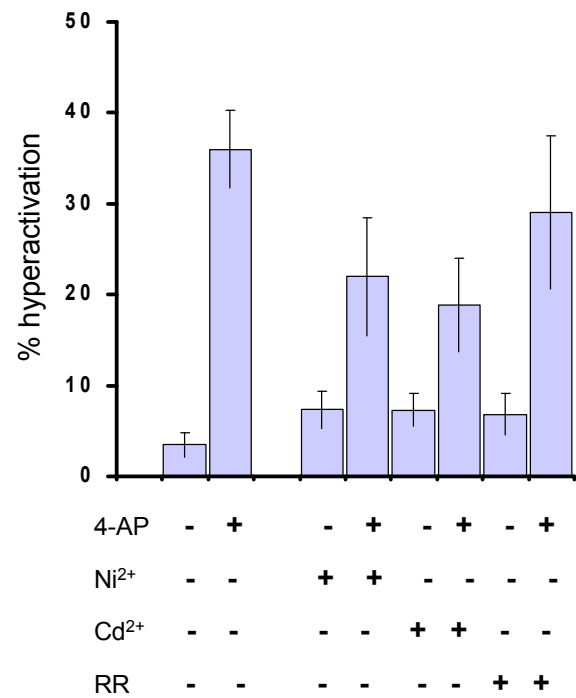


**Figure 4.1** 4-aminopyridine (2mM) induced hyperactivation on capacitated human spermatozoa (assessed by CASA) in the presence of Ni<sup>2+</sup> (300μM), Cd<sup>2+</sup> (200μM) and Ruthenium Red (10μM). **(a)** 4-AP causes an increase in the % of hyperactivated sperm from control conditions. Pre-incubation of cells with Ni<sup>2+</sup> (300μM) or Cd<sup>2+</sup> (200μM) significantly decreased the 4-AP induced hyperactivation by 54.9-64.4% (paired *t*-test, *P*<0.05). Pre-incubation with RR (10μM) decreased the 4-AP induced hyperactivation by 31.8% (NS). Each bar shows mean ± SEM. of 6 experiments

**Table 4.1. Effect of Ni<sup>2+</sup> (300μM), Cd<sup>2+</sup> (200μM) and RR (10μM) ± 4-aminopyridine (2mM) on sperm motility, VCL, ALH and LIN (mean±SEM; n=6donors)**

	Motile(%)	VCL (μm/sec)	ALH (μm)	LIN (%)
Control	79.0±4.0	126.8±8.3	4.8±0.4	62.7±2.2
+ 4AP	78.0 ±7.1	171.2±13.0	6.8±0.5	41.3±1.7
+ Ni <sup>2+</sup>	79.2±2.8	122.6±8.2	4.9±0.3	58.7±1.9
+ Ni <sup>2+</sup> and 4AP	80.2±2.9	131.2±16.8	5.4±0.6	44.0±6.5
+ Cd <sup>2+</sup>	78.9±3.7	118.2±8.2	5.0±0.2	55.4±1.6
+ Cd <sup>2+</sup> and 4AP	73.3±5.2	143.0±15.1	6.1±0.5	44.9±3.6
+ RR	73.8±4.1	121.2±8.0	5.1±0.2	56.0±2.4
+ RR and 4AP	75.0±4.6	159.8±20.2	6.9±0.7	42.1±2.5

**Table 4.1** Effects of Ni<sup>2+</sup>(300μM), Cd<sup>2+</sup> (200μM) and RR (10μM) ± 4-AP on human sperm motility, VCL, ALH and LIN. Sperm were treated with saline only (Cntrl), Ni<sup>2+</sup>(300μM), Cd<sup>2+</sup> (200μM) and RR (10μM) ± 4-AP (mean ± SEM, n=6 donors).

#### 4.4.2 Effect of $\text{Ni}^{2+}$ and 4-aminopyridine on OGB fluorescence emission

To investigate the effect of  $\text{Ni}^{2+}$  on OGB fluorescence emission, de-esterified OGB was prepared as described in previously (section 2.3.5) ( $[\text{Ca}^{2+}]_0 = 3.6 \times 10^{-4}\text{M}$ ,  $25^\circ\text{C}$ , pH 7.3) and steady state fluorescence emission ( $\lambda_{\text{em}}=522\text{nm}$ ) was recorded in the presence and absence of  $\text{Ni}^{2+}$  (0.1-0.5mM at  $25^\circ\text{C}$ ) (figure 4.2 a). Addition of  $\text{Ni}^{2+}$  enhanced the emission signal and enhancement factor of 0.6 ( $1/Q$ ) was obtained from the intercept of the double reciprocal Stern-Volmer plot (figure 4.2 b).

Steady state emission spectra were also recorded for OGB containing  $300\mu\text{M}$   $\text{Ni}^{2+}$  with additions of 4-aminopyridine (0.5-5mM) (figure 4.2 c). Addition of 4-aminopyridine (0.5-5mM) (at  $25^\circ\text{C}$ , pH 7.3,  $[\text{Ca}^{2+}]_0 = 3.6 \times 10^{-4}\text{M}$ ) had a slight quenching effect on fluorescence emission (Stern-Volmer constant= 0.0012). 4-aminopyridine in the presence of  $\text{Ni}^{2+}$  ( $300\mu\text{M}$ ) did not significantly effect OGB emission (figure 4.2c).

**Figure 4.2**

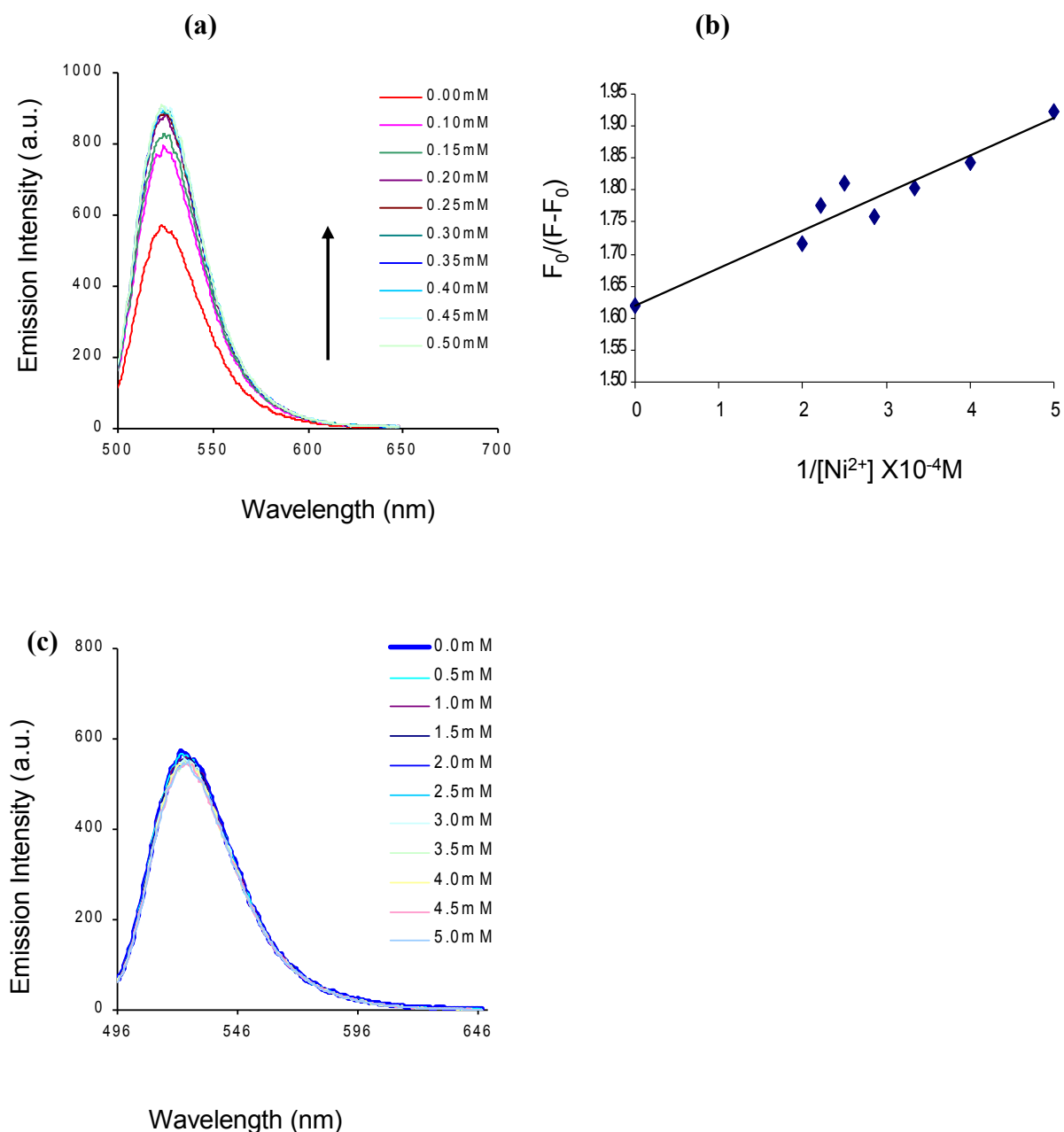


**Figure 4.2:** The effect of  $\text{Ni}^{2+}$  ( $\pm$  4-aminopyridine) on Oregon Green Bapta1 (OGB) emission (irradiation  $\lambda_{\text{ex}} = 488 \text{nm}$ , emission at  $\lambda_{\text{em}} = 522 \text{nm}$ ) (a) Emission spectra of OGB (red trace) was enhanced with the addition of  $\text{Ni}^{2+}$  (0.10-0.50 mM). (b) The enhancement factor  $Q$  for  $\text{Ni}^{2+}$  was obtained from the intercept of the linear double reciprocal plot ( $F_0/(F-F_0)$  vs  $1/[\text{Ni}^{2+}]$ ) (as described in Rai and Kasturi, 1994) (c) Emission spectra for de-esterified OGB and  $\text{Ni}^{2+}$  (300  $\mu\text{M}$ ) in the absence (blue trace) and presence of 4-aminopyridine in saline ( $[\text{Ca}^{2+}]_0 = 3.6 \times 10^{-4} \text{M}$ ).



#### 4.4.3. Effect of nickel on 4-aminopyridine induced $[Ca^{2+}]_i$ fluorescence response

Nickel is a non-specific inhibitor of numerous  $Ca^{2+}$  channels including CatSper channels (300 $\mu$ M) (Kirichok *et al.*, 2006). The application of  $Ni^{2+}$  in standard media resulted in immediate transient fluorescent signal of  $\sim 35\%$  in the majority of cells, indicating uptake and binding of  $Ni^{2+}$  to a fraction of the fluorescent indicator (figure 4.3a). However, pre-treatment with  $Ni^{2+}$  did not necessarily occlude a subsequent transient  $[Ca^{2+}]_i$  fluorescence response to 4-aminopyridine in a proportion of cells. Visual examination of individual single cell traces pre-treated with  $Ni^{2+}$  followed by 4-aminopyridine showed that  $\sim 20\%$  of cells responded with a transient increase in  $[Ca^{2+}]_i$  fluorescence of  $25.9 \pm 2.1\%$  (n=4 experiments, 291 cells; figure 4.3b). The kinetics of this response was significantly different from the 4-aminopyridine induced sustained response in paired control experiments (in the absence of  $Ni^{2+}$ , 70% of cells respond with a tonic increase of  $17.8 \pm 2.2\%$  (pH 7.3, n=5 experiments, 401 cells, paired *t*-test,  $P < 0.05$ ).

In order to minimize  $Ni^{2+}$  precipitation a further set of experiments were carried out with simplified saline lacking bicarbonate and phosphates. Cells were initially superfused with standard saline to remove excess dye and unattached cells before switching to simplified saline. However, transition to simplified saline resulted in an increase in  $[Ca^{2+}]_i$  of  $\sim 20\%$  in the majority of cells. Once a control period had been established in simple saline the cells were briefly treated with  $Ni^{2+}$  (300 $\mu$ M). As before, the majority of cells responded to  $Ni^{2+}$  with an increase in fluorescent signal indicating  $Ni^{2+}$  uptake and interaction with the dye (figure 4.3c). Although, the response to 4-aminopyridine was not discernible from the mean population response, visual examination of individual traces demonstrated that in a proportion of cells (12.0%) responded with a transient increase in  $[Ca^{2+}]_i$  fluorescence ( $20.5 \pm 1.7\%$  (n=3 experiments, 259 cells, figure 4.3 c). The response to 4-aminopyridine only in simplified saline was lower in comparison to standard saline, (30.7% of cells responded with a sustained response of  $6.6 \pm 1.6\%$  (pH 7.3, n=3 experiments, 127 cells; figure 4.3d).

**Figure 4.3**

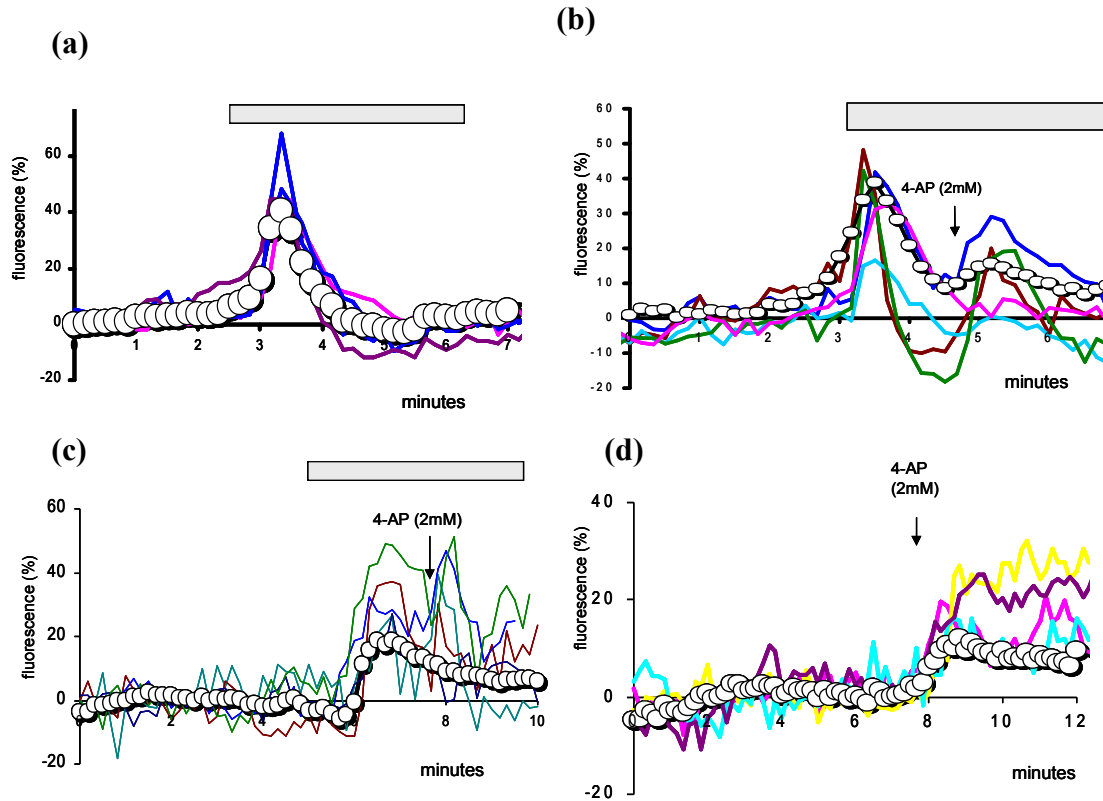


**Figure 4.3** Pre-treatment of human spermatozoa with  $\text{Ni}^{2+}$  (300  $\mu\text{M}$ ; grey bar) in standard or simplified saline altered the kinetics of the 4-aminopyridine elevation of  $[\text{Ca}^{2+}]_i$  in a proportion of OGB loaded human sperm. **(a)** Superfusion with  $\text{Ni}^{2+}$  (300  $\mu\text{M}$ ) only in standard saline caused an immediate transient fluorescent artifact in the majority of cells. Responses of 5 representative cells are shown and also mean response (o-o) of all the 87 cells in the experiment. **(b)** The application of 4-aminopyridine (2mM) in the continued presence of  $\text{Ni}^{2+}$  caused a transient rise in  $[\text{Ca}^{2+}]_i$  in ~20% of cells. Coloured lines show responses of 8 representative cells. Open circles (o-o) show mean response of 4 experiments (291 cells). **(c)** The application of 4-aminopyridine (2mM) in the continued presence of  $\text{Ni}^{2+}$  caused a transient rise in  $[\text{Ca}^{2+}]_i$  in ~12% of cells (in simplified saline). Coloured lines show responses of 6 representative cells. Open circles (o-o) show mean response of 259 cells in 3 experiments. **(d)** Control experiment where the application of 4-aminopyridine (2mM) caused a sustained response in simplified saline. Coloured lines show responses of 4 representative cells. Open circles (o-o) show mean response of 97 cells in the experiment.

## 4.5 Discussion

There is little doubt that increased intracellular calcium is essential in sperm, enabling transition from activated to hyperactivated motility in mammalian sperm.  $[Ca^{2+}]_i$  is increased as  $Ca^{2+}$  enters the cytoplasm through plasma membrane calcium channels or as  $Ca^{2+}$  is released from intracellular stores (Marquez *et al.*, 2007; Navarro *et al.*, 2008). Plasma membrane  $Ca^{2+}$  channels identified in mammalian sperm include voltage-gated  $Ca^{2+}$  channels (section 1.6.1), cyclic nucleotide gated  $Ca^{2+}$  channels (1.6.2), canonical transient receptor potential channels (section 1.5.1) and the sperm specific pH sensitive CatSper channels (section 1.5.1) (Wennemuth *et al.*, 2000; Ren *et al.*, 2001; Castellano *et al.*, 2003; Quill *et al.*, 2003; Trevino *et al.*, 2001, 2004; Kirichok *et al.*, 2006; Xia *et al.*, 2007). The CatSper channels have been shown to be important for hyperactivated sperm motility, CatSper proteins (1-4) mutations result in a loss of function phenotype and sterility in mice (Carlson *et al.*, 2005; Marquez *et al.*, 2007; Qi *et al.*, 2007). Indeed many recent papers (examining mouse sperm) have implicated CatSper dependent  $Ca^{2+}$  influx with a BSA induced  $Ca^{2+}$  influx (Xia and Ren, 2009a), maintenance of basal  $Ca^{2+}$  levels for activated motility (Marquez *et al.*, 2007; Qi *et al.*, 2007), ATP homeostasis (Xia *et al.*, 2007) and ZP3 induced acrosome reaction (Xia and Ren, 2009b).

*Treatment with  $Ni^{2+}$ ,  $Cd^{2+}$  or ruthenium red did not occlude 4-aminopyridine induced hyperactivation in human sperm*

The divalent metal ions cadmium ( $Cd^{2+}$ , 200 $\mu$ M) and nickel ( $Ni^{2+}$ , 300 $\mu$ M) and the ruthenium red dye (10 $\mu$ M) were found to reversibly block  $I_{CatSper}$  in mouse sperm (Kirichok *et al.*, 2006). Although pre-treatment with  $Ni^{2+}$  and  $Cd^{2+}$  decreased 4-aminopyridine induced hyperactivation rates in human spermatozoa approximately ~35-40% of cells were unaffected. Pre-treatment with ruthenium red did not significantly affect 4-aminopyridine induced hyperactivation response or motility parameters. These results demonstrate that 4-aminopyridine induced

hyperactivation is not solely CatSper dependent and store-mobilisation and  $\text{Ca}^{2+}$  influx through channels resistant to  $\text{Ni}^{2+}$ ,  $\text{Cd}^{2+}$  and ruthenium red may play a significant role in human sperm hyperactivation. These results are in agreement with Marquez *et al.*, (2007) who reported that in the presence of 1mM  $\text{Ni}^{2+}$  approximately 30% of mice sperm hyperactivate in response to thimerosol induced store mobilisation (Marqueuz *et al.*, 2007).

*Intracellular calcium response to 4-aminopyridine in OGB loaded human spermatozoa pre-treated with Nickel or Cadmium*

Divalent metal ions have relatively high affinities for ion channel binding sites and typically inhibit  $\text{Ca}^{2+}$  influx by competing for the channel site. Since metal ions can move through the channel slowly, endogenous metal cations may interact with fluorescence dye to quench or enhance fluorescence signal (Snitsarev *et al.*, 1996). Superfusion of spermatozoa with  $\text{Ni}^{2+}$  in standard saline or simplified saline resulted in a fluorescence artifact although it is unclear how  $\text{Ni}^{2+}$  entered the cell. Addition of  $\text{Ni}^{2+}$  (100 $\mu\text{M}$ ) was found to enhance de-esterified OGB fluorescence emission whereas 4-aminopyridine had a negligible quenching effect on OGB emission signal in the presence of  $\text{Ni}^{2+}$  (300 $\mu\text{M}$ ).

Despite the presence of a nickel induced fluorescent artifact, a 4-aminopyridine induced transient response was evident in a significant proportion of cells (18% in standard saline and 12% in simplified saline). We have previously demonstrated that both 4-aminopyridine and  $\text{NH}_4\text{Cl}$  have a similar effect on  $\text{pH}_i$  (figure 3.4b) and cytoplasmic alkalinisation should activate available CatSper channels. Inhibition by  $\text{Ni}^{2+}$  would not only block CatSper dependent  $\text{Ca}^{2+}$  influx, but various other channels including voltage-operated channels (VOC) (Fox *et al.*, 1987; Zamponi *et al.*, 1996), receptor operated channels (ROC) (Hughes and Barritt, 1989) and capacitative calcium entry (CCE) channels (Hoth and Penner, 1993; Kerschbaum and Cahalan 1998). 4-aminopyridine induced a transient  $[\text{Ca}^{2+}]_i$  fluorescence response in a population of cells which reflects intracellular  $\text{Ca}^{2+}$  store mobilisation however the sustained response is lost

apparently due to inhibition of store-operated channels (SOC) or CatSper dependent  $\text{Ca}^{2+}$  influx. These results indicate that release of  $\text{Ca}^{2+}$  from an internal store is sufficient to initiate 4-aminopyridine induced hyperactivation. Similar results from the Suarez group demonstrated that hyperactivation could also be induced in CatSper null mice (Marquez *et al.*, 2007). This group demonstrated that addition of  $\text{Ca}^{2+}$  releasing agents (thimerosal and high dose thapsigargin) induced hyperactivation in bovine sperm in the absence of extracellular  $\text{Ca}^{2+}$  (Ho and Suarez, 2001b). Suarez *et al.*, (1993) demonstrated the sustained increase in  $[\text{Ca}^{2+}]_i$  in the post-acrosomal head was greater than the proximal/distal midpiece of hyperactivated hamster sperm. Intracellular calcium store mobilisation and consequential sustained CCE in sperm has been observed by a number of groups (Blackmore, 1993; Dragileva *et al.*, 1999; Williams and Ford, 2003; Espino *et al.*, 2009).

### *Conclusion*

The presence of a population of 4-aminopyridine responsive cells suggest that store mobilisation and channels resistant to  $\text{Ni}^{2+}$ ,  $\text{Cd}^{2+}$  and ruthenium red play a significant role in human sperm hyperactivation. Furthermore application of 4-aminopyridine induced a transient  $[\text{Ca}^{2+}]_i$  response in a similar proportion of cells indicating a role for store mobilisation in human sperm hyperactivation.

## **CHAPTER FIVE**

### **4-AMINOPYRIDINE INDUCED INTRACELLULAR**

### **Ca<sup>2+</sup> STORE MOBILISATION**

<b>5.1 Abstract</b>	116
<b>5.2 Introduction</b>	117
<b>5.3 Materials and method</b>	119
5.3.1 Materials	119
5.3.2 Spermatozoa preparation and capacitation	119
5.3.3 Single cell imaging	120
5.3.4 Evaluation of sperm hyperactivation	120
5.3.5 Evaluation of Ca <sup>2+</sup> uptake and release in microsomal vesicles	121
5.3.6 Evaluation of acrosome reaction	122
5.3.7 Statistical analysis	123
<b>5.4 Results</b>	
5.4.1 The response to 4-aminopyridine initiates at the sperm neck	124
5.4.2 4-aminopyridine mobilises stored Ca <sup>2+</sup>	126
5.4.3 4-aminopyridine induced Ca <sup>2+</sup> mobilisation and hyperactivation in sperm	130
5.4.4 Effects of 4-aminopyridine on intracellular Ca <sup>2+</sup> transport and release proteins	132
5.4.4.1 Effect of 4-aminopyridine on fluo3 emission	132
5.4.4.2 Effect of 4-aminopyridine on Ca <sup>2+</sup> uptake and Ca <sup>2+</sup> -ATPase activity	133
5.4.4.3 Effect of 4-aminopyridine on IP <sub>3</sub> Ca <sup>2+</sup> release channels	133
5.4.4.4 Effect of 4-aminopyridine on the ryanodine receptor Ca <sup>2+</sup> release channel	134
5.4.5 Effect of low dose P <sub>4</sub> on the 4-aminopyridine induced [Ca <sup>2+</sup> ] <sub>i</sub> response	137
5.4.6 Effect of tetracaine on the 4-aminopyridine induced [Ca <sup>2+</sup> ] <sub>i</sub> response	138
5.4.7 4-aminopyridine and sperm mitochondrial Ca <sup>2+</sup>	140
5.4.8 4-aminopyridine and the acrosome reaction	142
<b>5.5 Discussion</b>	143

## 5.1 Abstract

4-aminopyridine caused a robust and persistent hyperactivation of motility in human sperm. Furthermore  $\text{Ca}^{2+}$  imaging showed that treatment with 4-aminopyridine induced a parallel elevation of  $[\text{Ca}^{2+}]_i$ , which initiated at the sperm neck/midpiece and was associated with asymmetric flagellar bending in this region. In low  $\text{Ca}^{2+}$  saline ( $\leq 5 \mu\text{M Ca}^{2+}$ ) the ability of 4-aminopyridine to cause an elevation of  $[\text{Ca}^{2+}]_i$  was similar to that seen in standard saline. Application of 4-aminopyridine to cells briefly (4-5min) exposed to EGTA-buffered saline ( $<10^{-7} \text{ M Ca}^{2+}$ ) induced a  $[\text{Ca}^{2+}]_i$  transient. Hyperactivation induced by 4-aminopyridine was similarly transient (10-15min) in EGTA-buffered saline, though motility persisted for 20-30 min. 4-aminopyridine acted as a non-specific intra-calcium store agonist however it remains unclear how this compound triggers store mobilisation in microsomal vesicles. In conclusion 4-aminopyridine induced hyperactivation is not solely pH or CatSper channel dependent and intracellular  $\text{Ca}^{2+}$  store mobilisation contributes to the induction of hyperactivation in human sperm.

## 5.2 Introduction

Despite their small size and apparent structural simplicity, it is evident that sperm are capable of generating and regulating complex, compartmentalised  $\text{Ca}^{2+}$  signals directly controlling a range of activities including the acrosome reaction, chemotaxis and hyperactivation (Jimenez-Gonzalez *et al.*, 2006; Publicover *et al.*, 2007). Various studies from a number of species demonstrated the presence of a  $\text{Ca}^{2+}$  store in the neck region of mammalian sperm (Kuroda *et al.*, 1999; Ho and Suarez, 2001b, 2003; Naaby-Hansen *et al.*, 2001; Harper *et al.*, 2004; Lefièvre *et al.*, 2007; Marquez *et al.*, 2007). Investigations in rodent and bovine sperm has provided strong evidence that the elevation of  $[\text{Ca}^{2+}]_i$  that occurs upon mobilisation of this store regulates flagellar activity, including (or at least facilitating) aspects of hyperactivation (Ho *et al.*, 2001b; 2003). Importantly hyperactivation can be induced independently of CatSper channels with store mobilisation induced hyperactivation occurring in mouse sperm lacking CatSper channels (Marquez *et al.*, 2007). Since capacitative calcium entry (CCE) has been observed in sperm (Blackmore, 1993; Dragileva *et al.*, 1999; Williams and Ford, 2003; Espino *et al.*, 2009; Costello *et al.*, 2009), store mobilisation might even recruit this mechanism to supplement  $\text{Ca}^{2+}$  influx through CatSper channels (Olson *et al.*, 2010). This second pathway for induction of hyperactivation may play a separate role from that mediated by CatSper channels enabling sperm to switch hyperactivated motility on and off in response to *in vivo* triggers (e.g. nitric oxide, low dose progesterone). Mobilisation of stored  $\text{Ca}^{2+}$ , which is rapidly reversible and localised, may be better suited to such transient regulation of motility whereas pH regulated activation of CatSper channels could support the prolonged hyperactivation that permits ‘permanent’ detachment from the cells of the female tract (Ho *et al.*, 2009) and penetration of the zona pellucida.

4-aminopyridine disrupts intra-cellular calcium homeostasis in a number of cell types (Ishida and Honda, 1993; Guse *et al.*, 1994; Gobet *et al.*, 1995, Grimaldi *et al.*, 2001) including mammalian sperm (Navarro *et al.*, 2007). 4-aminopyridine induced hyperactivation and



$[Ca^{2+}]_i$  fluorescence response in human spermatozoa is not solely dependent on cytoplasmic alkalinisation and concomitant CatSper channel activation. In this report, the effects of 4-aminopyridine on  $[Ca^{2+}]_i$  fluorescence and rates of hyperactivation in  $Ca^{2+}$  free condition ( $[Ca^{2+}]_o < 10^{-7}$  M) are examined. Furthermore, the effects of 4-aminopyridine on  $Ca^{2+}$  uptake and  $Ca^{2+}$  release channels in microsomal vesicles (sarcoplasmic reticulum (SR) and brain microsomes) are investigated so that results are independent of cytoplasmic alkalinisation,  $K^+$  channel inhibition and CatSper channel activation.

## 5.3 Materials and Methods

### 5.3.1 Materials

Ca<sup>2+</sup>-free sEBSS (no added Ca<sup>2+</sup>, ([Ca<sup>2+</sup>]<sub>o</sub> ≤ 5μM)) and EGTA buffered medium (5mM Ca<sup>2+</sup>, 6mM EGTA) were prepared in the laboratory ([Ca<sup>2+</sup>]<sub>o</sub> < 10<sup>-7</sup> M). Osmotic strength was maintained by adjusting NaCl. The calcium concentration calculator Maxchelator (V2.2) written by Chris Patton from Stanford University

(<http://www.stanford.edu/~cpatton/maxc.html>) was used to calculate the calcium concentration in saline containing EGTA.

Creatine Kinase was purchased from Boehringer, Mannheim. D-myo-Inositol-1,4,5-triphosphate hexapotassium salt (IP<sub>3</sub> – 2mM stock made up in H<sub>2</sub>O) was purchased from Enzo Life Sciences (Exeter). All other materials were purchased from Sigma Aldrich (Poole, Dorset) including 1-[2-Amino-5-(2,7-dichloro-6-hydroxy-3-oxy-9-xanthenyl)phenoxy]-2-(2-amino-5-methylphenoxy)ethane-N,N,N',N'-tetraacetic acid ammonium potassium salt (fluo-3 ammonium salt - 0.5mM stock concentration made up in H<sub>2</sub>O), 2-(6-Amino-3-imino-3H-xanthen-9-yl)benzoic acid methyl ester (Rhodamine123 - 15mM stock concentration dispersed with Pluronic F-127), progesterone [4-pregnene-3,20-dione] (6mM stock concentration prepared in DMSO), thapsigargin (0.1mM stock concentration prepared in DMSO), 2-(dimethylamino)ethyl 4-(butylamino)benzoate (tetracaine hydroxide, 50mM stock in H<sub>2</sub>O), phosphocreatine from bovine heart, adenosine 5'-triphosphate disodium salt (ATP – made up with MgSO<sub>4</sub> in water, pH 7.0) and calcimycin A32187 (1mM stock in DMSO). All chemicals were cell culture-tested grade were available.

### 5.3.2 Spermatozoa preparation and capacitation

As in chapter two.

### 5.3.3 Single Cell Imaging

Investigation of 4-aminopyridine on Oregon Green Bapta1 loaded cells were as previously described (chapter two). All experiments were performed at  $25\pm0.5^{\circ}\text{C}$  in a continuous flow of medium (sEBSS,  $\text{Ca}^{2+}$ -free' sEBSS ( $[\text{Ca}^{2+}]_0 \leq 5 \mu\text{M}$ ) or EGTA-buffered saline ( $[\text{Ca}^{2+}]_0 < 10^{-7} \text{M}$ ). For high speed fluorescence imaging (9 Hz) the protocol was as described previously (chapter two) but cells were viewed using a 60x oil immersion objective and images were captured with an EMCCD camera controlled by a PC running iQ software.

To investigate the effect of 4-aminopyridine on mitochondrial membrane potential, 200  $\mu\text{l}$  aliquots of capacitated spermatozoa at  $3\text{--}6 \times 10^6$  cells/ml were loaded with Rhodamine123 (6.5  $\mu\text{M}$  final concentration dispersed with Pluronic F-127) and transferred to an imaging chamber (volume 180  $\mu\text{l}$ ) in which the lower surface was a 1% (w/v) poly-D-lysine coated coverslip and allowed to adhere during a 30 min incubation at  $37^{\circ}\text{C}$  and 5.5%  $\text{CO}_2$ . The chamber was connected to the perfusion apparatus (peristaltic pump and header tank; superfusion rate  $0.4 \text{ml min}^{-1}$ ) and cells were superfused with approximately 10 ml of fresh medium to remove unattached cells and excess dye. All experiments were performed at  $25\pm0.5^{\circ}\text{C}$  in a continuous flow of medium. Spermatozoa were imaged on a Nikon TE200 inverted fluorescence microscope. Images were obtained at 10s intervals using a 60x oil objective and a Andor iXon EM<sup>+</sup> camera controlled by a PC running iQ software (Andor Technology, Belfast, UK). To minimize photobleaching EM gain was set to 70 (to improve signal to noise ratio), exposure was reduced to 1ms.

### 5.3.4 Evaluation of sperm hyperactivation

For motility assessment in nominal  $\text{Ca}^{2+}$  free medium (no added  $\text{Ca}^{2+}$ ), 200  $\mu\text{l}$  aliquots of spermatozoa ( $\geq 6 \times 10^6$  cells. $\text{ml}^{-1}$ ) were prepared by direct swim and incubated for  $\sim 1\text{--}1.5$  hours. For experiments involving EGTA-buffered medium, cells were centrifuged (300 g for 5 min) and the pellet re-suspended in 1ml EGTA buffered saline immediately prior to the

experiment. 200µl aliquots were treated with either saline (control) or 4-aminopyridine and immediately (or after an appropriate period of incubation for time-course experiments) introduced into a chamber (depth 20µm) (Microcell, Conception Technologies Ltd.) at a concentration of 6-7 million/ml on a Hamilton Thorne HTM IVOS semen analyzer (37°C). Hyperactivation was defined as previously described (chapter two).

### **5.3.5 Evaluation of Ca<sup>2+</sup> uptake and release in microsomal vesicles**

#### *Evaluation of 4-aminopyridine induced fluo-3 fluorescence quenching*

Fluorescence quenching experiments were performed with 250nM fluo-3 (free acid) in 2ml of 40mM Tris, 100mM KCL saline (pH 7.2) in a magnetically stirred methylacrylate cuvette maintained at 25°C or 37°C by a water jacket. Emission spectra were recorded with 4-aminopyridine (0-4mM final concentration) with fixed excitation wavelength held at 506nm, slit width set at 3nm. Emission was scanned at 1000 nm/min between 506 and 650nm. Fluorescence quenching was measured quantitatively using the Stern-Volmer equation as described in chapter two.

#### *Microsomal membrane purification*

Sarcoplasmic reticulum microsomes (SR) and porcine brain microsomes were kindly donated by Dr F. Michelangeli (Department of Biosciences, University of Birmingham).

#### *Calcium uptake and release assay*

Experiments were carried out using a Perkin-Elmer LS50B fluorescence spectrofluorimeter running FLWinlab version 3.0. Fluorimetry was performed with 2ml of 40mM Tris, 100mM KCL (pH 7.2) in a magnetically stirred methylacrylate cuvette maintained at 37°C by a water jacket. Rabbit sarcoplasmic reticulum (SR) (2µg) (Michelangeli and Munkonge, 1991) or porcine brain vesicles (40-50µg) were added in the presence of 250nM Fluo-3 (free acid),

10µg/ml creatine kinase and 10mM phosphocreatine.  $\text{Ca}^{2+}$  uptake was initiated by the addition of Mg-ATP. To examine the effect of 4-aminopyridine on  $\text{Ca}^{2+}$ -ATPases,  $\text{Ca}^{2+}$  uptake was measured by addition of the drug prior to the start of the experiment.  $\text{Ca}^{2+}$  release was measured by addition of 4-aminopyridine (0.5-4mM) following ATP uptake in the presence of thapsigargin (~1-1.5µM). Fluorescence changes were monitored using excitation and emission wavelengths of 506nm and 526nm, respectively. Calcium concentrations were determined using the following equation:

$$[\text{Ca}^{2+}]_i = K_d \times [(F - F_{\min}) / (F_{\max} - F)]$$

where  $K_d$  is the dissociation constant for  $\text{Ca}^{2+}$  binding to fluo-3 (900nM at 37°C, pH 7.2, in 40mM Tris and 100mM KCL),  $F$  is the fluorescence intensity of the sample and  $F_{\min}$  and  $F_{\max}$  are the fluorescence intensities of 1.25mM EGTA and 2mM  $\text{CaCl}_2$ , respectively (Michelangeli, 1991; Menza and Michelangeli, 1996). Percentage  $\text{Ca}^{2+}$  release (%) was determined by comparing the amount of  $\text{Ca}^{2+}$  released by 4-aminopyridine with that observed with 12.5µg/ml A23187.

### **5.3.6 Evaluation of acrosome reaction**

After capacitation (in sEBSS + 0.3% BSA, incubated at 37°C and 5.5%  $\text{CO}_2$  for 5-6 hours), 200 µl aliquots of spermatozoa were then stimulated with 4-aminopyridine (2 mM), progesterone (final concentration of 3.2 µM) or A23187 (10 µM) or solvent control (0.05% DMSO). After an incubation period of 1 hour (37°C) cells were centrifuged (500 g for 5 min). The supernatant was removed and the spermatozoa re-suspended in 0.5 ml of hypo-osmotic swelling (HOS) medium (0.74% sodium citrate, 1.35% fructose in double-distilled  $\text{H}_2\text{O}$ ). After 45 min cells were centrifuged (500 g for 5 min), supernatant was removed and pellets were smeared on poly-L-lysine coated slides and air-dried. The cells were permeabilised in methanol

for  $\approx 30$  seconds. 15 $\mu$ l of FITC-labelled *Pisum sativum* agglutinin (FITC-PSA) in PBS was spread on each slide and incubated for 45 min in a humid chamber at 37° C. Slides were then washed in a constant flow of tap water for 5 min before air drying and mounting with hydromount. Acrosomal status of viable (curly tailed) spermatozoa was assessed by fluorescence microscopy (Cross *et al.*, 1988). A total of 200 cells were scored for each treatment (100 each from 2 slides).

### **5.3.7 Statistical Analysis**

As in chapter two.

## 5.4 Results

### 5.4.1 The response to 4-aminopyridine initiates at the sperm neck.

To localise the point(s) of initiation of the  $[Ca^{2+}]_i$  signal in cells exposed to 4-aminopyridine, we collected images for a brief period (2 min) at 9 Hz. In many cells it was impossible to identify the point of origin of the  $Ca^{2+}$  signal, intensity rising rapidly in both the anterior flagellum (which often remained in focus despite flagellar beating) and the posterior head/neck (not the anterior head). However, in a minority of cells a focus of  $Ca^{2+}$  mobilisation was clearly visible at the sperm neck, the signal spreading rapidly ( $\approx 5s$ ) into the posterior head, midpiece and anterior principal piece (fig. 5.1b). In a very small number of cells ( $<1\%$ ) a gradual rise in fluorescence in the neck and posterior sperm head apparently ‘triggered’ a  $[Ca^{2+}]_i$  response in the midpiece (figure 5.1c). A common observation in 4-aminopyridine treated cells was the occurrence of a unilateral bend at the midpiece, which developed as  $[Ca^{2+}]$  increased. The example in fig. 5.1b is particularly striking, bending by  $\geq 45^\circ$ , but most cells in which this occurred showed a more conservative response with a bend of  $10-20^\circ$ . The principal piece of the flagellum continued to beat but was displaced laterally. Upon washout of 4-aminopyridine bending of the flagellum ‘relaxed’ with the fall in  $[Ca^{2+}]_i$ . Re-application of the drug restored both  $[Ca^{2+}]_i$  elevation and bending of the proximal flagellum repeated.

**Figure 5.1**

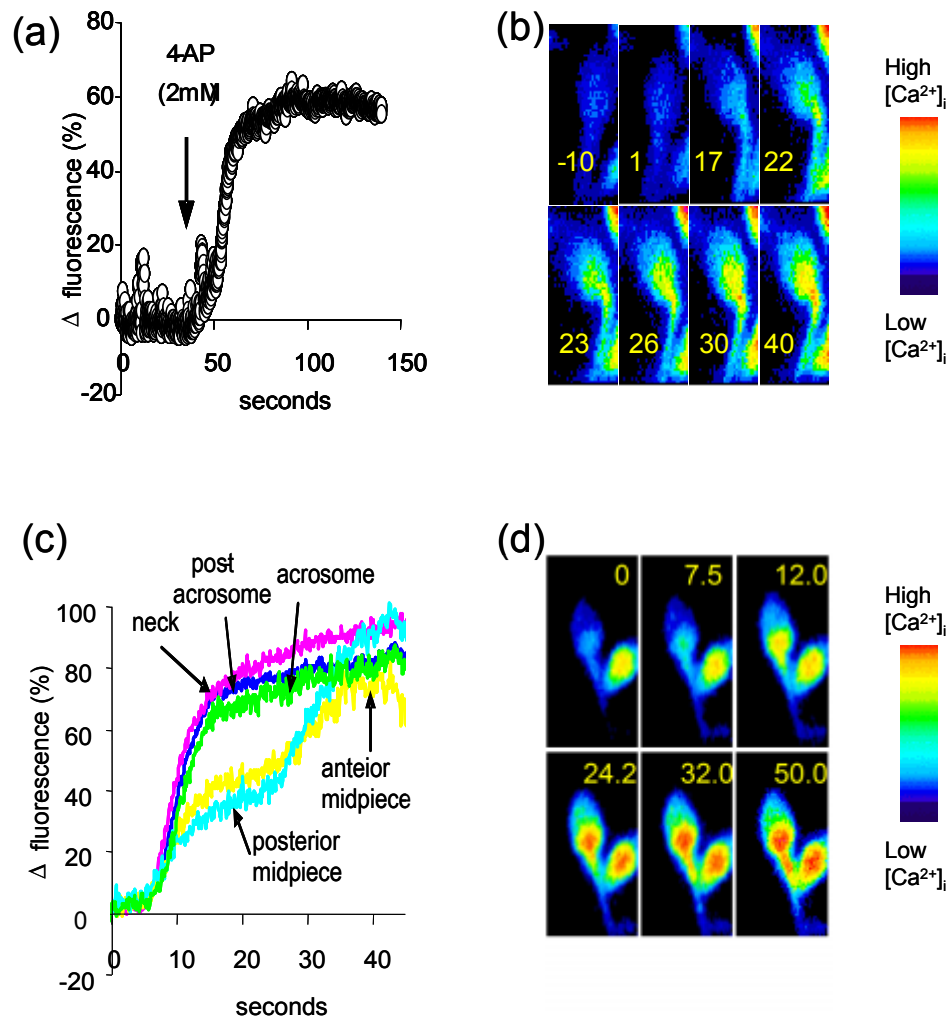


**Figure 5.1.** Imaging of 4-aminopyridine-induced hyperactivation and  $\text{Ca}^{2+}$  mobilisation. **(a)** plot showing 4-aminopyridine-induced (arrow) increase in fluorescence of Oregon Green BAPTA-1 in the cell shown in **(b)** Pseudocolour image series showing  $[\text{Ca}^{2+}]_i$  (Oregon Green-1 BAPTA fluorescence) in a cell (bathed in sEBSS) exposed to 2mM 4-aminopyridine. The  $[\text{Ca}^{2+}]_i$  response originates at the sperm neck and anterior midpiece then spreads into the posterior head and flagellum. Figures in each image shows the time in seconds with respect to application of 2mM 4-aminopyridine. **(c)** Delayed mobilisation of  $\text{Ca}^{2+}$  in the sperm neck/midpiece. Plot shows  $[\text{Ca}^{2+}]_i$  (normalized Oregon Green BAPTA-1 fluorescence) at various points in a sperm stimulated with 2mM 4-aminopyridine (applied at 0 seconds). An initial rise in fluorescence increases fastest in the sperm neck (cerise), preceding the other areas by <1 s. In the midpiece (yellow and turquoise)  $[\text{Ca}^{2+}]_i$  initially rises with similar kinetics but after 20-25 s a second mobilisation of  $\text{Ca}^{2+}$  is triggered. **(d)** Pseudocolour images of Oregon Green-1



BAPTA fluorescence) in the same cell (left hand cell in each picture) at various times points after stimulation. Figure in each image shows the time in seconds with respect to application of 2mM 4-aminopyridine.

#### 5.4.2 4-aminopyridine mobilises stored $\text{Ca}^{2+}$

Previous studies on excitable cells have shown that 4-aminopyridine can mobilise stored  $\text{Ca}^{2+}$ . To investigate whether stored  $\text{Ca}^{2+}$  is involved in the action of 4-aminopyridine in human sperm we imaged cells superfused with modified bathing medium. To reduce any contribution of  $\text{Ca}^{2+}$  influx, we used sEBSS with no added  $\text{Ca}^{2+}$  (no added  $\text{Ca}^{2+}$  sEBSS; measured contaminating  $[\text{Ca}^{2+}] < 5\mu\text{M}$ ) (Harper *et al.*, 2004). When  $\text{Ca}^{2+}$  was simply omitted from the medium, 4-aminopyridine still induced a clear rise in  $[\text{Ca}^{2+}]_i$  in >75% of cells. Fluorescence increased by  $29.4 \pm 0.7\%$  within 5 min (5 experiments; 353 cells; figure 5.2b) an effect slightly greater than that seen in standard sEBSS ( $24.5 \pm 0.7\%$ ; paired *t*-test,  $P > 0.05$ ). Analysis of single cell records showed that, within the same experiment, responses to 4-aminopyridine in ‘ $\text{Ca}^{2+}$ -free’ medium were of two types.  $[\text{Ca}^{2+}]_i$  either peaked within 1-2 min ( $\approx 20\%$  of responsive cells) or rose more slowly but reached a similar level after  $\approx 5$  min exposure to 4-aminopyridine (figure 5.2a). When  $\text{Ca}^{2+}$  was reintroduced to the recording >90% of cells showed a clear increase in  $[\text{Ca}^{2+}]_i$ . 15-20% of cells generated  $[\text{Ca}^{2+}]_i$  oscillations, this occurring almost exclusively in those cells that had responded to application of 4-aminopyridine with a rapid rise in  $[\text{Ca}^{2+}]_i$  (figure 5.2a;  $P < 10^{-120}$ , chi square test).

Exposure of human sperm to EGTA-buffered medium causes an immediate fall in  $[\text{Ca}^{2+}]_i$  which rapidly depletes intracellular  $\text{Ca}^{2+}$  stores (Harper *et al.*, 2004; Bedu-Addo *et al.*, 2007). Cells incubated in EGTA-buffered saline ( $[\text{Ca}^{2+}] < 10^{-7}$  M) for 10-15 min showed no response to 4-aminopyridine. However, when the drug was applied after exposure to EGTA-buffered saline for  $\leq 10$  min a clear transient increase in  $[\text{Ca}^{2+}]_i$  was detectable in a proportion of the cells ( $23.8 \pm 8.2\%$ ;  $n=7$ ; figure 5.2c). In cells showing a detectable response the size of the transient (expressed as change compared to fluorescence intensity immediately before

application of 4-aminopyridine) was highly variable, amplitude ranging from 2.5-55% of control fluorescence (figure 5.2c; mean =  $8.7 \pm 1.4\%$ ) and duration was typically 5-10 min. In some cells 4-aminopyridine caused a slowly developing elevation of  $[Ca^{2+}]$  followed by a 'spike', suggesting the occurrence of  $Ca^{2+}$ -induced  $Ca^{2+}$  release (fig. 5.2c). Upon re-introduction of  $Ca^{2+}$  to the imaging chamber there was a large increase in  $[Ca^{2+}]_i$  in most cells, consistent with activation of capacitative  $Ca^{2+}$  influx.

**Figure 5.2**

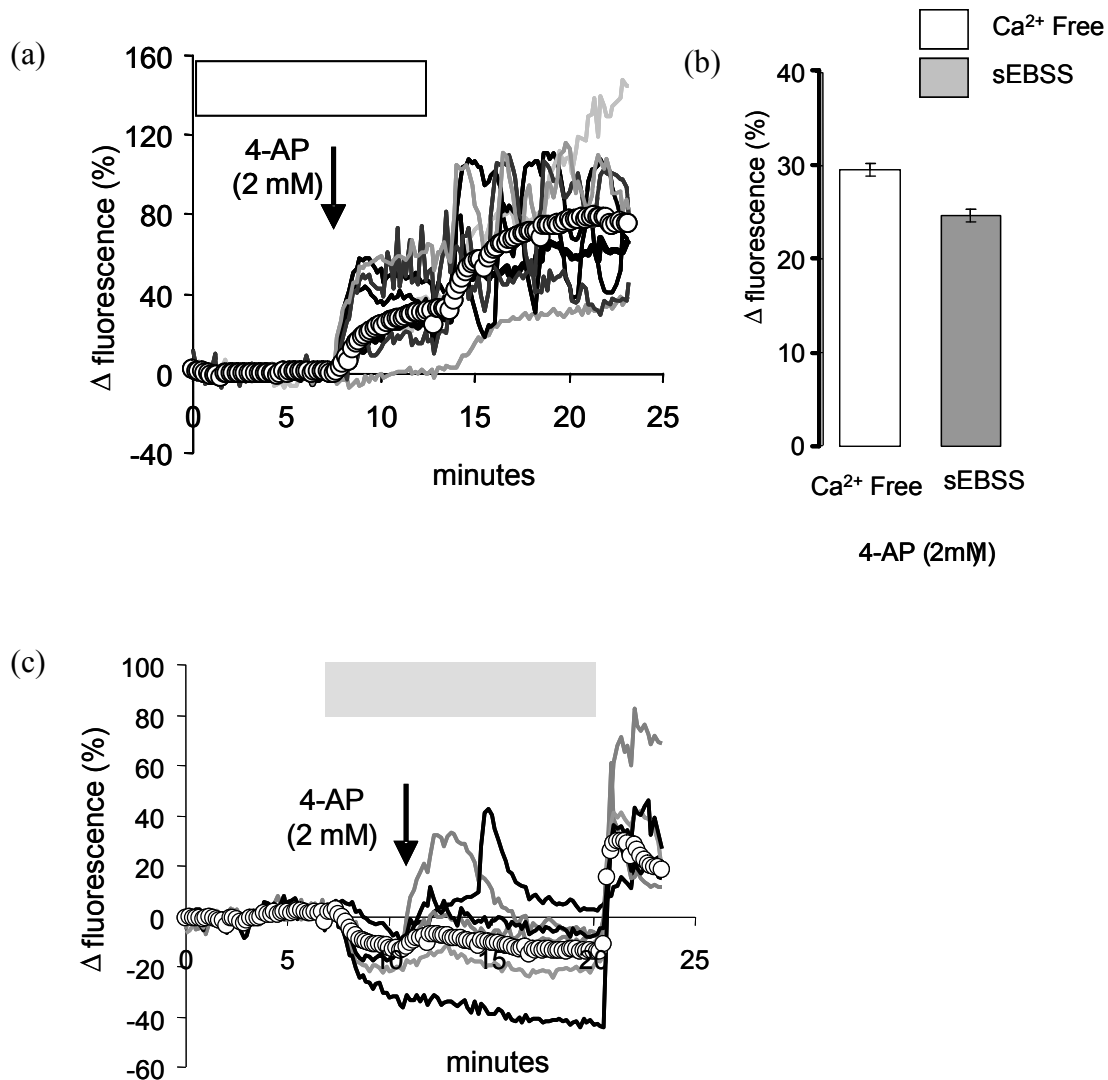


**Figure 5.2.** 4-aminopyridine mobilises stored  $\text{Ca}^{2+}$ . **(a)** Effect of 2 mM 4-aminopyridine on  $[\text{Ca}^{2+}]_i$  in cells superfused with nominally  $\text{Ca}^{2+}$ -free sEBSS (no added  $\text{Ca}^{2+}$ ;  $[\text{Ca}^{2+}] \leq 5 \mu\text{M}$ ; shown by white bar). Upon application of 4-aminopyridine (arrow) most cells responded to 4-aminopyridine. Responses of 7 representative cells are shown and also mean response ( $\circ-\circ$ ) of all the 234 cells in the experiment. In most cells  $[\text{Ca}^{2+}]_i$  rose slowly, similarly to the mean response, but in  $\approx 20\%$  there was a more rapid rise, comprising an initial transient and a plateau. Upon introduction of standard sEBSS ( $1.8\text{mM } \text{Ca}^{2+}$ ) to the recording chamber there was a further increase in  $[\text{Ca}^{2+}]_i$  (including some cells that showed no initial response) and most of those cells that had showed an initial transient response to 4-aminopyridine generated  $[\text{Ca}^{2+}]_i$  oscillations. **(b)** Elevation of  $[\text{Ca}^{2+}]_i$  by 4-aminopyridine in cells superfused with  $\text{Ca}^{2+}$ -free sEBSS and standard sEBSS. Each bar shows mean increase in fluorescence (at plateau) of 144-364 cells from 4 experiments. **(c)** Effect of 4-aminopyridine on cells superfused

with EGTA-buffered sEBSS ( $[Ca^{2+}] < 10^{-7}$  M). Responses of 6 representative cells are shown and also mean response ( $\circ-\circ$ ) of all the 95 cells in the experiment. Superfusion with EGTA-buffered saline ( $[Ca^{2+}] < 10^{-7}$  M; shown by grey bar) caused a rapid fall in  $[Ca^{2+}]_i$ . Application of 4-aminopyridine  $\approx 5$  min after EGTA caused a transient rise in  $[Ca^{2+}]_i$ , lasting 5-10 min, in a subset (24%) of cells. Upon re-introduction of standard sEBSS  $[Ca^{2+}]_i$  in all cells rose rapidly.

#### 5.4.3 4-aminopyridine induced $\text{Ca}^{2+}$ mobilisation and hyperactivation in sperm

Experiments on sperm bathed in EGTA-buffered saline show that the action of 4-aminopyridine on  $[\text{Ca}^{2+}]_i$  in human sperm involves both  $\text{Ca}^{2+}$  influx and an initial mobilisation of stored  $\text{Ca}^{2+}$  in the neck/midpiece region of the cell. To investigate whether stored  $\text{Ca}^{2+}$  contributes to the strong hyper-activating action of 4-aminopyridine, we assessed the motility of cells exposed to the drug in medium with modified  $[\text{Ca}^{2+}]$ . The ability of 4-aminopyridine to dramatically increase the proportion of hyperactivated cells was not inhibited by simple omission of  $\text{Ca}^{2+}$  from the medium. In 12 paired experiments in which cells from the same sample were exposed to 4-aminopyridine both in standard medium and medium from which  $\text{Ca}^{2+}$  had been omitted, ( $[\text{Ca}^{2+}] \leq 5 \mu\text{M}$ ) the mean proportion of hyperactivated cells was not significantly reduced (4-aminopyridine induced hyperactivation in standard saline =  $21.3.2 \pm 4.4\%$  (grey bar) and in nominal calcium free saline =  $33.2 \pm 5.2\%$  (open bar), paired  $t$ -test,  $P > 0.05$ , figure 5.3a).

4-aminopyridine-induced elevation of  $[\text{Ca}^{2+}]_i$  in cells suspended in EGTA-buffered medium ( $< 10^{-7} \text{ M}$ ), which reflects mobilisation of stored  $\text{Ca}^{2+}$ , is transient (figure 5.2c). We therefore examined the persistence of the hyperactivating effect of 4-aminopyridine in cells suspended in EGTA-buffered medium compared to that in cells in standard sEBSS. Whereas the action of 4-aminopyridine on cells in sEBSS was stable over a period of 45 min, when cells were re-suspended in EGTA-buffered medium 2 min before stimulation with 4-aminopyridine hyperactivation decayed to zero within 10-15 min (figure 5.3b). Incubation in EGTA-buffered saline also caused gradual loss of motility but a significant proportion of the cells remained motile for  $> 30$  min (figure 5.3c), almost twice as long as the persistence of 4-aminopyridine-induced hyperactivation.

**Figure 5.3**

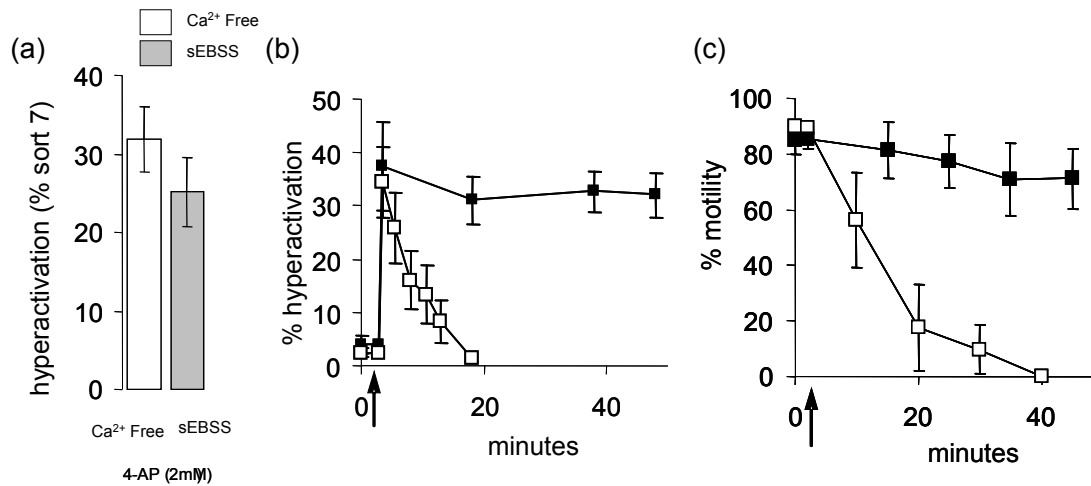


**Figure 5.3** Stored  $\text{Ca}^{2+}$  and 4-aminopyridine induced hyperactivation. **(a)** Induction of hyperactivation (% cells) by 2 mM 4-aminopyridine in cells suspended in standard sEBSS (1.8 mM  $\text{Ca}^{2+}$ ; grey bar) and in saline with no added  $\text{Ca}^{2+}$  ( $[\text{Ca}^{2+}]_0 \leq 5 \mu\text{M}$ ; Harper *et al*, 2004; open bar). Each bar shows mean  $\pm$ sem of 12 experiments. Hyperactivation was measured  $\approx 2$  min after application of 4-aminopyridine ( $P > 0.05$ ; paired t-test). The effect of suspension in EGTA-buffered medium on motility and hyperactivation was also assessed. Cells were suspended in EGTA-buffered medium  $< 10^{-7}$  M at 0 min and aliquots were withdrawn at intervals to assess motility (c) and induction of hyperactivation by 4-aminopyridine hyperactivation (b). Each point shows mean  $\pm$ sem of 4 experiments. **(b)** Decay of 4-aminopyridine-induced hyperactivation. After suspension of cells in appropriate medium an aliquot was immediately assessed for hyperactivation. 2 mM 4-aminopyridine was then applied to the cells (arrow) and time-dependence of hyperactivation was assessed by withdrawing aliquots at a series of time points as shown. Filled squares (■) shows cells suspended in sEBSS (mean  $\pm$ sem of 4 experiments). Open squares (□) shows cells re-suspended in EGTA-buffered medium 2 min before application of 4-aminopyridine (mean  $\pm$ sem of 4 experiments). **(c)** Decay of 4-aminopyridine-induced motility. After suspension of cells in appropriate medium an aliquot was immediately assessed for motility 2 mM 4-aminopyridine was then applied to the cells (arrow) and time-dependence of motility was assessed by withdrawing aliquots at a series of time points as shown. Filled squares (■) shows cells suspended in sEBSS (mean  $\pm$ sem of 4 experiments). Open squares (□) shows cells re-suspended in EGTA buffered medium 2 min before application of 4-aminopyridine (mean  $\pm$ sem of 4 experiments).

#### **5.4.4 Effects of 4-aminopyridine on intracellular $\text{Ca}^{2+}$ transport and release proteins**

The elevation of  $[\text{Ca}^{2+}]_i$  caused by 4-aminopyridine in EGTA buffered saline reflected mobilisation (figure 5.2c) of intracellular stored  $\text{Ca}^{2+}$  located at the posterior head. Although the structure of this putative store is not fully elucidated, evidence suggests the presence of calreticulin (a  $\text{Ca}^{2+}$  storage protein) (Naaby-Hansen *et al.*, 2001; Ho and Suarez, 2003), inositol 1,4,5-trisphosphate receptors ( $\text{IP}_3\text{Rs}$ ) (Kuroda *et al.*, 1999; Ho and Suarez, 2001b, 2003) and ryanodine receptor (Giannini *et al.*, 1995; Harper *et al.*, 2004). There is also some evidence of  $\text{Ca}^{2+}$ -ATPase localised to this area including SERCA (sarcoplasmic endoplasmic reticulum  $\text{Ca}^{2+}$ -ATPase) and SPCA (secretory pathway  $\text{Ca}^{2+}$ -ATPase) (Harper *et al.*, 2005; Lawson *et al.*, 2007). In an attempt to isolate the effects of 4-aminopyridine on individual components of intracellular store calcium uptake pumps and release channels uptake and release of  $\text{Ca}^{2+}$  by sarcoplasmic reticulum (SR) and brain microsome vesicles suspended in medium containing the calcium indicating dye fluo3 (acid free) was examined.

##### *5.4.4.1 Effects of 4-aminopyridine fluo3 emission*

Since previous data demonstrated that 4-aminopyridine had a quenching effect on OGB fluorescent signal (chapter two), the quenching effects of this compound on fluo3 was investigated. Fluorescence emission spectra were recorded in the presence and absence of 4-aminopyridine (0.5–4.0mM). As expected, there was a decrease in fluorescence signal in the presence of 4-aminopyridine however neither the emission spectrum shape nor wavelength were affected. The Stern-Volmer quenching constant was 0.05 at 25°C (figure 5.4).

**Figure 5.4**

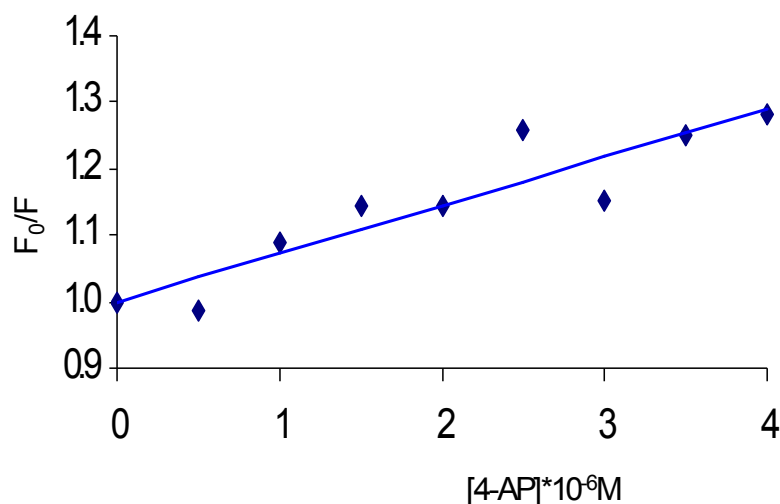


**Figure 5.4:** Stern-Volmer plot of fluorescence lifetime of fluo-3 (250nM in 40mM Tris and 100mM KCL, pH 7.2) containing increasing concentrations of 4-aminopyridine (0.5-4mM) at 25°C. Irradiation wavelength was held at 506nm.

#### 5.4.4.2 *Effects of 4-aminopyridine on $\text{Ca}^{2+}$ uptake and $\text{Ca}^{2+}$ ATP-ase activity*

4-aminopyridine has previously been shown to inhibit the ATP-driven  $\text{Ca}^{2+}$  uptake in guinea pig sarcoplasmic reticulum (Ishida and Honda, 1993). Figure 5.5 (a) shows typical traces of ATP-dependent  $\text{Ca}^{2+}$  uptake in rabbit skeletal muscle sarcoplasmic reticulum (SR) (SERCA isoform 1 predominantly expressed) in the absence (blue trace) and presence (pink trace) of 4-aminopyridine. The membranes were pre-incubated with 4-aminopyridine (2mM) for ~2 mins prior to the addition of 1.5mM ATP to initiate  $\text{Ca}^{2+}$  uptake (arrow). The rate of ATP-dependent  $\text{Ca}^{2+}$  uptake did not differ significantly different in the presence of 4-aminopyridine (2mM) (n=3 experiments, paired *t*-test,  $P>0.05$ ).

#### 5.4.4.3 *Effects of 4-aminopyridine on the $\text{IP}_3$ $\text{Ca}^{2+}$ release channels*

Porcine cerebellar microsomes are relatively enriched in intracellular pumps (predominantly SERCA2) and channels (predominantly  $\text{IP}_3\text{R}$ ). As described in the methods, brain microsomes were loaded with  $\text{Ca}^{2+}$ , initiated by the addition of 1.5mM Mg-ATP (at 100s). Adequate  $\text{Ca}^{2+}$  accumulation required a prolonged period due to the age of the microsomal preparation



(~1000s). Additions of 2mM 4-aminopyridine to the cuvette (at ~1050s) caused a clear mobilisation of  $\text{Ca}^{2+}$  (figure 5.5b insert). Application of  $\text{IP}_3$  (10 $\mu\text{M}$  at 1155s) resulted in further release. Total accumulated  $\text{Ca}^{2+}$  within the brain microsomes was measured by the addition of 12.5 $\mu\text{g/ml}$  A23187 and the degree of 4-aminopyridine induced  $\text{Ca}^{2+}$  release was calculated as a % of the maximum. Average 4-aminopyridine induced  $\text{Ca}^{2+}$  release was 6.9% followed by  $\text{IP}_3$  induced release of 3.8% (mean  $n=3$  experiments, 3 different microsomal aliquots). These results demonstrate that 4-aminopyridine can trigger partial store release probably by  $\text{IP}_3\text{R}$  activation but may not occupy or is displaced from the  $\text{IP}_3$  binding site since the application of  $\text{IP}_3$  triggered further  $\text{Ca}^{2+}$  release.

#### 5.4.4.4 *Effects of 4-aminopyridine on the ryanodine receptor $\text{Ca}^{2+}$ release channel*

Immunolocalisation studies from our laboratory demonstrate the presence of ryanodine receptors proteins (isoforms 1 and 2) expressed in the posterior head of human sperm (Harper *et al.*, 2004; Lefièvre *et al.*, 2007). Since both  $\text{IP}_3\text{R}$  and  $\text{RyR}$  have similar structures 4-aminopyridine-induced  $\text{Ca}^{2+}$  release (0.1 to 3.0mM) on ryanodine receptor1 predominantly expressed in rabbit skeletal muscle heavy sarcoplasmic reticulum was investigated. A typical experimental trace is presented in figure 5.5(c).  $\text{Ca}^{2+}$  uptake was initiated by the addition of 1.5mM Mg-ATP (at ~185s) and once sufficient  $\text{Ca}^{2+}$  had accumulated further  $\text{Ca}^{2+}$  uptake was inhibited with thapsigargin (1-1.5 $\mu\text{M}$ , at ~200s) prior to the addition of 4-aminopyridine (at ~400s) (figure 5.5c insert). Total accumulated  $\text{Ca}^{2+}$  within the SR microsomes was measured by the addition of 12.5 $\mu\text{g/ml}$  A23187 and the degree of 4-aminopyridine induced  $\text{Ca}^{2+}$  release was represented as a % of the maximum. Figure 5.5(d) shows the dose-dependent mobilisation of  $\text{Ca}^{2+}$  release from skeletal muscle SR induced by 4-aminopyridine. Average 4-aminopyridine (2mM) induced  $\text{Ca}^{2+}$  release was  $5.0 \pm 1.1\%$  slightly lower than brain microsomal vesicles ( $\text{IP}_3\text{R}$ ) ( $n=12$  experiments, mean $\pm$ s.e.m.).

**Figure 5.5**

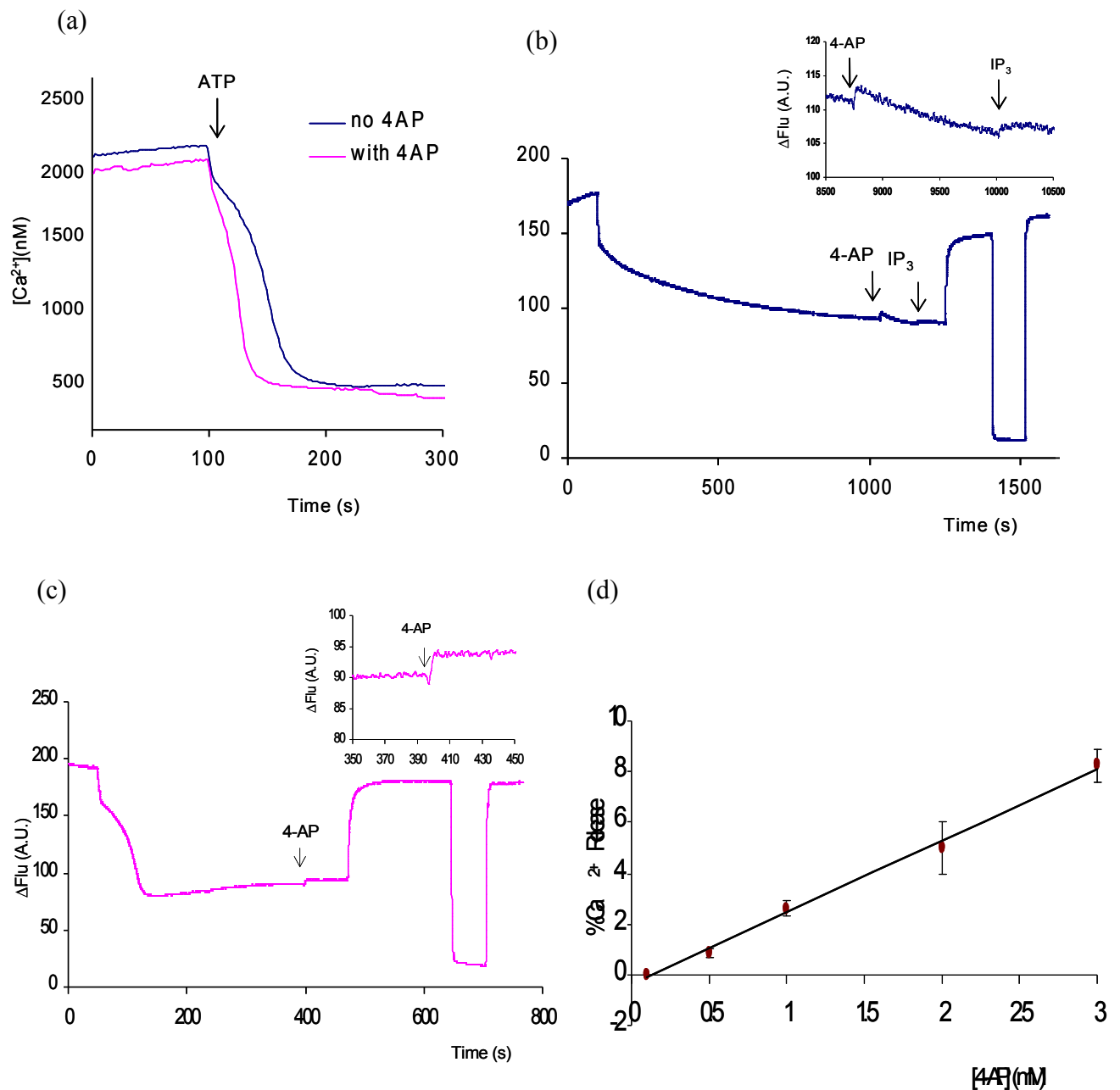


**Figure 5.5** Effect of 2mM 4-aminopyridine on  $\text{Ca}^{2+}$  uptake and release in microsomal vesicles (rabbit skeletal muscle vesicles or brain microsomes) at pH7.2 and 37°C **(a)** Typical traces showing  $\text{Ca}^{2+}$  uptake initiated by addition of 1.5mM Mg-ATP (indicated by arrow) in SR vesicles in the presence (pink line) and absence (blue line) of 4-aminopyridine (2mM) (representative of 3 experiments). **(b)** Effect of 2mM 4-aminopyridine on  $\text{Ca}^{2+}$  release in brain microsomal vesicles. Typical traces showing  $\text{Ca}^{2+}$  uptake initiated by addition of 1.5mM Mg-ATP (at ~100s) followed by 4-aminopyridine (2mM, arrow at 1050s) and  $\text{IP}_3$  (arrow at 1155s) resulting in  $\text{Ca}^{2+}$  release (insert). Maximal store release was achieved by addition of the calcium ionophore A23187 (~1250s). **(c)** Effect of 2mM 4-aminopyridine on  $\text{Ca}^{2+}$  release in rabbit skeletal muscle microsomal vesicles. Typical traces showing

$\text{Ca}^{2+}$  uptake initiated by addition of 1.5mM Mg-ATP (at ~185s) followed by thapsigargin (1 $\mu$ M) at ~200s. 4-aminopyridine (2mM arrow at 400s, insert) resulting in  $\text{Ca}^{2+}$  release. Maximal store release was achieved by addition of the calcium ionophore A23187 (~475s). **(d)** Dose-dependency of  $\text{Ca}^{2+}$  release induced by 4-aminopyridine presented as a percentage of  $\text{Ca}^{2+}$  release compared to that released by A23187 (vertical bars indicate s.e.m.).

#### 5.4.5 Effect of low dose $P_4$ on the 4-aminopyridine induced $[Ca^{2+}]_i$ response

Previous studies from this laboratory indicate that exposure of human spermatozoa to very low concentrations of progesterone produced a low tonic ‘background’ influx of  $Ca^{2+}$  that allowed the store in the neck/midpiece to fill up which was mobilised when cells were exposed to nitric oxide donors (Machado-Oliveira *et al.*, 2008). Exposure of sperm to 100pM progesterone in standard saline for approximately 10mins increased resting  $[Ca^{2+}]_i$  by  $10.7 \pm 0.7\%$  (figure 5.6, 5mins after exposure) in the majority of cells. Furthermore the subsequent 4-aminopyridine induced  $[Ca^{2+}]_i$  response was altered in many cells with approximately 50% of cell responding with a transient increase (amplitude  $34.5 \pm 2.4\%$ ), followed by oscillations in ~15% of cells. Approximately 40% of cells responded with a sustained elevation  $[Ca^{2+}]_i$  of  $17.0 \pm 0.9\%$ .

**Figure 5.6**

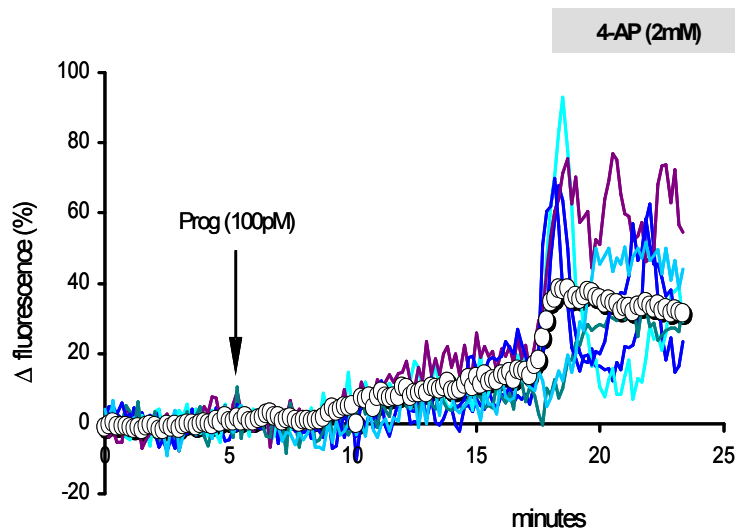


**Figure 5.6** Effect of progesterone (100pM) pre-treatment on the response to 4-aminopyridine.  $[Ca^{2+}]_i$  responses of 7 representative cells are shown and also mean response ( $\circ-\circ$ ) of all the 135 cells in the experiment. Cells were exposed to 100pM progesterone for  $\approx 10$  min, causing a sustained elevation of  $[Ca^{2+}]_i$ . Application of 2mM 4-aminopyridine (grey bar) caused a further rise in  $[Ca^{2+}]_i$ .

#### **5.4.6 Effects of tetracaine on 4-aminopyridine induced $[Ca^{2+}]_i$ response**

Harper *et al.*, (2004) demonstrated that application of tetracaine inhibited progesterone (3 $\mu$ M) induced oscillations (Harper *et al.*, 2004). Tetracaine has been shown to inhibit the ryanodine receptor/ $Ca^{2+}$  release channel in SR microsomal membranes (Martin *et al.*, 1993; Tovey *et al.*, 1998). In these experiments, sperm have been pretreated to 1mM tetracaine for approximately 10mins which in 66% of cells resulted in a no change or a decrease in resting  $[Ca^{2+}]_i$  of  $9.8 \pm 0.7\%$  (5 mins after exposure) and the remaining cells (34%) responded with a tonic increase  $[Ca^{2+}]_i$  of  $7.8 \pm 0.7\%$ . The overall kinetics (response) of the subsequent 4-aminopyridine induced  $[Ca^{2+}]_i$  response was similar to controls (non-tetracaine experiments) as the majority of cells responded with a sustained increase in  $[Ca^{2+}]_i$  of  $23.8 \pm 1.2\%$ . However upon washout of tetracaine, the 4-aminopyridine response was altered to a transient response (amplitude  $34.9 \pm 1.7\%$ ) in the majority of cells (figure 5.7a). This transient was absent in parallel experiments upon washout of 4-aminopyridine (figure 5.7b).

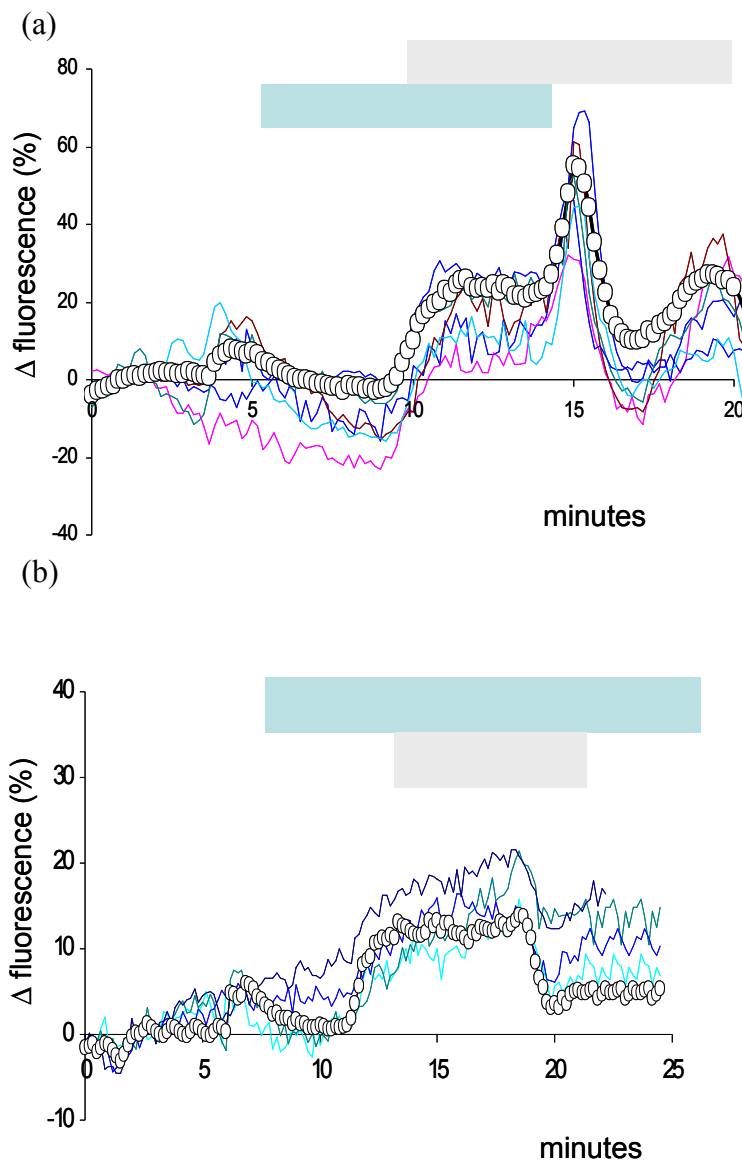


**Figure 5.7** Effect of tetracaine (1mM, blue bar) pre-treatment on the response to 4-aminopyridine (2mM, grey bar).

(a)  $[Ca^{2+}]_i$  responses of 7 representative cells and mean response ( $\circ-\circ$ ) of all the 55 cells in the experiment are shown. Cells were exposed to 1mM tetracaine (blue bar) for  $\approx 10$  min prior to the application of 2 mM 4-aminopyridine (grey bar), resulting in transient rise in  $[Ca^{2+}]_i$ . Washout of tetracaine altered the 4-aminopyridine response to a transient  $[Ca^{2+}]_i$  signal in  $>90\%$  of cells.

(b) This transient response is lost upon washout of 4-aminopyridine (grey bar). Responses of 6 representative cells and mean response ( $\circ-\circ$ ) of all the 60 cells in the experiment.

#### 5.4.7 4-aminopyridine and sperm mitochondrial $\text{Ca}^{2+}$

To investigate whether mitochondria are involved in the generation of 4-aminopyridine induced calcium increase, we pre-treated cells with the mitochondrial uncoupler 2,4-dinitrophenol (100 $\mu\text{M}$  for  $\sim 6$  mins), to collapse the mitochondrial inner membrane potential, prior to the application of 4-aminopyridine. In the majority of cells ( $\sim 60\%$ ) application of 2,4-dinitrophenol caused a tonic increase in  $[\text{Ca}^{2+}]_i$  of  $5.6 \pm 0.4\%$  ( $n=2$  experiments, 145 cells, figure 5.8a), probably due to release of mitochondrial  $\text{Ca}^{2+}$ . However, the 4-aminopyridine induced response was not significantly altered in comparison to non-pretreated controls (figure 5.8b)- amplitude of 4-aminopyridine response in pretreated cells ( $21.4 \pm 0.4\%$ ) and non-pretreated cells ( $20.5 \pm 0.7$ ,  $n=2$  experiments; paired  $t$ -test,  $P>0.05$ ). A further convenient method of measuring mitochondrial membrane depolarisation and membrane integrity was to record any decrease in fluorescence of the mitochondrial compartmentalizing probe, Rhodamine 123 (Rh123) (Ogunbayo *et al.*, 2008). Rh123 is a cationic, lipophilic species that accumulates in the matrix of the polarised mitochondria. Upon depolarisation or loss of mitochondrial membrane integrity (release of pro-apoptotic factors through the permeability transient pore (PTP)) Rh123 fluorescent signal is lost. Rh123 is light sensitive and photobleaching results in a gradual slow decrease of signal. Figure 5.8(c) shows the fluorescence intensity of Rhodamine 123-loaded sperm cells. 4-aminopyridine (2mM) was added to the cells at 100 sec after the start of the recording. Although a small degree of fluorescence decrease could be observed in some cells which was attributed to photobleaching, the mean rate of fluorescence decrease was not enhanced upon exposure to 4-aminopyridine.

**Figure 5.8**

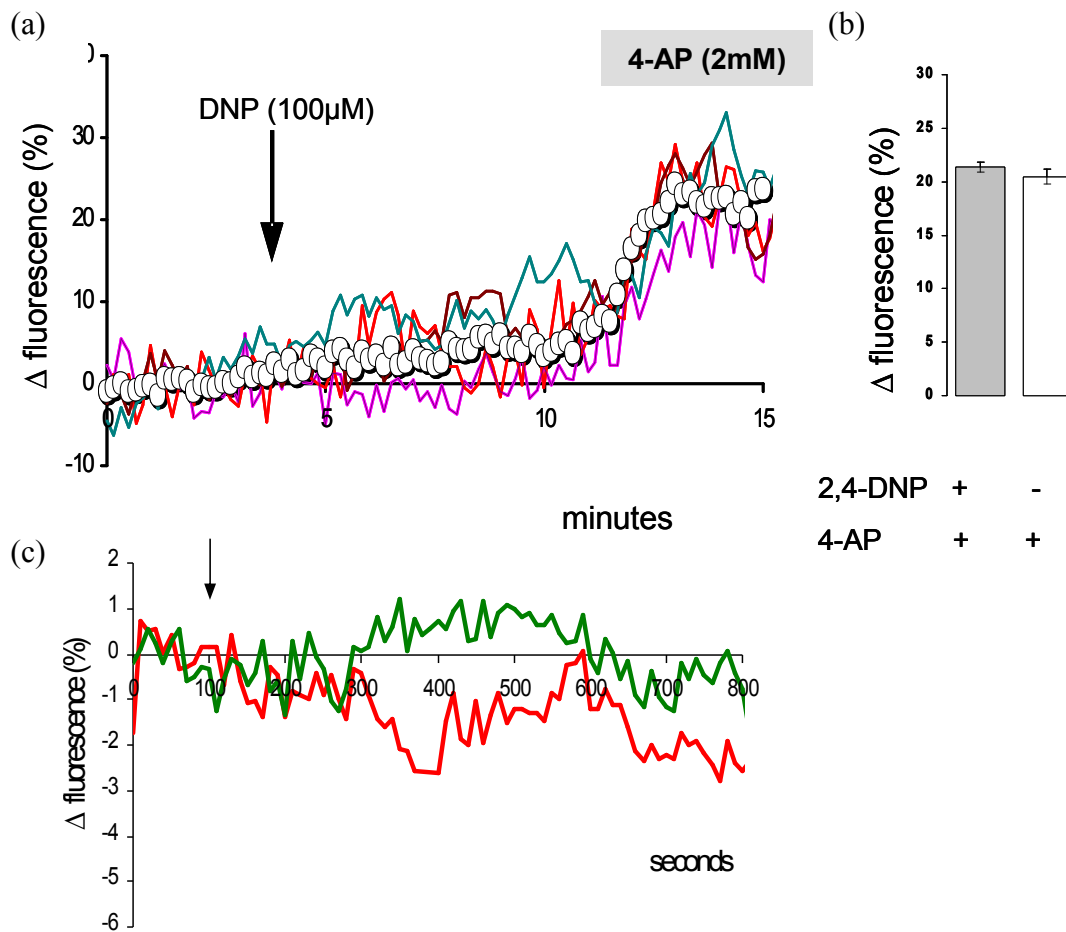


**Figure 5.8** Effect of 4-aminopyridine on mitochondrial  $Ca^{2+}$  (a)  $[Ca^{2+}]_i$  responses of 6 representative cells are shown and also mean response ( $\circ-\circ$ ) of all the 92 cells in the experiment. Cells were exposed to 100  $\mu$ M 2,4-dinitrophenol for  $\approx$ 5 min, causing a sustained elevation of  $[Ca^{2+}]_i$ . Application of 2 mM 4-aminopyridine (grey bar) caused a further large rise in  $[Ca^{2+}]_i$  (b) Elevation of  $[Ca^{2+}]_i$  by 4-aminopyridine (2mM) in cells pre-treated with 2,4-DNP (grey bar, n=2 expts, 145 cells) and non-pretreated control (open bar, n=2exps, 150 cells) . Each bar shows mean increase in fluorescence (at plateau)  $\pm$  s.e.m. (c) The effects of 4-aminopyridine (2mM) on mitochondrial membrane potential in human sperm cells loaded with Rhodamine 123. Green trace is a combination of 16 cells exposed to 4-aminopyridine (black arrow) and red trace is a combination of 15 cells exposed to saline only. Downward drift due to photobleaching.



#### 5.4.8 4-aminopyridine and the acrosome reaction

Mammalian spermatozoa are relatively hard wired cells. We have shown previously that  $\text{Ca}^{2+}$  signals in human sperm are compartmentalised, permitting the sperm separately to regulate different activities (e.g. hyperactivation and acrosome reaction) even though both are activated by  $\text{Ca}^{2+}$ -mediated signalling cascades (Bedu-Addo *et al.*, 2007). 4-aminopyridine induces hyperactivation in human sperm, apparently through prolonged elevation of  $[\text{Ca}^{2+}]_i$ . To investigate whether the sperm were capable of restricting the effects of this signal to regulation of flagellar activity, we exposed sperm, suspended in standard saline, to 4-aminopyridine (2mM). After one hour the sperm were processed for assessment of acrosomal status. Whereas A23187 (10  $\mu\text{M}$ ) increased the proportion of acrosome reacted cells from  $6.6 \pm 1.7\%$  to  $67.6 \pm 5.4\%$  (paired *t*-test,  $P < 5 \times 10^{-5}$ ; paired-t,  $n=7$ ), 4-aminopyridine had no effect on the rate of acrosome reaction ( $5.0 \pm 1.2\%$ ; paired *t*-test,  $P > 0.4$ ;  $n=7$ ; figure 5.8).

**Figure 5.9**

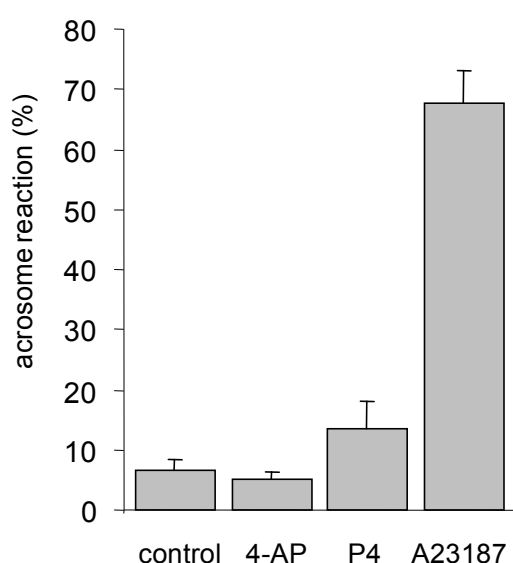


**Figure 5.9.** 4-aminopyridine does not induce acrosome reaction. Histogram shows proportion of cells which had undergone acrosome reaction (failure to stain with *Pisum sativum* agglutinin; see methods). A23187 increases the rate of acrosome reaction to  $>65\%$ . Progesterone ( $\text{P}_4$ ) also increased the proportion of acrosome reacted cells but 2 mM 4-aminopyridine failed to cause any stimulation.

## 5.5 Discussion

Although sperm are specialised cells they have a limited number of intracellular organelles (in comparison to somatic cells) there is evidence to suggest they contain at least two separate intracellular calcium stores. While the  $\text{Ca}^{2+}$  content of any putative intracellular stores would be small and difficult to quantify, mobilisation could induce capacitative calcium entry (CCE) and the opening of plasma membrane  $\text{Ca}^{2+}$  channels to prolong  $\text{Ca}^{2+}$  influx (Blackmore, 1993; Williams & Ford, 2003). Calcium channel opening and depletion of  $\text{Ca}^{2+}$  from acrosomal stores results in elevation of calcium which drives exocytosis and the acrosome reaction (Florman *et al.*, 1989; Florman, 1994; O'Toole *et al.*, 2000; Jungnickel *et al.*, 2001). Furthermore, mobilisation of the neck/midpiece store and resulting CCE may contribute significantly to regulation of motility (Castellano *et al.*, 2003; Yoshida *et al.*, 2003). The neck/midpiece region of mammalian and sea urchin sperm  $\text{Ca}^{2+}$  store is composed of the redundant nuclear envelope (RNE), which is retained following nuclear condensation and located behind the nucleus of mammalian sperm. Membrane vesicles have been observed closely opposed to the plasmalemma, in the cytoplasmic droplet of human sperm. Both these structures have calreticulin (a  $\text{Ca}^{2+}$  storage protein) and  $\text{IP}_3$  receptors and  $\text{Ca}^{2+}$  mobilisation in this region is sensitive to ryanodine (a  $\text{Ca}^{2+}$  activated  $\text{Ca}^{2+}$  channel) (Ho and Suarez, 2001b, 2003; Naaby-Hansen *et al.*, 2001; Harper *et al.*, 2005). Accumulation and mobilisation of  $\text{Ca}^{2+}$  from one or both these structures is believed to initiate and or control hyperactivation in mouse and bovine sperm and regulation of flagellar beat mode in human sperm (Ho and Suarez, 2001a, 2003; Harper *et al.*, 2007; Bedu-Addo *et al.*, 2008; Machado-Oliveira *et al.*, 2008). In the previous chapters results have demonstrated that in a population of human sperm 4-aminoopyridine induced hyperactivation and increased  $[\text{Ca}^{2+}]_i$  is not solely pH or CatSper dependent.

### ***Ca<sup>2+</sup> store mobilisation and asymmetric bending of the midpiece.***

In imaging experiments of 4-aminopyridine-treated cells (both fluorescence imaging of  $[Ca^{2+}]_i$  and high speed acquisition of phase contrast images), a common observation was a strong bending of the sperm flagellum in the midpiece and (sometimes) proximal part of the principal piece. In fluorescence image series it was clear that this bending was tightly associated with elevation of  $[Ca^{2+}]_i$  at the neck/midpiece (Suarez and Dai, 1992; Carlson *et al.*, 2003; Quill *et al.*, 2003; Harper *et al.*, 2004; Marquez *et al.*, 2007; Bedu-Addo *et al.*, 2007, 2008). The most extreme examples of this occurred in cells showing very strong  $[Ca^{2+}]_i$  responses and 'relaxation' of the bend occurred upon the return of  $[Ca^{2+}]_i$  to resting levels. Similar reversible effects on bending of the proximal flagellum are observed during  $[Ca^{2+}]_i$  oscillations induced by progesterone (Harper *et al.*, 2004, Bedu-Addo *et al.*, 2007, Machado-Oliveira *et al.*, 2008) and NO (Machado-Oliveira *et al.*, 2008). Increased bending of the midpiece and anterior flagellum is characteristic of hyperactivated motility and will lead to exaggerated lateral movement of the sperm head (Suarez and Ho, 2003a, 2003b; Ishijima *et al.*, 2006; Ohmuro and Ishijima, 2006). Bedu-Addo *et al.*, (2007) suggested that mobilisation of  $Ca^{2+}$  at the sperm neck/midpiece and consequent bending in this region is an important contribution to hyperactivation.

### ***Stored Ca<sup>2+</sup> and 4-aminopyridine-induced $[Ca^{2+}]_i$ response***

Assessment of  $[Ca^{2+}]_i$  in 4-aminopyridine stimulated cells showed a sustained elevation of  $[Ca^{2+}]_i$  originating in the neck/midpiece of the sperm. Omission of  $Ca^{2+}$  from the bathing medium had little, if any, effect on the ability of 4-aminopyridine either to elevate  $[Ca^{2+}]_i$  (figure 5.2 a,b) or to induce hyperactivation of the cells (figure 5.3a). However, when cells were superfused with EGTA-buffered medium ( $[Ca^{2+}]_o < 10^{-7}M$ ) the response to 2mM 4-aminopyridine (applied within a few minutes of exposure to EGTA) was a transient elevation of  $[Ca^{2+}]_i$  which decayed completely within 5-10 min (figure 5.2c). It appears unlikely that the

action of 4-aminopyridine in human sperm was to inhibit ATPases since, when cells were treated with the drug in low- $\text{Ca}^{2+}$  saline, subsequent addition of  $\text{Ca}^{2+}$  evoked large oscillations of  $[\text{Ca}^{2+}]_i$ , (indicating repeated accumulation and release of stored  $\text{Ca}^{2+}$ ) which occurred almost exclusively in those cells that had previously shown a 4-aminopyridine-induced  $[\text{Ca}^{2+}]_i$  transient (figure 5.2 a). Thus an action actively to mobilise  $\text{Ca}^{2+}$ , or to sensitise  $\text{Ca}^{2+}$  release, is more likely.

Exposure of human sperm to EGTA-buffered, ' $\text{Ca}^{2+}$  free' medium causes an immediate and large fall in  $[\text{Ca}^{2+}]_i$  and rapidly depletes intracellular  $\text{Ca}^{2+}$  stores (Harper *et al*, 2004; Bedu-Addo *et al*, 2007). Cells incubated in EGTA-buffered saline for 10 -15 min showed no response to 4-aminopyridine, but application of the drug 4-5 min after exposure to EGTA induced a clear response in almost 25% of cells . Under these circumstances the rise in  $[\text{Ca}^{2+}]_i$  was transient and was of diminished amplitude. Thus it appears that at least part of the elevation in  $[\text{Ca}^{2+}]_i$  that occurs in human sperm exposed to 4-aminopyridine reflects the mobilisation of stored  $\text{Ca}^{2+}$ , though the prolonged effect is probably dependent upon  $\text{Ca}^{2+}$ -influx.

### ***Effect of 4-aminopyridine on microsomal $\text{Ca}^{2+}$ uptake and release***

The asynchronous behaviour and minute size of human sperm presents many technical difficulties. As discussed above, single cell imaging experiments in  $\text{Ca}^{2+}$  free conditions indicated that 4-aminopyridine was mobilising stored calcium however it is difficult to isolate and identify the channels or pumps involved. Furthermore, 4-aminopyridine has potentially numerous other effects on human sperm including blocking  $\text{K}_v$  channels, cytoplasmic alkalisation and activation of KSper and CatSper channels. In an attempt to isolate the components of the calcium signalling 'toolkit' targeted by 4-aminopyridine, microsomes (brain and sarcoplasmic reticulum) were utilized to examine calcium uptake and mobilisation. Application of 2mM 4-aminopyridine to rabbit SR did not significantly alter the rate or kinetics

of  $\text{Ca}^{2+}$ -ATPase uptake, although an increased dose of 4-aminopyridine may have an effect. These results are in agreement with Ishida and Honda (1993) who examined the effects of 4-aminopyridine on guinea pig SR  $\text{Ca}^{2+}$ -ATPase activity. High doses of 4-aminopyridine (10mM) were required to inhibit guinea pig SR  $\text{Ca}^{2+}$ -ATPase uptake whereas lower dose (<3mM) 4-aminopyridine did not have a significant effect.

As yet there is no consensus to the identity of the  $\text{Ca}^{2+}$  channel localised in the neck/midpiece region of mammalian sperm. Suarez and co report the presence of  $\text{IP}_3\text{R}$  however high, non-specific doses of thapsigargin are required to mobilise this store. Despite the slow  $\text{Ca}^{2+}$  uptake by brain microsomes,  $\text{Ca}^{2+}$  release occurred in response to 4-aminopyridine (~7% of total accumulated) but did not occlude a subsequent response to  $\text{IP}_3$  indicating that 4-aminopyridine and  $\text{IP}_3$  act at different sites on the channels. These results are contrary to Palade and co-workers (1989) who reported that 4-aminopyridine inhibited  $\text{IP}_3$  induced  $\text{Ca}^{2+}$  release from brain microsomes by direct interaction with the  $\text{Ca}^{2+}$  channel. However these results are in agreement with Guse *et al.*, 1994 who report 4-aminopyridine induced a dose-dependent  $\text{IP}_3\text{R}$  calcium release followed by a sustained elevation of  $[\text{Ca}^{2+}]_i$  in Jurkat T-lymphocytes. Furthermore, Grimaldi and co-workers (2001) demonstrated that 4-aminopyridine enhanced phospholipase C (PLC)/ $\text{IP}_3$  pathways in neurons and astrocytes resulting in store mobilisation. It is possible that 4-aminopyridine induced store mobilisation in intact human spermatozoa directly or indirectly by enhanced  $\text{IP}_3$  production.

Immunolocalisation studies from our laboratory demonstrate the presence of ryanodine receptors (RyR) proteins (isoforms 1 and 2) expressed in the posterior head of human sperm (Harper *et al.*, 2004; Lefièvre *et al.*, 2007). The ryanodine receptors are large ion channels, positively regulated by S-nitrosylation and the recent report by Machado-Oliveira *et al.*, (2008) demonstrated that nitric oxide donors and progesterone converge and act synergistically to enhance calcium mobilisation in human sperm. Ryanodine receptors have high conductance (>100pS; Zalk *et al.*, 2007) so it is likely that any sperm RyRs are expressed at extremely low

levels (Costello *et al.*, 2009). We have examined the dose-dependent effects of 4-aminopyridine on RyR1, the predominant isoform expressed in rabbit skeletal muscle (figure 5.5c). Following  $\text{Ca}^{2+}$  uptake  $\text{Ca}^{2+}$ -ATPase activity was inhibited with thapsigargin prior to the addition of 4-aminopyridine. In the majority of experiments a definite increase in fluorescence signal was observed reflecting  $\text{Ca}^{2+}$  release. This data demonstrates that 4-aminopyridine is a relatively effective ryanodine receptor activator of  $\text{Ca}^{2+}$  release (~5% release, figure 5.5d). For comparison the commonly used ryanodine receptor activator, 4-chloro-m-cresol (4CmC) was recently shown to release ~10% of SR vesicle stored calcium (Al-Mousa and Michelangeli, 2009). These results agree with Ishida *et al.*, (1992) who demonstrated that 4-aminopyridine (1mM) induced a transient  $\text{Ca}^{2+}$  release from guinea pig SR.

Treatments which induce  $\text{Ca}^{2+}$  influx can 'switch on' cyclical mobilisation of this store (causing cytoplasmic  $[\text{Ca}^{2+}]_i$  oscillations) apparently due to a form of calcium induced calcium release (CICR) (Kirkman-Brown *et al.*, 2004; Harper *et al.*, 2005; Bedu-Addo *et al.*, 2007). Previous work in this laboratory has provided evidence for participation of stored  $\text{Ca}^{2+}$  in complex  $[\text{Ca}^{2+}]_i$  signals that occur in human sperm stimulated with progesterone or NO, both products of the female tract and cumulus-oocyte complex (COC) (Publicover *et al.*, 2007; Machado-Oliveira *et al.*, 2008). Pre-treatment of sperm with low dose progesterone (100pM) induced a small rise in  $[\text{Ca}^{2+}]_i$  and altered the NO induced response from a tonic increase in  $[\text{Ca}^{2+}]_i$  to a large transient which was often followed by oscillations (Machado-Oliveira *et al.*, 2008). Similar results are reported in this study, low dose progesterone caused a modest background (tonic) increase in  $\text{Ca}^{2+}$  'leak' into the sperm leading to elevation of resting  $[\text{Ca}^{2+}]_i$  and possible accumulation of  $\text{Ca}^{2+}$  into the neck/midpiece store. The response to 4-aminopyridine is altered in cells pre-treated with low dose progesterone to a transient increase in  $[\text{Ca}^{2+}]_i$  which is followed by oscillations in ~15% of cells, providing further evidence of 4-aminopyridine induced store mobilisation in human sperm. 4-aminopyridine induced  $\text{Ca}^{2+}$

release from brain and SR microsomal vesicles provides evidence that this compound can activate intracellular  $\text{Ca}^{2+}$  stores mobilisation.

***Stored  $\text{Ca}^{2+}$  and 4-aminopyridine-induced hyperactivation.***

CASA was used to examine whether mobilisation of stored  $\text{Ca}^{2+}$  might contribute to the strong hyperactivating action of 4-aminopyridine on human sperm. The ability of 4-aminopyridine dramatically to increase the proportion of hyperactivated cells was not inhibited by simple omission of  $\text{Ca}^{2+}$  from the medium, the ability of the drug to induce hyperactivation being, if anything, enhanced (figure 5.3a). Furthermore, following brief re-suspension in EGTA-buffered saline (~2 mins), application of 2mM 4-aminopyridine induced hyperactivation in a proportion of cells only slightly lower than that in controls (standard medium; figure 5.3b). Induction of hyperactivation by 4-aminopyridine was truncated in cells re-suspended in EGTA-buffered medium, lasting for a maximum of 12 min (figure 5.3b) even though motility of the cells persisted for 20-30 min (figure 5.3c). The decay of 4-aminopyridine-induced elevation of  $[\text{Ca}^{2+}]_i$  in the presence of EGTA appeared to be more rapid than the decay of hyperactivation in 'parallel' CASA experiments (figure 5.3b), but this probably reflects the fact that, for CASA, the cells were pelleted and re-suspended in EGTA buffered medium. Though this procedure was done with care to minimize carry over of sEBSS in the pellet,  $[\text{Ca}^{2+}]_o$  may well have been slightly less stringently buffered in these experiments. It appears that mobilisation of  $\text{Ca}^{2+}$  from a labile, EGTA-sensitive store, contributes to the ability of 4-aminopyridine to induce hyperactivation. These findings are consistent with previous reports that extra-cellular calcium is not a requirement for initiation of hyperactivation in bovine and murine sperm. Suarez and colleagues concluded that mobilisation of stored  $\text{Ca}^{2+}$  (possibly from the redundant nuclear envelope) is sufficient to initiate but cannot sustain hyperactivated motility (Ho and Suarez 2001b; Marquez *et al*, 2007; Olson *et al.*, 2010; Chang and Suarez, 2010).

### ***Inhibition of sperm intracellular $\text{Ca}^{2+}$ store channels and 4-aminopyridine-induced $[\text{Ca}^{2+}]_i$ response***

In an attempt to inhibit intracellular  $\text{Ca}^{2+}$  store release cells were treated with a local anesthetic tetracaine (1mM for 10mins) prior to application of 4-aminopyridine (2mM). Tetracaine (1mM) has previously been shown to inhibit ryanodine receptor calcium release in brain microsomal membranes (Martin *et al.*, 1993) and diminish motility in human sperm (2mM, tetracaine) (Teves *et al.*, 2009).

Tetracaine contains an aromatic amine (pKa8.3) and like 4-aminopyridine its activity and membrane permeability are dependent on the ionisation state of the compound. At higher extracellular pH, the compound is membrane permeable but the charged compound is active intracellular. Pre-treatment of cells with tetracaine did not significantly effect the response to 4-aminopyridine, the majority of cells responded with a sustained increase in  $[\text{Ca}^{2+}]_i$  fluorescence. However removal of the inhibitor altered the 4-aminopyridine response to a transient increase in  $[\text{Ca}^{2+}]_i$  fluorescence (figure 5.7a), possibly due to store mobilisation. This response was absent in experiments where cells continue to be exposed to tetracaine (figure 5.7b). However, tetracaine does not specifically inhibit intracellular  $\text{Ca}^{2+}$  release channels, this compound also affects  $\text{Ca}^{2+}$ -ATPases, sodium potassium ATPase (NaK-ATPases), mitochondrial membrane integrity and estrogen receptor all of which are present in mammalian sperm cells.

### ***4-aminopyridine induced $[\text{Ca}^{2+}]_i$ response is not due to mobilisation of mitochondrial $\text{Ca}^{2+}$ in human sperm***

The mitochondria of mammalian sperm can accumulate  $\text{Ca}^{2+}$  in the matrix compartment *in situ* (Wennemuth *et al.*, 2003b) through the mitochondrial  $\text{Ca}^{2+}$  uniporter (MCU) and controlled release occurs through the  $\text{Na}^+$   $\text{Ca}^{2+}$  exchanger (NCX) (Bernardi *et al.*, 1999). Excessive  $\text{Ca}^{2+}$  accumulation can lead to activation of the permeability transition pore, which permits release



of apoptotic factors leading to cell death (Jeong and Seol, 2008). Previously, we have shown that mitochondrial  $\text{Ca}^{2+}$  uptake is not involved in store-mediated calcium oscillations (stimulated with low dose progesterone or NO) (Machado-Oliveira *et al.*, 2008). We report that uncoupling of mitochondrial respiration (with 2,4 dinitrophenol) did not inhibit the 4-aminopyridine induced tonic increase in  $[\text{Ca}^{2+}]_i$  (figure 5.8b). These results are in agreement with other studies which have demonstrated that mitochondrial function did not contribute significantly to store mobilisation (Ho and Suarez, 2003; Machado-Oliveira *et al.*, 2008). Evidence suggests that excessive  $\text{K}^+$  efflux and intracellular  $\text{K}^+$  depletion are key early stages in apoptosis. Mitochondrial viability (retention of rhodamine 123 as described in Ogunbayo *et al.*, 2008), did not differ significantly in the presence or absence of 4-aminopyridine (figure 5.8c). Furthermore recent investigations on cerebellar granule neurons demonstrated that 4-aminopyridine did not significantly depolarise the resting mitochondrial membrane potential but enhanced cell viability. In summary 4-aminopyridine does not significantly mobilise mitochondrial  $\text{Ca}^{2+}$  or induce cell death (apoptosis).

#### *4-aminopyridine does not induce the acrosome reaction in human sperm*

The acrosomal store is strongly implicated in regulation of exocytosis of the acrosomal vesicle itself (acrosome reaction) (O'Toole *et al.*, 2000; Herrick *et al.*, 2005). Despite the sustained effect of 4-aminopyridine on  $[\text{Ca}^{2+}]_i$ , we observed no increase in the proportion of acrosome reacted cells (figure 5.9) further illustrating the ability of sperm to maintain specific 'targeting' of responses mediated through  $[\text{Ca}^{2+}]_i$  signalling (Publicover *et al.*, 2007).

#### *Conclusion*

4-aminopyridine caused reversible, repeatable mobilisation of  $\text{Ca}^{2+}$  stored in the neck/midpiece accompanied by parallel, reversible and repeatable asymmetric bending of the flagellum. Investigations of the  $\text{Ca}^{2+}$  dependence of 4-aminopyridine-induced hyperactivation clearly

show that, as in mouse and bovine sperm, mobilisation of stored  $\text{Ca}^{2+}$  is sufficient to initiate hyperactivation, but also suggest that store-operated  $\text{Ca}^{2+}$  influx contributes to maintenance of this mode of motility.

Previous studies on the effects of 4-aminopyridine on cellular  $\text{Ca}^{2+}$ -homeostasis have shown that the drug mobilises stored  $\text{Ca}^{2+}$  in other cell types, though the mechanism by which this may be achieved is not clear (Guse *et al.*, 1994; Ishida and Honda, 1993; Gobet *et al.*, 1995; Grimaldi *et al.*, 2001). These results demonstrate that 4-aminopyridine induced store mobilisation is non-specific having a similar effect on  $\text{IP}_3\text{R}$  and  $\text{RyR}$  in microsomal preparations. It seems likely that 4-aminopyridine induced  $\text{Ca}^{2+}$  mobilisation (in  $\text{Ca}^{2+}$  free conditions) of the neck/midpiece store would involve activation of the ryanodine receptor channel or  $\text{IP}_3\text{R}$  channel although the exact mechanism and target remains unclear. Store depletion may also trigger  $\text{Ca}^{2+}$  influx via flagellar store operated calcium mechanisms to refill the depleted neck region store.

## **CHAPTER SIX**

### **4-AMINOPYRIDINE AND CAPACITATIVE $\text{Ca}^{2+}$ ENTRY**

<b>6.1 Abstract</b>	153
<b>6.2 Introduction</b>	154
<b>6.3 Materials and methods</b>	156
6.3.1 Materials	156
6.3.2 Spermatozoa preparation and capacitation	156
6.3.3 Evaluation of sperm hyperactivation	156
6.3.4 Single cell imaging	156
6.3.5 Data analysis	156
<b>6.4 Results</b>	
6.4.1 4-aminopyridine enhanced $\text{Ca}^{2+}$ influx in $\text{Ca}^{2+}$ store depleted sperm cells	157
6.4.2 Pharmacological inhibition of store operated $\text{Ca}^{2+}$ channels modified the 4-aminopyridine induced $[\text{Ca}^{2+}]_i$ response	163
<b>6.5 Discussion</b>	167

## 6.1 Abstract

4-aminopyridine, at concentrations comparable with those used here, strongly potentiates capacitative  $\text{Ca}^{2+}$  entry (CCE) in astrocytes and skeletal muscle cells (Grimaldi *et al.*, 2001). 4-aminopyridine has previously been shown to induce store mobilisation in microsomal vesicles and in human sperm briefly treated with EGTA buffered saline (chapter 5). In experiments designed to activate store-operated channels (SOCs) (treatment with bis-phenol or incubation in EGTA buffered saline) this report demonstrates that  $\text{Ca}^{2+}$  influx in the presence of 4-aminopyridine was enhanced. Furthermore pharmacological inhibition of SOC (with 2-APB and SFF-96365) had a significant effect on the 4-aminopyridine induced response. In the presence of inhibitors, 4-aminopyridine induced a transient  $[\text{Ca}^{2+}]_i$  response, the SOC sustained influx was inhibited in a population of cells. Significantly this effect was absent when CatSper channel influx was activated by cytoplasmic alkalinisation (2-APB pretreatment did not significantly effect the  $\text{NH}_4\text{Cl}$  induced  $[\text{Ca}^{2+}]_i$  response). These results indicate that the 4-aminopyridine induced  $[\text{Ca}^{2+}]_i$  store mobilisation response may potentiate SOC within a population of human sperm.

## 6.2 Introduction

Mammalian sperm use  $\text{Ca}^{2+}$ -signalling to regulate or contribute to the regulation of many different functions including hyperactivation (Ho and Suarez, 2003; Jimenez-Gonzalez *et al.*, 2006; Publicover *et al.*, 2007).

Numerous studies have demonstrated that the CatSper channel proteins are required for normal hyperactivated motility in mouse sperm (Ren *et al.*, 2001; Quill *et al.*, 2003; Carlson *et al.*, 2005; Qi *et al.*, 2007; Xia *et al.*, 2007). In addition, studies on sperm from rodents, bulls and humans have provided strong evidence that  $\text{Ca}^{2+}$  stored in the region of the sperm neck contributes to regulation of flagellar activity (Ho and Suarez, 2001b, 2003; Naaby-Hansen *et al.* 2001). Triggering mobilisation of this stored  $\text{Ca}^{2+}$  can induce hyperactivation in mouse sperm lacking CatSper (Marquez *et al.*, 2007). Recent data from this laboratory has demonstrated the presence of stromal interacting protein 1 (STIM1, a protein containing a calcium sensor located in the intracellular calcium store) and Orai proteins (a protein that forms a calcium channel in the plasma membrane) in human sperm, immunolocalised primarily to the neck/midpiece (Lefièvre *et al.*, in prep), both these proteins are required for calcium release activated channel (CRAC) activity. Since capacitative calcium entry (CCE) has been observed in sperm (Blackmore 1993; Yoshida *et al.*, 2003; Harper *et al.*, 2003, 2005; Bedu-Addo *et al.*, 2007; Costello *et al.*, 2009), store mobilisation might even recruit this mechanism to supplement  $\text{Ca}^{2+}$  influx through CatSper channels (Olson *et al.*, 2010). Alternatively this pathway for induction of hyperactivation may play a separate role from that mediated by CatSper. Observations of sperm, primarily in humans but also other mammals, suggest that the cells can ‘switch’ rapidly and probably repeatedly between activated and hyperactivated motility (Katz *et al.*, 1989; Pacey *et al.*, 1995a, 1995b; Mortimer and Swan 1995), a behaviour that may mediate interactions with cells of the female tract (Pacey *et al.*, 1995a, 1995b). Mobilisation of stored  $\text{Ca}^{2+}$ , which is rapidly reversible and localised, may be better suited to such transient regulation of motility whereas pH regulated activation of CatSper could support the prolonged

hyperactivation that permits 'permanent' detachment from the cells of the female tract (Ho *et al.*, 2009) and penetration of the zona.

Results have shown that 4-aminopyridine causes dramatic hyperactivation of human sperm, whereas cytoplasmic alkalinisation with 25mM NH<sub>4</sub>Cl which hyperactivates bovine sperm (Marquez and Suarez, 2007) had a negligible effect on human sperm motility (chapter 3). Furthermore 4-aminopyridine can induce store mobilisation in microsomal vesicles although the exact mechanism involved remains unclear (chapter 5). Since 4-aminopyridine has been shown to potentiate capacitative calcium entry (CCE) in a number of cell types (Grimaldi *et al.*, 2001) store mobilisation was investigated and whether the 4-aminopyridine induced [Ca<sup>2+</sup>]<sub>i</sub> fluorescence response involves CCE.

The effects of a number of store operated Ca<sup>2+</sup> channel (SOC) inhibitors (high dose 2-APB and SKF-96365) and agonist (low dose 2-APB) on 4-aminopyridine induced [Ca<sup>2+</sup>]<sub>i</sub> signals in OGB loaded spermatozoa was examined.

## **6.3 Materials and Methods**

### **6.3.1 Materials**

As described in chapter two. 1-[ $\beta$ -[3-(4-Methoxyphenyl)propoxy]-4-methoxyphenethyl]-1H-imidazole, HCL (SKF-96365 stock conc. 10mM was made up in H<sub>2</sub>O) purchased from Calbiochem (UK). bis(2-hydroxy-3-tert-butyl-5-methyl-phenyl)methane (bis-phenol, stock conc. 20mM made up in DMSO) was purchased from Pfaltz and Bauer, Waterbury, CT. 2-aminoethoxydiphenylborane (2-APB, stock conc. 200mM, made up in DMSO) was from Sigma Aldrich (Poole, Dorset, UK). All chemicals were cell-culture-tested grade where available. Nominal Ca<sup>2+</sup> free saline (no added Ca<sup>2+</sup>, ([Ca<sup>2+</sup>]<sub>o</sub> ≤ 5μM)) and EGTA buffered medium (5mM Ca<sup>2+</sup>, 6mM EGTA, 25°C ([Ca<sup>2+</sup>]<sub>o</sub> 10<sup>-7</sup> M)) were prepared as described in chapter 5. The calcium concentration calculator Maxchelator (V2.2) written by Chris Patton from Stanford University (<http://www.stanford.edu/~cpatton/maxc.html>) was used to calculate the free calcium concentration in saline containing EGTA.

### **6.3.2 Spermatozoa preparation and capacitation**

As described in chapter two.

### **6.3.3 Evaluation of sperm hyperactivation**

As described in chapter two.

### **6.3.4 Single cell Imaging**

As described in chapter two.

### **6.3.5 Data Analysis**

As described in chapter two.

## 6.4 Results

### 6.4.1 4-aminopyridine enhanced $\text{Ca}^{2+}$ influx in $\text{Ca}^{2+}$ store depleted sperm cells

To investigate whether mobilisation of stored  $\text{Ca}^{2+}$  (potentially activating store-operated  $\text{Ca}^{2+}$  influx mechanisms) might enhance the cells response to the 4-aminopyridine response, we used a protocol designed to evacuate the sperm's intracellular stores. Since high, non-specific doses of thapsigargin are required to mobilise stored  $\text{Ca}^{2+}$  in sperm, attempts to assess  $[\text{Ca}^{2+}]_i$  may reflect effects on other  $\text{Ca}^{2+}$  pumps. Cells were exposed to EGTA-buffered medium ( $<10^{-7}\text{M}$   $\text{Ca}^{2+}$ ), conditions which cause a rapid fall in  $[\text{Ca}^{2+}]_i$  and consequent depletion of  $\text{Ca}^{2+}$  from the sperm's intracellular stores (Harper *et al.*, 2004; Bedu-Addo *et al.*, 2007). A proportion of sperm cells briefly ( $\sim 2$  mins) treated with EGTA buffered saline ( $[\text{Ca}^{2+}]_o$  at  $10^{-7}\text{M}$   $\text{Ca}^{2+}$ ), respond to 2mM 4-aminopyridine with a small transient increase in  $[\text{Ca}^{2+}]_i$  fluorescence (figure 5.2c), this response is lost when cells are continually superfused for longer periods ( $\sim 10$ mins decreased  $[\text{Ca}^{2+}]_i$  fluorescence by  $36.3 \pm 4.1\%$  below basal levels, figure 6.1a and b). Extracellular  $\text{Ca}^{2+}$  was re-introduced to the imaging chamber at a lower dose ( $10^{-5}\text{M}$ ) to prevent saturation of the fluorescent signal (intracellular OGB saturated at  $1\text{-}2\mu\text{M}$   $\text{Ca}^{2+}$ ) (Haugland, 2001). Restoration of extracellular  $\text{Ca}^{2+}$  resulted in a rapid recovery to baseline levels of  $[\text{Ca}^{2+}]_i$  fluorescence (figure 6.1b,  $n=3$  experiments, 128 cells). When the same experiments were performed in the presence of 4-aminopyridine  $[\text{Ca}^{2+}]_i$  fluorescence increased 40-50% above baseline (figure 6.1a,  $n=5$  experiments, 504 cells) a response maintained in the presence of 4-aminopyridine which promptly reversed upon washout.



Figure 6.1

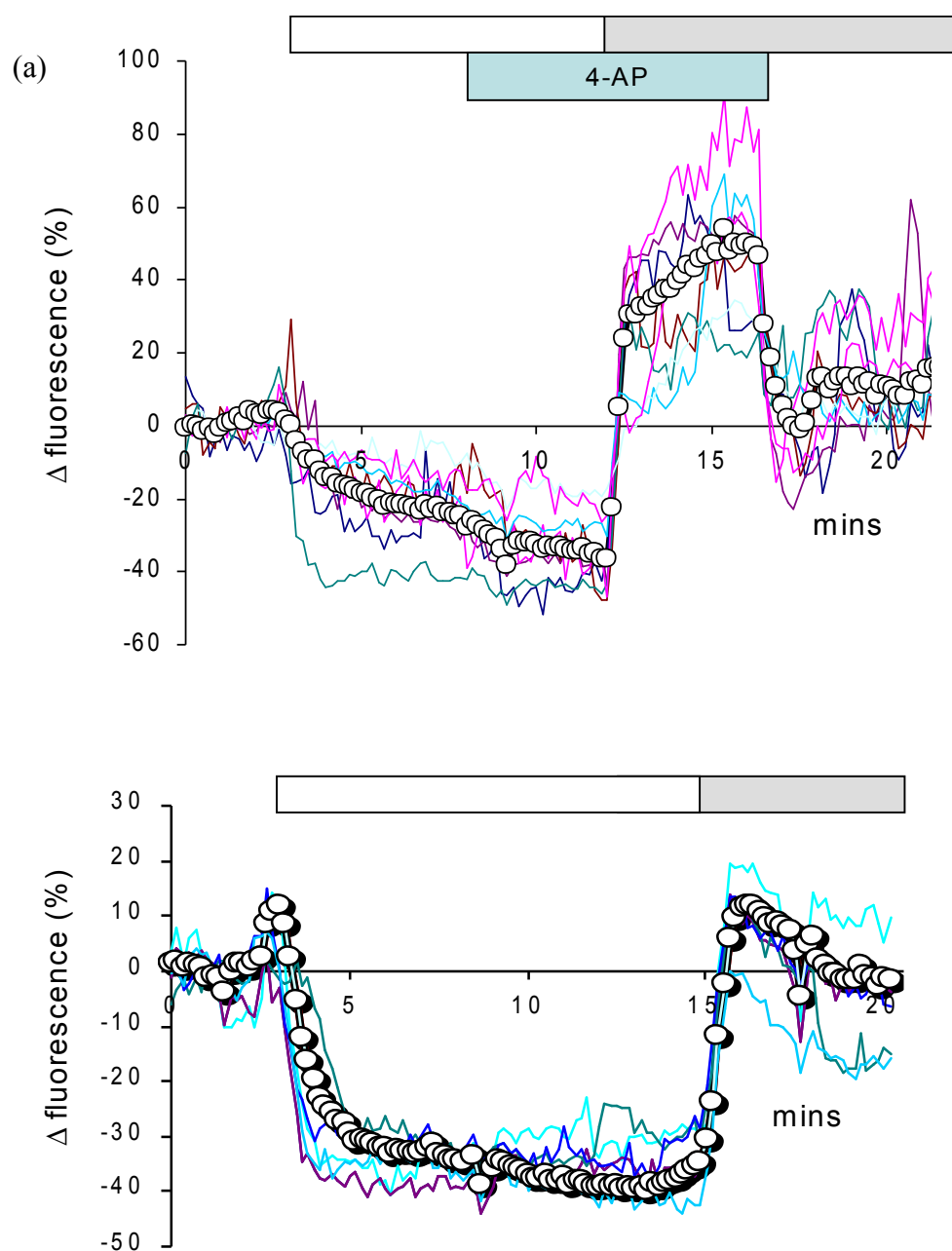


**Figure 6.1.** 4-aminopyridine enhanced  $\text{Ca}^{2+}$  influx in EGTA  $[\text{Ca}^{2+}]_i$  depleted cells. **(a)** Plot showing cells pretreated with EGTA buffered saline ( $<10^{-7}$  M  $\text{Ca}^{2+}$ , white bar) to deplete stored calcium, decreased  $[\text{Ca}^{2+}]_i$  fluorescent by 36.3% (n=5 experiments, 376 cells). Cells were exposed to 4-aminopyridine (blue bar) for ~5mins prior to the restoration of  $\text{Ca}^{2+}$  ( $[\text{Ca}^{2+}]_o = 10^{-5}$  M, grey bar) which resulted in a ~50% increase in fluorescence above baseline. Responses of 7 representative cells are shown and also mean response ( $\circ-\circ$ ) of all the 77 cells in the experiment. Upon 4-aminopyridine washout  $[\text{Ca}^{2+}]_i$  fluorescence decreased rapidly. **(b)** Superfusion of cells with EGTA buffered saline to deplete stored calcium decreased  $[\text{Ca}^{2+}]_i$  fluorescent by ~40% (n=3 experiments,

128 cells). Restoration of ( $[Ca^{2+}]_o = 10^{-5}$  M, grey bar) resulted in a  $[Ca^{2+}]_i$  fluorescence recovering to ~10% above baseline which promptly returned to basal levels. Responses of 5 representative cells are shown and also mean response ( $\circ-\circ$ ) of all the 66 cells.

In sperm, high non-specific doses of thapsigargin (to inhibit SERCA) does not induce a rapid elevation of  $[Ca^{2+}]_i$  but a gradual release, the effect is irreversible resulting in a loss of motility (Williams and Ford, 2003). In human cells data from this laboratory has shown that the neck/midpiece store is not mobilised by thapsigargin, but is sensitive to bis-phenol, an inhibitor of  $Ca^{2+}$  ATPases (both SERCA and SPCA) (Brown *et al.*, 1994; Harper *et al.*, 2001, 2005; Bedu-Addo *et al.*, 2007). Bis-phenol mobilises stored  $Ca^{2+}$  in human sperm and prevents generation of store-mediated  $Ca^{2+}$ -oscillations (Harper *et al.*, 2005; Bedu-Addo *et al.*, 2007).

When cells were incubated in the presence of bis-phenol (20  $\mu$ M) a sustained increase in  $[Ca^{2+}]_i$  was observed due to impairment of  $Ca^{2+}$  clearance mechanisms (Brown *et al.*, 1994; Bedu-Addo *et al.*, 2007). An increase in fluorescence (calculated with respect to steady-state level in the presence of bis-phenol) upon application of 2mM 4-aminopyridine was not only still evident, but was enhanced, (mean =  $52.9 \pm 0.9\%$ ; 597 cells from 5 experiments; figure 6.2a), significantly greater than the response in cells not pretreated with bis-phenol ( $P < 10^{-5}$ ). When these experiments were repeated in medium with no added  $Ca^{2+}$  ( $[Ca^{2+}]_o \leq 5$   $\mu$ M) (Harper *et al.*, 2004), to reduce  $Ca^{2+}$  influx at the plasma membrane, bis-phenol again caused a sustained (though smaller) rise in  $[Ca^{2+}]_i$  (Bedu-Addo *et al.*, 2007), the effect of 4-aminopyridine was greatly reduced. The increase in fluorescence 5 min after application of 4-aminopyridine was just  $12.2 \pm 0.5\%$ , significantly smaller than in non-pretreated preparations (paired *t*-test,  $P < 0.0005$ ) and in some experiments was barely detectable (figure 6.2b).

Treatment with bis-phenol in the presence or absence of extracellular  $Ca^{2+}$  does not significantly enhance hyperactivation in human spermatozoa. Application of 4-aminopyridine

was required to significantly enhance hyperactivation (figure 6.2c). Examination of VCL (the total distance the sperm covered in the observation period) highlighted the potent effect of 4-aminopyridine on motility (increased from  $85.0 \pm 4.9$  to  $129.7 \pm 7.6$   $\mu\text{m}/\text{sec}$  in NCFsEBSS) an effect not mirrored in cells treated with bis-phenol. However, treatment with bis-phenol decreased % motility in both normal and nominal free  $\text{Ca}^{2+}$  saline (table 6.1) and with addition of 4-aminopyridine many cells were observed to ‘freeze’ with tightly bent flagella (arrested with angulated flagellum), which is typical cytoplasmic  $\text{Ca}^{2+}$  overload (apparently due to impaired  $\text{Ca}^{2+}$  clearance and  $\text{Ca}^{2+}$  influx).

**Figure 6.2**

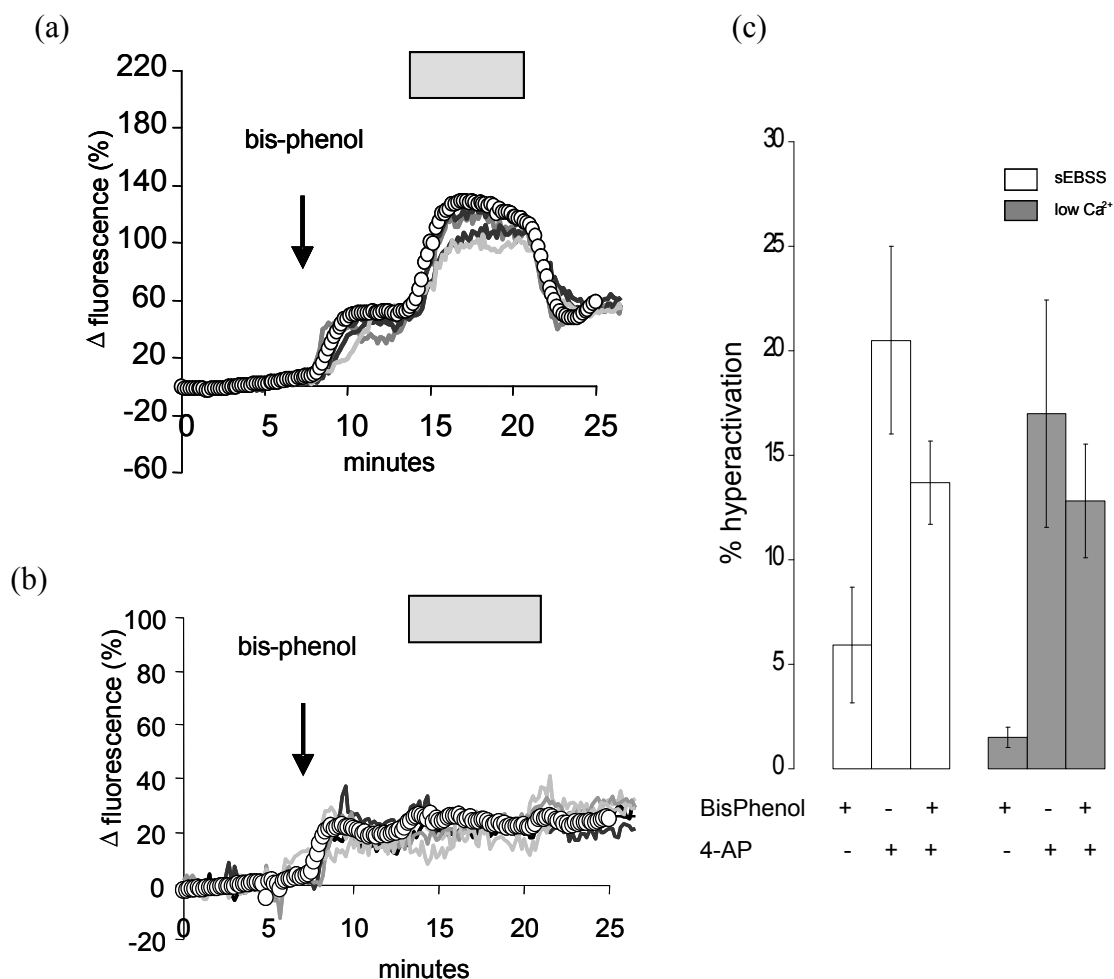


**Table 6.1. Effect of bis-phenol (20 $\mu$ M)  $\pm$  4-aminopyridine (2mM) on sperm motility, VCL, ALH and LIN (mean $\pm$ SEM; n=6donors) in normal saline and saline with no added  $Ca^{2+}$  ( $[Ca^{2+}]_o \leq 5$  mM)**

	Motile(%)	VCL ( $\mu$ m/sec)	ALH ( $\mu$ m)	LIN (%)
Cntrl ( $[Ca^{2+}]_o$ 1.8mM)	83.0 $\pm$ 3.5	113.4 $\pm$ 12.1	4.5 $\pm$ 0.6	59.6 $\pm$ 1.4
+ 4AP	81.2 $\pm$ 3.6	149.5 $\pm$ 8.2	6.1 $\pm$ 0.3	49.6 $\pm$ 1.4
+ bis-phenol	74.6 $\pm$ 4.7	117.8 $\pm$ 6.8	4.8 $\pm$ 0.1	53.6 $\pm$ 1.2
+ bis-phenol and 4AP	59.0 $\pm$ 9.0	123.6 $\pm$ 4.8	5.1 $\pm$ 0.1	16.5 $\pm$ 2.9
Cntrl ( $[Ca^{2+}]_o \leq 5 \mu$ M)	75.8 $\pm$ 4.6	85.0 $\pm$ 4.9	3.4 $\pm$ 0.2	64.2 $\pm$ 1.4
+ 4AP	75.5 $\pm$ 4.1	129.70 $\pm$ 7.7	5.5 $\pm$ 0.3	52.0 $\pm$ 1.0
+ bis-phenol	62.0 $\pm$ 2.6	87.6 $\pm$ 3.1	4.0 $\pm$ 0.2	55.0 $\pm$ 0.9
+ bis-phenol and 4AP	53.2 $\pm$ 6.1	115.2 $\pm$ 9.1	5.4 $\pm$ 0.5	46.3 $\pm$ 1.4

**Figure 6.2:** Effect of prior mobilisation of stored  $\text{Ca}^{2+}$  (by inhibition intracellular  $\text{Ca}^{2+}$  store uptake with bis-phenol) on the response to 4-aminopyridine in normal and nominal  $\text{Ca}^{2+}$  free saline. **(a)** Pre-treatment of cells with bis-phenol in standard saline. Responses of 7 representative cells are shown and also mean response ( $\circ-\circ$ ) of all the 150 cells in the experiment. Cells were exposed to 20  $\mu\text{M}$  bis-phenol (arrow) for  $\approx 5$  min, causing a sustained elevation of  $[\text{Ca}^{2+}]_i$ . Application of 2mM 4-aminopyridine (grey bar) caused a further large rise in  $[\text{Ca}^{2+}]_i$  which exceeded that seen in non-pretreated cells. This effect reversed upon washout of 4-aminopyridine. **(b)** Response to 4-aminopyridine in bis-phenol pretreated cells is dependent upon  $\text{Ca}^{2+}$  influx. Cells superfused with nominally  $\text{Ca}^{2+}$  free sEBSS (no added  $\text{Ca}^{2+}$ ;  $[\text{Ca}^{2+}] \leq 5 \mu\text{M}$ ) were exposed to 20  $\mu\text{M}$  bis-phenol (arrow) for  $\approx 5$  min, causing a sustained elevation of  $[\text{Ca}^{2+}]_i$  that was  $< 50\%$  of that seen in standard sEBSS (Harper *et al.*, 2005). Application of 2mM 4-aminopyridine (grey bar) caused only a small further rise in  $[\text{Ca}^{2+}]_i$ , the effect being negligible in many cells. Responses of 6 representative cells are shown and also mean response ( $\circ-\circ$ ) of all the 103 cells in the experiment. **(c)** Proportion of hyperactivated cells (mean  $\pm$  SEM) in response of bis-phenol  $\pm$  4-aminopyridine in normal saline (white bars) and nominal  $\text{Ca}^{2+}$  free saline (grey bars). **Table 6.1** Effects of bis-phenol  $\pm$  4-AP on human sperm motility, VCL, ALH and LIN in standard or nominal  $\text{Ca}^{2+}$  free saline ( $[\text{Ca}^{2+}]_o \leq 5 \mu\text{M}$ ) (mean  $\pm$  SEM,  $n=6$  donors).

#### **6.4.2 Pharmacological inhibition of store operated $\text{Ca}^{2+}$ channels modified the 4-aminopyridine induced $[\text{Ca}^{2+}]_i$ response**

Previous reports have shown that treatment of sperm with store-operated channel blockers (high dose 2-APB and SKF-96365) inhibits asymmetrical flagellar beating patterns and chemotaxis in ascidian and human sperm (Yoshida *et al.*, 2003; Teves *et al.*, 2009).

2-APB has a reported bimodal effect on CRAC channel activity, low doses ( $<10\mu\text{M}$ ) enhance  $\text{Ca}^{2+}$  entry whereas high doses ( $<50\mu\text{M}$ ) are inhibitory (Peinelt *et al.*, 2008). Pre-treatment of sperm cells with 2-APB ( $10\mu\text{M}$  and  $50\mu\text{M}$ ) resulted in a slow tonic increase in  $[\text{Ca}^{2+}]_i$  fluorescence of  $\sim 10\%$  in  $\sim 50\text{-}60\%$  of cells. Application of 4-aminopyridine induced a transient increase of  $[\text{Ca}^{2+}]_i$  (amplitude  $20\text{-}30\%$ ) in  $50\text{-}60\%$  of sperm ( $n=6$  experiments, 596 cells, figure 6.3a) while the remaining cells ( $\sim 30\%$ ) responded with a sustained increase in  $[\text{Ca}^{2+}]_i$  (amplitude  $\sim 10\%$ ). The 4-aminopyridine induced transient response was absent from parallel control experiments, where the majority of cells ( $\sim 80\%$ ) responded to with a sustained increase of  $24.0\pm 1.7\%$  ( $n=3$  experiments, 269 cells). The effect of 2-APB on the 4-aminopyridine induced response was independent of cytoplasmic alkalinisation. In parallel experiments where 4-aminopyridine was replaced with  $\text{NH}_4\text{Cl}$  ( $25\text{mM}$ ), pre-treatment with 2-APB ( $10\mu\text{M}$  and  $50\mu\text{M}$ ) did not significantly alter the kinetics or amplitude of the  $\text{NH}_4\text{Cl}$  induced  $[\text{Ca}^{2+}]_i$  response (figure 6.3b,  $n=7$  experiments, 450 cells, paired *t*-test,  $P>0.05$ ).

The compound SKF-96365 is widely used to block  $\text{Ca}^{2+}$  channels including store operated channels (Merritt *et al.*, 1990; Hirohashi and Vacquier, 2003). Treatment of sperm cells with SKF-96365 ( $10\mu\text{M}$  for 10 minutes, figure 6.3c, white bar) resulted in a increase in  $[\text{Ca}^{2+}]_i$  of  $\sim 10\pm 2.7\%$  in the majority ( $\sim 80\%$ ) of cells. Application of 4-aminopyridine (black arrow) induced a transient  $[\text{Ca}^{2+}]_i$  fluorescence response in  $\sim 64\%$  of cells of  $26.8\pm 5.8\%$  ( $n=4$  experiments, 353 cells) (calculated with respect to steady-state level in the presence of

SKF-96365). In parallel control experiments (non-SKF-96365 treated) ~80% responded to 4-aminopyridine with a sustained response of  $27.0 \pm 1.7\%$  (n=4 experiments, 511 cells).

There was no significant correlation between the gradual tonic increase in  $[Ca^{2+}]_i$  fluorescence (induced by 2-APB or SKF96395) with the 4-aminopyridine induced transient  $[Ca^{2+}]_i$  response ( $P > 0.05$ ; chi square test).

**Figure 6.3**

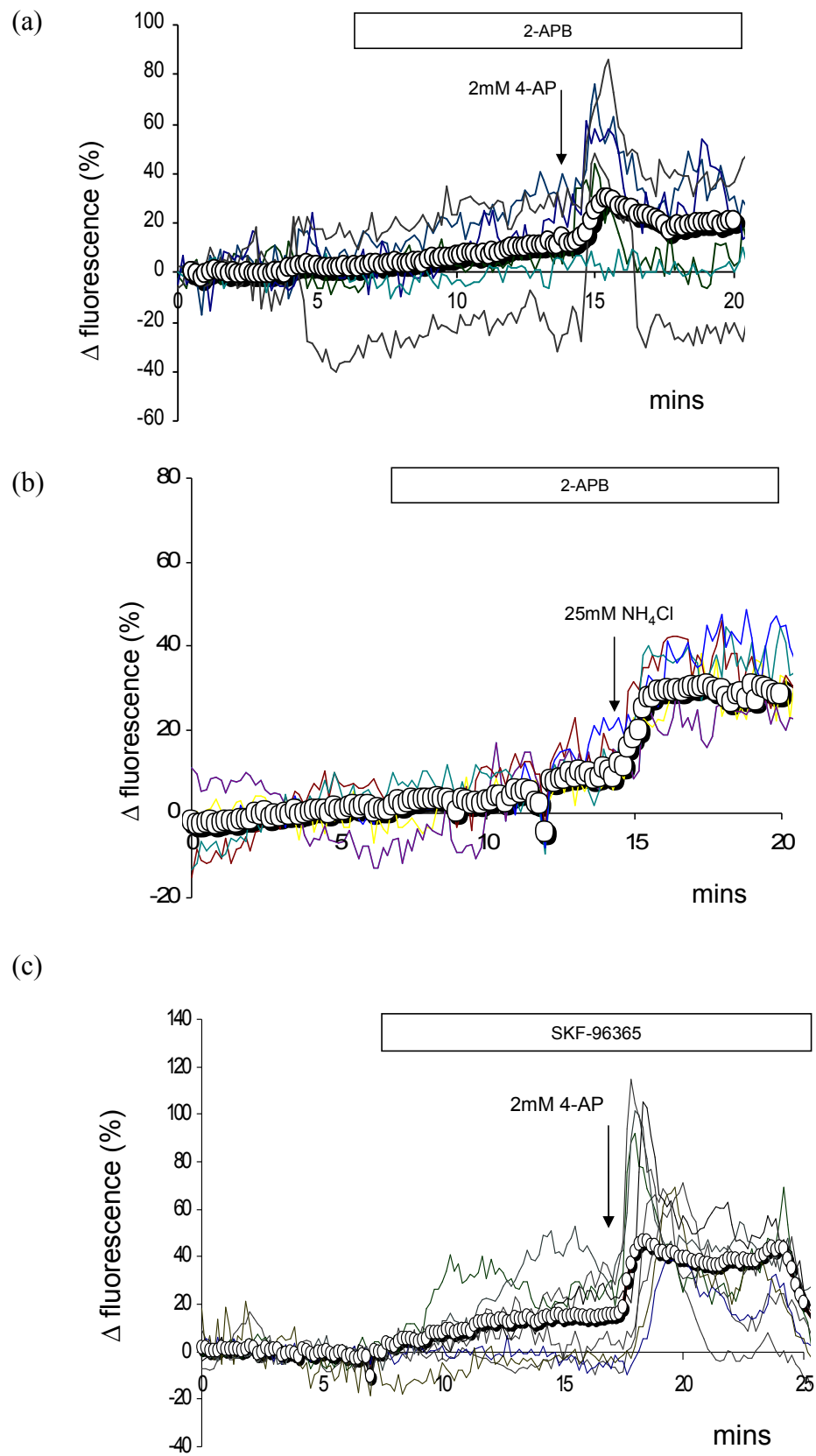




**Figure 6.3.** Pre-treatment with store operated channel (SOC) inhibitors (50 $\mu$ M 2-APB or 10 $\mu$ M SKF-96365) (white bar) altered the 4-aminopyridine induced  $[Ca^{2+}]_i$  fluorescence response in a proportion of sperm cells. **(a)** 2-APB (50 $\mu$ M) pretreatment (10 mins, white bar) causes a tonic increase of  $[Ca^{2+}]_i$  fluorescence in cells superfused with sEBSS. Upon application of 4-aminopyridine (arrow) many cells respond with a transient increase in  $[Ca^{2+}]_i$  fluorescence cells. Responses of 5 representative cells are shown and also mean response ( $\circ-\circ$ ) of all the 95 cells in the experiment. **(b)** Pre-treatment with 2-APB (50 $\mu$ M, for 10 mins, white bar) did not significantly alter the  $NH_4Cl$  (25mM, arrow) induced  $[Ca^{2+}]_i$  fluorescence response (paired *t*-test,  $P>0.05$ ). Responses of 6 representative cells are shown and also mean response ( $\circ-\circ$ ) of all the 79 cells in the experiment. **(c)** SKF-96365 (10 $\mu$ M) pretreatment (10mins, white bar) causes a tonic increase of  $[Ca^{2+}]_i$  fluorescence in cells superfused with standard saline. Upon application of 4-aminopyridine ~60% of cells respond with a transient increase in  $[Ca^{2+}]_i$  fluorescence cells. Responses of 10 representative cells are shown and also mean response ( $\circ-\circ$ ) of all the 94 cells in the experiment.

## 6.5 Discussion

The role of hyperactivated motility is not restricted to penetration of the zona pellucida. It facilitates mucus penetration (Suarez and Ho, 2003a, 2003b) and aids detachment of cells bound to the walls of the female tract (Suarez and Pacey, 2006). The ability to control and rapidly 'switch' hyperactivation is likely to be important in interaction of human and animal sperm with the fluids and cells of the female tract (Pacey *et al.*, 1995a, 1995b; Suarez and Pacey, 2006). Increased  $\text{pH}_i$ , leading to activation of CatSper channels (Navarro *et al.*, 2007), could provide prolonged hyperactivation in capacitated cells at the site of fertilisation and may even cause hyperactivation of cells upon binding to zona proteins (Xia and Ren, 2009b). In contrast, activation by  $\text{Ca}^{2+}$  store mobilisation and capacitative calcium entry (CCE) may be better suited to generation of bursts of hyperactivation 'on demand', regulated by a range of factors encountered at various points within the female tract such as progesterone and nitric oxide (Harper *et al.*, 2004, 2005; Machado-Oliveira *et al.*, 2008). Marquez *et al.*, (2007) demonstrated that store mobilisation induced hyperactivation in CatSper null sperm providing strong evidence that store mobilisation and CCE play a role in regulating flagellar activity.

CCE is carried by store-operated channels and the calcium release-activated  $\text{Ca}^{2+}$  current ( $I_{\text{CRAC}}$ ) is the best characterised. The molecular components of  $I_{\text{crac}}$  have been identified, depletion of stored calcium is sensed by the ER membrane protein STIM which reorganize into distinct puncta to interact with Orai subunits to form a functional  $\text{Ca}^{2+}$  channel (Frischauf *et al.*, 2008). The ubiquitously expressed STIM and Orai proteins have recently been identified in human sperm, immunolocalised primarily to the posterior neck/midpiece region (Lefièvre *et al.*, in prep). Due to the small size of sperm there seems little scope for STIM reorganisation indeed  $\text{Ca}^{2+}$  mobilisation from the posterior head/midpiece store would be negligible, it is likely that STIM and Orai proteins are already primed and in place. The transient receptor potential (TRP) channels activated by STIM1 can act as store operated  $\text{Ca}^{2+}$  channels, several TRP channels have been identified in human sperm (TPRC and TRPM) are linked with

motility regulation and the acrosome reaction (Castellano *et al.*, 2003; De Blas *et al.*, 2009).

#### *4-aminopyridine potentiates CCE in store depleted human sperm*

4-aminopyridine, at concentrations comparable with those used here, strongly potentiated CCE in astrocytes and skeletal muscle cells (Grimaldi *et al.*, 2001). To investigate the effect of 4-aminopyridine on CCE spermatozoa were exposed to EGTA-buffered medium ( $<10^{-7}$  M  $\text{Ca}^{2+}$ ), conditions which cause a rapid fall in  $[\text{Ca}^{2+}]_i$  and concomitant depletion of  $\text{Ca}^{2+}$  from the sperm's intracellular stores (Harper *et al.*, 2004; Bedu-Addo *et al.*, 2007) before application of 2mM 4-aminopyridine. Restoration of extracellular calcium ( $10^{-5}$  M) caused a significant sustained increase in  $[\text{Ca}^{2+}]_i$  fluorescence which was maintained in the presence of 4-aminopyridine. CRAC channels have high  $\text{Ca}^{2+}$  selectivity but in calcium free conditions readily allow  $\text{Na}^+$  permeation until extracellular  $\text{Ca}^{2+}$  is restored (Parekh and Putney, 2005). Torres-Flores and colleagues (2008) recently demonstrated  $\text{Na}^+$  dependent depolarisation of human spermatozoa when  $[\text{Ca}^{2+}]_o < 10^{-8}$  M due to  $\text{Na}^+$  permeation presumably through a  $\text{Ca}^{2+}$  channel. Calcium restoration resulted in  $E_m$  hyperpolarisation and a large  $\text{Ca}^{2+}$  influx although the identity of the  $\text{Ca}^{2+}$  influx channel is unclear (Gonzalez-Martinez *et al.*, 2002; Gonzalez-Martinez, 2003; Trevino *et al.*, 2004; Torres-Flores *et al.*, 2008). Since  $[\text{Ca}^{2+}]_o$  was maintained at  $10^{-7}$  M in these experiments it is probable that the 4-aminopyridine enhanced  $\text{Ca}^{2+}$  influx was SOC dependent however depolarisation induced  $\text{Ca}^{2+}$  influx may occur through other channels including the CatSper channels or voltage-gated  $\text{Ca}^{2+}$  channels (Darszon *et al.*, 2007).

The site within human sperm at which the  $[\text{Ca}^{2+}]_i$  response to 4-aminopyridine initiates, the sperm neck/midpiece (figure 5.1a), is consistent with previous reports of a store in the neck region of mammalian sperm (Ho and Suarez, 2001b, 2003; Naaby-Hansen *et al.*, 2001; Harper *et al.*, 2004). In human cells we have shown that this store is not mobilised by SERCA inhibition, but is sensitive to bis-phenol (Harper *et al.*, 2001, 2005). In cells superfused with

sEBSS the elevation of  $[Ca^{2+}]_i$  induced by 4-aminopyridine was strongly enhanced by pre-treatment with 20  $\mu$ M bis-phenol (figure 6.2a), probably reflecting induction of  $Ca^{2+}$  influx by 4-aminopyridine against a background of impaired  $Ca^{2+}$  clearance due to the effect of bis-phenol on the plasma membrane  $Ca^{2+}$ -ATPase (Brown *et al.*, 1994; Bedu-Addo *et al.*, 2007). In contrast, when these experiments were repeated in medium with no added  $Ca^{2+}$  ( $[Ca^{2+}]_o \leq 5 \mu$ M) the action of 4-aminopyridine in bis-phenol pretreated cells was greatly reduced compared to parallel experiments without pre-treatment, sometimes being barely detectable (compare responses in figures 6.2a and 6.2b). The proportion of 4-aminopyridine induced hyperactivated cells was reduced in the presence of bis-phenol, although many cells arrested with angulated flagellum (Gibbons and Gibbons, 1980; Sale, 1986).

Regardless of the method used to activate CCE (store mobilisation with bis-phenol or EGTA induced  $[Ca^{2+}]_i$  depletion) the presence of 4-aminopyridine maintained a considerably enhanced influx of calcium which reversed upon washout.

#### *Inhibition of store operated channels altered the 4-aminopyridine induced $[Ca^{2+}]_i$ response*

Despite the physiological importance of store operated channels only a few pharmacological tools are available including 2-APB and SKF-96365 (Parekh and Putney, 2005). The reported bimodal effect of 2-APB on CRAC current are complex with potentiation at low doses (5-10 $\mu$ M) whereas higher dose (>10 $\mu$ M) are inhibitory (Prakriya and Lewis, 2001; Parekh and Putney, 2005; Peinelt *et al.*, 2008). The reported dual effect of 2-APB was not evident in these experiments as both low and high dose 2-APB (10 $\mu$ M and 50 $\mu$ M) altered the 4-aminopyridine response in ~50-60% of cells to a transient which indicated store mobilisation. Human sperm may be particularly sensitive to the effects with 10 $\mu$ M 2-APB having an inhibitory effect on  $Ca^{2+}$  influx. Recent data by Lefièvre *et al.*, (in prep) demonstrates that 2-APB (5 $\mu$ M) enhanced CCE in EGTA  $[Ca^{2+}]_i$  depleted human sperm and significantly enhanced the progesterone

induced transient response. The effects of high dose 2-APB (50 $\mu$ M) are complex and has different effects depending on the molecular components of  $I_{CRAC}$  (Peinelt *et al.* 2008).

Previously results have shown that increased  $pH_i$  induced by  $NH_4Cl$  (25mM) enhanced  $[Ca^{2+}]_i$  fluorescence in human sperm presumably apparently due to CatSper channels activation (chapter 3). Pre-treatment with 2-APB (10 or 50 $\mu$ M) had little effect on  $NH_4Cl$  induced  $[Ca^{2+}]_i$  fluorescence response indicating that CatSper dependent  $Ca^{2+}$  influx was unaffected. These results signify that the sustained part of the 4-aminopyridine induced  $Ca^{2+}$  response is carried by SOC which is absent in the presence of 2-APB.

Similarly pre-treatment with SKF-96365 altered the 4-aminopyridine induced  $[Ca^{2+}]_i$  response in many cells. These results indicate that the sustained part of the 4-aminopyridine induced response is dependent on SOC. Both 2-APB and SKF-96365 have non-specific responses which may account for the increase in  $[Ca^{2+}]_i$  fluorescence prior to the application of 4-aminopyridine.

### *Conclusion*

This report provides further evidence that SOC play a role and contribute to the 4-aminopyridine induced  $[Ca^{2+}]_i$  response in human spermatzoa. Whether mobilisation of stored  $Ca^{2+}$  may affect CatSper channels is not known. It is possible that the different sources of  $Ca^{2+}$  have different functions in human sperm, transient bursts of hyperactivation facilitated by  $Ca^{2+}$  mobilisations and concomitant CCE whereas prolonged hyperactivation is facilitated by CatSper activation.

## **CHAPTER SEVEN**

### **GENERAL DISCUSSION**

It has been 40 years since Ryuzo Yanagimachi observed that hamster sperm swimming in the oviduct exhibited a vigorous motility pattern which he termed hyperactivation (Yanagimachi, 1970). Since then hyperactivation has been studied extensively however the physiological factor(s) that activate hyperactivation *in vivo* remains elusive. Due to ethical constraints knowledge of *in vivo* human sperm hyperactivation is particularly limited.

Previous data from this laboratory demonstrated that 4-aminopyridine is a potent inducer of hyperactivation in human spermatozoa (Gu *et al.*, 2004). The aim of this thesis was to elucidate the effects of 4-aminopyridine on  $[Ca^{2+}]_i$ , examine its target and mechanism of action and to assess the importance of store mobilisation on  $[Ca^{2+}]_i$  and its potential to regulate human sperm hyperactivation.

#### **Key findings**

This report examined in detail the effects of 4-aminopyridine on  $[Ca^{2+}]_i$  fluorescence and hyperactivation on human spermatozoa.  $Ca^{2+}$  imaging showed that treatment with 4-aminopyridine induced a parallel elevation of  $[Ca^{2+}]_i$  (chapter 2) which initiated at the sperm neck/midpiece and was associated with asymmetric flagellar bending in this region (section 5.4.1). ‘Clamping’ of  $E_m$  at  $E_K$  (1  $\mu$ M valinomycin) had no effect on these actions of 4-aminopyridine (section 2.4.5).

Elevation of  $[Ca^{2+}]_i$  and hyperactivation showed similar dose-dependence and both were enhanced at elevated  $pH_o$ , which facilitates entry of 4-aminopyridine across the plasmalemma (chapter 3). Since various studies have shown that a pH-stimulated  $Ca^{2+}$  increase in sperm, triggers hyperactivation (Mújica *et al.*, 1994; Marquez and Suarez, 2004, 2007) the effects of 4-aminopyridine on cytoplasmic alkalinisation was examined (chapter 3). Assessment using BCECF confirmed that 2mM 4-aminopyridine caused an immediate increase in  $pH_i$  of  $\approx 0.2$  units in human sperm. To investigate whether cytoplasmic alkalinisation of human sperm might underlie the effect of 4-aminopyridine on  $[Ca^{2+}]_i$  and hyperactivation  $NH_4Cl$  was used directly to increase  $pH_i$ . Exposure of sperm to  $NH_4Cl$  had an almost identical effect on  $pH_i$  and also caused a sustained increase in  $[Ca^{2+}]_i$  only slightly less than that seen with 2mM 4-aminopyridine. However, there was negligible induction of hyperactivation compared to cells treated with 4-aminopyridine. Treatment of sperm with propionate (to decrease  $pH_i$  and inhibit CatSper channel) did not significantly effect 4-aminopyridine induced hyperactivation but enhanced the effect of 4-aminopyridine on  $[Ca^{2+}]_i$ . In summary the 4-aminopyridine induced hyperactivation response in human sperm is not solely pH dependent.

The sperm specific pH-sensitive flagellar CatSper channels have been shown to be an important contributor to hyperactivation in mouse spermatozoa (Ren *et al.*, 2001; Quill *et al.*, 2001). The effect of calcium channel inhibition (with  $Ni^{2+}$ ,  $Cd^{2+}$  and ruthenium red) on 4-aminopyridine induced hyperactivation was therefore investigated (chapter 4). Inhibition of CatSper channels did not occlude the 4-aminopyridine induced hyperactivation in a population of human spermatozoa. The application of 4-aminopyridine to cells briefly pre-treated with  $Ni^{2+}$  triggered a transient increase in  $[Ca^{2+}]_i$  fluorescence indicative of stored  $Ca^{2+}$  mobilisation in a small proportion of cells. These results provide further evidence that 4-aminopyridine induced hyperactivation is not solely dependent on CatSper dependent calcium influx. The presence of a population of 4-aminopyridine responsive cells suggest that store mobilisation

and channels resistant to the divalent metals ( $\text{Ni}^{2+}$  and  $\text{Cd}^{2+}$ ) play a significant role in human sperm hyperactivation.

Evidence suggests that  $\text{Ca}^{2+}$  store mobilisation plays a key role in hyperactivation (Marequez *et al.*, 2007). In low  $\text{Ca}^{2+}$  saline the ability of 4-aminopyridine to cause an elevation of  $[\text{Ca}^{2+}]_i$  was similar to that seen in standard saline (chapter 5). Application of 4-aminopyridine to cells briefly (4-5min) exposed to EGTA-buffered saline ( $<10^{-7}$  M  $\text{Ca}^{2+}$ ) induced a  $[\text{Ca}^{2+}]_i$  transient. Hyperactivation induced by 4-aminopyridine was similarly transient (10-15min) in EGTA-buffered saline, though motility persisted for 20-30 min. 4-aminopyridine acted as a non-specific intra-calcium store agonist however it remains unclear how this compound triggers store mobilisation in microsomal vesicles. In conclusion intracellular  $\text{Ca}^{2+}$  store mobilisation contributes to 4-aminopyridine induced hyperactivation in human sperm.

4-aminopyridine, at concentrations comparable with those used here, strongly potentiates capacitative  $\text{Ca}^{2+}$  entry (CCE) in astrocytes and skeletal muscle cells (Grimaldi *et al.*, 2001). In experiments designed to activate store-operated channels (SOCs) (treatment with bis-phenol or incubation in EGTA buffered saline) this report demonstrates that  $\text{Ca}^{2+}$  influx in the presence of 4-aminopyridine was enhanced (chapter 6). Furthermore pharmacological inhibition of SOC (with 2-APB and SFF-96365) had a significant effect on the 4-aminopyridine induced response. In the presence of inhibitors, 4-aminopyridine induced a transient  $[\text{Ca}^{2+}]_i$  response, the SOC sustained influx was inhibited in a population of cells. Significantly this effect was absent when CatSper channel influx was activated by cytoplasmic alkalisation (2-APB pretreatment did not significantly effect the  $\text{NH}_4\text{Cl}$  induced  $[\text{Ca}^{2+}]_i$  response). These results indicate that the 4-aminopyridine induced  $[\text{Ca}^{2+}]_i$  store mobilisation response may potentiate SOC within a population of human sperm.



In summary, this report demonstrates that the elevation of  $[Ca^{2+}]_i$  that occurs upon mobilisation from a store in the sperm neck/mid-piece region regulates hyperactivation at least in a population of cells.

***Why would human sperm cells require two mechanisms for hyperactivation? Could the different sources of  $Ca^{2+}$  have different functions?***

The female tract represents a formidable barrier for sperm where numerous poorly understood interactions occur to ensure that only sperm of good quality, characterised by normal morphology and vigorous motility, will meet the oocyte (figure 7.1a, Suarez and Pacey, 2006). Human sperm are deposited in the vagina but only ~1% of sperm are retained by the female reproductive tract (~95% is lost following coitus due to 'flowback' and ~4% trapped by cervical mucus). This suggests that the female is exercising sperm selection favouring particular sperm from the ejaculate (Suarez and Pacey, 2006). In other species such as the pig, boar sperm are ejaculated directly into the uterine cavity hence female sperm selection is likely to occur elsewhere. The role of hyperactivated motility is not restricted to penetration of the zona pellucida. It also facilitates mucus penetration (Suarez and Dai, 1992; Suarez and Ho, 2003a; 2003b) and aids detachment of cells bound to the walls of the female tract (Suarez and Pacey, 2006; Suarez, 2007; Ho *et al.*, 2009). The ability to control and rapidly 'switch' hyperactivation is likely to be important for interaction of human and animal sperm with the fluids and cells of the female tract (Pacey *et al.*, 1995a, 1995b; Suarez and Pacey, 2006). The utero-tubal junction presents another major anatomical challenge. In some mammals (rabbits, pigs, cows) the narrow mucus filled lumen is complicated by mucosal folds, in mouse/rat the junction is patent for only a short time after coitus, whereas in humans the entrance is fairly simple. As sperm pass through the utero-tubal junction they enter the tubal isthmus which serves as a sperm storage reservoir by binding sperm tightly to the endosalpingeal (oviductal) epithelium (De Mott and Suarez, 1992; Suarez, 2002a, 2007, 2008b). The storage reservoir

preserves sperm viability/fertility until ovulation and may serve to prevent polyspermic fertilisation (Hunter and Leglise, 1971; Suarez *et al.*, 1991; Pollard *et al.*, 1991). Capacitation associated changes within the sperm plasma membrane reduce binding affinity and hyperactivation is required to provide the force to gradually free sperm cells from endosalpinal epithelium (De Mott and Suarez, 1992; Ho *et al.*, 2009). The human oviduct differs from other mammals in that no distinct anatomical tubal reservoir has been located. Although human sperm do associate intermittently with oviduct epithelium, *in vitro* they do not bind as quickly or tightly as those of other non-primate mammals (De Mott *et al.*, 1995; Pacey *et al.*, 1995a, 1995b; De Jonge, 2005; Suarez and Pacey, 2006). It is possible that activation of  $\text{Ca}^{2+}$  store mobilisation and capacitative  $\text{Ca}^{2+}$  entry may be better suited in human sperm to generate bursts of hyperactivation ‘on demand’ regulated by mediators of  $\text{Ca}^{2+}$  influx (such as progesterone) or direct inducers of store mobilisation (such as  $\text{NO}\bullet$ ) (Machado-Oliveira *et al.*, 2008). Finally, only hyperactivated sperm can penetrate the outer vestments of the mouse oocyte in order to reach and fuse with the oocyte plasma membrane (figure 7.1b) (Overstreet and Cooper, 1979; Ren *et al.*, 2001; Quill *et al.*, 2003). Increased  $\text{pH}_i$ , leading to activation of CatSper channels, could provide prolonged hyperactivation in capacitated cells at the site of fertilisation and may even cause hyperactivation of cells upon binding to zona proteins (Xia and Ren, 2009b).

***How important are CatSper channels in human sperm and are they absolutely necessary for hyperactivation?***

Evidence suggests that sperm competition is a potent driving force in the evolution of sperm traits and likely to influence the diversity of design, total sperm size and midpiece volume associated with sperm competition (Immler *et al.*, 2007). It is physiologically ‘costly’ for male mammals to engage in sperm competition but compared with rodents and other mammals, humans are unlikely to face sperm competition or sexual conflict. Of the millions of human

sperm ejaculated, a small proportion of sperm actually reach the site of fertilisation and of these only a fraction may be competent to fertilise (De Jonge, 2005; Suarez and Pacey, 2006; Lefièvre *et al.*, 2009). Furthermore, reproduction in humans is relatively inefficient, the probability of conceiving during a menstrual cycle is about 40% and approximately 30% of conceptions will not result in a live birth (Dey, 2010).

Although basic biological processes are usually conserved in mammals, reproductive system proteins are subjected to selective evolutionary forces and often undergo accelerated evolution and functional divergence so that a degree of redundancy is often observed. Since fertilisation occurs deep within the female tract, sperm have evolved the ability to alter motility pattern, indeed the CatSper channels are a recent evolutionary invention, since CatSper-like channels have not been detected in species lower than mouse (Lobley *et al.*, 2003; Cai and Clapham, 2008). The intriguing observation that, whereas 4-aminopyridine causes dramatic hyperactivation of human sperm, cytoplasmic alkalinisation with 25mM NH<sub>4</sub>Cl (which hyperactivates bovine sperm (Marquez and Suarez, 2007) had a negligible effect on motility, may reflect species variation in the mechanisms of control of hyperactivation (and thus in sensitivity to hyperactivating stimuli) due to differences in the behavioural requirements for sperm.

Approximately 1:15 human male are sub-fertile or infertile (HFEA, 2005, [www.hfea.gov.uk](http://www.hfea.gov.uk)) and of these approximately 15% are linked with genetic abnormalities (Lefièvre *et al.*, 2007). Since large proportions of infertile males are diagnosed as idiopathic, genetic causes of male infertility may be underestimated. However, it is almost 10 years since Ren *et al.*, (2001) first identified the CatSper channels in mouse sperm but to date there are very little data on CatSper related infertility in humans. Avenarius *et al.*, (2009) identified two males in an Iranian family with nonsyndromic male fertility resulting from insertion mutations in the CatSper1 gene (Avenarius *et al.*, 2009). Nikpoor *et al.*, (2004) report a positive correlation between lowered

CatSper gene expression and immotile sperm in humans, but the study was very small (18 patients in total). Only one group have examined human sperm motility in relation to CatSper channels. Li *et al.*, (2007) demonstrated that CatSper1 immunolocalised to the principal piece of human sperm and incubation with an antibody reduced % progressive motility by ~25% after a 6 hour incubation. The same group report that human sperm hyperactivation (12/173 cells) was inhibited in the presence of CatSper antibody (Li *et al.*, 2009). Without more evidence on gene expression/mutations and availability of specific inhibitors of CatSper channel activation, it is impossible to determine their importance in human sperm motility and hyperactivation.

We can speculate that due to a lack of sperm competition and the physiology/anatomy of the female reproductive tract, human sperm motility may require periods of quiescence followed by 'bursts' of hyperactivation to respond rapidly upon receiving the signals that ovulation has occurred. In other mammals where insemination is synchronised with ovulation, spermatozoa may require more prolonged hyperactivation (CatSper dependent). Prolonged and sustained hyperactivation may confer an advantage (over sperm from rival males) enabling spermatozoa to quickly reach the oviduct, pull free from the sperm reservoir and fertilise the egg(s) (Dixson and Anderson, 2004; Pennisi, 2010).

The data presented here demonstrates that 4-aminopyridine induced hyperactivation in human sperm is not solely pH/CatSper channel dependent and that mobilisation of stored  $\text{Ca}^{2+}$ , possibly causing activation of store-operated  $\text{Ca}^{2+}$  influx, is essential for hyperactivation in a population of human sperm (figure 7.1d). Of course there are many aspects of the activation and control of store mobilisation of which we are still ignorant and further characterisation of the store is required. Although basic semen analysis is rudimentary, 4-aminopyridine could provide a simple, non-invasive pharmacological tool to identify patients with motility related

sub-fertility. In addition, these data have important implications for the development of the elusive male contraceptive. Pharmaceutical targeting of native CatSper channel in mouse sperm produced a CatSper null phenocopy (Carlson *et al.*, 2009) but may be insufficient to fully inhibit hyperactivation in human sperm.

**Figure 7.1**

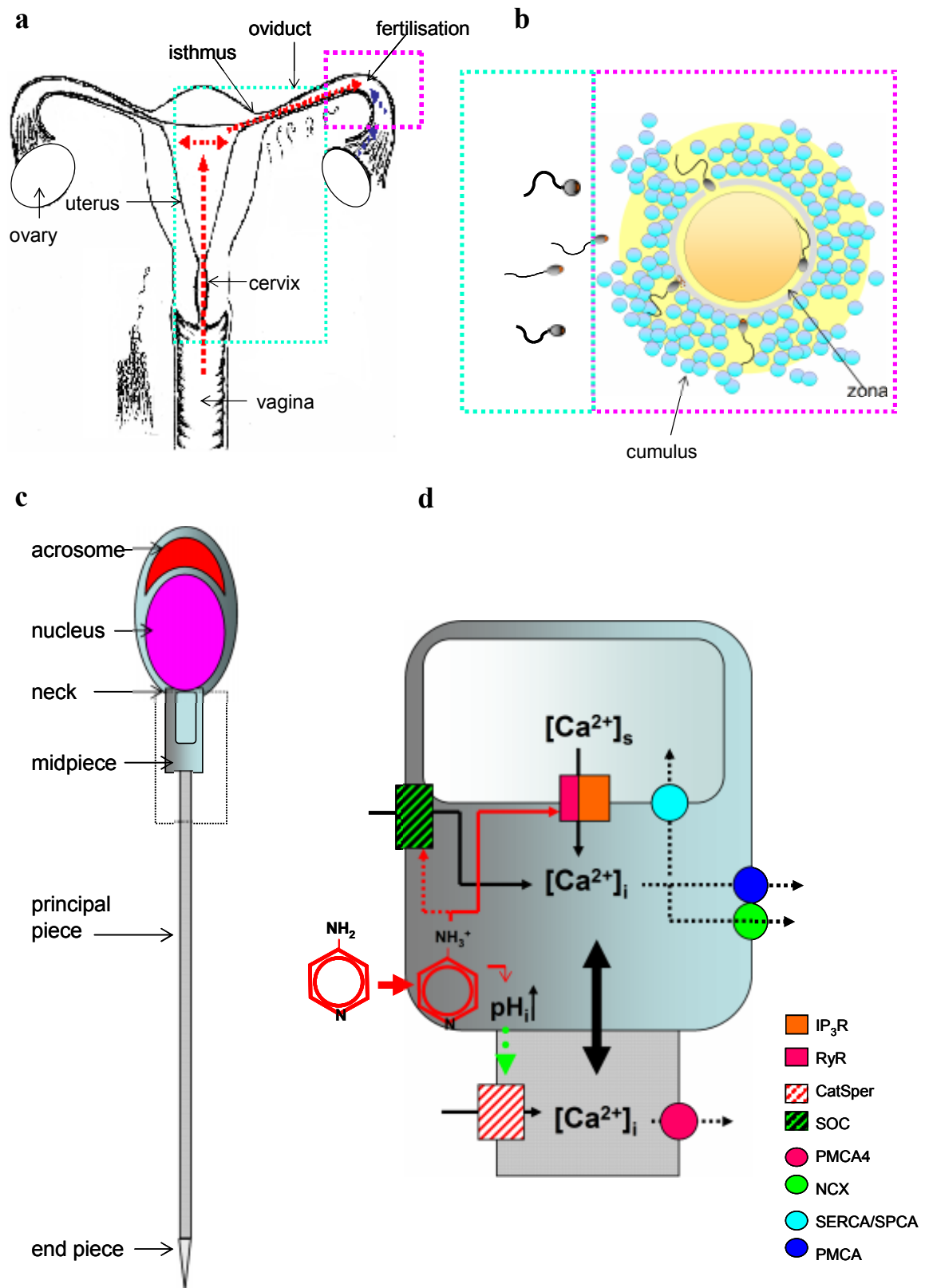


Figure 7.1: **(a)** Schematic representation of the female reproductive tract illustrating the transport of gametes to the site of fertilisation. Sperm (red arrow) are deposited in the vagina, from where a limited number quickly swim through the cervix/cervical mucus. Transport through the uterus is aided by uterine contractions. Sperm must then swim through the isthmus and oviduct to the ampulla where fertilisation can occur. The oocyte (blue arrow) is released from the ovary and is moved along to the site of fertilisation. **(b)** In order to successfully complete the journey through the female reproductive tract human sperm may switch between periods of quiescence followed by ‘bursts’ of hyperactivation on demand. However prolonged (possibly CatSper dependent) hyperactivation may be required upon receiving ovulation signals and to enable penetration of the cumulus oocyte complex. **(c)** Schematic structure of human sperm, boxed area shows the position of the  $\text{Ca}^{2+}$  store at the neck/midpiece and a short segment of the principal piece. **(d)** Model for the effects of 4-aminopyridine on  $[\text{Ca}^{2+}]_i$  in human sperm. 4-aminopyridine crosses the plasma membrane in an uncharged form however it is the charged form which is biologically active. 4-aminopyridine can activate store mobilisation (via RyR or  $\text{IP}_3\text{R}$  in microsomal vesicles) in sperm in the absence of extracellular  $\text{Ca}^{2+}$  (buffered with EGTA) (chapter 5). 4-aminopyridine induced store mobilisation is likely to activate store operated  $\text{Ca}^{2+}$  channels and enhance  $\text{Ca}^{2+}$  influx. 4-aminopyridine has been shown to potentiate CCE following store mobilisation (bis-phenol or depletion with EGTA buffered saline) (chapter 6). Store mobilisation and concomitant SOC activation may provide a localised signal to facilitate short bursts of hyperactivation on demand. Furthermore 4-aminopyridine acting as weak base could induce cytoplasmic alkalinisation and CatSper channels activation. Surprisingly cytoplasmic alkalinisation with  $\text{NH}_4\text{Cl}$  did not induce hyperactivation in human sperm. In conclusion the actions of 4-aminopyridine are not solely pH/CatSper dependent in a population of human sperm. However it is likely that combined activation of CatSper channels and store mobilisation/SOC activation is required to maintain high  $[\text{Ca}^{2+}]_i$  and sustain hyperactivation enabling penetration of the outer vestments of the oocyte.

## 7.1 Future research

Strict regulation of sperm functions (including motility) is essential to achieve successful fertilisation. Although *in vitro* studies have been carried out to understand the complex events that precede human fertilisation, translation to what happens *in vivo* is far from being simple. Evidence from this study indicates a central role for  $\text{Ca}^{2+}$  stores in hyperactivation of human sperm. This report focused on 4-aminopyridine which is a remarkably effective inducer of hyperactivation in human sperm. Although 4-aminopyridine can induce cytoplasmic alkalinisation and CatSper channel activation these results demonstrate a key role for mobilisation of stored  $\text{Ca}^{2+}$  in the sperm neck and human sperm hyperactivation. Although this compound is a useful tool in studying store mobilisation and hyperactivation in human sperm it is difficult to isolate these responses from CatSper channel activation. A specific CatSper channel inhibitor is currently not available commercially however the compound HC-056456 has been shown to cause a rapid reversible loss of CatSper dependent hyperactivation in the mouse (Carlson *et al.*, 2009). The effect of this compound on human sperm remains unknown. Further characterisation of the neck/midpiece store is essential to understanding the signalling pathways involved in the regulation of motility and hyperactivation. 4-aminopyridine presents a useful non-invasive tool for examination of sperm hyperactivation response. Investigation of 4-aminopyridine induced hyperactivation in assisted conception patients would provide an opportunity to determine the biological role of defective,  $\text{Ca}^{2+}$  stores and hyperactivation. We would hypothesise that failure of  $\text{Ca}^{2+}$  store mobilisation/CCE would result in sperm dysfunction and infertility.



## **APPENDIX I: Supplement calcium channel information**

### **Voltage gated calcium channel subunits and currents**

The voltage-gated  $\text{Ca}^{2+}$  channels (VGCC) (Table 7.0, figure 8.0) that have been characterised bio-chemically are complex proteins composed of four or five distinct subunits that are encoded by multiple genes (Catterall *et al.*, 2005). The  $\alpha_1$  subunit of 190 to 250 kDa is the largest subunit and it incorporates the conductance pore, the voltage sensor and gating apparatus and most of the known sites of channel regulation by second messengers, drugs and toxins. Like the  $\alpha$  subunits of sodium channels, the  $\alpha_1$  subunit of voltage-gated  $\text{Ca}^{2+}$  channels (VOCC) is organised into four homologous domains (I-IV), with six trans-membrane segments (6TM) (S1-S6) in each. The S4 segment serves as the voltage sensor. The pore loop between transmembrane segments S5 and S6 in each domain determines ion conductance and selectivity. An intracellular  $\beta$  subunit and a transmembrane disulphide-linked  $\alpha_2\delta$  subunit complex are components of most  $\text{Ca}^{2+}$  channels. A  $\gamma$  subunit has been found in skeletal muscle  $\text{Ca}^{2+}$  channels. Although the auxiliary subunits modulate the properties of the channel complex, the pharmacological and electrophysiological diversity of calcium channels arise primarily from the existence of multiple  $\alpha_1$  subunits (Catterall *et al.*, 2005).

Figure 8.0.

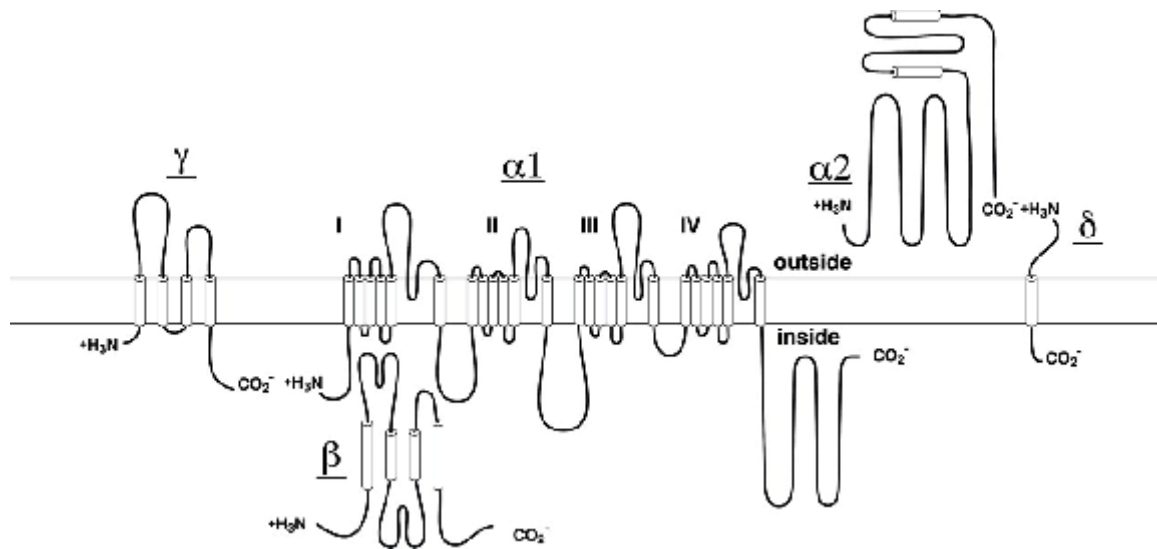


Figure 8.0 Subunit structure of  $\text{Ca}_v1$  channels. The subunit composition and structure of calcium channels purified from skeletal muscle are illustrated. Predicted  $\alpha$  helices are depicted as cylinders (Catterall *et al.*, 2005).

Calcium currents recorded in different cell types have diverse physiological and pharmacological properties. L-type  $\text{Ca}^{2+}$  currents typically require strong depolarisation for activation, are long lasting and are blocked by organic L-type channel antagonists (including dihydropyridines, phenylalkylamines and benzothiazepines). They are the main  $\text{Ca}^{2+}$  currents recorded in muscle and endocrine cells where they initiate contraction and secretion. N-type, P/Q-type and R-type  $\text{Ca}^{2+}$  currents also require strong depolarisation of activation. They are relatively unaffected by L-type  $\text{Ca}^{2+}$  channel antagonist but are blocked by specific polypeptide toxins from snail and spider venom. They are expressed primarily in neurons where they initiate neurotransmission. T-type  $\text{Ca}^{2+}$  currents are activated by weak depolarisation and are transient. They are resistant to both organic antagonists and to the snail and snake toxins used to define N- and P/Q-type  $\text{Ca}^{2+}$  currents. They are expressed in a wide variety of cells.

Application of electrophysiological techniques is technically difficult but patch clamping of immature male germ cells (both rodent and human) has shown consistently that these cells display both L-type and T-type currents. Immunostaining experiments using specific antibodies

detected the presence and distribution of T-type, L-, R- and P/Q-type and N-type channels in rodent sperm (Wennemuth *et al.*, 2000).

### **CatSper channels**

CatSpers (Table 8.0) are putative 6TM voltage-gated  $\text{Ca}^{2+}$ -permeant channels that are specific to sperm (Clapham and Garbers, 2005). CatSpers are structurally related to the 6TM voltage-gated  $\text{Na}^+$  channel classes. Patch-clamp experiments on mouse spermatozoa demonstrated an alkaline-potentiated, voltage-activated, calcium selective channel (Kirichok *et al.*, 2006). The two-pore channels TPC1 and TPC2 are putative cation-selective ion channels related to CatSper and transient receptor potential channels.

### **Transient receptor potential (TRP) channels**

The TRP ion channels (Table 9.0) are named after the *Drosophila* phototransduction channels. There are six mammalian protein families including the classical TRPs (TRPC). TRPs are generally assumed to have 6TM domains, one (S1-S4) containing the S4 voltage sensor and a second (S5-S6) containing the 2TM pore and gate. A high resolution structure of a TRP channel has not yet been solved. However, the 2TM structure of a bacterial  $\text{K}^+$  channel is analogous to the S5 and S6 domain (Clapham *et al.*, 2005).

TRP channels are relatively non-selective. Upon opening they depolarise cells from resting  $E_m$  to around 0mV (raise intracellular  $\text{N}^+$  and usually  $\text{Ca}^{2+}$ ) (Clapham *et al.*, 2005).

### **Cyclic-nucleotide-regulated channels**

The family of cyclic nucleotide-regulated channels comprises two groups: the cyclic nucleotide gated (CNG) and the hyperpolarisation-activated nucleotide-gated (HNG) channels (Hofmann *et al.*, 2005). CNG cation channels activation is mediated by the direct binding of cGMP or cAMP to the channel protein. CNG channels are expressed in the cilia of olfactory neurons where they

play a key role in sensory transduction. CNG channels are heterotetramers composed of an A subunit and a B subunit. Both types of subunits are members of 6TM segment channel superfamily. In the cytosolic C terminus, CNG channel subunits carry a cyclic nucleotide binding domain that serves as an activation domain. CNG channels pass monovalent cations ( $\text{Na}^+$  and  $\text{K}^+$ ),  $\text{Ca}^{2+}$  is also permeable and provides feedback when bound to calmodulin. A CNG,  $\text{Ca}^{2+}$  permeable channel has been described in human spermatozoa.

Table 7.0: Supplement Ca <sub>v</sub> channel information (including channel current, specific antagonists, male germ cell tissue (human or rodent), localisation and method used) (adapted from Catterall <i>et al.</i> , 2005; Jimenez-Gonzalez <i>et al.</i> , 2006).						
Channel	Current	Specific Antagonists	Tissue Present	Method	Knock-out mouse	
Ca <sub>v</sub> 1.1	L	Dihydropyridines, phenylalkylamines, benzothiazepines	Rat testis sections (Goodwin <i>et al.</i> , 1997)	Immunostaining		
Ca <sub>v</sub> 1.2	L	Dihydropyridines, phenylalkylamines, benzothiazepines	Rat Testis sections (Goodwin <i>et al.</i> , 2000) Human spermatozoa (Goodwin <i>et al.</i> , 2000; Park <i>et al.</i> , 2003)	<i>In situ</i> RT-PCR <i>In situ</i> RT-PCR, Immunogold transmission EM		
Ca <sub>v</sub> 1.3	L	Dihydropyridines, phenylalkylamines, benzothiazepines	Not detected			
Ca <sub>v</sub> 1.4	L	Dihydropyridines, phenylalkylamines, benzothiazepines	Not detected			
Ca <sub>v</sub> 2.1	P/Q	ω-Agatoxin IVA (funnel web spider)	Mouse spermatozoa (Wennemuth <i>et al.</i> , 2000).	Immunostaining/immunoblotting		
Ca <sub>v</sub> 2.2	N	ω-Conotoxin-GVIA (cone snail toxin)	Mouse spermatozoa (Wennemuth <i>et al.</i> , 2000)	Immunostaining/immunoblotting	KO mouse fertile (Sakata <i>et al.</i> , 2001)	
Ca <sub>v</sub> 2.3	R	SNX-482 (tarantula venom)	Mouse spermatozoa (Wennemuth <i>et al.</i> , 2000). Human spermatozoa (Trevino <i>et al.</i> , 2004).	Immunostaining/immunoblotting Immunostaining	KO mouse remain fertile (Sakata <i>et al.</i> , 2001).	
Ca <sub>v</sub> 3.1	T	None	Human sperm head regions (Trevino <i>et al.</i> , 2004)	Immunostaining	KO mouse fertile (Escoffier <i>et al.</i> , 2007)	
Ca <sub>v</sub> 3.2	T	None	Human sperm head region (Trevino <i>et al.</i> , 2004)	Immunostaining	KO mouse remain fertile (Escoffier <i>et al.</i> , 2007)	
Ca <sub>v</sub> 3.3	T	None	Human sperm midpiece region (Trevino <i>et al.</i> , 2004)	Immunostaining		

Table 8.0: Supplement CatSper channel information (including channel current, specific antagonists, male germ cell tissue (human), localisation and method used) (adapted from Clapham and Garbers, 2005).

Channel name	Current	Specific Antagonists	Tissue Present	Method
CatSper 1	$\text{Ca}^{2+}$ selective, voltage dependent, potentiated at pH8	Not established HC-056456 (Carlson <i>et al.</i> , 2009)	Mouse spermatozoa	$\text{Ca}^{2+}$ imaging, patch clamp Ren <i>et al.</i> , 2001)
CatSper 2	Putative $\text{Ca}^{2+}$ current	Not established	Mouse spermatozoa	$\text{Ca}^{2+}$ imaging (Quilley <i>et al.</i> , 2001)
CatSper 3	Putative $\text{Ca}^{2+}$ current	Not established	Mouse Testis	Lobley <i>et al.</i> , 2003
CatSper 4	Putative $\text{Ca}^{2+}$ current	Not established	Mouse Testis	Lobley <i>et al.</i> , 2003

Table 9.0: Supplement TRPC channel information (including channel current, specific antagonists, male germ cell tissue (human or rodent), localisation and method used) (adapted from Clapham *et al.*, 2005).

Channel name	Current	Specific Antagonists	Tissue Present	Method
TRPC1	$\text{Na}^+/\text{Ca}^{2+}$	2-APB, SKF96365 and $\text{Gd}^{3+}$	Human spermatozoa	Immunolocalised flagellum Castellano <i>et al.</i> , 2003)
TRPC2	Mouse pheromone channel	None	Mouse sperm	Immunolocalised acrosome region (Agannathan <i>et al.</i> , 2002) Pseudogene in human and bovine Vannier <i>et al.</i> , 1999).
TRPC3	$\text{Na}^+/\text{Ca}^{2+}$	2-APB, 1-25 $\mu\text{M}$ $\text{Gd}^{3+}$ , $\text{La}^{3+}$ , RR	Human spermatozoa	Immunolocalised flagellum Castellano <i>et al.</i> , 2003)
TRPC4	$\text{Na}^+/\text{Ca}^{2+}$	2-APB, mM $\text{La}^{3+}$	Human spermatozoa	Immunolocalised flagellum Castellano <i>et al.</i> , 2003)
TRPC6	$\text{Na}^+/\text{Ca}^{2+}$	100 $\mu\text{M}$ 2-APB, 2 $\mu\text{M}$ $\text{Gd}^{3+}$ , 4 $\mu\text{M}$ $\text{La}^{3+}$ , 4 $\mu\text{M}$ SKF96365	Human spermatozoa	Immunolocalised flagellum Castellano <i>et al.</i> , 2003)

## **APPENDIX II: Media**

### **Supplemented Earle's Balanced Salt Solution (sEBSS)**

Sodium Dihyd. Phosphate (1.0167 mM)

Potassium Chloride (5.4 mM)

Magnesium Sulphate.7H<sub>2</sub>O (0.811 mM)

Dextrose Anhydrous (5.5 mM)

Sodium Pyruvate (2.5 mM)

DL-Lactic Acid, Sodium (19.0 mM)

Calcium Chloride.2H<sub>2</sub>O (1.8 mM) Sodium

Bicarbonatel (25.0 mM)

Sodium Chloride (≈116.4 mM)

HEPES (15.0mM)

Sodium chloride was added in increments until osmolarity was 285-295 mOsm (Advanced Micro Osmometer, Vitech Scientific Ltd, West Sussex, UK, which has been pre-calibrated using a 50 mOsm/Kg H<sub>2</sub>O and a 850 mOsm/Kg H<sub>2</sub>O calibration standards). sEBSS pH was adjusted to 7.3-7.4 with 1M HCl and 1M NaOH and subsequently stored as 100 ml volumes in glass bottles at 4°C until use. 0.3% Bovine serum albumin (BSA) (0.3%) was added on experimental day.

### **Nominal Ca<sup>2+</sup>-free sEBSS (NCFsEBSS)**

Sodium Dihyd. Phosphate (1.0167 mM)

Potassium Chloride (5.4 mM)

Magnesium Sulphate.7H<sub>2</sub>O (0.811 mM)

Dextrose Anhydrous (5.5 mM)

Sodium Pyruvate (2.5 mM)

DL-Lactic Acid, Sodium (19.0 mM)

Sodium Bicarbonate (25.0 mM)

Sodium Chloride (≈ 118.4 mM)

Prepared as for standard sEBSS but stored as 100 ml volumes in polystyrene bottles at 4°C, pH was adjusted to 7.3-7.4, 0.3% BSA was added on experimental day.

### **Non-capacitating sEBSS (NCsEBSS)**

Sodium Dihyd. Phosphate (1.0167 mM)

Potassium Chloride (5.4 mM)

Magnesium Sulphate.7H<sub>2</sub>O (0.811 mM)

Dextrose Anhydrous (5.5 mM)

Sodium Pyruvate (2.5 mM)

DL-Lactic Acid, Sodium (19.0 mM)

Calcium Chloride.2H<sub>2</sub>O (1.8 mM)

Sodium Chloride ( $\approx 116.4$  mM)

NCsEBSS recipe was based upon standard sEBSS recipe (osmolarity was 285-295 mOsm as before), pH was adjusted to 7.3-7.4. NCsEBSS was stored as 100 ml volumes in glass bottles at 4°C until use, 0.3% BSA added on day of use.

**sEBSS-Ethylene glycol-bis ( $\beta$ -amino-ethylether)-N,N,N',N'-tetraacetic acid (sEBSS-EGTA)**

Sodium Phosphate Monobasic (1.018 mM)

Potassium Chloride (5.366 mM)

Magnesium Sulphate.7H<sub>2</sub>O (0.811 mM)

Dextrose Anhydrous (5.551 mM)

Sodium Pyruvate (2.724 mM)

DL-Lactic Acid, Sodium (41.763 mM)

Calcium Chloride.2H<sub>2</sub>O (4.966 mM)

Sodium Bicarbonate (26.187 mM)

Sodium Chloride ( $\approx 85.0$  mM)

EGTA (5.994 mM)

Prepared as for standard sEBSS. 0.3% BSA was added on experimental day.

The calcium concentration calculator Maxchelor (V2.2) written by Chris Patton from Stanford University (<http://www.stanford.edu/~cpatton/maxc.html>) was used to calculate the free calcium concentration in saline containing EGTA: 25°C ( $[Ca^{2+}]_o$   $10^{-7}$  M)

### **Simplified Saline**

Potassium Chloride (5.4 mM)

Magnesium Chloride 6H<sub>2</sub>O (1.0 mM)

Dextrose Anhydrous (9.0 mM)

Calcium Chloride.2H<sub>2</sub>O (1.8 mM)

Sodium Chloride (approx 132.0 mM)

Osmolarity was 285-295 mOsm as before, pH adjusted to 7.2-7.4, saline stored as 100 ml volumes in glass bottles at 4°C until use, 0.3% BSA added on day of use.



### **APPENDIX III: Research Publications**

#### **In prep**

**Costello, S.** Barratt, C.L.R., Kirkman-Brown, J. and Publicover, S. Hyperactivation of human sperm by 4-aminopyridine: key role for mobilisation of stored  $\text{Ca}^{2+}$  in the sperm neck (in prep)

#### **Reviews**

**Costello, S.** Michelangeli, F., Nash, K., Lefièvre, L., Morris, J., Machado-Oliveira, G., Barratt, C., Kirkman-Brown, J.K., and Publicover, S. (2009).  $\text{Ca}^{2+}$  - stores in sperm: their identities and functions. *Reproduction* **138**, 425-437.

Bedu-Addo, K., **Costello, S.**, Harper, C., Machado-Oliveira, G., Lefièvre, L., Ford, C., Barratt, C. and Publicover, S. (2008). Mobilisation of stored calcium in the neck region of human sperm – a mechanism for regulation of flagellar activity. *International Journal of Developmental Biology* **52**, 615-26.

#### **Abstracts**

4-aminopyridine mobilises calcium in human sperm

Young Physiologist Symposium (Cations 2008) at University of Manchester 2008

4-aminopyridine mobilises calcium in human sperm

Society for Reproduction and Fertility Meeting (2008)

4-aminopyridine mobilises calcium in human sperm

Proceedings of the Physiological Society (2008)

The modulation of  $[\text{Ca}^{2+}]_i$  homeostasis by 4-aminopyridine in human spermatozoa

Fertilization & Activation of Development Gordon Research Conference (July 2007), U.S.

## **REFERENCES**

- Abou-haila, A. and Tulsiani, D.R.** (2009). Signal transduction pathways that regulate sperm capacitation and the acrosome reaction. *Arch Biochem Biophys* **485**, 72-81.
- Abramowitz, J and Birnbaumer, L.** (2009). Physiology and pathophysiology of canonical transient receptor potential channels. *FASEB J* **23**, 297-328.
- Acevedo, J.J., Mendoza-Lujambio, I., de la Vega-Beltrán, J.L., Treviño, C.L., Felix, R. and Darszon, A.** (2006). KATP channels in mouse spermatogenic cells and sperm, and their role in capacitation. *Dev Biol.* **289**, 395-405.
- Acott, T.S. and Carr, D.W.** (1984). Inhibition of bovine spermatozoa by caudal epididymal fluid: II. Interaction of pH and a quiescence factor. *Biol Reprod.* **30**, 926-35.
- Aitken, R. J., Buckingham, D. W. and Irvine, D. S.** (1996). The extragenomic action of progesterone on human spermatozoa: evidence for a ubiquitous response that is rapidly down-regulated. *Endocrinology* **137**, 3999-4009.
- Albert, A., Goldacre, R. And Phillips, J.** (1948). The strength of heterocyclic bases. *J Chem Soc* 2240-2249
- Al-Mousa, F. and Michelangeli, F.** (2009). Commonly used ryanodine receptor activator, 4-chloro-m-cresol (4CmC), is also an inhibitor of SERCA Ca<sup>2+</sup> pumps. *Pharmacol Rep.* **61**, 838-42.
- Amaral, A. And Ramalho-Santos, J.** (2009). Assessment of mitochondrial potential: implications for the correct monitoring of human sperm function. *Int J Androl.* **33**, e180-e186
- Arnoult, C., Cardullo, R. A., Lemos, J. R. and Florman, H. M.** (1996a). Activation of mouse sperm T-type Ca<sup>2+</sup> channels by adhesion to the egg zona pellucida. *Proc Natl Acad Sci U S A* **93**, 13004-9.
- Arnoult, C., Zeng, Y. and Florman, H. M.** (1996b). ZP3-dependent activation of sperm cation channels regulates acrosomal secretion during mammalian fertilization. *J Cell Biol* **134**, 637-45.
- Arnoult, C., Villaz, M. and Florman, H. M.** (1998). Pharmacological properties of the T- type Ca<sup>2+</sup> current of mouse spermatogenic cells. *Mol Pharmacol* **53**, 1104-11.
- Arnoult, C., Kazam, I. G., Visconti, P. E., Kopf, G. S., Villaz, M. and Florman, H. M.** (1999). Control of the low voltage-activated calcium channel of mouse sperm by egg ZP3 and by membrane hyperpolarization during capacitation. *Proc Natl Acad Sci U S A* **96**, 6757-62.
- Aronson, J.K.** (1992). Potassium channels in nervous tissue. *Biochem Pharmacol.* **43**, 11-4.

**Austin, C. R.** (1951). Observations on the penetration of the sperm in the mammalian cell. *Aust J Sci Res (B)* **4**, 581-596.

**Austin, C. R.** (1957). Fate of spermatozoa in the uterus of the mouse and rat. *J Endocrinol* **14**, 335-42.

**Avenarius, M.R., Hildebrand, M.S., Zhang, Y., Meyer, N.C., Smith, L.L., Kahrizi, K., Najmabadi, H and Smith, R.J.** (2009), Human male infertility caused by mutations in the CatSper channel protein. *Am J Genet* **84**, 505-10.

**Baba, D., Kashiwabara, S., Honda, A., Yamagata, K., Wu, Q., Ikawa, M., Okabe, M. and Baba, T.** (2002). Mouse sperm lacking cell surface hyaluronidase PH-20 can pass through the layer of cumulus cells and fertilize the egg. *J Biol Chem* **277**, 30310-30314.

**Babcock, D.F.** (2007) Wrath of the wraiths of CatSper3 and CatSper4. *PNAS* **104**, 1107-8.

**Babiak, S. and Testa, A.C.** (1976). Fluorescence lifetime study of aminopyridines. *J Physical Chem* **80**, 1882-1885.

**Baibakov, B., Gauthier, L., Talbot, P., Rankin, T.L. and Dean, J.** (2007). Sperm binding to the zona pellucida is not sufficient to induce acrosome reaction. *Development* **134**, 933-943.

**Bailey, J. L. and Storey, B. T.** (1994). Calcium influx into mouse spermatozoa activated by solubilized mouse zona pellucida, monitored with the calcium fluorescent indicator, fluo-3. Inhibition of the influx by three inhibitors of the zona pellucida induced acrosome reaction: tyrphostin A48, pertussis toxin, and 3-quinuclidinyl benzilate. *Mol Reprod Dev* **39**, 297-308.

**Baker, M. A. and Aitken, R. J.** (2004). The importance of redox regulated pathways in sperm cell biology. *Mol Cell Endocrinol* **216**, 47-54.

**Baldi, E., Casano, R., Falsetti, C., Krausz, C., Maggi, M. and Forti, G.** (1991). Intracellular calcium accumulation and responsiveness to progesterone in capacitating human spermatozoa. *J Androl* **12**, 323-30.

**Baldi, E., Luconi, M., Bonaccorsi, L., Maggi, M., Francavilla, S., Gabriele, A., Properzi, G. And Forti. G.** (1999). Nongenomic progesterone receptor on human spermatozoa: biochemical aspects and clinical implications. *Steroids*. **64**,143-8.

**Baldi, E., Luconi, M., Bonaccorsi, L., Muratori, M. and Forti, G.** (2000). Intracellular events and signaling pathways involved in sperm acquisition of fertilizing capacity and acrosome reaction. *Front Biosci* **5**, E110-23.

- Baldi, E., Luconi, M., Bonaccorsi, L. and Forti, G.** (2002). Signal transduction pathways in human spermatozoa. *J Reprod Immunol* **53**, 121-31.
- Barfield, J.P., Yeung, C.H. and Cooper, T.G.** (2005). Characterization of potassium channels involved in volume regulation of human spermatozoa. *Mol Hum Reprod*. **11**, 891-7.
- Barratt, C.L.R.** (1995). Spermatogenesis. In: *Gametes, the spermatozoon* (ed J.G. Grundzinskas and J.L. Yovich) pp 250-262, Cambridge UK: Cambridge University Press.
- Barratt, C.L, Kay, V and Oxenham, S.K.** (2009). The human spermatozoon – a stripped down but refined machine. *J Biol* **8**, 63.
- Battalia, D. E. and Yanagimachi, R.** (1979). Enhanced and co-ordinated movement of the hamster oviduct during the periovulatory period. *J Reprod Fertil* **56**, 515-20.
- Bedu-Addo, K., Barratt, C. L., Kirkman-Brown, J. C. and Publicover, S. J.** (2007). Patterns of  $[Ca^{2+}]_i$  mobilization and cell response in human spermatozoa exposed to progesterone. *Dev Biol* **302**, 324-32.
- Bedu-Addo, K., Costello, S., Harper, C., Machado-Oliveira, G., Lefièvre, L., Ford, C., Barratt, C. and Publicover, S.** (2008). Mobilization of stored calcium in the neck region of human sperm – a mechanism for regulation of flagellar activity. *Int J Dev Biol* **52**, 615-26.
- Bernardi, P.** (1999). Mitochondrial transport of cations: channels, exchangers, and permeability transition. *Physiol Rev*. **79**, 1127-55.
- Berridge, M.J.** (1997). The AM and FM of calcium signalling. *Nature* **386**, 759-60.
- Berridge, M.J.** (2005). Unlocking the secrets of cell signaling. *Annu Rev Physiol* **67**, 1-21
- Blackmore, P. F., Beebe, S. J., Danforth, D. R. and Alexander, N.** (1990). Progesterone and 17  $\alpha$ -hydroxyprogesterone. Novel stimulators of calcium influx in human sperm. *J Biol Chem* **265**, 1376-80.
- Blackmore, P. F.** (1993). Thapsigargin elevates and potentiates the ability of progesterone to increase intracellular free calcium in human sperm: possible role of perinuclear calcium. *Cell Calcium* **14**, 53-60.
- Blackmore, P. F. and Eisoldt, S.** (1999). The neoglycoprotein mannose-bovine serum albumin, but not progesterone, activates T-type calcium channels in human spermatozoa. *Mol Hum Reprod* **5**, 498-506.
- Bleil, J. D. and Wassarman, P. M.** (1980a). Mammalian sperm-egg interaction: identification of a glycoprotein in mouse egg zonae pellucidae possessing receptor activity for sperm. *Cell* **20**, 873-82.

- Bleil, J. D. and Wassarman, P. M.** (1980b). Structure and function of the zona pellucida: identification and characterization of the proteins of the mouse oocyte's zona pellucida. *Dev Biol* **76**, 185-202.
- Bleil, J. D. and Wassarman, P. M.** (1983). Sperm-egg interactions in the mouse: sequence of events and induction of the acrosome reaction by a zona pellucida glycoprotein. *Dev Biol* **95**, 317-24.
- Bleil, J. D., Beall, C. F. and Wassarman, P. M.** (1981). Mammalian sperm-egg interaction: fertilization of mouse eggs triggers modification of the major zona pellucida glycoprotein, ZP2. *Dev Biol* **86**, 189-97.
- Boatman, D. E. and Robbins, R. S.** (1991). Bicarbonate: carbon-dioxide regulation of sperm capacitation, hyperactivated motility, and acrosome reactions. *Biol Reprod* **44**, 806-13.
- Böhmer, M., Van ,Q., Weyand, I., Hagen, V., Beyermann, M., Matsumoto, M., Hoshi, M., Hildebrand, E. and Kaupp, U.B.** (2005).  $\text{Ca}^{2+}$  spikes in the flagellum control chemotactic behavior of sperm. *EMBO J.* **24**, 2741-52.
- Bönigk, W., Loogen, A., Seifert, R., Kashikar, N., Klemm, C., Krause, E., Hagen, V., Kremmer, E., Strücker and T., Kaupp, UB.** (2009). An atypical CNG channel activated by a single cGMP molecule controls sperm chemotaxis. *Sci Signal.* **2**, (94)
- Breitbart, H., Stern, B. and Rubinstein, S.** (1983). Calcium transport and  $\text{Ca}^{2+}$ -ATPase activity in ram spermatozoa plasma membrane vesicles. *Biochim Biophys Acta.* **728**, 349-55.
- Breitbart, H., Rubinstein, S. and Gruberger, M.** (1996). Calcium efflux mechanism in sperm mitochondria. *Biochim Biophys Acta.* **1312**, 79-84.
- Breitbart, H. and Spungin, B.** (1997). The biochemistry of the acrosome reaction. *Mol Hum Reprod.* **3**, 195-202.
- Breitbart, H.** (2003). Signaling pathways in sperm capacitation and acrosome reaction. *Cell Mol Biol (Noisy-le-grand)* **49**, 321-7.
- Brokaw, C. J.** (1972). Flagellar movement: a sliding filament model. *Science* **178**, 455-62.
- Brokaw, C.J., Josslin, R. and Bobrow, L.** (1974). Calcium ion regulation of flagellar beat symmetry in reactivated sea urchin spermatozoa. *Biochem Biophys Res Commun.* **4**, 795-800.
- Brokaw, C.J.** (1979). Calcium-induced asymmetrical beating of triton-demembranated sea urchin sperm flagella. *J Cell Biol.* **82**, 401-11.

- Brokaw, C.J.** (1987). Regulation of sperm flagellar motility by calcium and cAMP-dependent phosphorylation. *J Cell Biochem.* **35**, 175-84.
- Brokaw, C. J.** (1989). Direct measurements of sliding between outer doublet microtubules in swimming sperm flagella. *Science* **243**, 1593-6.
- Brown, G.R., Benyon, S.L., Kirk, C.J., Wictome, M., East, J.M., Lee, A.G. and Michelangeli, F.** (1994). Characterisation of a novel Ca<sup>2+</sup> pump inhibitor (bis-phenol) and its effects on intracellular Ca<sup>2+</sup> mobilization. *Biochimica et Biophysica Acta* **1195**, 252-258.
- Brown, P.R., Miki, K., Harper, D.B. and Eddy, E.M.** (2003) A-kinase anchoring protein 4 binding proteins in the fibrous sheath of the sperm flagellum. *Biol Reprod.* **68**, 2241- 8
- Buck, J., Sinclair, M. L., Schapal, L., Cann, M. J. and Levin, L. R.** (1999). Cytosolic adenylyl cyclase defines a unique signaling molecule in mammals. *Proc Natl Acad Sci U S A* **96**, 79-84.
- Buffone, M.G., Rodriguez-Miranda, E., Storey, B.T. and Gerton. G.L.** (2009). Acrosomal exocytosis of mouse sperm progresses in a consistent direction in response to zona pellucida. *J Cell Physiol* **220**, 611-20.
- Bultynck, G., Szlufcik, K., Kasri, N.N., Assefa, Z., Callewaert, G., Missiaen, L., Parys, J.B. and De Smedt, H.** (2004). Thimerosal stimulates Ca<sup>2+</sup> flux through inositol 1,4,5-trisphosphate receptor type 1, but not type 3, via modulation of an isoform-specific Ca<sup>2+</sup>-dependent intramolecular interaction. *Biochem J.* **381**(Pt 1):87-96.
- Bunch, D. O., Welch, J. E., Magyar, P. L., Eddy, E. M. and O'Brien, D. A.** (1998). Glyceraldehyde-3-phosphate dehydrogenase-S protein distribution during mouse spermatogenesis. *Biol Reprod* **58**, 834-41.
- Burkman, L.J., Overstreet, J.W. and Katz, D.F.** (1984). A possible role for potassium and pyruvate in the modulation of sperm motility in the rabbit oviducal isthmus. *J Reprod Fertil.* **71**, 367-76.
- Burkman, L.J.** (1995). The motility of human spermatozoa before and after capacitation. In: *Gametes, the spermatozoon* (ed J.G. Grundzinskas and J.L. Yovich) pp 122-139, Cambridge UK: Cambridge University Press.
- Burks, D. J., Carballada, R., Moore, H. D. and Saling, P. M.** (1995). Interaction of a tyrosine kinase from human sperm with the zona pellucida at fertilization. *Science* **269**, 83-6.
- Cabello-Agueros, J.F., Hernandez-Gonzalez, E.O. and Mujica, A.** (2003). The role of F-actin cytoskeleton-associated gelsolin in the guinea pig capacitation and acrosome reaction. *Cell Motil Cytoskeleton* **56**, 94-108.
- Cai, X. and Clapham, D.E.** (2008). Evolutionary genomics reveals lineage-specific gene loss and rapid evolution of a sperm-specific ion channel complex: CatSper and CatSperbeta. *PLoS One.* **3**, e3569.

- Calogero, A. E., Burrello, N., Ferrara, E., Hall, J., Fishel, S. and D'Agata, R. (1999).** Gamma-aminobutyric acid (GABA) A and B receptors mediate the stimulatory effects of GABA on the human sperm acrosome reaction: interaction with progesterone. *Fertil Steril* **71**, 930-6.
- Carlson, A. E., Westenbroek, R. E., Quill, T., Ren, D., Clapham, D. E., Hille, B., Garbers, D. L. and Babcock, O. F. (2003).** CatSper 1 required for evoked Ca<sup>2+</sup> entry and control of flagellar function in sperm. *Proc Natl Acad Sci USA* **100**, 14864-8.
- Carlson, A. E., Quill, T., Westenbroek, R. E., Schuh, S.M., B. and Babcock, O. F. (2005).** Identical phenotypes of CatSper1 and CatSper2 null sperm. *J Biol Chem* **280**, 32238-44.
- Carlson, A. E., Hille, B. and Babcock, O. F. (2007).** External Ca<sup>2+</sup> acts upstream of adenylyl cyclase SACY in the bicarbonate signalled activation of sperm motility. *Dev Biol* **312**, 183-92.
- Carlson, A. E., Burnett, L.A., del Camino, D., Quill, T.A., Hille, B., Chong, J.A., Moran, M.M. and Babcock, D.F. (2009).** Pharmacological targeting of native CatSper channels reveals a required role in maintenance of sperm hyperactivation. *PloS One* **4(8)** e6844
- Carr, D.W. and Acott, T.S. (1989).** Intracellular pH regulates bovine sperm motility and protein phosphorylation. *Biol Reprod.* **41**, 907-20.
- Carrera, A., Moos, J., Ning, X. P., Gerton, G. L., Tesarik, J., Kopf, G. S. and Moss, S. B. (1996).** Regulation of protein tyrosine phosphorylation in human sperm by a calcium/calmodulin-dependent mechanism: identification of A kinase anchor proteins as major substrates for tyrosine phosphorylation. *Dev Biol* **180**, 284-96.
- Castellano, L. E., Trevino, C. L., Rodriguez, D., Serrano, C.J., Pacheco, J., Tsutsumi, V., Felix, R. and Darszon, A. (2003).** Transient receptor potential (TRPC) channel in human sperm: expression, cellular localization and involvement in the regulation of flagellar motility. *FEBS Lett* **541**, 69-74.
- Cataldo, L., Baig, K., Oko, R., Mastrangelo, M. A. and Kleene, K. C. (1996).** Developmental expression, intracellular localization, and selenium content of the cysteine- rich protein associated with the mitochondrial capsules of mouse sperm. *Mol Reprod Dev* **45**, 320-31.
- Catterall, W.A., Perez-Reyes, E., Snutch, T.P. and Striessnig, J. (2005).** International Union of Pharmacology. XLVIII. Nomenclature and structure-function relationships of voltage-gated calcium channels. *Pharmacol Rev.* **57(4)**:411-25.
- Chakravarty, S., Kadunganattil, S., Bansal, P., Sharma, R.K. and Gupta, S.K. (2008).** Relevance of glycosylation of human zona pellucida glycoproteins for their binding to capacitated human spermatozoa and

subsequent induction of acrosomal exocytosis. *Mol Reprod Dev* **75**, 75-88.

**Chandler, J.A. and Battersby, S.** (1976). X-ray microanalysis of ultrathin frozen and freeze dried section of human sperm cells. *J Microsc* **107**, 55-65.

**Chang, M.C.** (1951). Fertilizing capacity of spermatozoa deposited in the fallopian tubes. *Nature* **168**, 697-8.

**Chang, H. and Suarez, S.S.** (2010). Rethinking the relationship Between Hyperactivation and Chemotaxis in Mammalian Sperm. *Biol Reprod*. May 12. [Epub ahead of print]

**Chen, Y., Cann, M. J., Litvin, T. N., Iourgenko, V., Sinclair, M. L., Levin, L. R. and Buck, J.** (2000). Soluble adenylyl cyclase as an evolutionarily conserved bicarbonate sensor. *Science* **289**, 625-8.

**Chiarella, P., Puglisi, R., Sorrentino, V., Boitani, C. and Stefanini, M.** (2004). Ryanodine receptors are expressed and functionally active in mouse spermatogenic cells and their inhibition interferes with spermatogonial differentiation. *J Cell Sci* **117**, 4127-34.

**Choi, D., Lee, E., Hwang, S., Jun, K., Kim, D., Yoon, B.K., Shin, H.S. and Lee, J.H.** (2001). The biological significance of phospholipase C beta 1 gene mutation in mouse sperm in the acrosome reaction, fertilization, and embryo development. *J Assist Reprod Genet.* **18**, 305-10.

**Ciapa, B. and Chiri, S.** (2000). Egg activation: upstream of the fertilization calcium signal. *Biol of the Cell* **92**, 215-233

**Clapham, D.E. and Garbers, D.L.**(2005). International Union of Pharmacology. L. Nomenclature and structure-function relationships of CatSper and two-pore channels. *Pharmacol Rev.* **57**, 451-4.

**Clapham, D. E., Julius, D., Montell, C. and Schultz, G.** (2005). International Union of Pharmacology. XLIX. Nomenclature and structure-function relationships of transient receptor potential channels. *Pharmacol Rev* **57**, 427-50.

**Coffey, D.** (1995). What is the prostate and what is its function? in: *Handbook of Andrology* (ed. B. Robaire, J. L. Pryor and J. M. Trasler), pp. 21-4. Lawrence, Kans: Allen Press Inc.

**Cohen-Dayag, A., Ralt, D., Tur-Kaspa, I., Manor, M., Makler, A., Dor, J., Mashiach, S. and Eisenbach, M.** (1994). Sequential acquisition of chemotactic responsiveness by human spermatozoa. *Biol Reprod* **50**, 786-90.

**Conner, S. J., Lefièvre, L., Hughes, D.C. and Barratt, C. L.** (2005). Cracking the egg: increased complexity in the zona pellucida. *Hum Reprod* **20**, 1148-52.



- Conner, S. J., Lefièvre, L., Kirkman-Brown, J., Michelangeli, F., Jimenez-Gonzalez, C., Machado-Oliveira, G. S., Pixton, K. L., Brewis, I. A., Barratt, C. L. and Publicover, S. J.** (2007). Understanding the physiology of pre-fertilisation events in the human spermatozoa- a necessary prerequisite to developing rational therapy. *Soc Reprod Fertil Suppl* **63**, 237-55.
- Cook, S.P. and Babcock, D.F.** (1993). Activation of  $\text{Ca}^{2+}$  permeability by cAMP is coordinated through the pHi increase induced by speract. *J Biol Chem*. **268**, 22408-13.
- Cooper, T.G., Barfield, J.P. and Yeung, C.H.** (2005). Changes in osmolality during liquefaction of human semen. *Int J Androl*. **28**, 58-60.
- Correia, J. N., Conner, S. J. and Kirkman-Brown, J. C.** (2007). Non-genomic steroid actions in human spermatozoa. "Persistent tickling from a laden environment". *Semin Reprod Med* **25**, 208-19.
- Costello, S., Michelangeli, F., Nash, K., Lefievre, L., Morris, J., Machado-Oliveira, G., Barratt, C., Kirkman-Brown, J. and Publicover, S.** (2009).  $\text{Ca}^{2+}$ -stores in sperm: their identities and functions. *Reproduction*. **138**, 425-37.
- Cross, N.L., Morales, P., Overstreet, J.W. and Hanson, F.W.** (1988). Induction of the acrosome reactions by the human zona pellucida. *Biol Reprod* **38**, 235-44.
- Cross, N.L. and Razy-Faulkner, P.** (1997). Control of human sperm intracellular pH by cholesterol and its relationship to the response of the acrosome to progesterone. *Biol Reprod*. **56**, 1169-74.
- Cross, N.L.** (2007) Effect of pH on the development of acrosomal responsiveness of human sperm. *Andrologia*. **39**(2):55-9.
- Cummins, J. M. and Yanagimachi, R.** (1986). Development of ability to penetrate the cumulus oophorus by hamster spermatozoa capacitated *in vitro*, in relation to the timing of the acrosome reaction. *Gamete Res* **15**, 187-212.
- Curry, M.R. and Watson, P.F.** (1995). Sperm structure and function. In: *Gametes, the spermatozoon* (ed J.G. Grundzinskas and J.L. Yovich) pp 122-139, Cambridge UK: Cambridge University Press.
- Dale, B., Wilding, M., Coppola, G. and Toshi, E.** (2010). How do spermatozoa activate oocytes? *Reprod Biomed Online* Feb 14 [Epub ahead of print].
- Darszon, A., Beltran, C., Felix, R., Nishigaki, T. and Trevino, C. L.** (2001). Ion transport in sperm signaling. *Dev Biol* **240**, 1-14.
- Darszon, A., Lopez-Martinez, P., Acevedo, J.J., Hernandez-Cruz, A. and Trevino, C. L.** (2006). T-

type Ca(2+) channels in sperm function. *Cell Calcium* **40**, 241-52.

**Darszon, A., Treviño, C.L., Wood, C., Galindo, B., Rodríguez-Miranda, E., Acevedo, J.J., Hernandez-González, E.O., Beltrán, C., Martínez-López, P. and Nishigaki, T.** (2007). Ion channels in sperm motility and capacitation. *Soc Reprod Fertil Suppl.* **65**:229-44.

**De Blas, G., Michaut, M., Trevino, C. L., Tomes, C. N., Yunes, R., Darszon, A. and Mayorga, L. S.** (2002). The intraacrosomal calcium pool plays a direct role in acrosomal exocytosis. *J Biol Chem* **277**, 49326-31.

**De Blas, G., Darszon, A., Ocampo, A.Y., Serrani, C.J. Castellano, L.E., Hernandez-Gonzalez, E.O., Chirinos, M., Larrea, F., Beltran, C. and Trevino, C. L.** (2009). TRPM8, a versatile channel in mouse sperm. *Plos One* **4**, e6095.

**Dega-Szafran, Z., Kania, A., Nowak-Wydra, B. and Szafran, M.** (1994). UV,1H and 13C NMR spectra and AM1 studies of protonation of aminopyridines. *J Molecular Structure* **322**, 223-232.

**De Jonge, C.J., Han, H.L., Mack, S.R. and Zaneveld, L.J.** (1991). Effect of phorbol diesters, synthetic diacylglycerols, and a protein kinase C inhibitor on the human sperm acrosome reaction. *J Androl* **12**, 62-70.

**De Jonge, C.** (2005). Biological basis for human capacitation. *Hum Reprod Update* **11**, 205-14.

**de Lamirande, E., Leclerc, P and Gagnon, C.** (1997). Capacitation as a regulatory event that primes spermatozoa for the acrosome reaction and fertilization. *Mol Hum Reprod* **3**, 175-194.

**Demarco, I.A., Espinosa, F., Edwards, J., Sosnik, J., De La Vega-Beltran, J.L., Hockensmith, J.W., Kopf, G.S., Darszon, A. and Visconti, P.E.** (2003). Involvement of a Na<sup>+</sup>/HCO<sub>3</sub><sup>-</sup> cotransporter in mouse sperm capacitation. *J Biol Chem.* **278**, 7001-9.

**De Mott, R.P. and Suarez, S.S.** (1992). Hyperactivated sperm progress in the mouse oviduct. *Biol Reprod.* **46**, 779-85.

**De Mott, R.P., Lefebvre, R. and Suarez, S.S.** (1995). Carbohydrates mediate the adherence of hamster sperm to oviductal epithelium. *Biop Reprod* **52**, 1395-1403.

**Dey, S.K.** (2010). How we are born. *J Clin Invest.* **120**(4):952-5.

**Dixson, A.F. and Anderson, M.J.** (2004). Sexual behavior, reproductive physiology and sperm competition in male mammals. *Physiol Behav.* **83**, 361-71.

- Dragileva, E., Rubinstein, S. and Breitbart, H.** (1999). Intracellular  $\text{Ca}^{2+}$ - $\text{Mg}^{2+}$ -ATPase regulates calcium influx and acrosomal exocytosis in bull and ram spermatozoa. *Biol Reprod.* 61, 1226-34.
- Dymek, E.E. and Smith, E.F.** (2007). A conserved CaM- and radial spoke associated complex mediates regulation of flagellar dynein activity. *J Cell Biol.* 179, 515-26.
- Eddy, E.M.** (2007). The scaffold role of the fibrous sheath. *Soc Reprod Fertil Suppl.* 65,45-62.
- Eisenbach, M.** (1999). Mammalian sperm chemotaxis and its association with capacitation. *Dev Genet* 25, 87-94.
- Eisenbach, M. and Giojalas, L. C.** (2006). Sperm guidance in mammals - an unpaved road to the egg. *Nat Rev Mol Cell Biol* 7, 276-85.
- Ellerman, D.A., Pei, J., Guptas, S., Snell, W.J., Myles, D. and Primokoff, P.** (2009). Izumo is part of a multiprotein family whose members form long complexes on mammalian sperm. *Mol Reprod Dev* 76, 1188-99.
- Ensslin, M.A. and Shur, B.D.** (2003). Identification of mouse sperm SED1, a bi-motif EGF repeat and discoidin domain protein involved in sperm-egg binding. *Cell* 114, 405-417.
- Escoffier, J., Boisseuu, S., Serres, C., Chen, C.C., Kim, D., Stamboulia, S., Shin, H.S., Campbell, K.P., De Ward, M. and Arnoult, C.** (2007). Expression, localization and functions in acrosome reaction and sperm motility of  $\text{Ca}_v3.1$  and  $\text{Ca}_v3.2$  channels in sperm: an evaluation from  $\text{Ca}_v3.1$  and  $\text{Ca}_v3.2$  deficient mice. *J Cell Physiol* 212, 753-63.
- Espinosa, F. and Darszon, A.** (1995). Mouse sperm membrane potential: changes induced by  $\text{Ca}^{2+}$ . *FEBS Lett.* 372, 119-25.
- Esposito, G., Jaiswal, B. S., Xie, F., Krajnc-Franken, M. A., Robben, T. J., Strik, A. M., Kuil, C., Philipsen, R. L., van Duin, M., Conti, M. et al.** (2004). Mice deficient for soluble adenylyl cyclase are infertile because of a severe sperm-motility defect. *Proc Natl Acad Sci U S A* 101, 2993-8.
- Espino, J., Mediero, M., Lozano, G.M., Bejarano, I., Ortiz, A., Garcia, J.F., Pariente, J.A. and Rodriguez, A.B.** (2009). Reduced levels of intracellular calcium releasing in spermatozoa from asthenozoospermic patients. *Reprod Biol Endocrinol* 6, 7-11.
- Evans, J. P. and Florman, H. M.** (2002). The state of the union: the cell biology of fertilization. *Nat Cell Biol* 4 Suppl, s57-63.
- Fawcett, D. W.** (1975). The mammalian spermatozoon. *Dev Biol* 44, 394-436.

- Felix, R.** (2005) Molecular physiology and pathology of Ca<sup>2+</sup> conducting channels in the plasma membrane of mammalian sperm. *Reproduction* **129**, 251-62.
- Feske, S., Gwack, Y., Prakriya, M., Srikanth, S., Puppel, S.H., Tanasa, B., Hogan, P.G., Lewis, R.S., Daly, M. and Rao, A.** (2006). A mutation in Orai1 causes immune deficiency by abrogating CRAC channel function. *Nature* **441**, 179-85.
- Flesch, F.M. and Gadella, B.M.** (2000). Dynamics of the mammalian sperm plasma membrane in the process of fertilization. *Biochim Biophys Acta*, **1469**, 197-235
- Florman, H. M., Tombes, R. M., First, N. L. and Babcock, D. F.** (1989). An adhesion- associated agonist from the zona pellucida activates G protein-promoted elevations of internal Ca<sup>2+</sup> and pH that mediate mammalian sperm acrosomal exocytosis. *Dev Biol* **135**, 133-46.
- Florman, H. M.** (1994). Sequential focal and global elevations of sperm intracellular Ca<sup>2+</sup> are initiated by the zona pellucida during acrosomal exocytosis. *Dev Biol* **165**, 152-64.
- Florman, H. M., Arnoult, C., Kazam, I. G., Li, C. and O'Toole, C. M. B.** (1999). An intimate biochemistry: egg-regulated acrosome reactions of mammalian sperm. *Adv. Devel Biochem* **5**, 147-186.
- Florman, H. M., Jungnickel, M.K. and Sutton, K.A.** (2008). Regulating the acrosome reaction. *Int J Dev Biol* **52**, 503-10.
- Florman, H.M., Jungnickel, M.K. and Sutton, K.A.** (2010). Shedding light on sperm pHertility. *Cell*. **140**, 310-2.
- Ford, W.C.** (2006). Glycolysis and sperm motility: does a spoonful of sugar help the flagellum go round? *Hum Reprod Update*. **12**, 269-74.
- Foreman, M.A., Smith, J. and Publicover, S.J.** (2006). Characterisation of serum-induced intracellular Ca<sup>2+</sup> oscillations in primary bone marrow stromal cells. *J Cell Physiol*. **206**, 664-71.
- Foresta, C., Rossato, M. and Di Virgilio, F.** (1993). Ion fluxes through the progesterone- activated channel of the sperm plasma membrane. *Biochem J* **294 ( Pt 1)**, 279-83.
- Fox, A.P., Nowycky, M.C. and Tsien, R.W.** (1987). Kinetic and pharmacological properties distinguishing three types of calcium currents in chick sensory neurones. *J Physiol*. **394**, 149-72.
- Fraire-Zamora, J. J. and Gonzalez-Martinez, M. T.** (2004). Effect of intracellular pH on depolarization-evoked calcium influx in human sperm. *Am J Physiol Cell Physiol* **287**, C1688-96.

- Fraser, L.R., Adeoya-Osiguwa, S., Baxendale, R.W., Mededovic, S. and Osiguwa, O.O.** (2005). First messenger regulation of mammalian sperm function via adenylyl cyclase/cAMP. *J Reprod Devel* **51**, 37-46.
- Fraser, L. R.** (2010). The “switching on” of mammalian spermatozoa: molecular events involved in promotion and regulation of capacitation. *Mol Reprod Dev* **77**, 197-208
- Frayne, J., Dimsey, E.A.C., Jury, J.A. and Hall, J.** (1999). Transcripts encoding the sperm surface protein tMDC II are non-functional in the human. *Biochem J* **341**, 771-775.
- Frischauf, I., Schindl, R., Derler, I., Bergsmann, J., Fahrner, M. and Romanin, C.** (2008). The STIM/Orai coupling machinery. *Channels (Austin)*. **2**, 261-8.
- Fukami, K., Nakao, K., Inoue, T., Kataoka, Y., Kurokawa, M., Fissore, R. A., Nakamura, K., Katsuki, M., Mikoshiba, K., Yoshida, N. et al.** (2001). Requirement of phospholipase Cdelta4 for the zona pellucida-induced acrosome reaction. *Science* **292**, 920-3.
- Fukami, K., Yoshida, M., Inoue, T., Kurokawa, M., Fissore, R. A., Yoshida, N., Mikoshiba, K. and Takenawa, T.** (2003). Phospholipase Cdelta4 is required for Ca<sup>2+</sup> mobilization essential for acrosome reaction in sperm. *J Cell Biol* **161**, 79-88.
- Fukuda, N., Yomogida, K., Okabe, M. and Touhara, K.** (2004). Functional characterization of a mouse testicular olfactory receptor and its role in chemosensing and in regulation of sperm motility. *J Cell Sci* **117**, 5835-45.
- Gadella, B. and Visconti, P.E.** (2006). Regulation of capacitation. in *The Sperm Cell: Production, Maturation, Fertilization and Regeneration* (ed. C. de Jonge and C. Barratt), pp. 134-169. Cambridge, UK: Cambridge University Press.
- Galantino-Homer, H.L., Florman, H.M., Storey, B.T., Dobrinski, I. and Kopf, G.S.** (2004). Bovine sperm capacitation: assessment of phosphodiesterase activity and intracellular alkalinization on capacitation-associated protein tyrosine phosphorylation. *Mol Reprod Dev.* **67**, 487-500.
- Garcia, M. A. and Meizel, S.** (1999). Progesterone-mediated calcium influx and acrosome reaction of human spermatozoa: pharmacological investigation of T-type calcium channels. *Biol Reprod* **60**, 102-9.
- Giannini, G., Conti, A., Mammarella, S., Scrobogna, M. and Sorrentino, V.** (1995). The ryanodine receptor/calcium channel genes are widely and differentially expressed in murine brain and peripheral tissues. *J Cell Biol* **128**, 893-904.
- Gibbons, I. R. and Rowe, A. J.** (1965). Dynein: A Protein with Adenosine Triphosphatase Activity from Cilia. *Science* **149**, 424-6.

- Gibbons, I.R. and Gibbons, B.H.** (1980). Transient flagellar waveforms during intermittent swimming in sea urchin sperm. I. Wave parameters. *J Muscle Res Cell Motil.* **1**,31-59
- Giroux-Widemann, V., Jouannet, P., Pignot-Paintrand, I. and Feneux, D.** (1991). Effects of pH on the reactivation of human spermatozoa demembranated with Triton X-100. *Mol Reprod Dev.* **29**, 157-62.
- Glover, T.D., Barratt, C.L.R., Tyler, J.J.P. and Hennessey, R.** (1990). Human male fertility and semen analysis. London: Academic Press, pp. 247.
- Gobet, I., Lippai, M., Tomkowiak, M., Durocher, Y., Leclerc, C., Moreau, M. and Guerrier, P.** (1995). 4-aminopyridine acts as a weak base and a  $\text{Ca}^{2+}$  mobilizing agent in triggering oocyte meiosis reinitiation and activation in the Japanese clam *Ruditapes philippinarum*. *Int J Dev Biol.* **39**, 485-91.
- Gonzalez-Martinez, M. T., Galindo, B. E., de De La Torre, L., Zapata, O., Rodriguez, E., Florman, H. M. and Darszon, A.** (2001). A sustained increase in intracellular  $\text{Ca}^{2+}$  is required for the acrosome reaction in sea urchin sperm. *Dev Biol* **236**, 220-9.
- Gonzalez-Martinez, M. T., Bonilla-Hernandez, M.A. and Guzman-Grenfell, A.M.** (2002). Stimulation of voltage-dependent calcium channels during capacitation and by progesterone in human sperm. *Arch Biochem Biophys* **408**, 205-10.
- González-Martínez, M.T.** (2003). Induction of a sodium-dependent depolarization by external calcium removal in human sperm. *J Biol Chem.* **278**(38):36304-10.
- Goodwin, L.O., Leeds, N.B., Hurley, I., Mandel, F.S., Pergolizzi, R.G. and Benoff, S.** (1997). Isolation and characterization of the primary structure of testis-specific L-type calcium channel: implications for contraception. *Mol Hum Reprod.* **3**(3):255-68.
- Goodwin, L.O., Karabinus, D.S., Pergolizzi, R.G. and Benoff, S.** (2000). L-type voltage-dependent calcium channel  $\alpha\text{-1C}$  subunit mRNA is present in ejaculated human spermatozoa. *Mol Hum Reprod.* **6**(2):127-36.
- Goto, N. and Harayama, H.** (2009). Calyculin A-sensitive protein phosphatases are involved in maintenance of progressive movement in mouse spermatozoa in vitro by suppression of autophosphorylation of protein kinase A. *J Reprod Dev.* **55**, 327-34..
- Green, D. P.** (1997). Three-dimensional structure of the zona pellucida. *Rev Reprod* **2**, 147-56.
- Greve, J. M. and Wassarman, P. M.** (1985). Mouse egg extracellular coat is a matrix of interconnected filaments possessing a structural repeat. *J Mol Biol* **181**, 253-64.

- Grimaldi, M., Atzori, M., Ray, P. and Alkon, D.L.** (2001). Mobilization of calcium from intracellular stores, potentiation of neurotransmitter-induced calcium transients, and capacitative calcium entry by 4-aminopyridine. *J Neurosci.* **21**, 3135-43.
- Grynkiewicz, G., Poenie, M. and Tsien, R.Y.** (1985). A new generation of  $\text{Ca}^{2+}$  indicators with greatly improved fluorescence properties. *J Biol Chem.* **260**, 3440-50.
- Gu, Y., Kirkman-Brown, J.C., Korchev, Y., Barratt, C.L. and Publicover, S.J.** (2004). Multi-state, 4-aminopyridine-sensitive ion channels in human spermatozoa. *Dev Biol.* **274**, 308-17.
- Gunarathne, H.J. and Vacquier, V.D.** (2006). Evidence for a secretory pathway  $\text{Ca}^{2+}$ -ATPase in sea urchin spermatozoa. *FEBS Lett.* **580**, 3900-4.
- Gunter, T.E., Buntinas, L., Sparagna, G., Eliseev, R. and Gunter, K.** (2000). Mitochondrial calcium transport: mechanism and functions. *Cell Calcium* **28**, 285-96.
- Gupta, S.K., Bansal, P., Ganguly, A., Bhandari, B. and Chakrabarti, K.** (2009). Human zona pellucida glycoproteins: functional relevance during fertilization. *J Reprod Immun* **83**, 50-55.
- Guse, A.H., Roth, E. and Emmrich, F.** (1994).  $\text{Ca}^{2+}$  release and  $\text{Ca}^{2+}$  entry induced by rapid cytosolic alkalization in Jurkat T-lymphocytes. *Biochem J.* **301** ( Pt 1), 83-8.
- Hagaman, J.R., Moyer, J.S., Bachman, E.S., Sibony, M., Magyar, P.L., Welch, J.E. Smithies, O., Kregge, J.H. and O'Brien, D.A.** (1998). Angiotensin-converting enzyme and male fertility. *PNAS* **95**, 2552-7.
- Hamamah, S. and Gatti, J.L.** (1998). Role of the ionic environment and internal pH on sperm activity. *Hum Reprod. 13 Suppl* **4**, 20-30.
- Harayama, H., Okada, K. and Miyake, M.** (2003). Involvement of cytoplasmic free calcium in boar sperm: head-to-head agglutination induced by a cell-permeable cyclic adenosine monophosphate analog. *J Androl.* **24**, 91-9.
- Harper, C. V., Kirkman-Brown, J. C., Barratt, C. L. and Publicover, S. J.** (2003). Encoding of progesterone stimulus intensity by intracellular  $[\text{Ca}^{2+}]$  ( $[\text{Ca}^{2+}]_i$ ) in human spermatozoa. *Biochem J* **372**, 407-17.
- Harper, C. V., Barratt, C. L. and Publicover, S. J.** (2004). Stimulation of human spermatozoa with progesterone gradients to simulate approach to the oocyte. Induction of  $[\text{Ca}^{2+}]_i$  oscillations and cyclical transitions in flagellar beating. *J Biol Chem* **279**, 46315-25.
- Harper, C., Wootton, L., Michelangeli, F., Lefievre, L., Barratt, C. and Publicover, S.** (2005). Secretory

pathway  $\text{Ca}(2+)\text{-ATPase}$  (SPCA1)  $\text{Ca}(2+)\text{ pumps}$ , not SERCAs, regulate complex  $[\text{Ca}(2+)](i)$  signals in human spermatozoa. *J Cell Sci* **118**, 1673-85.

**Harper, C. V. and Publicover, S. J.** (2005). Reassessing the role of progesterone in fertilization--compartmentalized calcium signalling in human spermatozoa? *Hum Reprod* **20**, 2675-80.

**Harper, C. V., Barratt, C. L., Publicover, S.J. and Kirkman-Brown, J. C.** (2006). Dynamics of the progesterone-induced acrosome reaction and its relation to intracellular calcium responses in individual human spermatozoa. *Biol Reprod* **75**, 933-9.

**Harper, C. V., Cumerson, J.A. White, M.R., Publicover, S. J. and Johnson, P.M.** (2008). Dynamic resolution of acrosomal exocytosis in human spermatozoa. *J Cell Sci* **121**, 2130-5.

**Harrison, R. A.** (2004). Rapid PKA-catalysed phosphorylation of boar sperm proteins induced by the capacitating agent bicarbonate. *Mol Reprod Dev* **67**, 337-52.

**Haugland, R.P.** (2001) Handbook of Molecular Probes and Research Products, 8<sup>th</sup> Ed

**Haugland, R.P. and You, W.W.** (2008). Coupling of antibodies with biotin. *Methods Mol Biol*, **418**, 13-24.

**Hayashi, S. and Shingyoji, C.** (2008). Mechanism of flagellar oscillation-bending-induced switching of dynein activity in elastase-treated axonemes of sea urchin sperm. *J Cell Sci.* **121**, (Pt 17):2833-43.

**Hayashi, S. and Shingyoji, C.** (2009). Bending-induced switching of dynein activity in elastase-treated axonemes of sea urchin sperm--roles of  $\text{Ca}^{2+}$  and ADP. *Cell Motil Cytoskeleton.* **66**, 292-301.

**Hernandez-Gonzalez, E.O., Sosnik, J., Edwards, J, Acevedo, J.J., Mendoza-Lujambio, I., Lopez-Gonzalez, I., Demarco, I., Wertheimer, E., Darszon, A. and Visconti, P.E.** (2006). Sodium and epithelial sodium channels participate in the regulation of the capacitation-associated hyperpolarisation in mouse sperm. *J Biol Chem* **281**, 5623-33.

**Hernandez-Gonzalez, E.O., Trevino, C.L. Castellano, L.E., de la Vega-Beltran, J.L., Ocampo, A.Y., Wertheimer, E., Visconti, P.E. and Darszon, A.** (2007). Involvement of the cystic fibrosis transmembrane conductance regulator in mouse sperm capacitation. *J Biol Chem* **282**, 24397-406.

**Herrero, M. B., Cebal, E., Boquet, M., Viggiano, J. M., Vitullo, A. and Gimeno, M. A.** (1994). Effect of nitric oxide on mouse sperm hyperactivation. *Acta Physiol Pharmacol Ther Latinoam* **44**, 65-9.

**Herrero, M. B. and Gagnon, C.** (2001). Nitric oxide: a novel mediator of sperm function. *J Androl* **22**, 349-56.

**Herrick, S. B., Schweissinger, D. L., Kim, S. W., Bayan, K. R., Mann, S. and Cardullo, R. A.** (2005). The



acrosomal vesicle of mouse sperm is a calcium store. *J Cell Physiol* **202**, 663-71.

**Hess, K.C., Jones, B.H., Marquez, B., Chen, Y., Ord, T.S., Kamenetsky, M., Miyamoto, C., Zippin, J.H., Kopf, G.S., Suarez, S.S., Levin, L.R., Williams, C.J., Buck, J. and Moss, S.B.** (2005). The "soluble" adenylyl cyclase in sperm mediates multiple signaling events required for fertilization. *Dev Cell*. **9**, 249-59

**Hirohashi, N. and Vacquier, V. D.** (2003). Store-operated calcium channels trigger exocytosis of the sea urchin sperm acrosomal vesicle. *Biochem Biophys Res Commun* **304**, 285-92.

**Ho, H. C. and Suarez, S. S.** (2001a). Hyperactivation of mammalian spermatozoa: function and regulation. *Reproduction* **122**, 519-26.

**Ho, H. C. and Suarez, S. S.** (2001b). An inositol 1,4,5-trisphosphate receptor-gated intracellular  $\text{Ca}^{2+}$  store is involved in regulating sperm hyperactivated motility. *Biol Reprod* **65**, 1606-15.

**Ho, H.C., Granish, K.A. and Suarez, S.S.** (2002). Hyperactivated motility of bull sperm is triggered at the axoneme by  $\text{Ca}^{2+}$  and not cAMP. *Dev Biol*. **250**, 208-17.

**Ho, H. C. and Suarez, S. S.** (2003). Characterization of the intracellular calcium store at the base of the sperm flagellum that regulates hyperactivated motility. *Biol Reprod* **68**, 1590-6.

**Ho, H. C., Wolff, C.A. and Suarez, S. S.** (2009). CatSper-null mutant spermatozoa are unable to ascend beyond the oviductal reservoir. *Reprod Fertil Dev* **21**, 345-50.

**Ho, H.C.** (2010). Redistribution of nuclear pores during formation of the redundant nuclear envelope in mouse spermatids. *J. Anat* **216**, 525-32.

**Hoffhines, A.J., Jen, C.H., Leary, J.A. and Moore, K.L.** (2009). Tyrosylprotein sulfotransferase-2 expression is required for sulfation of RNase 9 and Mfge8 in vivo. *J Biol Chem* **284**, 3096-105.

**Hofmann, F., Biel, M. and Kaupp, U.B.** (2005) International Union of Pharmacology. LI. Nomenclature and structure-function relationships of cyclic nucleotide-regulated channels. *Pharmacol Rev* **57**, 455-62

**Hoth, M. and Penner, R.** (1993). Calcium release-activated calcium current in rat mast cells. *J Physiol*. **465**, 359-86.

**Howe, J.R. and Ritchie, J.M.** (1991). On the active form of 4-aminopyridine: block of  $\text{K}^{+}$  currents in rabbit Schwann cells. *J Physiol*. **433**, 183-205.

- Huang, Z., Somanath, P.R., Chakrabarti, R., Eddy, E.M. and Vijayaraghavan, S.** (2005) Changes in intracellular distribution and activity of protein phosphatase PP1gamma2 and its regulating proteins in spermatozoa lacking AKAP4. *Biol Reprod* **72**, 384-92.
- Hughes, B.P. and Barritt, G.J.** (1989). Inhibition of the liver cell receptor-activated Ca<sup>2+</sup> inflow system by metal ion inhibitors of voltage-operated Ca<sup>2+</sup> channels but not by other inhibitors of Ca<sup>2+</sup> inflow. *Biochim Biophys Acta*. **1013**, 197-205.
- Hunter, R.H. and Léglise, P.C.** (1971). Polyspermic fertilization following tubal surgery in pigs, with particular reference to the rôle of the isthmus. *J Reprod Fertil*. **24**, 233-46.
- Hutt, D. M., Cardullo, R. A., Baltz, J. M. and Ngsee, J. K.** (2002). Synaptotagmin VIII is localized to the mouse sperm head and may function in acrosomal exocytosis. *Biol Reprod* **66**, 50-6.
- Ignotz, G.G. and Suarez, S.S.** (2005). Calcium/calmodulin and calmodulin kinase II stimulate hyperactivation in demembranated bovine sperm. *Biol Reprod*. **73**, 519-26.
- Ikawa, M., Wada, I., Kominami, K., Watanabe, D., Toshimori, K., Nishimune, Y and Okabe, M.** (1997). The putative chaperone calmeglin is required for sperm fertility. *Nature* **387**, 607-11.
- Ikawa, M., Inoune, N. and Okabe, M.** (2008). Mechanism of sperm-egg interactions emerging from gene-manipulated animals. *Int J Dev Biol* **52**, 657-64.
- Ikawa, M., Inoune, N., Benham AM, Okabe M.** (2010). Fertilization: a sperm's journey to and interaction with the oocyte. *J Clin Invest*. **120**, 984-94.
- Immler, S., Moore, H.D.M., Breed, W.G. and Birkhead TR.** (2007). By hook or by crook? Morphometry, competition and cooperation in rodent sperm. *PloS One*, e170
- Inoue, N., Ikawa, M., Isotani, A. and Okabe, M.** (2005). The immunoglobulin superfamily protein Izumo is required for sperm to fuse with eggs. *Nature*. **434**, 234-8.
- Inoue, Y. and Shingyoji, C.** (2007). The roles of noncatalytic ATP binding and ADP binding in the regulation of dynein motile activity in flagella. *Cell Motil Cytoskeleton*. **64**, 690-704.
- Inoune, N., Kasahara, T., Ikawa, M., and Okabe, M.** (2010). Identification and disruption of sperm-specific angiotensin converting enzyme-3 (ACE-3) in mouse. *Plos one* **5**, e10301.
- Irino, Y., Ichinohe, M., Nakamura, Y., Nakahara, M. and Fukami, K.** (2005). Phospholipase Cdelta4 associates with glutamate receptor interacting protein 1 in testis. *J Biochem*. **138**, 451-6.

**Isotani, A. and Okabe, M.** (2005). The immunoglobulin superfamily protein Izumo is required from sperm to fuse with eggs. *Nature*, **434**, 234-8.

**Ishida, Y., Honda, H. and Watanabe, T.X.** (1992).  $\text{Ca}^{2+}$  release from isolated sarcoplasmic reticulum of guinea-pig psoas muscle induced by  $\text{K}^{+}$ -channel blockers. *Br J Pharmacol*. **106**, 764-5.

**Ishida, Y. and Honda, H.** (1993). Inhibitory action of 4-aminopyridine on  $\text{Ca}^{2+}$ -ATPase of the mammalian sarcoplasmic reticulum. *J Biol Chem*. **268**, 4021-4.

**Ishijima, S., Hamaguchi, M.S., Naruse, M., Ishijima, S.A. and Hamaguchi, Y.** (1992). Rotational movement of a spermatozoon around its long axis. *J Exp Biol*. **163**, 15-31.

**Ishijima, S. and Hamaguchi, Y.** (1993). Calcium ion regulation of chirality of beating flagellum of reactivated sea urchin spermatozoa. *Biophys J*. **65**, 1445-8.

**Ishijima, S.** (1995). High-speed video microscopy of flagella and cilia. *Methods Cell Biol*. **47**, 239-43.

**Ishijima, S., Kubo-Irie, M., Mohri, H. and Hamaguchi, Y.** (1996). Calcium-dependent bidirectional power stroke of the dynein arms in sea urchin sperm axonemes. *J Cell Sci*. **109**, 2833-42.

**Ishijima, S., Iwamoto, T., Nozawa, S. and Matsushita, K.** (2002a). Motor apparatus in human spermatozoa that lack central pair microtubules. *Mol Reprod Dev*. **63**, 459-63.

**Ishijima, S., Baba, S. A., Mohri, H. and Suarez, S. S.** (2002b). Quantitative analysis of flagellar movement in hyperactivated and acrosome-reacted golden hamster spermatozoa. *Mol Reprod Dev* **61**, 376-84.

**Ishijima, S., Mohri, H., Overstreet, J.W. and Yudin, A.I.** (2006). Hyperactivation of monkey spermatozoa is triggered by  $\text{Ca}^{2+}$  and completed by cAMP. *Mol Reprod Dev*. **73**, 1129-39.

**Ishijima, S.** (2007a). Digital image analysis of flagellar beating and microtubule sliding of activated and hyperactivated sperm flagella. *Soc Reprod Fertil Suppl*. **65**:327-30.

**Ishijima, S.** (2007b) The velocity of microtubule sliding: its stability and load dependency. *Cell Motil Cytoskeleton*. **64**, 809-13.

**Jagannathan, S., Punt, E. L., Gu, Y., Arnoult, C., Sakkas, D., Barratt, C. L. and Publicover, S. J.** (2002). Identification and localization of T-type voltage-operated calcium channel subunits in human male germ cells. Expression of multiple isoforms. *J Biol Chem* **277**, 8449-56.

**Jaiswal, B. S., Cohen-Dayag, A., Tur-Kaspa, I. and Eisenbach, M.** (1998). Sperm capacitation is, after all, a prerequisite for both partial and complete acrosome reaction. *FEBS Lett* **427**,

**Jaiswal, B. S., Tur-Kaspa, I., Dor, J., Mashiach, S. and Eisenbach, M.** (1999). Human sperm chemotaxis: is progesterone a chemoattractant? *Biol Reprod* **60**, 1314-9.

**Jaiswal, B. S. and Conti, M.** (2003). Calcium regulation of the soluble adenylyl cyclase expressed in mammalian spermatozoa. *Proc Natl Acad Sci U S A* **100**, 10676-81.

**Jeong, S.Y. and Seol, D.W.** (2008). The role of mitochondria in apoptosis. *BMB Rep.* **41**, 11-22.

**Jimenez-Gonzalez, C., Michelangeli, F., Harper, C. V., Barratt, C. L. and Publicover, S. J.** (2006). Calcium signalling in human spermatozoa: a specialized 'toolkit' of channels, transporters and stores. *Hum Reprod Update* **12**, 253-67.

**Jin, J., Jin, N., Zheng, H., Ro, S., Tafolla, D., Sanders, K.M. and Yan, W.** (2007). CatSper3 and CatSper4 are essential for sperm hyperactivated motility and male fertility in the mouse. *Biol Reprod* **77**, 37-44.

**Jones, H.P., Lenz, R.W., Palevitz, B.A. and Cormier, M.J.** (1980). Calmodulin localization in mammalian spermatozoa. *Proc Natl Acad Sci U S A.* **77**, 2772-6.

**Jones, J.M. and Bavister, B.D.** (2000). Acidification of intracellular pH in bovine spermatozoa suppresses motility and extends viable life. *J Androl.* **21**, 616-24.

**José, O., Hernández-Hernández, O., Chirinos, M., González-González, M.E., Larrea, F., Almanza, A., Felix, R., Darszon, A. and Treviño, C.L.** (2010). Recombinant human ZP3-induced sperm acrosome reaction: evidence for the involvement of T- and L-type voltage-gated calcium channels. *Biochem Biophys Res Commun.* **395**, 530-4.

**Jungnickel, M. K., Marrero, H., Birnbaumer, L., Lemos, J. R. and Florman, H. M.** (2001). Trp2 regulates entry of Ca<sup>2+</sup> into mouse sperm triggered by egg ZP3. *Nat Cell Biol* **3**, 499-502.

**Kaneto, M., Krisfalusi, M., Eddy, E.M., O'Brien, D.A. and Miki, K.** (2008). Bicarbonate-induced phosphorylation of p270 protein in mouse sperm by cAMP-dependent protein kinase. *Mol Reprod Dev.* **75**, 1045-53.

**Katz, D.F., Mills, R.N. and Pritchett, T.R.** (1978a). The movement of human spermatozoa in cervical mucus. *J Reprod Fertil.* **53**, 259-65.

**Katz, D.F., Yanagimachi, R. and Dresdner, R.D.** (1978b). Movement characteristics and power output of guinea-pig and hamster spermatozoa in relation to activation. *J Reprod Fertil.* **52**, 167-72.

**Katz, D. F. and Yanagimachi, R.** (1980). Movement characteristics of hamster spermatozoa within the oviduct. *Biol Reprod* **22**, 759-64.

**Katz, D.F., Drobnis, E.Z. and Overstreet, J.W.** (1989). Factors regulating mammalian sperm migration through the female reproductive tract and oocyte vestments. *Gamete Res.* 1989 (**4**):443-69.

**Kaupp, U. B.** (1995). Family of cyclic nucleotide gated ion channels. *Curr Opin Neurobiol* **5**, 434-42.

**Kaupp, U. B., Solzin, J., Hildebrand, E., Brown, J. E., Helbig, A., Hagen, V., Beyermann, M., Pampaloni, F. and Weyand, I.** (2003). The signal flow and motor response controlling chemotaxis of sea urchin sperm. *Nat Cell Biol* **5**, 109-17.

**Kaupp, U.B., Kashikar, N.D. and Weyand, I.** (2008). Mechanisms of sperm chemotaxis. *Annu Rev Physiol.* 70, 93-117.

**Kerschbaum, H.H. and Cahalan, M.D.** (1998). Monovalent permeability, rectification, and ionic block of store-operated calcium channels in Jurkat T lymphocytes. *J Gen Physiol.* **111**, 521-37.

**Kim, E., Yamashita, M., Nakanishi, T., Park, K.E., Kimura, M., Kashiwabara, S. and Baba, R.** (2006). Mouse lacking ADAM1b/ADAM2 fertilin can fuse with the egg membrane and effect fertilization. *J Biol Chem* **281**, 5634-9.

**Kirichok, Y., Navarro, B. and Clapham, D.E.** (2006) Whole-cell patch-clamp measurements of spermatozoa reveal an alkaline-activated Ca<sup>2+</sup> channel. *Nature* **439** 737-40.

**Kirkman-Brown, J. C., Bray, C., Stewart, P. M., Barratt, C. L. and Publicover, S. J.** (2000). Biphasic elevation of [Ca<sup>2+</sup>]<sub>i</sub> in individual human spermatozoa exposed to progesterone. *Dev Biol* **222**, 326-35.

**Kirkman-Brown, J. C., Punt, E. L., Barratt, C. L. and Publicover, S. J.** (2002). Zona pellucida and progesterone-induced Ca<sup>2+</sup> signaling and acrosome reaction in human spermatozoa. *J Androl* **23**, 306-15.

**Kirkman-Brown, J. C., Barratt, C. L. and Publicover, S. J.** (2003). Nifedipine reveals the existence of two discrete components of the progesterone-induced [Ca<sup>2+</sup>]<sub>i</sub> transient in human spermatozoa. *Dev Biol* **259**, 71-82.

**Kirkman-Brown, J. C., Barratt, C. L. and Publicover, S. J.** (2004). Slow calcium oscillations in human spermatozoa. *Biochem J* **378**, 827-32.

**Kobori, H., Miyazaki, S. and Kuwabara, Y.** (2000). Characterization of intracellular Ca<sup>2+</sup> increase in response to progesterone and cyclic nucleotides in mouse spermatozoa. *Biol Reprod* **63**, 113-20.

**Krietsch, T., Fernandes, M. S., Kero, J., Losel, R., Heyens, M., Lam, E. W., Huhtaniemi, I., Brosens, J. J. and Gellersen, B.** (2006). Human homologs of the putative G protein- coupled membrane progestin

receptors (mPR $\alpha$ ,  $\beta$ , and  $\gamma$ ) localize to the endoplasmic reticulum and are not activated by progesterone. *Mol Endocrinol* **20**, 3146-64.

**Kulkarni, S.B., Sauna, Z.E., Somlata, V. and Sitaramam, V. (1997).** Volume regulation of spermatozoa by quinine-sensitive channels. *Mol Reprod Dev.* **46**, 535-50.

**Kunz, G., Beil, D., Deininger, H, Wildt, L. and Leyendecker, G. (1996).** The dynamics of rapid sperm transport through the female genital tract: evidence from vaginal sonography or uterine peristalsis and hysterosalpingoscintigraphy. *Hum Reprod* **11**, 627-32.

**Kuroda, Y., Kaneko, S., Yoshimura, Y., Nozawa, S. and Mikoshiba, K. (1999).** Are there inositol 1,4,5-triphosphate (IP3) receptors in human sperm? *Life Sci* **65**, 135-43.

**Laufer, N., DeCherney, A. H., Haseltine, F. P. and Behrman, H. R. (1984).** Steroid secretion by the human egg-corona-cumulus complex in culture. *J Clin Endocrinol Metab* **58**, 1153-7.

**Lawson, C., Dorval, V., Goupil, S. and Leclerc, P. (2007).** Identification and localisation of SERCA2 isoform in mammalian sperm. *Mol Hum Reprod* **13**, 307-16.

**Leclerc, P., de Lamirande, E. and Gagnon, C. (1996).** Cyclic adenosine 3',5'-monophosphate-dependent regulation of protein tyrosine phosphorylation in relation to human sperm capacitation and motility. *Biol Reprod* **55**, 684-92.

**Lefièvre, L., De Lamirande, E. and Gagnon, C. (2000).** The cyclic GMP-specific phosphodiesterase inhibitor, sildenafil, stimulates human sperm motility and capacitation but not acrosome reaction. *J Androl* **21**, 929-37.

**Lefièvre, L., Jha, K. N., de Lamirande, E., Visconti, P. E. and Gagnon, C. (2002).** Activation of protein kinase A during human sperm capacitation and acrosome reaction. *J Androl* **23**, 709-16.

**Lefièvre, L., Conner, S. J., Salpekar, A., Olufowobi, O., Ashton, P., Pavlovic, B., Lenton, W., Afnan, M., Brewis, I. A., Monk, M. et al. (2004).** Four zona pellucida glycoproteins are expressed in the human. *Hum Reprod* **19**, 1580-6.

**Lefièvre, L., Bedu-Addo, K., Conner, S.J., Machado-Oliveira, G.S., Chen, Y., Kirkman-Brown J.C., Afnan, M.A., Publicover, S.J., Ford, W.C, and Barratt, C.L. (2007).** Counting sperm does not add up any more: time for a new equation? *Reproduction.* **133**, 675-84.

**Lefièvre, L., Machado-Oliveira, G., Ford, C., Kirkman-Brown, J., Barratt, C. and Publicover, S. (2009).** Communication between female tract and sperm: saying No when you mean yes. *Commun Intedr Biol* **2**, 82-5.

- Lewis, R.S.** (2007). The molecular choreography of a store-operated calcium channel. *Nature* **446**, 284-7.
- Leypold, B.G., Yu, C.R., Leinders-Zufall, T., Kims, M.M., Zufall, F and Axel, R.** (2002). Altered sexual and social behaviours in *trp2* mutant mice. *PNAS* **99**, 6376-6381.
- Li, H.G., Ding, X.F., Liao, A.H., Kong, X.B. and Xiong, C.L.** (2007). Expression of CatSper family transcripts in the mouse testis during post-natal development and human ejaculated spermatozoa: relationship to sperm motility. *Mol Hum Reprod.* **13**, 299-306.
- Li, H., Ding, X., Guan, H. and Xiong, C.** (2009). Inhibition of human sperm function and mouse fertilization in vitro by an antibody against cation channel of sperm 1: the contraceptive potential of its transmembrane domains and pore region. *Fertil Steril.* **92**, 1141-6.
- Lin Y-N., Roy, A., Yan, W., Burns, K.H. and Matzuk, M.M.** (2007). Loss of zona pellucida binding proteins in the acrosomal matrix disrupts acrosome biogenesis and sperm morphogenesis. *Mol Cell Biol* **27**, 6794-6895.
- Linck, B., Qiu, Z., He, Z., Tong, Q., Hilgemann, D.W. and Philipson, K.D.** (1998). Functional comparison of the three isoforms of the Na<sup>+</sup>/Ca<sup>2+</sup> exchanger (NCX1, NCX2, NCX3). *Am J Physiol.* **274**(2 Pt 1):C415-23.
- Lindemann, C. B. and Goltz, J. S.** (1988). Calcium regulation of flagellar curvature and swimming pattern in triton X-100--extracted rat sperm. *Cell Motil Cytoskeleton* **10**, 420-31.
- Lindemann, C.B., Gardner, T.K., Westbrook, E. and Kanous, K.S.** (1991). The calcium-induced curvature reversal of rat sperm is potentiated by cAMP and inhibited by anti-calmodulin. *Cell Motil Cytoskeleton.* **20**, 316-24.
- Lishko, P.V., Botchkina, I.L., Fedorenko, A. and Kirichok, Y.** (2010). Acid extrusion from human spermatozoa is mediated by flagellar voltage-gated proton channel. *Cell.* **140**, 327-37.
- Litvin, T. N., Kamenetsky, M., Zarifyan, A., Buck, J. and Levin, L. R.** (2003). Kinetic properties of "soluble" adenylyl cyclase. Synergism between calcium and bicarbonate. *J Biol Chem* **278**, 15922-6.
- Lobley, A., Pierron, V., Reynolds, L., Allen, L. and Michalovich, D.** (2003). Identification of human and mouse CatSper3 and CatSper4 genes: characterisation of a common interaction domain and evidence for expression in testis. *Reprod Biol Endocrinol* **1**, 53.
- Losel, R., Dorn-Beineke, A., Falkenstein, E., Wheling, M. and Feuring, M.** (2004). Porcine spermatozoa contain more than one membrane progesterone receptor. *Int J Biochem Cell Biol* **36**, 1532-41.
- Losel, R., Breiter, S., Seyfert, M., Wehling, M. and Falkenstein, E.** (2005). Classic and non-classic progesterone receptors are both expressed in human spermatozoa. *Horm Metab Res* **37**, 10-4.

- Lu, Q., and Shur, B.D.** (1997). Sperm from  $\beta$ 1,4-galactosyltransferase null mice are refractory to ZP3-acrosome reaction and penetrate the zona pellucida poorly. *Development* **124**, 4121-4131.
- Luconi, M., Muratori, M., Maggi, M., Pecchioli, P., Peri, A., Mabcini, M., Filimberti, E., Forti, G. and Baldi, E.** (2000). Uteroglobulin and transglutaminase modulate human sperm functions. *J Androl*, **21**, 676-88
- Luik, R.M., Wang, B., Prakriya, M., Wu, M.M. and Lewis, R.S.** (2008). Oligomerization of STIM1 couples ER calcium depletion to CRAC channel activation. *Nature* **454**, 538-42.
- Machado-Oliveira, G., Lefievre, L., Ford, C., Herrero, M.B., Barratt, C., Connolly, T.J., Nash, K., Morales-Garcia, A., Kirkman-Brown, J. and Publicover, S.** (2008). Mobilisation of  $\text{Ca}^{2+}$  stores and flagellar regulation in human sperm by S-nitrosylation: a role for NO synthesised in the female reproductive tract. *Development* **135**, 3677-86.
- Mann, T. and Lutwak-Mann, C.** (1981). Male Reproductive Function and Semen: Themes and Trends in: *Physiology, Biochemistry and Investigative Andrology* New York, NY: Springer-Verlag.
- Marengo, S.R.** (2008). Maturing the sperm, unique mechanism for modifying integral proteins in the sperm plasma membrane. *Anim Reprod Sci* **105**, 52-63.
- Marín-Briggiler, C.I., Jha, K.N., Chertihin, O., Buffone, M.G., Herr, J.C., Vazquez-Levin, M.H. and Visconti, P.E.** (2005). Evidence of the presence of calcium/calmodulin-dependent protein kinase IV in human sperm and its involvement in motility regulation. *J Cell Sci.*, **118**, 2013-22.
- Martin, C., Ashley, R. and Shoshan-Barmatz, V.** (1993). The effect of local anaesthetics on the ryanodine receptor/ $\text{Ca}^{2+}$  release channel of brain microsomal membranes. *FEBS Lett.* **328**, 77-81.
- Martínez-López, P., Santi, C.M., Treviño, C.L., Ocampo-Gutiérrez, A.Y., Acevedo, J.J., Alisio, A., Salkoff, L.B. and Darszon, A.** (2009). Mouse sperm  $\text{K}^{+}$  currents stimulated by pH and cAMP possibly coded by Slo3 channels. *Biochem Biophys Res Commun.* **381**, 204-9.
- Marquez, B. and Suarez, S. S.** (2004). Different signaling pathways in bovine sperm regulate capacitation and hyperactivation. *Biol Reprod* **70**, 1626-33.
- Marquez, B. and Suarez, S.S.** (2007). Bovine sperm hyperactivation is promoted by alkaline-stimulated  $\text{Ca}^{2+}$  influx. *Biol Reprod.* **76**, 660-5
- Marquez, B., Ignatz, G. and Suarez, S.S.** (2007). Contributions of extracellular and intracellular  $\text{Ca}^{2+}$  to regulation of sperm motility: Release of intracellular stores can hyperactivate CatSper1 and CatSper2 null sperm. *Dev Biol.* **303**, 214-21.



- Marquez, B. and Suarez, S.S.** (2008). Soluble adenylyl cyclase is required for activation of sperm but does not have a direct effect on hyperactivation. *Reprod Fertil Dev.* 20, 247-52
- McPartlin, L.A., Suarez, S.S., Czaya, C.A., Hinrichs, K. and Bedford-Guaus, S.J.** (2009). Hyperactivation of stallion sperm is required for successful in vitro fertilization of equine oocytes. *Biol Reprod.* **81**, 199-206.
- Meizel, S. and Turner, K. O.** (1991). Progesterone acts at the plasma membrane of human sperm. *Mol Cell Endocrinol* **77**, R1-5.
- Meizel, S., Turner, K. O. and Nuccitelli, R.** (1997). Progesterone triggers a wave of increased free calcium during the human sperm acrosome reaction. *Dev Biol* **182**, 67-75.
- Mendoza, C. and Tesarik, J.** (1990). Effect of follicular fluid on sperm movement characteristics. *Fertil Steril* **54**, 1135-9.
- Menge, A. C. and Edwards, R. P.** (1993). Mucosal immunity of the reproductive tract and infertility. in: *Immunology of Reproduction* (ed. R. K. Zaz), pp. 19-36. Boca Raton, FL: CRC Press.
- Menza, M. and Michelangeli, F.** (1996). The effects of inositol 1,4,5-trisphosphate (InsP3) analogues on the transient kinetics of Ca<sup>2+</sup> release from cerebellar microsomes. InsP3 analogues act as partial agonists. *J Biol Chem* **271**, 31818-23
- Merritt, J.E., Armstrong, W.P., Benham, C.D., Hallam, T.J., Jacob, R., Jaxa-Chamiec, A., Leigh, B.K., McCarthy, S.A., Moores, K.E. and Rink, T.J.** (1990). SK&F 96365, a novel inhibitor of receptor-mediated calcium entry. *Biochem J.* **271**, 515-22.
- Michaut, M., Tomez, C. N., De Blas, G., Yunes, R. and Mayorga, L. S.** (2000). Calcium- triggered acrosomal exocytosis in human spermatozoa requires the coordinated activation of Rab3A and N-ethylmaleimide-sensitive factor. *Proc Natl Acad Sci U S A* **97**, 9996-10001.
- Michelangeli, F.** (1991). Measuring calcium uptake and inositol 1,4,5-trisphosphate-induced calcium release in cerebellum microsomes using fluo3. *J Fluorescence* **1**, 203-206
- Michelangeli, F. and Munkonge, F.M.** (1991). Methods of reconstitution of the purified sarcoplasmic reticulum (Ca(2+)-Mg(2+)-ATPase using bile salt detergents to form membranes of defined lipid to protein ratios or sealed vesicles. *Anal Biochem.* **194**, 231-6.
- Michelangeli, F., Ogunbayo, O. A. and Wootton, L. L.** (2005). A plethora of interacting organellar Ca<sup>2+</sup> stores. *Curr Opin Cell Biol* **17**, 135-40.

**Miki, K., Willis, W.D., Brown, P.R., Goulding, E.H., Fulcher, K.D. and Eddy, E.M.** (2002). Targeted disruption of the Akap4 gene causes defects in sperm flagellum and motility. *Dev Biol.* **248**, 331-42.

**Miki, K., Qu, W., Goulding, E. H., Willis, W. D., Bunch, D. O., Strader, L. F., Perreault, S. D., Eddy, E. M. and O'Brien, D. A.** (2004). Glyceraldehyde 3-phosphate dehydrogenase- S, a sperm-specific glycolytic enzyme, is required for sperm motility and male fertility. *Proc Natl Acad Sci U S A* **101**, 16501-6.

**Minelli, A., Allegrucci, C., Rosati, R. and Mezzasoma, I.** (2000). Molecular and binding characteristics of IP3 receptors in bovine spermatozoa. *Mol Reprod Dev* **56**, 527-33.

**Miyado, K., Yamada, G., Yamada, S., Hasuwa, H., Nakamura, Y., Tyu, F., Suzuki, K., Kosai, K., Inoune, K., Ogura, A., Okabe, M. and Mekada, E.** (2000). Requirement of CD9 on the egg plasma membrane for fertilization. *Science* **287**, 321-324.

**Miyado, K., Yoshida, K., Yamagata, K., Sakakibara, K., Okabe, M., Wang, X., Miyamoto, K., Akutsu, H., Kondo, T., Takahashi, Y., Ban, T., Ito, C., Toshimori, K., Nakamura, A., Ito, M., Miyado, M., Mekada, E. and Umezawa, A.** (2008). The fusing ability of sperm is bestowed by CD9-containing vesicles released from eggs in mice. *PNAS* **105**, 12921-12926.

**Morales, P., Overstreet, J. W. and Katz, D. F.** (1988). Changes in human sperm motion during capacitation *in vitro*. *J Reprod Fertil* **83**, 119-28.

**Morales, P., and Llanos, M.** (1996). Interaction of human spermatozoa with the zona pellucida of oocyte: development of the acrosome reaction. *Front Biosci* **1**, d146-60.

**Moreno, R. D., Ramalho-Santos, J., Sutovsky, P., Chan, E. K. and Schatten, G.** (2000). Vesicular traffic and golgi apparatus dynamics during mammalian spermatogenesis: implications for acrosome architecture. *Biol Reprod* **63**, 89-98.

**Morgan, D.J., Weisenhaus, M., Shum, S., Su, T., Zheng, R., Zhang, C., Shokat, K.M., Hille, B., Babcock, D.F. and McKnight, G.S.** (2008). Tissue-specific PKA inhibition using a chemical genetic approach and its application to studies on sperm capacitation. *Proc Natl Acad Sci U S A.* **105**, 20740-5.

**Morita, M., Iguchi, A. and Takemura, A.** (2009). Roles of calmodulin and calcium/calmodulin-dependent protein kinase in flagellar motility regulation in the coral *Acropora digitifera*. *Mar Biotechnol (NY)*. 111, 118-23.

**Mortimer, D., Courtot, A.M., Giovangrandi, Y., Jeulin C. and David, G.** (1984). Human sperm motility after migration into, and incubation in, synthetic media. *Gamete Res* **9**, 131-144.

**Mortimer, D.** (1994). Practical Laboratory Andrology. Oxford, UK: Oxford University Press.

- Mortimer, D.** (1995). Sperm transport in the female reproductive tract. In: *Gametes, the spermatozoon* (ed J.G. Grundzinskas and J.L. Yovich) pp 157-174, Cambridge UK: Cambridge University Press.
- Mortimer, S.T. and Swan, M.A.** (1995). Variable kinematics of capacitating human spermatozoa. *Hum Reprod.* **10**, 3178-82.
- Mortimer, S.T., Schëvæert, D., Swan, M.A. and Mortimer, D.** (1997). Quantitative observations of flagellar motility of capacitating human spermatozoa. *Hum Reprod.* **12**, 1006-12.
- Mortimer, S.T.** (2000). CASA-practical aspects. *J Androl.* **21**, 515-24.
- Mújica, A., Neri-Bazan, L., Tash, J.S. and Uribe, S.** (1994). Mechanism for procaine-mediated hyperactivated motility in guinea pig spermatozoa. *Mol Reprod Dev.* **38**, 285-92.
- Mukai, C. and Okuno, M.** (2004). Glycolysis plays a major role for adenosine triphosphate supplementation in mouse sperm flagellar movement. *Biol Reprod.* **71**, 540-7.
- Muñoz-Garay, C., De la Vega-Beltrán, J.L., Delgado, R., Labarca, P., Felix, R. and Darszon, A.** (2001). Inwardly rectifying K(+) channels in spermatogenic cells: functional expression and implication in sperm capacitation. *Dev Biol.* **234**, 261-74.
- Naaby-Hansen, S., Wolkowicz, M. J., Klotz, K., Bush, L. A., Westbrook, V. A., Shibahara, H., Shetty, J., Coonrod, S. A., Reddi, P. P., Shannon, J. et al.** (2001). Co- localization of the inositol 1,4,5-trisphosphate receptor and calreticulin in the equatorial segment and in membrane bounded vesicles in the cytoplasmic droplet of human spermatozoa. *Mol Hum Reprod* **7**, 923-33.
- Nagae, T., Yanagimachi, R., Srivastava, P. N. and Yanagimachi, H.** (1986). Acrosome reaction in human spermatozoa. *Fertil Steril* **45**, 701-7.
- Nakano, I., Kobayashi, T., Yoshimura, M. and Shingyoji, C.** (2003). Central-pair-linked regulation of microtubule sliding by calcium in flagellar axonemes. *J Cell Sci.* **116**, 1627-36.
- Narisawa, S., Hecht, N.B., Goldberg, E., Boatright, K.M., Reed, J.C. and Millán, J.L.** (2002) Testis-specific cytochrome c-null mice produce functional sperm but undergo early testicular atrophy. *Mol Cell Biol.* **15**:5554-62.
- Navarro, B., Kirichok, Y. and Clapham, D.E.** (2007). KSper, a pH-sensitive K<sup>+</sup> current that controls sperm membrane potential. *PNAS* **104**, 7688-92.
- Navarro, B., Kirichok, Y., Chung, J.J. and Clapham, D.E.** (2008) Ion channels that control fertility in mammalian spermatozoa. *Int J Develop Biol* **52**,607-613.

- Naz, R. K. and Rajesh, P. B.** (2004). Role of tyrosine phosphorylation in sperm capacitation/ acrosome reaction. *Reprod Biol Endocrinol* **2**, 75.
- Neill A.T. and Vacquier, V.D.** (2004). Ligands and receptors mediating signal transduction in sea urchin spermatozoa. *Reproduction*.**127**,141-9.
- Neri-Vidaurre Pdel, C., Torres-Flores, V. and Gonzalez-Martinez, M.T.** (2006). A remarkable increase in the pH<sub>i</sub> sensitivity of voltage-dependent calcium channels occurs in human sperm incubated in capacitating conditions. *Biochem Biophys Res Commun* **343**, 105-9.
- Nichols, C.G. and Lopatin, A.N.** (1997). Inward rectifier potassium channels. *Annu Rev Physiol*. **59**, 171-91.
- Nicholls, D.G. and Chalmers, S** (2004). The integration of mitochondrial calcium transport and storage. *J Bioenerg Biomembr* **36**, 277-81.
- Nikpoor, P., Mowla, S. J., Movahedin, M., Ziaee, S. A. and Tiraihi, T.** (2004). CatSper gene expression in postnatal development of mouse testis and in subfertile men with deficient sperm motility. *Hum Reprod* **19**, 124-8.
- Nolan, M.A., Babcock, D.F., Wennemuth, G., Brown, W., Burton, K.A. and McKnight, G.S.** (2004). Sperm-specific protein kinase A catalytic subunit Calpha2 orchestrates cAMP signaling for male fertility. *PNAS* **101**, 13483-8.
- Nomura M, Yoshida M, Morisawa M.** (2004). Calmodulin/calmodulin-dependent protein kinase II mediates SAAF-induced motility activation of ascidian sperm. *Cell Motil Cytoskeleton*, **59**, 28-37.
- Ogunbayo, O.A., Lai, P.F., Connolly, T.J. and Michelangeli, F.** (2008). Tetrabromobisphenol A (TBBPA), induces cell death in TM4 Sertoli cells by modulating Ca<sup>2+</sup> transport proteins and causing dysregulation of Ca<sup>2+</sup> homeostasis. *Toxicol In Vitro*. **22**, 943-52.
- Ohmuro, J. and Ishijima, S.** (2006). Hyperactivation is the mode conversion from constant-curvature beating to constant-frequency beating under a constant rate of microtubule sliding. *Mol Reprod Dev*. **73**,1412-21.
- Okunade, G.W., Miller, M.L., Pyne, G.J., Sutliff, R.L., O'Connor, K.T., Neumann, J.C., Andringa, A., Miller, D.A., Prasad, V., Doetschman, T., Paul, R.J. and Schull, G.E.** (2004). Targeted ablation of plasma membrane Ca<sup>2+</sup>-ATPase (PMCA) 1 and 4 indicate a major housekeeping function for PMCA1 and a critical role in hyperactivated sperm motility and male fertility for PMCA4. *J Biol Chem* **279**, 33742-50.
- Olson, S.D., Suarez, S.S. and Fauci, L.J.** (2010). A Model of CatSper Channel Mediated Calcium Dynamics in Mammalian Spermatozoa. *Bull Math Biol*. Feb 19. [Epub ahead of print]
- Osman, R. A., Andria, M. L., Jones, A. D. and Meizel, S.** (1989). Steroid induced exocytosis: the

human sperm acrosome reaction. *Biochem Biophys Res Commun* **160**, 828-33.

**O'Toole, C. M., Arnoult, C., Darszon, A., Steinhardt, R. A. and Florman, H. M. (2000).** Ca(2+) entry through store-operated channels in mouse sperm is initiated by egg ZP3 and drives the acrosome reaction. *Mol Biol Cell* **11**, 1571-84.

**Overstreet, J.W. and Cooper, G.W. (1979).** Effect of ovulation and sperm motility on the migration of rabbit spermatozoa to the site of fertilization. *J Reprod Fertil.* **55**, 53-9.

**Overstreet, J.W., Katz, D.F. and Johnson, L.L. (1980).** Motility of rabbit spermatozoa in the secretions of the oviduct. *Biol Reprod.* **22**, 1083-8.

**Pacey, A.A., Davies, N., Warren, W.A., Barratt, C.L. and Cooke, I.D. (1995a).** Hyperactivation may assist human spermatozoa to detach from intimate association with the endosalpinx. *Hum Reprod* **10**, 2603-2609.

**Pacey, A.A., Hill, C.J. Scudamore, I.W., Warren, W.A., Barratt, C.L. and Cooke, I.D. (1995b).** The interaction in vitro of human spermatozoa with epithelial cells from the human uterine (fallopian) tube. *Hum Reprod* **10**, 360-366.

**Palade, P., Dettbarn, C., Alderson, B. and Volpe, P. (1989).** Pharmacologic differentiation between inositol-1,4,5-trisphosphate-induced Ca2+ release and Ca2+-or caffeine-induced Ca2+ release from intracellular membrane systems. *Mol Pharmacol* **36**, 673-80

**Parekh, A.B. (2003).** Mitochondrial regulation of intracellular Ca2+ signaling: more than just simple Ca2+ buffers. *News Physiol Sci.* **18**, 252-6.

**Parekh, A.B. and Putney, J.W. Jr. (2005)** Store-operated calcium channels. *Physiol Reviews* **85**, 757-810.

**Park, J. Y., Ahn, H. J., Gu, J. G., Lee, K. H., Kim, J. S., Kang, H. W. and Lee, J. H. (2003).** Molecular identification of Ca2+ channels in human sperm. *Exp Mol Med* **35**, 285-92.

**Parmentier, M., Libert, F., Schurmans, S., Schiffmann, S., Lefort, A., Eggerickx, D., Ledent, C., Mollereau, C., Gerard, C., Perret, J. et al. (1992).** Expression of members of the putative olfactory receptor gene family in mammalian germ cells. *Nature* **355**, 453-5.

**Parrish, J.J., Susko-Parrish, J.L. and First, N.L. (1989).** Capacitation of bovine sperm by heparin: inhibitory effect of glucose and role of intracellular pH. *Biol Reprod* **41**, 683-99.

**Patrat, C., Serres, C. and Jouannet, P. (2000).** The acrosome reaction in human spermatozoa. *Biol Cell* **92**, 255-66.

**Peinelt, C., Lis, A., Beck, A., Fleig, A. and Penner, R.** (2008). 2-Aminoethoxydiphenyl borate directly facilitates and indirectly inhibits STIM1-dependent gating of CRAC channels. *J Physiol.* **586**, 3061-73.

**Pennisi, E.** (2010). Evolution. Male rivalry extends to sperm in female reproductive tract. *Science.* **327**, 1443.

**Pietrobon, E. O., Soria, M., Dominguez, L. A., Monclus Mde, L. and Fornes, M. W.** (2005). Simultaneous activation of PLA2 and PLC are required to promote acrosomal reaction stimulated by progesterone via G-proteins. *Mol Reprod Dev* **70**, 58-63.

**Plant, A., McLaughlin, E. A. and Ford, W. C.** (1995). Intracellular calcium measurements in individual human sperm demonstrate that the majority can respond to progesterone. *Fertil Steril* **64**, 1213-5.

**Polakoski, K. L., Syner, F. N. and Zaneveld, L. J. D.** (1976). Biochemistry of human seminal plasma. in: *Human Semen and Fertility Regulation in Men* (ed. E. S. E. Hafez), pp. 133-43. St. Louis, Mo: CV Mosby Company.

**Pollard, J.W., Plante, C., King, W.A., Hansen, P.J., Betteridge, K.J. and Suarez, S.S.** (1991). Fertilizing capacity of bovine sperm may be maintained by binding of oviductal epithelial cells. *Biol Reprod.* **44**, 102-7.

**Porter, M. E. and Johnson, K. A.** (1989). Dynein structure and function. *Annu Rev Cell Biol* **5**, 119-51.

**Primakoff, P. and Myles, D.G.** (2000). The ADAM gene family-surface proteins with adhesion and protease activity. *Trends Genet* **16**, 83-87.

**Primakoff, P. and Myles, D.G.** (2002). Penetration, adhesion and fusion in mammalian sperm-egg interaction. *Science* **296**, 2183-5.

**Prakriya, M. and Lewis, R.S.** (2001). Potentiation and inhibition of Ca(2+) release-activated Ca(2+) channels by 2-aminoethyldiphenyl borate (2-APB) occurs independently of IP(3) receptors. *J Physiol.* **536**, 3-19.

**Prakriya, M., Feske, S., Gwack, Y., Srikanth, Rao, R. and Hogan, P.G.** (2006). Orai1 is an essential pore subunit of the CRAC channel. *Nature* **443**, 230-3.

**Publicover, S., Harper, C.V. and Barratt, C.** (2007). [Ca(2+)](i) signalling in sperm - making the most of what you've got. *Nature Cell Biology* **9**, 235-242,

**Publicover, S.J., Giojalas, L.C., Teves, M.E., de Oliveira, G.S., Garcia, A.A., Barratt, C.L. and Harper, C.V.** (2008). Ca2+ signalling in the control of motility and guidance in mammalian sperm. *Front Biosci.* **13**, 5623-37.

**Putney, J. W., Jr.** (1990). Receptor-regulated calcium entry. *Pharmacol Ther* **48**, 427-34.

- Qi, H., Moran, M.M., Navarro, B., Chong, J.A., Krapivinsky, G., Krapivinsky, Y., Ramsey, I.S., Quill, T.A. and Clapham, D.E.** (2007). All four CatSper ion channel proteins are required for male fertility and sperm cell hyperactivated motility. *PNAS* **104**, 1219-23.
- Quill, T. A., Ren, D., Clapham, D. E. and Garbers, D. L.** (2001). A voltage-gated ion channel expressed specifically in spermatozoa. *Proc Natl Acad Sci U S A* **98**, 12527-31.
- Quill, T. A., Sugden, S. A., Rossi, K. L., Doolittle, L. K., Hammer, R. E. and Garbers, D. L.** (2003). Hyperactivated sperm motility driven by CatSper2 is required for fertilization. *Proc Natl Acad Sci U S A* **100**, 14869-74.
- Quill, T.A., Wang, D. and Garbers, D.L.** (2006). Insights into sperm cell motility signaling through sNHE and the CatSpers. *Mol Cell Endocrinol.* **250**, 84-92.
- Rai, S.S. and Kasturi, S.R.** (1994). Interaction of TNP-ATP with tubulin: a fluorescence spectroscopic study. *Biophysical Chemistry* **48**, 359-368.
- Ren, D., Navarro, B., Perez, G., Jackson, A. C., Hsu, S., Shi, Q., Tilly, J. L. and Clapham, D. E.** (2001). A sperm ion channel required for sperm motility and male fertility. *Nature* **413**, 603-9.
- Roldan, E. R. and Harrison, R.A.** (1993). Diacylglycerol in the exocytosis of the mammalian sperm acrosome. *Biochem Soc Trans* **21**, 284-9.
- Roldan, E. R., Murase, T. and Shi, Q. X.** (1994). Exocytosis in spermatozoa in response to progesterone and zona pellucida. *Science* **266**, 1578-81.
- Roldan, E.R. and Fraser, L.R.** (1998). Protein Kinase C and Exocytosis in Mammalian Spermatozoa. *Trends Endocrinol Metab.* **9**, 296-297.
- Roos, J., DiGregorio, P.J., Yeromin, A.V., Ohlsen, K., Lioduno, M., Zhang, S., Safrina, O., Kozak, J.A., Wagner, S.L., Cahalan, M.D., Velicelebi, G. and Stauderman, K.A.** (2005). STIM1, an essential an conserved component of store-operated Ca<sup>2+</sup> channel function. *J Cell Biol* **169**, 435-45.
- Rossato, M., Di Virgilio, F., Rizzuto, R., Galeazzi, C. and Foresta, C.** (2001). Intracellular calcium store depletion and acrosome reaction in human spermatozoa: role of calcium and plasma membrane potential. *Mol Hum Reprod.* **7**, 119-28.
- Sakata, Y., Saegusa, H., Zong, S., Osanai, M., Murakoshi, T., Shimizu, Y., Noda, T., Aso, T. and Tanabe, T.** (2002). Ca(v)2.3 (alpha1E) Ca<sup>2+</sup> channel participates in the control of sperm function. *FEBS Lett* **516**, 229-33.

**Sale, W.S.** (1986). The axonemal axis and  $\text{Ca}^{2+}$ -induced asymmetry of active microtubule sliding in sea urchin sperm tails. *J Cell Biol.* **102**, 2042-52.

**Salvioli, S., Barbi, C., Dobrucki, J., Moretti, L., Pinti, M., Pedrazzi, J., Pazienza, T.L., Bobyleva, V., Franceschi, C. and Cossarizza, A.** (2000). Opposite role of changes in mitochondrial membrane potential in different apoptotic processes. *FEBS Lett.* **469**, 186-90.

**San Agustin, J. T. and Witman, G. B.** (1994). Role of cAMP in the reactivation of demembranated ram spermatozoa. *Cell Motil Cytoskeleton* **27**, 206-18.

**Sandoval, A., Triviños, F., Sanhueza, A., Carretta, D., Hidalgo, M.A., Hancke, J.L. and Burgos, R.A.** (2007). Propionate induces pH(i) changes through calcium flux, ERK1/2, p38, and PKC in bovine neutrophils. *Vet Immunol Immunopathol.* **115**, 286-98.

**Santi, C.M., Martínez-López, P., de la Vega-Beltrán, J.L., Butler, A., Alisio, A., Darszon, A. and Salkoff, L.** (2010). The SLO3 sperm-specific potassium channel plays a vital role in male fertility. *FEBS Lett.* **584**, 1041-6.

**Satir, P.** (1968). Studies on cilia. 3. Further studies on the cilium tip and a "sliding filament" model of ciliary motility. *J Cell Biol* **39**, 77-94.

**Sato, Y., Son, J.H., Tucker, R.P. and Meizel, S.** (2000). The zona pellucida: initiated acrosome reaction: defect due to mutations in the sperm glycine receptor /Cl(-) channel. *Dev Biol* **227**, 211-8.

**Schlingmann, K., Michaut, M.A, McElwee. J.L., Wolff, C.A., Travis, A.J. and Turner, R.M.** (2007). Calmodulin and CaMKII in the sperm principal piece: evidence for a motility-related calcium/calmodulin pathway. *J Androl.* **706-16**.

**Schmidt, M., Evellin, S., Weernink, P.A., von Dorp, F., Rehmann, H., Lomasney, J.W. and Jakobs, K.H.** (2001). A new phospholipase-C-calcium signalling pathway mediated by cyclic AMP and a Rap GTPase. *Nat Cell Biol.* **3**(11):1020-4.

**Schreiber, M., Wei, A., Yuan, A., Gaut, J., Saito, M. and Salkoff, L.** (1998). Slo3, a novel pH-sensitive  $\text{K}^{+}$  channel from mammalian spermatocytes. *J Biol Chem.* **273**, 3509-16.

**Schuh, K., Cartwright, E.J., Jankevics, E., Bundschu, K., Liebermann, J., Williams, J.C., Armesilla, A.L., Emerson, M, Oceandy, D., Knobloch, K.P. and Neyes, L.** (2004). Plasma membrane  $\text{Ca}^{2+}$ -ATPase 4 is required for sperm motility and male fertility. *J Biol Chem* **279**, 28220-6.

**Schuffner, A.A., Bastiaan, H.S., Duran, H.E., Lin, Z.Y., Morshedi, M., Franken, D.R. and Oehninger, S.** (2002). Zona pellucida-induced acrosome reaction in human sperm dependency on activation of pertussis toxin-sensitive G(i) protein and extracellular calcium, and priming effect of progesterone and follicular fluid. *Mol*



*Hum Reprod* **8**, 722-7.

**Schulz, J. R., Wessel, G. M. and Vacquier, V. D.** (1997). The exocytosis regulatory proteins syntaxin and VAMP are shed from sea urchin sperm during the acrosome reaction. *Dev Biol* **191**, 80-7.

**Scott, J. D., Dell'Acqua, M. L., Fraser, I. D., Tavalin, S. J. and Lester, L. B.** (2000). Coordination of cAMP signaling events through PKA anchoring. *Adv Pharmacol* **47**, 175-207.

**Setchell, B.P.** (2008). Blood-testis barrier, junctional and transport proteins and spermatogenesis. *Adv Exp Biol Med*, **636**, 212-33

**Shi, Q. X. and Roldan, E. R.** (1995). Evidence that a GABAA-like receptor is involved in progesterone-induced acrosomal exocytosis in mouse spermatozoa. *Biol Reprod* **52**, 373-81.

**Shiba, K., Baba, S.A., Inoue, T. and Yoshida, M.** (2008). Ca<sup>2+</sup> bursts occur around a local minimal concentration of attractant and trigger sperm chemotactic response. *Proc Natl Acad Sci U S A*. **105**, 19312-7.

**Shur, B.D., Rodeheffer, C., Ensslin, M.A., Lyng, R. and Raymond, A.** (2006). Identification of novel gametes that mediate sperm adhesion to the egg coat. *Mol Cell Endocrinol* **250**, 137-148.

**Shur, B.D.** (2008). Reassessing the role of protein-carbohydrate complementarity during sperm-egg interactions in the mouse. *Int J Dev Biol* **52**, 7033-715.

**Sinclair, M.L., Wang, X.Y., Mattia, M., Conti, M., Buck, J., Wolgemuth, D.J. and Levin, L.R.** (2000). Specific expression of soluble adenylyl cyclase in male germ cells. *Mol Reprod Dev*. **56**, 6-11.

**Shingyoji, C., Murakami, A. and Takahashi, K.** (1977). Local reactivation of Triton- extracted flagella by iontophoretic application of ATP. *Nature* **265**, 269-70.

**Si, Y. and Okuno, M.** (1999). Role of tyrosine phosphorylation of flagellar proteins in hamster sperm hyperactivation. *Biol Reprod* **61**, 240-6.

**Si, Y. and Olds-Clarke, P.** (2000). Evidence for the involvement of calmodulin in mouse sperm capacitation. *Biol Reprod* **62**, 1231-9.

**Skalhegg, B. S., Huang, Y., Su, T., Idzerda, R. L., McKnight, G. S. and Burton, K. A.** (2002). Mutation of the Calpha subunit of PKA leads to growth retardation and sperm dysfunction. *Mol Endocrinol* **16**, 630-9.

**Smith, K.J., Felts, P.A. and John, G.R.** (2000). Effects of 4-aminopyridine on demyelinated axons, synapses and muscle tension. *Brain*. **123** ( Pt 1), 171-84.

**Smith, E.F.** (2002). Regulation of flagellar dynein by calcium and a role for an axonemal calmodulin and calmodulin-dependent kinase. *Mol Biol Cell*. **13**, 3303-13.

**Smith, D.J., Gaffney, E.A., Gadêlha, H., Kapur, N. and Kirkman-Brown, J.C.** (2009). Bend propagation in the flagella of migrating human sperm, and its modulation by viscosity. *Cell Motil Cytoskeleton*. **66**, 220-36.

**Snitsarev, V.A., McNulty, T.J., and Taylor, C.W.** (1996). Endogenous heavy metal ions perturb fura-2 measurements of basal and hormone-evoked Ca<sup>2+</sup> signals. *Biophys J*. **71**, 1048-56.

**Spehr, M., Gisselmann, G., Poplawski, A., Riffell, J. A., Wetzel, C. H., Zimmer, R. K. and Hatt, H.** (2003). Identification of a testicular odorant receptor mediating human sperm chemotaxis. *Science* **299**, 2054-8.

**Spehr, M., Schwane, K., Riffell, J. A., Barbour, J., Zimmer, R. K., Neuhaus, E. M. and Hatt, H.** (2004). Particulate adenylate cyclase plays a key role in human sperm olfactory receptor-mediated chemotaxis. *J Biol Chem* **279**, 40194-203.

**Stauss, C. R., Votta, T. J. and Suarez, S. S.** (1995). Sperm motility hyperactivation facilitates penetration of the hamster zona pellucida. *Biol Reprod* **53**, 1280-5.

**Steck, E.A, and Ewing, G.W.** (1948). Absorption spectra of heterocyclic compounds; amino-derivatives of pyridine, quinoline and isoquinoline. *J Am Chem Soc*. **70**, 3397-3406.

**Stephens, G.J., Garratt, J.C., Robertson, B. and Owen, D.G.** (1994). On the mechanism of 4-aminopyridine action on the cloned mouse brain potassium channel mKv1.1. *J. Physiol*. **477**, 187-96.

**Storey, B. T. and Kayne, F. J.** (1975). Energy metabolism of spermatozoa. V. The Embden- Myerhof pathway of glycolysis: activities of pathway enzymes in hypotonically treated rabbit epididymal spermatozoa. *Fertil Steril* **26**, 1257-65.

**Strange, K., Yan, X., Lorin-Nebel, C. and Xing, J.** (2007). Physiological roles of STIM1 and Orai1 homologs and CRAC channels in the genetic model organism *Caenorhabditis elegans*. *Cell Calcium* **42**, 193-203.

**Strünker, T., Weyand, I., Bönigk, W., Van, Q., Loogen, A., Brown, J.E., Kashikar, N., Hagen, V., Krause, E. and Kaupp, U.B.** (2006). A K<sup>+</sup>-selective cGMP-gated ion channel controls chemosensation of sperm. *Nat Cell Biol*. **8**, 1149-54.

**Suarez, S. S., Vincenti, L. and Ceglia, M. W.** (1987). Hyperactivated motility induced in mouse sperm by calcium ionophore A23187 is reversible. *J Exp Zool* **244**, 331-6.

**Suarez, S. S. and Osman, R. A.** (1987). Initiation of hyperactivated flagellar bending in mouse sperm within

the female reproductive tract. *Biol Reprod* **36**, 1191-8.

**Suarez, S. S., Katz, D. F., Owen, D. H., Andrew, J. B. and Powell, R. L.** (1991). Evidence for the function of hyperactivated motility in sperm. *Biol Reprod* **44**, 375-81.

**Suarez, S. S. and Dai, X.** (1992). Hyperactivation enhances mouse sperm capacity for penetrating viscoelastic media. *Biol Reprod* **46**, 686-91.

**Suarez, S.S., Varosi, S.M. and Dai, X.** (1993). Intracellular calcium increases with hyperactivation in intact, moving hamster sperm and oscillates with the flagellar beat cycle. *Proc Natl Acad Sci U S A.* **90**, 4660-4.

**Suarez, S.S.** (2002a). Formation of a reservoir of sperm in the oviduct. *Reprod Domest Anim.* **37**, 140-3.

**Suarez, S. S.** (2002b). Gamete transport. in: *Fertilization* (ed. D. M. Hardy), pp. 3-28. San Diego: Academic Press.

**Suarez, S.S. and Ho, H.C.** (2003a). Hyperactivation of mammalian sperm. *Cell Mol Biol (Noisy-le-grand).* **49**, 351-6.

**Suarez, S.S. and Ho, H.C.** (2003b). Hyperactivated motility in sperm. *Reprod Domest Anim.* **38**, 119-24.

**Suarez, S. S. and Pacey, A. A.** (2006). Sperm transport in the female reproductive tract. *Hum Reprod Update* **12**, 23-37.

**Suarez, S.S.** (2007). Interactions of spermatozoa with the female reproductive tract: inspiration for assisted reproduction. *Reprod Fertil Dev.* **19**, 103-10.

**Suarez, S.S., Marquez, B., Harris, T.P. and Schimenti, J.C.** (2007). Different regulatory systems operate in the midpiece and principal piece of the mammalian sperm flagellum. *Soc Reprod Fertil Suppl.* **65**, 331-4.

**Suarez, S. S.** (2008a). Control of hyperactivation in sperm. *Hum Reprod Update* **14**, 647-57.

**Suarez, S.S.** (2008b). Regulation of sperm storage and movement in the mammalian oviduct. *Int J Dev Biol.* **52**, 455-62.

**Summers, K. E. and Gibbons, I. R.** (1971). Adenosine triphosphate-induced sliding of tubules in trypsin-treated flagella of sea-urchin sperm. *Proc Natl Acad Sci U S A* **68**, 3092-6.

**Sun, F., Bahat, A., Gakamsky, A., Girsh, E., Katz, N., Giojalas, L. C., Tur-Kaspa, I. and Eisenbach, M.** (2005). Human sperm chemotaxis: both the oocyte and its surrounding cumulus cells secrete sperm chemoattractants. *Hum Reprod* **20**, 761-7.

- Sutovsky, P. and Manandhar, G.** (2006). Mammalian spermatogenesis and sperm structure: anatomical and compartmental analysis. in *The Sperm Cell: Production, Maturation, Fertilization and Regeneration* (ed. C. de Jonge and C. Barratt), pp. 1-30. Cambridge, UK: Cambridge University Press.
- Swann, K. and Lai, F.A.** (2002). PLC zeta: a sperm-specific trigger of  $\text{Ca}^{2+}$  oscillations in eggs and embryo development. *Development* **129**, 3533-44.
- Swann, K., Larman, M.G., Saunders, C.M. and Lai, F.A.** (2004). The cytosolic sperm factor that triggers  $\text{Ca}^{2+}$  oscillations and egg activation in mammals is a novel phospholipase C: PLCzeta. *Reproduction*. **127**, 431-9.
- Swann, K., Saunders, C.M., Rogers, N.T. and Lai, F.A.** (2006). PLC zeta(zeta): a sperm protein that triggers  $\text{Ca}^{2+}$  oscillations and egg activation in mammals. *Semin Cell Dev Biol* **17**, 264-73.
- Swann, K. and Yu, Y.** (2008). The dynamics of calcium oscillations that activate mammalian eggs. *Int J Dev Biol* **52**, 585-594.
- Tang, Q.Y., Zhang, Z., Xia, X.M. and Lingle, C.J.** (2010). Block of mouse Slo1 and Slo3  $\text{K}^{+}$  channels by CTX, IbTX, TEA, 4-AP and quinidine. *Channels (Austin)*. **4**, 22-41.
- Tanghe, S., Van Soom, A., Nauwynch, N., Coryn, M. and deKruif, A.** (2002). Minireview: Functions of the cumulus oophorus during oocyte maturation, ovulation and fertilization. *Mol Reprod Dev.* **61**, 414-24.
- Tash, J. S. and Means, A. R.** (1982). Regulation of protein phosphorylation and motility of sperm by cyclic adenosine monophosphate and calcium. *Biol Reprod* **26**, 745-63.
- Tash, J. S. and Means, A. R.** (1983). Cyclic adenosine 3',5' monophosphate, calcium and protein phosphorylation in flagellar motility. *Biol Reprod* **28**, 75-104.
- Tash, J. S. and Means, A. R.** (1987).  $\text{Ca}^{2+}$  regulation of sperm axonemal motility. *Methods Enzymol* **139**, 808-23.
- Tash, J. S., Krinks, M., Patel, J., Means, R. L., Klee, C. B. and Means, A. R.** (1988). Identification, characterization, and functional correlation of calmodulin-dependent protein phosphatase in sperm. *J Cell Biol* **106**, 1625-33.
- Tash, J. S. and Bracho, G. E.** (1998). Identification of phosphoproteins coupled to initiation of motility in live epididymal mouse sperm. *Biochem Biophys Res Commun* **251**, 557-63.
- Tash, J. S.** (1989). Protein phosphorylation: the second messenger signal transducer of flagellar motility. *Cell Motil Cytoskeleton* **14**, 332-9.

**Taylor, C.W., Rahman, T., Tovey, S.C., Dedos, S.G., Taylor, E.J. and Velamakanni, S.** (2009). IP3 receptors: some lessons from DT40 cells. *Immunol Rev.* **231**, 23-44.

**Tesarik, J., Pilka, L., Drahorad, J., Cechova, D. and Veselsky, L.** (1988). The role of cumulus cell-secreted proteins in the development of human sperm fertilizing ability: implication in IVF. *Hum Reprod* **3**, 129-32.

**Tesarik, J., Mendoza Oltras, C. and Testart, J.** (1990). Effect of the human cumulus oophorus on movement characteristics of human capacitated spermatozoa. *J Reprod Fertil* **88**, 65-75.

**Tesarik, J., Carreras, A. and Mendoza, C.** (1993). Differential sensitivity of progesterone and zona pellucida-induced acrosome reaction to pertussis toxin. *Mol Reprod Dev* **34**, 183-189.

**Teves, M. E., Barbano, F., Guidobaldi, H. A., Sanchez, R., Miska, W. and Giojalas, L. C.** (2006). Progesterone at the picomolar range is a chemoattractant for mammalian spermatozoa. *Fertil Steril* **86**, 745-9.

**Teves, M. E., Guidobaldi, H. A., Unates, D.R., Sanchez, R., Miska, W., Publicover, S.J., Morales Garcia, A.A. and Giojalas, L. C.** (2009). Molecular mechanism for human sperm chemotaxis mediated by progesterone. *Plos One* **8**, e8211.

**Thomas, P. and Meizel, S.** (1989). Phosphatidylinositol 4,5-bisphosphate hydrolysis in human sperm stimulated with follicular fluid or progesterone is dependent upon Ca<sup>2+</sup> influx. *Biochem J* **264**, 539-46.

**Tomes, C. N., Michaut, M., De Blas, G., Visconti, P., Matti, U. and Mayorga, L. S.** (2002). SNARE complex assembly is required for human sperm acrosome reaction. *Dev Biol* **243**, 326-38.

**Tomes, C. N., Roggero, C. M., De Blas, G., Saling, P. M. and Mayorga, L. S.** (2004). Requirement of protein tyrosine kinase and phosphatase activities for human sperm exocytosis. *Dev Biol* **265**, 399-415.

**Torres-Flores, V., García-Sánchez, N.L. and González-Martínez, M.T.** (2008). Intracellular sodium increase induced by external calcium removal in human sperm. *J Androl.* **29**, 63-9.

**Tovey, S.C., Longland, C.L., Mezna, M. and Michelangeli, F.** (1998). 2-Hydroxycarbazole induces Ca<sup>2+</sup> release from sarcoplasmic reticulum by activating the ryanodine receptor. *Eur J Pharmacol.* **354**(2-3), 245-51.

**Trevino, C. L., Santi, C. M., Beltran, C., Hernandez-Cruz, A., Darszon, A. and Lomeli, H.** (1998). Localisation of inositol trisphosphate and ryanodine receptors during mouse spermatogenesis: possible

functional implications. *Zygote* **6**, 159-72.

**Trevino, C. L., Serrano, C. J., Beltran, C., Felix, R. and Darszon, A.** (2001). Identification of mouse trp homologs and lipid rafts from spermatogenic cells and sperm. *FEBS Lett* **509**, 119-25.

**Trevino, C. L., Felix, R., Castellano, L. E., Gutierrez, C., Rodriguez, D., Pacheco, J., Lopez-Gonzalez, I., Gomora, J. C., Tsutsumi, V., Hernandez-Cruz, A. et al.** (2004). Expression and differential cell distribution of low-threshold Ca(2+) channels in mammalian male germ cells and sperm. *FEBS Lett* **563**, 87-92.

**Turner, R.M.** (2003). Tales from the tail: what do we really know about sperm motility? *J Androl.* **24**, 790-803.

**Turner, R. M.** (2006). Moving to the beat: a review of mammalian sperm motility regulation. *Reprod Fertil Dev* **18**, 25-38.

**Uhler, M. L., Leung, A., Chan, S. Y. and Wang, C.** (1992). Direct effects of progesterone and antiprogesterone on human sperm hyperactivated motility and acrosome reaction. *Fertil Steril* **58**, 1191-8.

**Vaca, L.** (2010). SOCIC: the store-operated calcium complex. *Cell Calcium* **47**, 199-209.

**Vannier, B., Peyton, M., Boulay, G., Brown, D., Qin, N., Jiang, M., Zhu, X. and Birnbaumer, L.** (1999). Mouse trp2, the homologue of the human trpc2 pseudogene, encodes mTrp2, a store depletion-activated capacitative Ca<sup>2+</sup> entry channel. *Proc Natl Acad Sci U S A* **96**, 2060-4.

**Várnai, P., Hunyady, L. and Balla, T.** (2009). STIM and Orai: the long-awaited constituents of store-operated calcium entry. *Trends Pharmacol Sci.* **30**, 118-28.

**Vijayaraghavan, S., Trautman, K. D., Goueli, S. A. and Carr, D. W.** (1997). A tyrosine- phosphorylated 55-kilodalton motility-associated bovine sperm protein is regulated by cyclic adenosine 3',5'-monophosphates and calcium. *Biol Reprod* **56**, 1450-7.

**Visconti, P. E., Moore, G. D., Bailey, J. L., Leclerc, P., Connors, S. A., Pan, D., Olds- Clarke, P. and Kopf, G. S.** (1995). Capacitation of mouse spermatozoa. II. Protein tyrosine phosphorylation and capacitation are regulated by a cAMP-dependent pathway. *Development* **121**, 1139-50.

**Visconti, P. E. and Kopf, G. S.** (1998). Regulation of protein phosphorylation during sperm capacitation. *Biol Reprod* **59**, 1-6.

**Visconti, P. E., Galantino-Homer, H., Moore, G. D., Bailey, J. L., Ning, X., Fornes, M. and Kopf, G. S.** (1998). The molecular basis of sperm capacitation. *J Androl* **19**, 242-8.

**Visconti, P. E., Westbrook, V. A., Chertihin, O., Demarco, I., Sleight, S. and Diekman, A. B.** (2002).

Novel signaling pathways involved in sperm acquisition of fertilizing capacity. *J Reprod Immunol* **53**, 133-50.

**Visconti, P.** (2009). Understanding the molecular basis of sperm capacitation through kinase design. *Pro Natl Acad Sci USA* **106**, 667-8

**Walensky, L. D. and Snyder, S. H.** (1995). Inositol 1,4,5-trisphosphate receptors selectively localized to the acrosomes of mammalian sperm. *J Cell Biol* **130**, 857-69.

**Wang, D., King, S.M., Quill, T.A., Doolittle, L.K. and Garbers, D.L.** (2003). A new sperm-specific Na<sup>+</sup>/H<sup>+</sup> exchanger required for sperm motility and fertility. *Nat Cell Biol.* **5**, 1117-22.

**Wang, D., Hu, J., Bobulescu, I.A., Quill, T.A., McLeroy, P., Moe, O.W. and Garbers, D.L.** (2007). A sperm-specific Na<sup>+</sup>/H<sup>+</sup> exchanger (sNHE) is critical for expression and in vivo bicarbonate regulation of the soluble adenylyl cyclase (sAC). *PNAS* **104**, 9325-30.

**Ward, C. R., Storey, B. T. and Kopf, G. S.** (1994). Selective activation of Gi1 and Gi2 in mouse sperm by the zona pellucida, the egg's extracellular matrix. *J Biol Chem* **269**, 13254-8.

**Wassarman, P. M., Florman, H. M.** (1997). Cellular mechanisms during mammalian fertilization. Handbook of physiology: Section 14- Cell Physiology 885-938. Oxford University Press, New York.

**Wassarman, P. M.** (1999). Mammalian fertilization: molecular aspects of gamete adhesion, exocytosis, and fusion. *Cell* **96**, 175-83.

**Wassarman, P. M., Jovine, L. and Litscher, E. S.** (2001). A profile of fertilization in mammals. *Nat Cell Biol* **3**, E59-64.

**Wassarman, P. M., Jovine, L., Litscher, E.S., Qi, H. and Williams Z.** (2004). Egg-sperm interactions at fertilization in mammals. *Eur J Obstet Gynecol Reprod Biol* **115** Suppl, S57-60.

**Wassarman, P. M.** (2009). Mammalian fertilization: the strange case of sperm protein 56. *Bioessays* **31**, 153-8.

**Wennemuth, G., Westenbroek, R. E., Xu, T., Hille, B. and Babcock, D. F.** (2000). CaV2.2 and CaV2.3 (N- and R-type) Ca<sup>2+</sup> channels in depolarization-evoked entry of Ca<sup>2+</sup> into mouse sperm. *J Biol Chem* **275**, 21210-7.

**Wennemuth, G., Carlson, A.E., Harper, A.J. and Babcock, D.F.** (2003a). Bicarbonate actions on flagellar and Ca<sup>2+</sup> -channel responses: initial events in sperm activation. *Development.* **130**, 1317-26.

**Wennemuth, G., Babcock, D. F. and Hille, B.** (2003b). Calcium clearance mechanisms of mouse sperm. *J*

*Gen Physiol* **122**,115-28.

**Wertheimer, E.V., Salicioni, A.M., Liu, W., Trevino, C.L., Chavez, J., Hernández-González, E.O, Darszon, A. and Visconti, P.E.** (2008). Chloride Is essential for capacitation and for the capacitation-associated increase in tyrosine phosphorylation. *J Biol Chem.* **283**, 35539-50.

**Wes, P. D., Chevesich, J., Jeromin, A., Rosenberg, C., Stetten, G. and Montell, C.** (1995). TRPC1, a human homolog of a Drosophila store-operated channel. *Proc Natl Acad Sci U S A* **92**, 9652-6.

**Westhoff, D. and Kamp, G.** (1997). Glyceraldehyde 3-phosphate dehydrogenase is bound to the fibrous sheath of mammalian spermatozoa. *J Cell Sci* **110 ( Pt 15)**, 1821-9.

**Wiesner, B., Weiner, J., Middendorff, R., Hagen, V., Kaupp, U. B. and Weyand, I.** (1998). Cyclic nucleotide-gated channels on the flagellum control Ca<sup>2+</sup> entry into sperm. *J Cell Biol* **142**, 473-84.

**Williams, K.M. and Ford, W.C.** (2003). Effects of Ca-ATPase inhibitors on the intracellular calcium activity and motility of human spermatozoa. *Int J Androl.* **26**, 366-75.

**Wissenbach, U., Schroth, G., Philipp, S. and Flockerzi, V.** (1998). Structure and mRNA expression of a bovine trp homologue related to mammalian trp2 transcripts. *FEBS Lett* **429**, 61-6.

**Wistrom, C. A. and Meizel, S.** (1993). Evidence suggesting involvement of a unique human sperm steroid receptor/Cl<sup>-</sup> channel complex in the progesterone-initiated acrosome reaction. *Dev Biol* **159**, 679-90.

**Woo, A.L., James, P.F. and Lingrel, J.B.** (2002). Roles of the Na,K-ATPase alpha4 isoform and the Na<sup>+</sup>/H<sup>+</sup> exchanger in sperm motility. *Mol Reprod Dev.* **62**, 348-56.

**World Health Organization (WHO)** (1999). *WHO Laboratory Manual for the Examination of Human Semen and Sperm-Cervical Mucus Interaction*. 4<sup>th</sup> ed., Cambridge, UK: Cambridge University Press.

**Wuttke, M. S., Buck, J. and Levin, L. R.** (2001). Bicarbonate-regulated soluble adenylyl cyclase. *Jop* **2**, 154-8.

**Xia, J., Reigada, D., Mitchell, C.H. and Ren, D.** (2007). CarSper channel-mediated Ca<sup>2+</sup> entry in mouse sperm triggers a tail-to-head propagation. *Biol Reprod* **77**, 551-9.

**Xia, J. and Ren, D.** (2009a). The BSA-induced Ca<sup>2+</sup> influx during sperm capacitation is CATSPER channel-dependent. *Reprod Biol Endocrinol* **7**, 119.

**Xia, J. and Ren, D.** (2009b). Egg coat proteins activate calcium entry into mouse sperm via CatSper channels. *Biol Reprod* **80**, 1092-1098.



- Xie, F., Garcia, M.A., Carlson, A. E., Schuh, S.M., Babcock, D.F., Jaiswal, B.S., Gossen, J.A., Esposito, G., van Duin, M. and Conti, M.** (2006). Soluble adenylyl cyclase (sAC) is indispensable for sperm function and fertilization. *Dev Biol* **296**, 353-62.
- Xu, W., Wilson, B.J., Huang, L., Parkinson, E.L., Hill, B.J., Milanick, M.A.** (2000). Probing the extracellular release site of the plasma membrane calcium pump. *Am J Physiol Cell Physiol*. **278**, C965-72.
- Yanagimachi, R.** (1970). The movement of golden hamster spermatozoa before and after capacitation. *J Reprod Fertil* **23**, 193-6.
- Yanagimachi, R. and Usui, N** (1974). Calcium dependence of the acrosome reaction and activation of guinea pig spermatozoa. *Exp Cell Biol* **89**, 161-74.
- Yanagimachi, R. and Mahi, C.A.** (1976). The sperm acrosome reaction and fertilization in the guinea-pig: a study in vivo. *J Reprod Fertil*. **46**, 49-54.
- Yanagimachi, R.** (1994a). Fertility of mammalian spermatozoa: its development and relativity. *Zygote* **2**, 371-2.
- Yanagimachi, R.** (1994b). Mammalian fertilization. in: *The Physiology of Reproduction* (ed. E. Knobil and J. D. Neill), pp. 189-317. New York, USA: Raven Press.
- Yamaguchi, R., Muro, Y., Isotani, A., Tokuhiko, K., Takumi, K., Adham, I., Ikawa, M. and Okabe, M.** (2009). Disruption of ADAM3 impairs the migration of sperm into oviduct in mouse. *Biol Reprod* **81**, 142-6.
- Yang, C., Jas, G.S. and Kuczera, K.** (2001). Structure and dynamics of calcium-activated calmodulin in solution. *J Biomol Struct Dyn*. **19**, 247-71.
- Yang, C.T., Zeng, X.H., Xia, X.M. and Lingle, C.J.** (2009). Interactions between beta subunits of the KCNMB family and Slo3: beta4 selectively modulates Slo3 expression and function. *PLoS One*. **4**, e6135.
- Yeoman, R. R., Jones, W. D. and Rizk, B. M.** (1998). Evidence for nitric oxide regulation of hamster sperm hyperactivation. *J Androl* **19**, 58-64.
- Yeung, C.H. and Cooper, T.G.** (2001). Effects of the ion-channel blocker quinine on human sperm volume, kinematics and mucus penetration, and the involvement of potassium channels. *Mol Hum Reprod*. **7**, 819-28.
- Yeung, C.H., Barfield, J.P., Anapolski, M. and Cooper, T.G.** (2004). Volume regulation of mature and immature spermatozoa in a primate model, and possible ion channels involved. *Hum Reprod*. **19**, 2587-93.

**Yeung, C.H., Barfield, J.P. and Cooper, T.G.** (2006). Physiological volume regulation by spermatozoa. *Mol Cell Endocrinol.* **250**, 98-105.

**Yoshida, M., Ishikawa, M., Izumi, H., De Santis, R. and Morisawa, M.** (2003). Store-operated calcium channel regulates the chemotactic behavior of ascidian sperm. *Proc Natl Acad Sci U S A* **100**, 149-54.

**Yoshimura, A., Nakano, I. and Shingyoji, C.** (2007). Inhibition by ATP and activation by ADP in the regulation of flagellar movement in sea urchin sperm. *Cell Motil Cytoskeleton.* **64**, 777-93.

**Yuan, Y.Y., Chen, W.Y., Shi, Q.X., Mao, L.Z., Yu, S.Q., Fang, X. and Roldan, E.R.** (2003). Zona pellucida induces activation of phospholipase A2 during acrosomal exocytosis in guinea pig spermatozoa. *Biol Reprod* **68**, 903-13.

**Yuan, J.P., Zeng, W., Huang, G.N., Worley, P.F. and Muallem, S.** (2007). STIM1 heteromultimerizes TRPC channels to determine their function as store-operated channels. *Nat Cell Biol.* **9**, 636-45.

**Zalk, R., Lehnart, S.E. and Marks, A.R.** (2007). Modulation of the ryanodine receptor and intracellular calcium. *Annu Rev Biochem.* **76**, 367-85.

**Zamponi, G.W., Bourinet, E. and Snutch, T.P.** (1996). Nickel block of a family of neuronal calcium channels: subtype- and subunit-dependent action at multiple sites. *J Membr Biol.* **151**, 77-90.

**Zeng, Y., Clark, E.N. and Florman, H.M. N.** (1995). Sperm membrane potential: hyperpolarization during capacitation regulates zona pellucida-dependent acrosomal secretion. *Dev Biol.* **171**, 554-63.

**Zeng, Y., Oberdorf, J.A. and Florman, H.M.** (1996). pH regulation in mouse sperm: identification of Na(+), Cl(-), and HCO<sub>3</sub>(-)-dependent and arylaminobenzoate-dependent regulatory mechanisms and characterization of their roles in sperm capacitation. *Dev Biol* **173**, 510-20.

**Zhang, H. and Zheng, R. L.** (1996). Possible role of nitric oxide on fertile and asthenozoospermic infertile human sperm functions. *Free Radic Res* **25**, 347-54.

**Zhang, H., Zhu, B., Yao, J.A. and Tseng, GN.** (1998). Differential effects of S6 mutations on binding of quinidine and 4-aminopyridine to rat isoform of Kv1.4: common site but different factors in determining blockers' binding affinity. *J Pharmacol Exp Ther.* **287**, 332-43.

**Zhang, S.L. Yu, Y., Roos, J., Kozak, J.A., Deerinck, T.J., Ellisman, M.H., Stauderman, K.A. and Cahalan, M.D.,** (2005). STIM1 is a Ca<sup>2+</sup> sensor that activates CRAC channels and migrates from the Ca<sup>2+</sup> store to the plasma membrane. *Nature* **437**, 902-5.

**Zhu, Y., Bond, J. and Thomas, P.** (2003). Identification, classification, and partial characterization of

genes in humans and other vertebrates homologous to a fish membrane progestin receptor. *Proc Natl Acad Sci USA* **100**, 2237-42.

